U.PORTO

FEUP FACULDADE DE ENGENHARIA
UNIVERSIDADE DO PORTO

FATIGUE ANALYSIS OF A JACKET-TYPE OFFSHORE PLATFORM BASED ON LOCAL APPROACHES

ANTÓNIO MANUEL DE BARROS FIGUEIREDO DA SILVA MOURÃO

Dissertação submetida para satisfação parcial dos requisitos do grau de

MESTRE EM ENGENHARIA CIVIL — ESPECIALIZAÇÃO EM ESTRUTURAS

Supervisor: Professor Doutor José António Fonseca de Oliveira Correia

Co-supervisors: Professor Doutor José Miguel de Freitas Castro

Professor Doutor Carlos Alberto da Silva Rebelo

JUNHO DE 2018

MESTRADO INTEGRADO EM ENGENHARIA CIVIL 2017/2018

DEPARTAMENTO DE ENGENHARIA CIVIL

Tel. +351-22-508 1901

Fax +351-22-508 1446

✉ miec@fe.up.pt

Editado por

FACULDADE DE ENGENHARIA DA UNIVERSIDADE DO PORTO

Rua Dr. Roberto Frias

4200-465 PORTO

Portugal

Tel. +351-22-508 1400

Fax +351-22-508 1440

✉ feup@fe.up.pt

http://www.fe.up.pt

Aos meus Pais, em agradecimento por todo o esforço e dedicação

Failure is simply the opportunity to begin again, this time more intelligently.

Henry Ford

ACKNOWLEDGMENTS

First and foremost, I would like to express a special thanks to my supervisor Prof. Doctor José Correia, researcher at Porto University for the invaluable dedication and guidance during this dissertation.

I would also like to thank my co-supervisors Prof. Doctor José Castro, researcher at Porto University and Prof. Doctor Calos Rebelo, researcher at Coimbra University.

A thank you to Force Technology, in particular to Eng. Miguel Correia and Eimund Gjerstad for the help and data provided, without which this this dissertation could not be possible.

For PhD student and Assistance Prof. at Rural Federal University of Semi-Árido (UFERSA), Joelton Barbosa, thanks for the all the advice and assistance provided.

For Prof. Milan Velikovic a note of appreciation for the invitation to attend the Internal Workshop INEGI-TUD: Prediction methods for fatigue resistance of bridge details at TU Delft.

To Faculty of Engineering of University of Porto (FEUP) and Institute of Science and Innovation in Mechanical and Industrial Engineering (INEGI), for making its facilities available to me.

Author gratefully acknowledges the funding of SciTech - Science and Technology for Competitive and Sustainable Industries (NORTE-01-0145-FEDER-000022), R&D project and FADEST - Competence Development in R&D in the fatigue design of structures and Structural Details (NORTE-01-0247-FEDER-015670), R&D project co-financed by Programa Operacional Regional do Norte ("NORTE2020"), through Fundo Europeu de Desenvolvimento Regional (FEDER).

Finally, for their constant and unconditional support in every step of the way, a thank you to my family.

António Mourão
University of Porto
June 25, 2018

RESUMO

Devido à sua localização, natureza e função, estruturas offshore têm sofrido uma melhoria ao longo dos anos convergindo em soluções e materiais inovadores de modo a dar resposta ao problema.

Com um carregamento cíclico constante por parte do ambiente circundante, nomeadamente, ações ambientais, estes tipos de estruturas são sujeitas à acumulação de dano por fadiga resultando no aparecimento de fendas que provocam a diminuição da vida em serviço da estrutura.

Com esta linha de pensamento, este estudo foca na avaliação das cargas ambientais às quais a estrutura está sujeita e posterior quantificação do nível de dano por fadiga presente.

Para tal, um caso de estudo é apresentado onde a estrutura offshore do tipo Jacket é analisada com base na ligação com os níveis de esforços mais críticos.

Dados de dispersão de onda são providenciados e, portanto, a fórmula de Morrison pode ser usada para obter um carregamento normal aplicável à estrutura. Para tal, diversas teorias de ondas são estudadas e comparadas, a teoria de onda linear e a teoria de Stokes de 5ª Ordem, resultando em diversas possibilidades de carregamento de onda onde mais pertinente será utilizada, Stokes de 5ª Ordem.

Uma vez que os esforços nos vários elementos da ligação critica são obtidos, o mais elevado resultando numa onda que será usada para o cálculo do dano à fadiga de acordo com diferentes tipos de análise.

Neste estudo foram empregues a regra de acumulação de dano de Palmgren-Miner e a preconizada na norma DNV-GL chamada de análise à fadiga simplificada usando a gama de tensões distribuída de Weibull. A regra de Palmgren-Miner foi aplicada usando abordagens baseadas nas tensões hot-spot, tensões nominais e tensões de entalhe. As tensões de entalhe foram obtidas usando uma abordagem na regra de Neuber e na relação de Ramberg-Osgood. Uma comparação e análise entre os diferentes métodos são feitas.

Foi verificado que o dano resultante das cargas marítimas cumpre o limite especificado proposto pela DNV-GL especificamente para estruturas offshore da mesma região que o caso de estudo.

PALAVRAS-CHAVE: Estruturas Offshore, Ações Ambientais, Teoria de Ondas, Fadiga, Dano por Fadiga, Previsão da vida à Fadiga.

ABSTRACT

Offshore structures have due to their location and function undergone a significant improvement over the years converging in innovative solutions and materials available to tackle the problems.

With constant cyclic loading from the environment, namely, environmental loads, this kind of structures are prompt to fatigue accumulative damage resulting in the appearance of cracks causing the reduction of the structures service life.

Under this line of thought, this study focuses in evaluating the environmental loads to which the structure is subjected to and posteriorly the quantification of the level of fatigue damage present.

For this, a case study is presented, where an offshore jacket-type structure will be analysed based on the joint with the most critical levels of stress.

Wave data scatter has been provided and so Morrison's formula can be used to achieve an applicable normal loading force to the structure. To do so, several wave theories are studied and compared, linear wave theory and Stokes 5^{th} order theory, resulting in several sea load possibilities, where only the most pertinent will be used, Stokes 5^{th} Order.

Once stresses at the various elements of the critical joint are obtained, the highest resulting in a wave that will be used to calculate fatigue damage according to different types of analysis.

In this study Palmgren-Miner rule for damage accumulation and the recommended in DNV-GL called simplified fatigue analysis using the stress range distribution.

It was verified that the damage resultant from the sea loads is under the specified limit put forward by DNV-GL specifically for offshore structures in the same region as this case study.

KEYWORDS: Offshore Structures, Sea Loads, Wave theory, Fatigue, Fracture Mechanics, Fatigue Damage, Fatigue Life.

GENERAL INDEX

LIST OF FIGURES

LIST OF TABLES

NUMENCLATURE

Chapter 2:

N_f – Total fatigue life

N_i – Nº of cycles associated with crack initiation

N_p – Nº of cycles associated with crack propagation

σ_{max} – Maximum stress [MPa]

σ_{min} – Minimum stress [MPa]

$\Delta\sigma$ – Stress range [MPa]

σ_a – Stress Amplitude [MPa]

σ_m – Mean stress [MPa]

R – stress R-ratio

C and m – material constants in Basquin's relation

$\Delta\sigma_C$ – Detail category

$\Delta\sigma_D$ – Constant amplitude fatigue limit

$\Delta\sigma_L$ – Cut-off-limit

σ – nominal stress

σ'_f - strength coefficient

b – fatigue strength exponent

$\Delta\varepsilon^e$ – strain elastic component

E – Young's modulus

$\Delta\varepsilon^p$ – strain plastic component

c – fatigue ductility exponent

ε'_f - fatigue ductility coefficient

ΔWP – Plastic strain energy density per cycle

ΔWt – total tensile strain energy density per cycle

n' - cyclic hardening exponent

$\delta\sigma_0$ – increase in the proportional stress limit

ν – Poisson coefficient

K_I – Stress Intensity Factor in mode I

K_{II} – Stress Intensity Factor in mode II

K_{III} – Stress Intensity Factor in mode III

r and θ – polar coordinates

K – Stress intensity factor

Y geometrical parameter

W – loading work per unit of volume

T – traction vector

$\bar{u}$ – displacement vector

da/dN – fatigue crack growth rate

ΔK – Stress intensity factor range

K_{max} – Maximum stress intensity factor

K_{min} – Minimum stress intensity factor

ΔK_{eff} – Effective stress intensity factor range

ΔK_{eq} – Equivalent stress intensity factor range

a – crack length

W – specimen width

t – specimen thickness

α – loading angle

K_{op} – Limit Stress intensity factor for crack closure effect

U – percentage of loading for crack propagation

Chapter 3:

H_s – significant wave height

λ – wave length

T – wave period

H_{max} – maximum wave height

d – water depth

ξ – wave profile

ω – wave frequency

k – wave number

x – position of the wave

ξ_a – Wave profile amplitude

Φ – velocity potencial

u – velocity component in x direction

w – velocity component in z direction

$\dot{u}$ – acceleration component in x direction

$\dot{w}$ – acceleration component in z direction

ρ – mass density of the fluid

C_A – added mass coefficient

C_D – drag coefficient

D – diameter

A – area of the cross section

v – velocity

$\dot{v}$ – acceleration

Chapter 4:

Px – Axial force

My – in plane bending moment

Mz – out of plane bending moment

D – fatigue damage

n_0 – number of occurrences

v_0 – average zero-up-crossing frequency

q and h – Weibull distribution parameters

Γ – function of the S-N curve slope and h

$\sigma_{0,t}$ – Hot-spot stress with thickness effect

$\sigma_{0,tref}$ – reference stress for thickness effect

t_{ref} – reference thickness

t – thickness of the element

k – thickness exponent

η – usage factor

ACRONYMS:

BS – British Standard

AASHTO – American Association of State Highway and Transportation Officials

EN – European Norm

DNV-GL – Det Norske Veritas Holding AS

ABS – American Bureau of Shipping

CCS - Chinese Classification Society

SWT – Smith-Watson-Topper

LEFM – Linear Elastic Fracture Mechanics

EPFM – Elastoplastic Fracture Mechanics

CTOD – Crack Tip Opening Displacement

SCF – Stress Concentration Factor

IIW – International Institute of Welding

SIF – Stress Intensity Factor

HAZ – Heat Affected Zone

API – American Petroleum Institute

FPS – Floating Production System

TLP – Tension Leg Platform

DFF – Design Fatigue Factor

1
INTRODUCTION AND OBJECTIVES

1.1. GLOBAL ASPECTS

With its beginnings dating back to the 1930's in the Gulf of Mexico and later expanding to the North Sea in the 1960's, offshore structures have played an important role in oil and gas exploration and production, having expanded to wind power in more recent years.

Given the increasing demand of these natural resources and the environmentally conscious mentality, never in the past has it been so important to fully understand the conditions to which these structures are exposed to.

Installed many times in locations with adverse conditions, offshore structures are mutually subjected to functional and environmental loads (sea loads being more dominant). Due to the dynamic nature of the sea loads, the structure is subjected to a range of stresses that even though below the yielding stress of the material, results in the diminishing life of the offshore platform by fatigue.

First contributions on the topic of fatigue where made in the 19th century and carried out by numerous authors. Trial and error being the main source of knowledge, there is no greater example of fatigue failure then the Liberty ship´s hull crack in WW2 or the Alexander L. Kielland offshore platform, where a fatigue crack was followed by an unstable collapse of the structure in both cases.

This way design codes such as the DNVGL require a fatigue analysis of the steel structure to mitigate such accidents.

1.2 AIM AND OBJECTIVES

With the use of sea load history provided for the specific location in which the platform is located, it is possible to obtain wave particle kinematics under several wave theories, both linear and nonlinear, to achieve the force applied in a specific critical joint of the structure by means of Morrison formula.

Being fatigue strength commonly described in the form of S-N curves obtained by experimental tests in laboratory, it is purposed with this study a fatigue damage evaluation by using current design standards as well local approaches. For this design codes such as the DNV-GL propose a simplified probabilistic fatigue analysis and a and the Palmgren-Miner rule for damage accumulation.

With this in mind an assessment of remaining life of a critical KT-type joint can be made and the remaining fatigue life of the structure obtained.

1.3 ORGANIZATION OF THE DISSERTATION

This document is organized under the following way. Starting in Chapter 2, a literature review on fatigue is provided, first with the major contributions on the subject, afterwards, several factors that have an impact in fatigue are presented. Next several types of damage parameters are presented, leading to different types of local approaches both uniaxial and multiaxial. To finalize this chapter a short review on studies for air and marine environment are pointed out as well as different approaches to fatigue in the specific case of offshore structures.

Following, in Chapter 3, a review on hydrodynamic and service loads is laid out, the necessary steps in the direction of wave simulation are expressed and linear and non-linear wave theories are studied.

From this linear and non-linear wave theories several normal load forces using Morrison formula are offered, from which one will be used to achieve forces at each member.

Next in Chapter 4, an overview on offshore structures is done followed by the description of the case study. Different approaches such as Palmgren-Miner rule based on hot-spot, nominal and notch stresses and simplified fatigue analysis are used. A comparison and discussion are presented.

Last, in Chapter 5, comprises the main conclusions of this paper and presents suggestions for future works.

2

FATIGUE AND FRACTURE MECHANICS IN OFFSHORE STRUCTURES

2.1. FATIGUE GENERAL CONSIDERATIONS

The term fatigue is described today as "The process of progressive localized permanent structural change occurring in a material subjected to conditions that produce fluctuating stresses and strains at some point or points and that may culminate in cracks or complete fracture after a sufficient number of fluctuations", ASTM E1823 [1].

The state of the art on the topic of fatigue covers over 180 years of history and several authors throughout the years have made countless contributions to the subject. This way, only the most significant contributions will be mentioned.

More on the topic of fatigue history can be found in the works of Schütz , Schijve and Mann the later which compiled numerous fatigue problems from 1838 to 1969 [2-4].

As presented by Schutz [2], fatigue history is divided into two eras, before and after Wöhler. Before Wöhler there is the work of German mines engineer Wilhelm Albert, who in 1837 associated the failure of iron chains to the small cyclic load to which these where subjected to, leading to the first experiments on fatigue.

Later in 1843, Rankine, known for his work in thermodynamics, discussed the fatigue strength of railway axles [5]. Braithwaite in 1854 was the first to introduce the term of fatigue.

The work of Wöhler was crucial to our current knowledge of the topic, not only is he responsible for the design and construction of the early testing machines but also for countless experimental tests which he passed on in a tabular manner. Afterwards his successor, Spangenberg, plotted the graphical representation of the data in what is called S-N curves or Wöhler curves, in memory of his predecessor.

S-N curves now presented in design codes worldwide are offered in the form of a bi-logarithmic axis, first suggested by Basquin in 1910 [6].

With his publications in 1870, often called "Whöler´s Laws" he concluded that the stress amplitude is the most important parameter in fatigue life, with the effect of mean stress playing a significant role. He went on to describing the need for safety factor for different components that reflects both mean stress and stress amplitude [2].

Whöler then describes in another paper, the crack propagation in railway axles that even though designed for infinite life, have collapsed in large numbers.

During the period 1870 to 1905 the works o Baushinger, Professor of Mechanics at the Munich Polytechnical School, now called Technical University of Munich, are vital to understand the elastic limit of metals when exposed to repeated stress, the basis for Low-Cycle-Fatigue developed by Coffin and Manson [7].

Kirsch, in 1898, was the first to arrive analytically at a concentration factor of 3.0 for a cylindrical hole in an infinite plate.

Slip bands commonly used to provide a metallurgical description of fatigue are introduced in the early 20th century by Ewing and Humfrey [7]

First full-scale fatigue test in large aircraft components were conducted in the U.K. at the same period, and names such as Smith, Haigh, Gough, Inglis, Kommers, Moore and Griffith are mentioned in the literature [2].

Griffith of the Royal Aircraft Establishment, U.K., made another major contribution to fatigue with the development of fracture mechanics, in 1920 [2].

Also important in the field of fatigue life, was the contribution of Gough, in his book, presenting the influence of surface roughness on fatigue limit as well as stress concentration factors.

Suggested by Palmgren, and later formulated mathematically by Miner in 1945, the Palmgren-Miner rule provides a cumulative damage criterion, which despite its limitation still is the most widely used cumulative damage model in fatigue [7].

In the 50s, with the numerous accidents concerning the Comet, due to fatigue failure, full-scale tests of the plane were conducted to assess fatigue life and were posteriorly made mandatory in the aeronautics industry along with the concept of “safe life”.

In 1958, Irwin realized that the stress intensity factor was the main factor when it came to cracked bodies leading to Linear Elastic Fracture Mechanics (LEFM) [2].

In his PhD Thesis at the University of New South Wales, Elber in 1968, found that after a tensile load the crack closes before ever reaching zero, giving birth to the “crack closure effect”.

In 1974, introduced by the US Air Force the Damage Tolerance Requirements, also present design codes, in which defects are considered in the structure.

2.1.1. Fatigue Damage Stages

“Microscopic investigations in the beginning of the 20th century have shown that fatigue crack nuclei start as invisible micro cracks in slip bands.” [8], usually micro cracks remain invisible to the naked eye for the majority of the total life, given that this percentage may fluctuate when applied to real structures, such as ships.

After the nucleation of a micro crack growth, it can be a slow process due to the microstructure [8], however once the crack as grown away from the nucleation site, a steadier growth can be observed.

Since several surface conditions take a toll in the initiation period but are almost negligible for the propagation period, it is important to differentiate the two, this way it is presented in Figure 2.1 a scheme of the both periods of fatigue life.

It is also important to mention that damage parameters existent in initiation phase such as stress concentration factor differ from the ones used to estimate fatigue life in propagation phase.

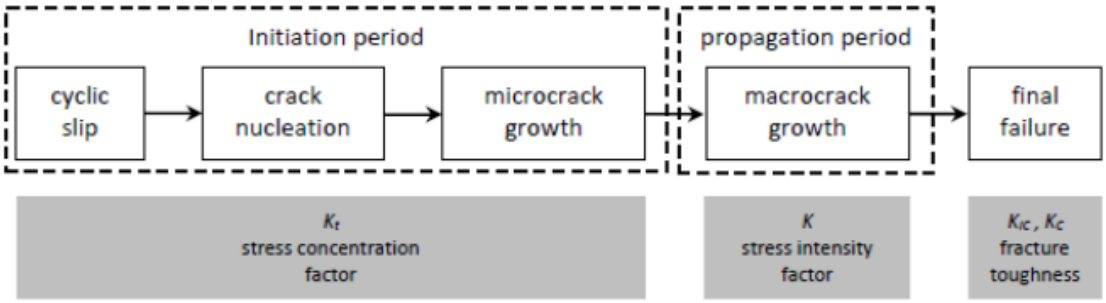

Figure 2.1 - Fatigue damage periods [9].

2.1.2. Crack Initiation

As a direct response to cyclic loading, slip bands are created on microscopic level at the material surface. Since fatigue occurs at a stress level below the yielding stress, the plastic deformation is limited to a handful of grains present at the material surface, since the grains are constricted only at one side. Plastic deformation of the grains can occur though slightly inside the material due to metallurgic imperfections, which then immediately propagates towards the material surface.

Since the material is not completely homogenous at a microscopic level, the stress distributions won´t be as well, as a result, some grains at the material surface present more favourable conditions for cyclic slip than others.

Slip bands are not fully reversible for two reasons, if a slip band is created then an oxidize layer will cover the new material which is not easily removed, and for the reason that strain hardening is not completely reversible. [8]

Taking into account the previous argument, inclusions appear in the material, as this is a repetitive mechanism, as can be seen in Figure 2.2, crack extension is to be expected.

Therefore, crack initiation is a predominantly a material surface phenomenon.

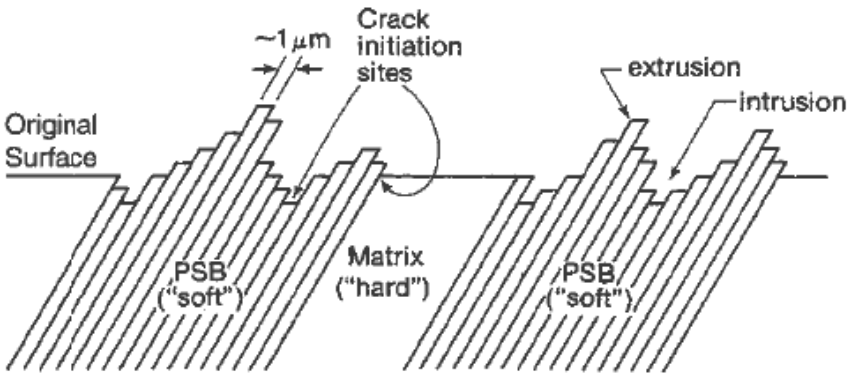

Figure 2.2 – Crack initiation phenomenon [10].

2.1.3. CRACK PROPAGATION

Since there can be formed several inclusions, stress concentration at the tip of the micro crack, can lead to the activation of more than one slip system, changing the direction of the original slip band. Usually crack growth direction will be perpendicular to the loading direction, supporting the idea that shear is the main influence for the appearance of slip bands, Fig.2.3 [8].

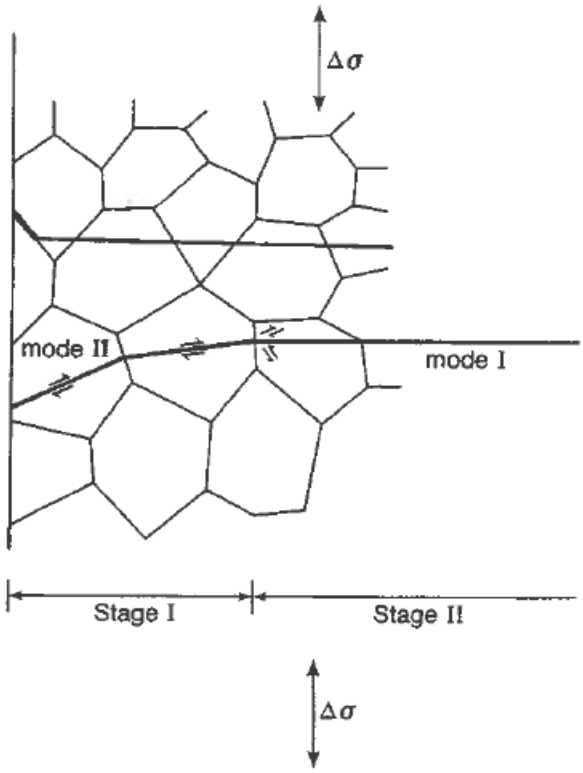

Figure 2.3 – Crack initiation and trans granular crack growth [10].

Crack propagation can however be stopped if the crack front encounters a crack growth barrier. Frost et al. [11] studied non-propagating fatigue cracks, they concluded that cracks in notched specimens stopped growing for stress amplitudes below the fatigue limit. Later on, it was recognized that non-propagating micro cracks could occur in unnotched specimens [8].

This way total life can be achieved as a summation of both initiation and propagation,

$$N_f = N_i + N_p \tag{2.1}$$

Where:

N_f - Total fatigue life

N_i – No. of cycles associated with crack initiation

N_p – No. of cycles associated with crack propagation

2.2. APPROACHES TO FATIGUE

To understand the following approaches, it is necessary to first comprehend the main factors behind fatigue damage.

As cited before, the work of Whöler has been paramount to the characterization of fatigue life with its relation to stress amplitude, nevertheless fatigue life can be related to numerous other stress related parameters, such as mean stress, which has been demonstrated to have a significant impact in data scatter.

As such, the different stress parameters used both in this document as well as in any literature concerning fatigue are shown in Figure 2.4.

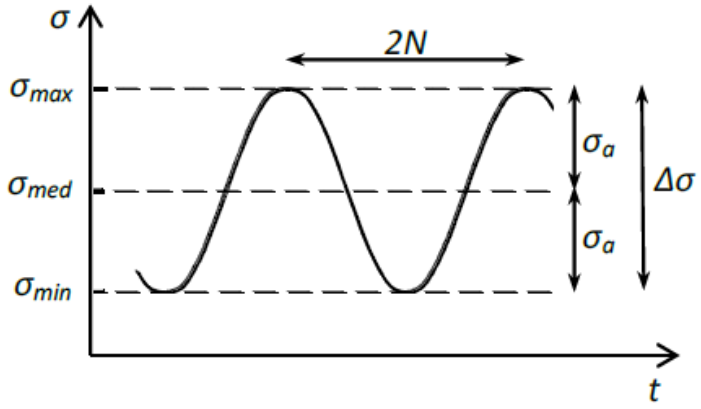

Figure 2.4 – General constant amplitude loading spectrum [9].

Where:

σ_{max}, Maximum stress;

σ_{min}, Minimum stress;

$\Delta\sigma = \sigma_{max} - \sigma_{min}$, Stress Range;

$\sigma_a = (\sigma_{max} - \sigma_{min})/2$, Stress Amplitude;

$\sigma_{med} = (\sigma_{max} + \sigma_{min})/2$, Mean Stress; and,

$R = {}^{\sigma_{min}}/_{\sigma_{max}}$, Stress R-ratio.

2.2.1. GLOBAL APPROACHES

Since fatigue includes numerous parameters that can be dependent of each other, the structural response to dynamic loading, cannot precisely be modelled [9], as a response design codes such as EN1993: 1-9[12], BS5400, AASHTO, DNVGL [13], American Bureau of Shipping [14], China Classification Society amongst others present an empirical procedure for design environment.

S-N curves in design codes, are expressed in a bi-logarithmic scale, like the one shown in Figure 2.5, where fatigue life, N_f, is often given as a function of the stress range, $\Delta\sigma$, to describe a specific structural detail to cyclic loading, using a mathematical expression developed by Basquin's Eq. (2.2).

$$\Delta\sigma^m N_f = C \tag{2.2}$$

Where *C* and *m* are constants related to both material and/or structural detail in question.

Regardless of Basquin's power law, several authors have proposed along the years different models to fit experimentally obtained data. Even though not all are physically viable the following are only a portion of the existing models (Table 2.1).

Table 2.1 – Proposed fatigue models for S-N curves [9].

Modelo	Equação
Wöhler (1870)	$\log N = A - B * \Delta\sigma;\ \Delta\sigma \geq\ \Delta\sigma_0$
Basquin (1910)	$\log N = A - B * \log\Delta\sigma\ ;\ \Delta\sigma \geq\ \Delta\sigma_0$
Strohmeyer (1914)	$\log N = A - B * \log(\Delta\sigma - \Delta\sigma_0)$
Palmgren (1924)	$\log(N + D) = A - B * \log(\Delta\sigma - \Delta\sigma_0)$
Palmgren (1924)	$\log N = A - B * \log(\Delta\sigma - \Delta\sigma_0)$
Weibull (1949)	$\log(N + D) = A - B * \log((\Delta\sigma - \Delta\sigma_0)/(\Delta\sigma_{st} - \Delta\sigma_0))$
Stüssi (1955)	$\log N = A - B * \log((\Delta\sigma - \Delta\sigma_0)/(\Delta\sigma_{st} - \Delta\sigma))$
Bastenaire (1972)	$(\log N - B) * (\Delta\sigma - \Delta\sigma_0) = A * \exp[-C * (\Delta\sigma - \Delta\sigma_0)]$
Spindel-Haibach (1981)	$\log\left(\frac{N}{N_0}\right) = \frac{\lambda + \delta * (-\log(1-\rho))^{1/\beta}}{\log(\Delta\sigma/\Delta\sigma_0)}$
Castillo et al. (1985)	$\log\left(\frac{N}{N_0}\right) = A * \log\left(\frac{\Delta\sigma}{\Delta\sigma_0}\right) - B * \log\left(\frac{\Delta\sigma}{\Delta\sigma_0}\right) + B\{\left(\frac{1}{\alpha}\right) * \log[1 + (\frac{\Delta\sigma}{\Delta\sigma_0})^{-2\alpha}$
Kohout and V**ě**chet (2001)	$\log\left(\frac{\Delta\sigma}{\Delta\sigma_\infty}\right) = \log\frac{N + N_1}{N + N_2}$
Pascual e Meeker (1999)	$\log N = A - B * \log(\Delta\sigma - \Delta\sigma_0)$

There have been recent developments [14-20] to achieve a unified theory considering both initiation and propagation crack phases, with the use of UniGrow model first developed by Noorozi [21].

Since a S-N curve is defined for a constant mean stress the figure below presents S-N curves for several stress levels as presented in EC3 (see Figure 2.5). It should be highlighted that as the stress increases the fatigue life consequently decreases.

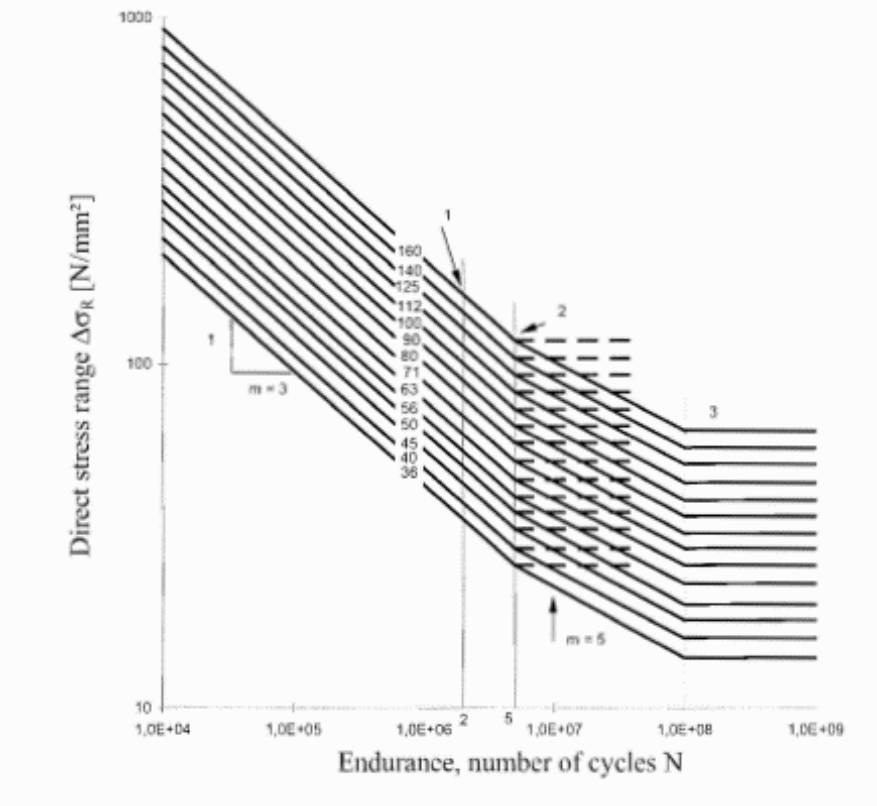

Figure 2.5 – EC3 typical S-N curves [12].

With:

1 - Detail Category, $\Delta\sigma_C$;

2 - Constant Amplitude Fatigue Limit, $\Delta\sigma_D$; and,

3 – Cut-off Limit, $\Delta\sigma_L$.

For this reason, it is advisable to represent fatigue life as a relation between stress amplitude and mean stress. Some relations have been proposed, with names such as Gerber (1874), Goodman (1899) and Soderberg (1939) being of relevance.

- Gerber relation: $\sigma_a = \sigma_e \left[1 - \left(\frac{\sigma_m}{\sigma_{UTS}}\right)^2\right]$ (2.3)
- Goodman relation: $\sigma_a = \sigma_e \left[1 - \frac{\sigma_m}{\sigma_{UTS}}\right]$ (2.4)
- Soderberg relation: $\sigma_a = \sigma_e \left[1 - \frac{\sigma_m}{\sigma_y}\right]$ (2.5)

The S-N method and the S-N curves are usually related either to the Nominal Stress Approach or the Hot Spot Stress Method Approach [14].

According to the definition of the, American Bureau of Shipping, nominal stress (σ) entails, the stress at a cross section of the specimen or structural detail away from the spot where fatigue cracking may occur (holes, welds, imperfections). On the other hand, hot spot stress (Shot) is defined as the surface value of the structural stress at the hot spot.

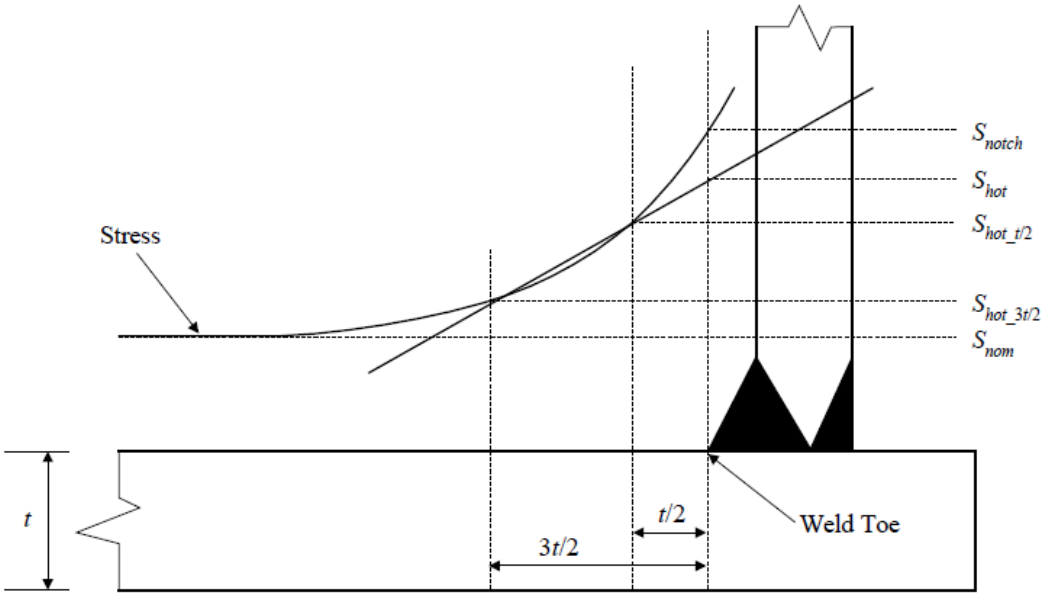

Figure 2.6 – Stresses at the weld detail [14]

Hot spot stress can also be obtained as the relation between nominal stress and the stress concentration factor, which will be mentioned later this document.

2.2.2. Local Approaches

Unlike the previous approach local approaches use fatigue damage parameters to link fatigue test results. For an accurate fatigue life prediction, several damage parameters have been proposed.

Local approaches can then be separated into three categories, stress-, strain- and energy-based, depending on the respective damage parameters.

2.2.2.1. Stress-based Method

Using alternating stresses as to predict the number of cycles until failure, this approach is more used for high-cycle fatigue (HCF) where the strains are mostly elastic, where in low cycle fatigue a non-linear relation between σ-ε can be observed.

$$\frac{\Delta\sigma}{2} = \sigma_a = (\sigma_f')\, {N_f}^b \tag{2.6}$$

According to Morrow, if the mean stress effect is taken in consideration, then Basquin's relation suffers a slight alteration to the following, which is the equivalent to a reduction of the fatigue strength coefficient, with a compressive stress having a reverse effect.

$$\frac{\Delta\sigma}{2} = \sigma_a = \left(\sigma_f' - \sigma_m\right) {N_f}^b \tag{2.7}$$

Where σ_f' and b are the strength coefficient and the fatigue strength exponent, respectively.

With the use of experimental data Basquin's coefficients are evaluated as to find the best fit possible. [10]

Another interesting model is the Kohout-Věchet model which covers all fatigue regimes and even though recently generalized for several fatigue damage parameters like strain-, SWT- and energy-based among others, proved to be sound with experimental results under uniaxial loading present in literature [22].

2.2.2.2. Strain-based Method

Similar to the previous methodology, strain-based approaches also use bi-logarithmic relation, where instead of stress vs fatigue life, strain is employed. The curve can be obtained in one of two ways, either by an amplitude of constant strains in different samples or by incremental test.

For a strain in a uniaxial stress state, the elastic component can be described as

$$\Delta\varepsilon^e = \frac{\Delta\sigma}{E} \tag{2.8}$$

If Basquin's relation, presented in Eq. (2.2), is divided by Young's modulus, then

$$\frac{\Delta\varepsilon^e}{2} = \frac{\left(\sigma_f'\right)\left(2N_f\right)^b}{E} \tag{2.9}$$

Where, σ_f' is the fatigue strength coefficient, and b is the fatigue strength exponent.

For high-cycle fatigue, plastic strain rounds zero as such Eqs. (2.8) and (2.9) are equivalent [10]. When it comes to low-cycle fatigue, Coffin and Manson arrived at a conclusion that plastic strain amplitude vs fatigue life could be linearized [23,24], which can be used according to Morrow's formulation [25],

$$\frac{\Delta\varepsilon^p}{2} = \varepsilon_f' * \left(2N_f\right)^c \tag{2.10}$$

Where c corresponds to the fatigue ductility exponent, and ε_f', the fatigue ductility coefficient.

By combining both elastic and plastic strains, we are left with the total strain amplitude as follows,

$$\frac{\Delta\varepsilon}{2} = \frac{(\sigma_f')\,(2N_f)^b}{E} + \varepsilon_f' * \,(2N_f)^c \tag{2.11}$$

Like stress-based methods, mean stress effect can be taken into consideration by applying the Smith, Watson and Topper (SWT) model, which shoulders the premise that fatigue life is a product of maximum stress, σ_{max} and strain amplitude $\frac{\Delta\varepsilon}{2}$ as shown below [9]:

$$\sigma_{max}\frac{\Delta\varepsilon}{2} = \frac{(\sigma_f')^2}{E}(2N_f)^{2b} + \sigma_f'\varepsilon_f'\,(2N_f)^{b+c} \tag{2.12}$$

More corrections have been made to the SWT model to consider the Bauschinger effect [26].

Manson and Halford on the other hand suggested an alteration to SWT, where both elastic and plastic terms of the equation should be arranged to include the mean stress effect, σ_m.

$$\frac{\Delta\varepsilon}{2} = \frac{(\sigma_f' - \sigma_m)(2\,N_f)^b}{E} + \varepsilon_f'\left(\frac{\sigma_f' - \sigma_m}{\sigma_f'}\right)^{c/b} * (\,2N_f)^c \tag{2.13}$$

It is important to emphasize that this method overestimates the mean stress effect on short life for plastic strain.

2.2.2.3. Energy-based Method

According to the basis of thermodynamics, when an object is loaded by an external force, part of that energy is dissipated, and the remaining is stored in the material [10]. It is the second which causes irreversible plastic deformation, representing hysteresis energy and first described by Bairstow in 1910.

The area of the hysteresis loop as the one presented below is believed to correlate to the fatigue damage suffered under each cycle.

The plastic strain energy density per cycle, ΔW^P, which has been proved advantageous especially for larger plastic strains. Thought out to predict the mean stress effect, the total tensile strain energy density per cycle, ΔW^t, uses both elastic and plastic strains, and as suggested by Ellyin and Kujawski can be written as,

$$\Delta W = \frac{1}{2}\Delta W^P + \frac{1}{2}\Delta\sigma\Delta\varepsilon \tag{2.14}$$

$$\Delta W^t = \Delta W^P + \frac{\sigma_{max}^2}{2E} \tag{2.15}$$

If ΔW^P is given by the following expression,

$$\Delta W^P = \frac{1-n'}{1+n'}\Delta\sigma\Delta\varepsilon^P + \frac{2n'}{1+n'}\delta\sigma_0\Delta\varepsilon^P \quad (2.16)$$

Where, n' is the cyclic strain-hardening exponent, $\delta\sigma_0$ the increase in the proportional stress limit and $\Delta\varepsilon^P$ the plastic strain range. In terms of total strain energy range,

$$\Delta W = k_t(2N_f)^\alpha + \Delta W_0{}^t \quad (2.17)$$

With $k>0$ and $\alpha<0$. Ellyin went on to formulate a more generalised formula to include mean stress [10].

2.2.2.4. Local Approaches based on Multiaxial Fatigue Criteria

Evaluation of multiaxial fatigue life is widely covered in literature, ranging from low to high-cycle fatigue in all manner of loading proportional or not.

Several authors [27-28] have gathered a wide range of both stress, strain and energy in literature ranging from low to high-cycle fatigue regardless of the loading (proportional or not) where multiaxial parameters are used for fatigue life evaluation, some of which are as follows.

Stress-based method:

Gough and Pollard for ductile metals under combined proportional bending and torsion loading conditions for the fatigue limit,

$$\left(\frac{\sigma_b}{\sigma_{FL}}\right)^2 + \left(\frac{\tau_t}{\tau_{FL}}\right)^2 = 1 \quad (2.18)$$

Sines proposed an alternative criterion in high-cycle fatigue (HCF), a similar one was proposed by Findley, Matake and McDiarmid using shear stress amplitude and normal stress on the critical plane as parameters [27].

$$\tau_{a,cr} + k\sigma_{n,cr} \leq \lambda \quad (2.19)$$

According to McDiarmid,

$$k = \frac{t_{A,B}}{2\sigma_u} \quad , \quad \lambda = t_{A,B} \quad (2.20)$$

Later in 2001, Papadopoulos, proposed a fatigue limit that can be of use for constant amplitude loading in high-cycle fatigue.

Strain-based method:

Defined by Brown and Miler the following mathematical formula, gives a relation between strain and fatigue life on multiaxial level for high-cycle regime, where *S* is a Brown Miller constant.

$$\left(S \cdot \Delta\varepsilon_n + \frac{\Delta\tau}{2}\right)_{max} = A\frac{\sigma_f'}{E}(2N_f)^b + B\varepsilon_f'(2N_f)^c \quad (2.21)$$

Fifteen years later, Fatemi and Socie modified the previous equation including Poisson's ration for both elastic and plastic regions.

Energy-based method:

As stated before, a damage parameter, SWT, was proposed by Smith and his co-authors, to consider the mean effect contribution. For multiaxial conditions, SWT parameter is corresponds to the maximum principal stress and strain:

$$SWT = \max\left(\sigma_n \cdot \frac{\Delta\varepsilon_1}{2}\right) \quad (2.22)$$

$$\sigma_n \cdot \frac{\Delta\varepsilon_1}{2} = \frac{(\sigma_f')^2}{E}(2N_f)^{2b} + \sigma_f'\varepsilon_f'(2N_f)^{b+c} \quad (2.23)$$

Where, σ_n is the maximum principal stress and the principal strain range, $\Delta\varepsilon_1$.

2.2.3. Fracture Mechanics based Approaches: LEFM and EPFM

Griffith postulated that the difference between theoretical and real resistance values could be explained by the presence of fissures in the material, since, according to his experimental results, for uncracked bodies the two values were almost similar.

Griffith stated that if the release of energy associated with cracking is higher than the energy that kept the material cohesive, than crack propagation would be verified [29]. Following the same train of thought, crack propagation can be avoided if the energy released remains below a certain limit, given by Griffith and for a plate under tension with a unitary thickness in plane stress with a crack.

$$U = \frac{\pi\sigma^2 a^2}{2E} \quad (2.24)$$

For crack propagation to occur,

$$\frac{\partial U}{\partial a} \geq \frac{\partial W}{\partial a} \rightarrow \frac{\pi\sigma^2 a^2}{2E} \geq 2\gamma a \quad (2.25)$$

$$G = \frac{\partial U}{\partial a} \tag{2.26}$$

For plane stress:

$$G = \frac{K^2}{E} \tag{2.27}$$

For plane strain:

$$G = \frac{K^2}{E}(1 - \upsilon^2) \tag{2.28}$$

However, above a certain threshold (a=a_c) these conditions invert given that the energy linked with elastic strain is proportional to crack opening square (a^2), whilst the cohesive energy is proportional to a.

It is then defined a critical value of stress for a certain crack length.

$$\sigma_c = \sqrt{\frac{2E\gamma}{\pi a}} \tag{2.29}$$

Depending on the size of the crack compared to the overall dimension of the element, fracture mechanics analysis can be divided into two, linear-elastic and elastoplastic fracture mechanics.

As mentioned before, Irwin realized that the stress intensity factor was the ruling parameter for cracked bodies, yet, this statement is only true for when the plastic strain region at the crack tip is small in comparison with other dimensions of the structure.

When the previous is not verified, the stress intensity factor is no longer applicable and so it becomes necessary to search other concepts with which to characterize fracture mechanics. For EPFM it is then used either CTOD or J-Integral, the latter being more precise since it relies on measurements which is subject to slight errors.

2.3. STRESS CONCENTRATION FACTOR

Construction is not without flaws, even though most of the welding and manufacturing for offshore structures is done in a controlled factory environment, there are always some irregularities from the design.

In this way, the most structural members present some sorts of discontinuity which should be taken into consideration for it will alter the response and distribution of stresses.

Design standards such as the IIW [30] imposes a mandatory minimum amount of discontinuity to be taken into account in design environment, be that a misalignment or a small deviation in angles.

As such design standards, present empirical formulas to determine the stress concentration factor (SCF) for those specific errors.

Stress concentration factor can so be considered a redistribution of stresses when a discontinuity in the member raising stresses in certain spots which may lead to cracking.

To me highlighted that SCF change depending on the type of loading, they need to be applied to the nominal stress used to obtain the same SCF and in the presence of combined loading, a superposition of the cases should be made where SCF is multiplied by the respective nominal stress [29].

Several author have developed parametric formulas for determination of SCF in joints connected to offshore engineering, Huang and Lloyd are amongst them, however, numerical simulations have been made which allows for comparison with the existing formulas [31].

There are many examples in literature where SCF are obtained for tubular joints with offshore structures in mind [32-34] and the interaction of different types on loading.

For offshore, DNVGL provides several formulas, suggested by Efthymiou, dependent on the type of connection and for several combinations of loading, none of which depends of the actual stress of the element.

From this could be stated that the stress concentration factors depend only on the type of loading and geometrical parameters.

2.4. STRESS INTENSITY FACTOR AND J-INTEGRAL

Given that stress and strain near a crack tip are described according to the mode of deformation, it is relevance to highlight all three different modes.

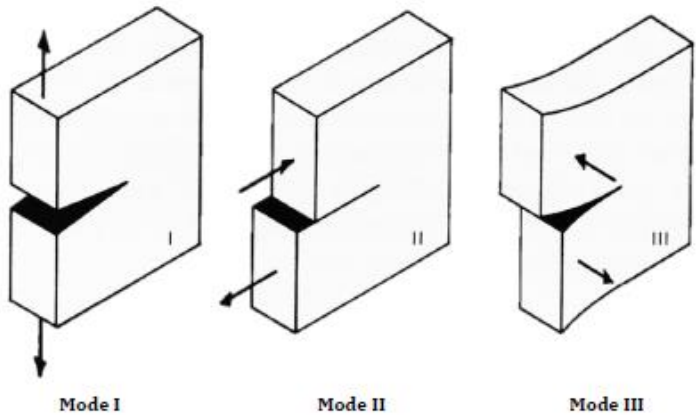

Figure 2.7 – Crack opening modes [35].

Mode I, associated with tensile loading where crack propagates in perpendicularly to the loading direction.

Mode II, or in-plane shear, where the direction of loading is perpendicular to the crack front.

Mode III, is commonly associated with out-of-plane shear, where the loading is parallel to the crack front.

Despite mode I being the most used when it comes to engineering applications, a combination of two or three modes can be found in literature for several materials.

Expressed by Irwin the elastic stress field near a crack tip under mode I loading conditions is:

$$\sigma_x = \frac{K_I}{\sqrt{2\pi r}}\cos\frac{\theta}{2}\left(1 - \sin\frac{\theta}{2}\sin\frac{3\theta}{2}\right) \tag{2.30}$$

$$\sigma_y = \frac{K_I}{\sqrt{2\pi r}}\cos\frac{\theta}{2}\left(1 + \sin\frac{\theta}{2}\sin\frac{3\theta}{2}\right) \tag{2.31}$$

$$\tau_{xy} = \frac{K_I}{\sqrt{2\pi r}}\cos\frac{\theta}{2}\sin\frac{\theta}{2}\cos\frac{3\theta}{2} \tag{2.32}$$

With ν is the Poisson coefficient, K_I is the stress intensity factor in mode I and r and θ are the polar coordinates.

Equivalently in mode II:

$$\sigma_x = \frac{-K_{II}}{\sqrt{2\pi r}}\sin\frac{\theta}{2}\left(2 + \cos\frac{\theta}{2}\cos\frac{3\theta}{2}\right) \tag{2.33}$$

$$\sigma_y = \frac{K_{II}}{\sqrt{2\pi r}}\sin\frac{\theta}{2}\cos\frac{\theta}{2}\cos\frac{3\theta}{2} \tag{2.34}$$

$$\tau_{xy} = \frac{K_{II}}{\sqrt{2\pi r}}\cos\frac{\theta}{2}\left(1 - \sin\frac{\theta}{2}\sin\frac{3\theta}{2}\right) \tag{2.35}$$

With K_{II} is the mode II stress intensity factor.

And last for mode III loading conditions:

$$\tau_{xy} = \frac{-K_{III}}{\sqrt{2\pi r}}\sin\frac{\theta}{2} \tag{2.36}$$

$$\tau_{yz} = \frac{K_{III}}{\sqrt{2\pi r}}\cos\frac{\theta}{2} \tag{2.37}$$

where K_{III} is the mode III stress intensity factor.

The stress intensity factor, *K*, which varies depending on the loading mode in question can be written as:

$$K = Y\sigma\sqrt{\pi a} \tag{2.38}$$

where *Y* is a geometrical parameter and σ the nominal stress.

By analysing the formulas above, it is noticeable that the stress intensity factor depends on the loading and geometry but not on the polar coordinates and so does not control the distribution of the stress, instead it outlines the intensity of the same.

For larger plastic zones at the crack tip, rendering stress intensity factor (*SIF* or *K*) invalid, the J-Integral is a valid option.

J-integral is used to characterize elastic or plastic stress-strain field around crack tip. The J- integral is nothing more than a surface integral that encloses the crack front from one crack tip to the next as showed in the figure below.

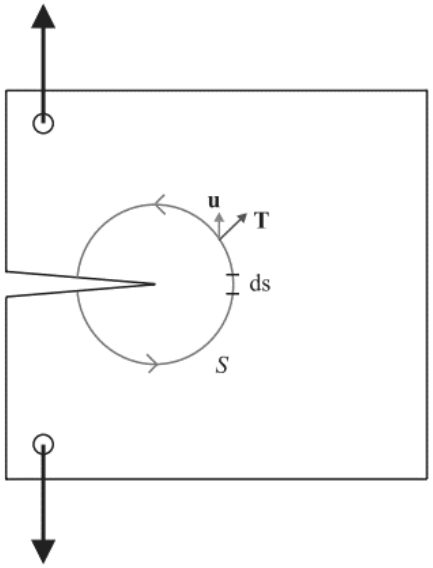

Figure 2.8 – J-Integral method [36].

The integral is the following:

$$J = \int_{\Gamma} W\,dy - T\left(\frac{\partial \bar{u}}{\partial X}\right) ds \tag{2.39}$$

where:

W is the loading work per unit of volume;

T, traction vector at *ds* according to the outward normal *n* along the contour; and,

$\bar{u}$, displacement vector at *ds*.

2.5. FATIGUE CRACK PROPAGATION

Having started with Griffith in 1920, even though only applicable to brittle materials, and later expanded to include materials with a certain degree of plasticity by Irwin and Orowan [37], fracture mechanics presents a major step forward to the field of fatigue. Not mentioned in section 2.1 but paramount to the subject at hand, Paris and his co-authors were the first to point out the stress intensity factor (SIF or K) as the chief parameter for the description of crack growth.

$$\frac{da}{dN} = f(\Delta K) \tag{2.40}$$

Where *da/dN* can be described as the fatigue crack growth rate (or speed), equivalent to a function of the stress intensity factor range (ΔK), which can be obtained with the equation below.

$$\Delta K = K_{max} - K_{min} \tag{2.41}$$

Proposed by Paris [38], a simplistic model relating crack growth rate and the intensity factor, adding only two parameters compared with Eq. (2.42), *C* and *m*, both material constants, which can be obtained by means of linear regression as to best fit experimental data.

$$\frac{da}{dN} = C(\Delta K)^m \tag{2.42}$$

Despite its theoretical validity proven by Rice [29], Paris law is only viable to describe one of the three regions associated with crack propagation (II), where in the other extreme regions the log-log relation is not verified.

Paris Law to achieve fatigue life needs to be integrated:

$$N_f = \int_{a_i}^{a_f} \frac{1}{C \cdot \Delta K^m} da \tag{2.43}$$

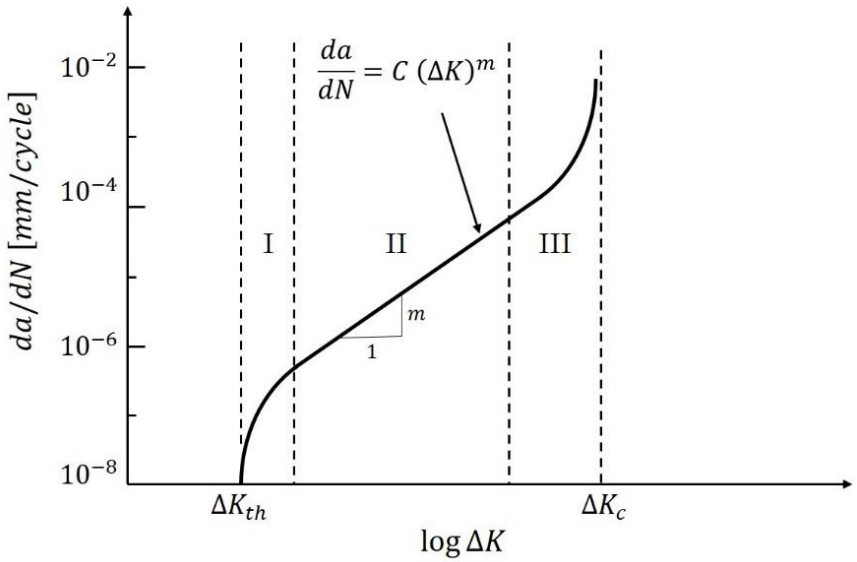

Figure 2.9 – Fatigue crack propagation rate [9].

Crack propagation can be divided into three regions, possible of observing in the picture above. Region I, denominated threshold region below which there is no crack propagation, region II called Paris Law region as a recognition of his work and the third, unstable crack growth region, where K_{max} approaches K_c leading to collapse (K_{max}=K_c).

The stress R-ratio can be written as a difference between K_{min} and K_{max}, this implies that *da/dN* depends on the stress R-ratio [3]. Tests have proved that different stress ratios produce different fatigue crack growth curves like the ones in Fig. 2.9, parallel, meaning that the constant C varies while the slope m remains the same.

Walker made a modification to include the stress ratio:

$$\frac{da}{dN} = C\ \left[\frac{\Delta K}{(1-R)^{1-\gamma}}\right]^m \tag{2.44}$$

Where γ is the Walker exponent.

Alongside the stress R-ratio, this relation adds another parameter to the Paris Law, γ, where if it takes a unitary value ($0 \leq \gamma \leq 1$), then the stress ratio has no influence in crack growth.

Foreman proposed an extension to the previous models, where it would not only be possible to describe region II but region III as well:

$$\frac{da}{dN} = \frac{C\ \Delta K^m}{(1-R)\ (K_c - K_{max})} \tag{2.45}$$

If K_{max} approaches K_c, then the crack growth rate becomes unstable, which serves as a validation of the model.

Hartman and Schijve went even further, making it possible for the model to cover all three regions of crack propagation regimes.

$$\frac{da}{dN} = \frac{C\ (\Delta K - \Delta K_{th})^m}{(1-R)\ (K_c - K_{max})} \tag{2.46}$$

Being that SIF (K) are only applicable for Linear-elastic Fracture Mechanics (LEFM), Begley and Dowling generalized the previous concept by replacing the stress intensity factor range by the J-Integral.

$$\frac{da}{dN} = C\ \Delta J^m \tag{2.47}$$

Identical the Paris Law, the last equation can only be used to accurately describe region II, not considering the stress ratio effect.

All the previous models consider constant amplitude loading, due to this fact, when variable amplitude loading is considered, Wheeler's model should be used to simulate the retardation effect on crack propagation.

Elber included the crack closure effect to the previous works of Paris, replacing stress intensity range, ΔK ,with effective stress intensity range, ΔK_{eff}.

2.5.1. Crack Propagation Models (Pure Mode I and Mixed-Mode)

The is always an uncertainty when it comes to service loading conditions, for this reason, it is cautionary to study fatigue crack propagation under a variety of loading conditions, covering pure mode and mixed mode alike.

Several authors have already covered this aspect in literature, what follows is but a brief content of their findings.

With aims to use Paris Law for loading conditions other than pure modes, it is necessary to arrive at an equivalent stress intensity range, this value can be obtained through the Huber-Mises for proportional loading:

$$\Delta K_{eq} = \sqrt{\Delta K_I^2 + 3\Delta K_{II}^2} \tag{2.48}$$

$$\Delta K_{eq} = \sqrt{\Delta K_I^2 + 3\Delta K_{III}^2} \tag{2.49}$$

The respective ΔK for each of the loading modes, is possible to calculate by using Richard's solution but only valid for slant cracks and a range of $0.5 \leq a/W \leq 0.7$ [39].

$$K_I = \frac{F\sqrt{\pi a}\ cos\theta}{Wt(1-a/W)} \sqrt{\frac{0.26 + 2.65(a/W - a)}{1 + 0.55(a/W - a) - 0.08(a/W - a)^2}} \tag{2.50}$$

$$K_{II} = \frac{F\sqrt{\pi a}\,cos\theta}{Wt(1-a/W)}\sqrt{\frac{-0.23+1.4(a/W-a)}{1+0.67(a/W-a)-2.08(a/W-a)^2}} \tag{2.51}$$

where, *F* is the applied load, *a* is the crack length, *W* is the specimen width, *t* is the specimen thickness and α describes the loading angle

According to Song and his co-authors the SIFs formula for K_I and K_{II} in CTS specimen is extended to a range $0.3 \leq a/W \leq 0.5$ in general form [39].

$$K_I = \frac{F\sqrt{\pi a}\cos(\alpha)\sqrt{\cos\left(\frac{\alpha}{3}\right)}}{Wt} f_I\left(\frac{a}{W}\right) \tag{2.52}$$

$$K_I = \frac{F\sqrt{\pi a}\sin(\alpha)}{Wt} f_{II}\left(\frac{a}{W}\right) \tag{2.53}$$

For mixed mode I+III the stress intensity factor ranges are, respectively:

$$\Delta K_I = Y_1 \Delta\sigma\, cos^2\alpha\sqrt{\pi(a_0+a)} \tag{2.54}$$

$$\Delta K_{III} = Y_3 \Delta\sigma sin\alpha\, cos\alpha\sqrt{\pi(a_0+a)} \tag{2.55}$$

where a_0 is the notch length. Stated by Harris Chell and Girvan the correction coefficients are:

$$Y_1 = \frac{5}{\sqrt{20-13\left(\frac{a_0+a}{w}\right)-7\left(\frac{a_0+a}{w}\right)^2}} \tag{2.56}$$

$$Y_3 = \sqrt{\left(\frac{\frac{2w}{a_0+a}}{w}\right)-7\left(\frac{a_0+a}{w}\right)^2} \tag{2.57}$$

2.5.2. Crack Closure Effects

Due to the work of Elber, which defended the notion that crack faces come into contact before the minimum stress value is ever reached, the load cycle is only effective for as long as the crack tip remains open [9], otherwise fatigue crack propagation would be overestimated.

$$U = \frac{\Delta K_{eff}}{\Delta K} = \frac{K_{max}-K_{op}}{K_{max}-K_{min}} \tag{2.58}$$

With K_{op}, being the stress intensity factor below which the crack remains closed and so there is no propagation.

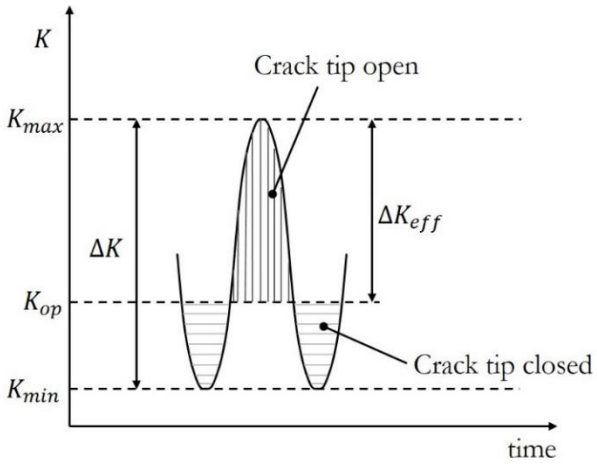

Figure 2.10 – Crack closure effect on stress intensity range [35].

By adjusting Paris Law to include crack closure effect we are left with:

$$\frac{da}{dN} = f\left(\Delta K_{eff}\right) \rightarrow \frac{da}{dN} = C\left(\Delta K_{eff}\right)^m = C(U\Delta K)^m \tag{2.59}$$

Using Aluminium alloys, Elber also found a relation between the percentage of the loading cycle that contributes to crack propagation (U), and the stress ratio, R.

$$U = 0.5 + 0.4R \tag{2.60}$$

Other authors have compiled different U-functions for both aluminium alloys and steels (see Table 2.2).

Table 2.2 – Different U-functions for crack closure [40]

U	Validity	Source	Comments
0.5*R*+0.4	0.1<*R*<0.7	(Elber, 1971)	Al-alloys, >3x10^{-9}m/cycle
0.75+0.25*R*	n/a	(Maddox et al., 1978)	steels
$U = 0.7 + 0.15R(2 + R)$	0<*R*<0.4	(Kumar and Singh, 1995)	steels >2xEner10^{-9}m/cycle
$U = 0.6684 - 2.4135\,R + 7.0077R^2$	0<*R*<0.5	(Singh et al., 2007)	steels, >1x10^{-10}m/cycle
$U = \left(1 - \frac{\Delta K_{th,0}}{K_{max}}\right)(1-R)^{\gamma-1}\ for\ K_{max} \leq K_L$ $U = 1\ for\ K_{max} \geq K_L$	n/a	(Correia et al., 2016)	steels

2.5.3. Studies into Crack Propagation in Structural Steels in Air and Marine environment

Until this point, a theoretical overview of fatigue and Fracture Mechanics were presented regardless of its applicability to the subject at hand. From this moment forward the aim of this document will shift more to its pertinence regarding offshore structures.

Some authors have dabbled into characterizing the fatigue crack propagation for structural steels in both air and marine environment. Adedipe and his co-authors, in their paper of review of corrosion fatigue in offshore structures, have presented the need for understanding the behaviour of the newer types of material and welding techniques, which may prove to be of significant influence in fatigue crack growth behaviour of these materials for both types of environments [41].

From the literature review, the existing experimental studies conducted in air and marine environment for crack propagation characterization are limited. Adedipe [41,42] and British standards, BS4360 and BS7910, present material constants for applying the fatigue crack propagation laws, though it may be limited.

BS4360 standard developed in the 70's and 80's provides data for medium strength steels, even though in large amounts of data. These structural steels are falling in disuse for offshore since newer grades of steel with improved properties due to improvement in fabrication techniques.

Adedipe [42] simulated the cyclic loading at constant amplitude in laboratory where marine environment simulation was the main goal. The marine environment was prepared according to the ASTM D1141 specifications and was circulated along the fully immerged specimens during their loading [42].

In the previous research work, the degree of magnitude of the initial crack needed for crack propagation wasn´t mentioned. The International Institute of Welding (IIW) has suggested a pre-crack at least 0.15mm from the weld toe, reducing the notch stresses [30].

Adedipe simulated the fatigue crack growth in seawater under different loading conditions and different types of detection instruments for stress R-ratios of 0.1, 0.5 and 0.7. Additionally, Adedipe also realized fatigue crack growth tests in weld material as in heat affected zone (HAZ).

In Figure 2.11 is showed the comparison between the base material, HAZ and the weld material for both sea and air environments, and design curves provided by BS7910 standard and should be pointed out that that some of the values obtained with experimental tests supersede the design lines provided by the BS7910 standard.

Other works was developed in the aim of European research fund for coal and steel under the name FATHOMS, where S460 and S355 steels under a stress R-ratio of 0.1 and 0.7 for air environment are also tested and fatigue crack propagation curves are obtained [43].

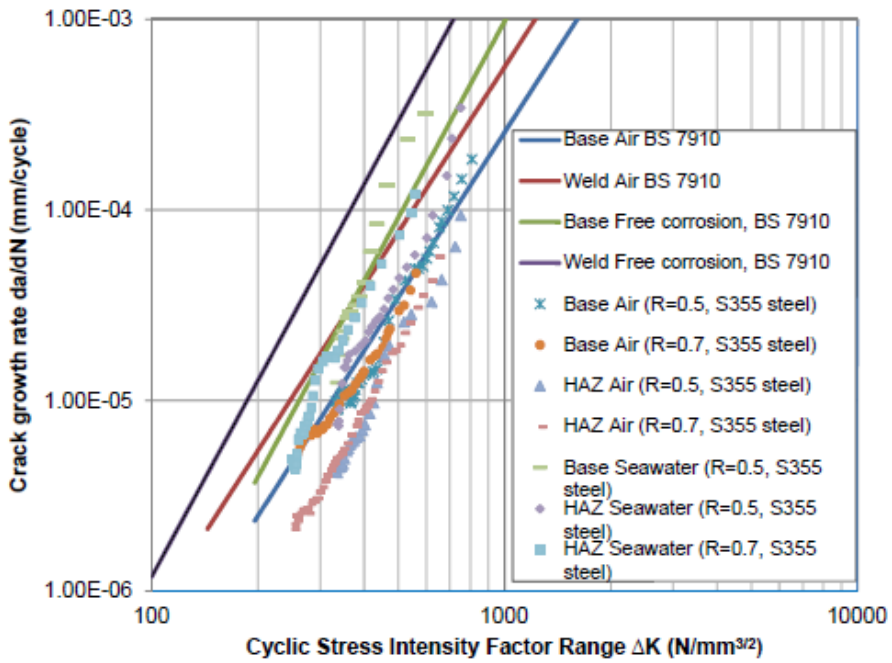

Figure 2.11 – Comparison of base material and HAZ data with BS7910 for sea and air environment [40].

2.6. FATIGUE SIMPLIFIED APPROACHES IN OFFSHORE STRUCTURES

There are several design codes that approach the subject of fatigue, some better suited than other.

Eurocode 3:1-9 presents a simplified fatigue approach based on Palmgren-Miner rule and global S-N curves.

Advanced design codes such as DNV-GL, provide several ways for the fatigue damage analysis in structures. One of them, simplified fatigue analysis based on Palmgren-Miner rule using the global S-N curves and a two-parameters Weibull distribution for the stresses. Another approach is based on global S-N curves and traditional fatigue damage.

Another simplified approach is based on S-N data, this approach assumes linear cumulative damage by Miner's rule. When the stress range is described in relation to a number of events, where damage can be obtained simply by the sum of the multiplication of each stress level raised to a parameter m, related to the inverse slope of the S-N curve either 3 or 5, and multiplied by the number of events for each stress level. This multiplication must be divided by a constant a, which is the interception of the design curve with the log N axis.

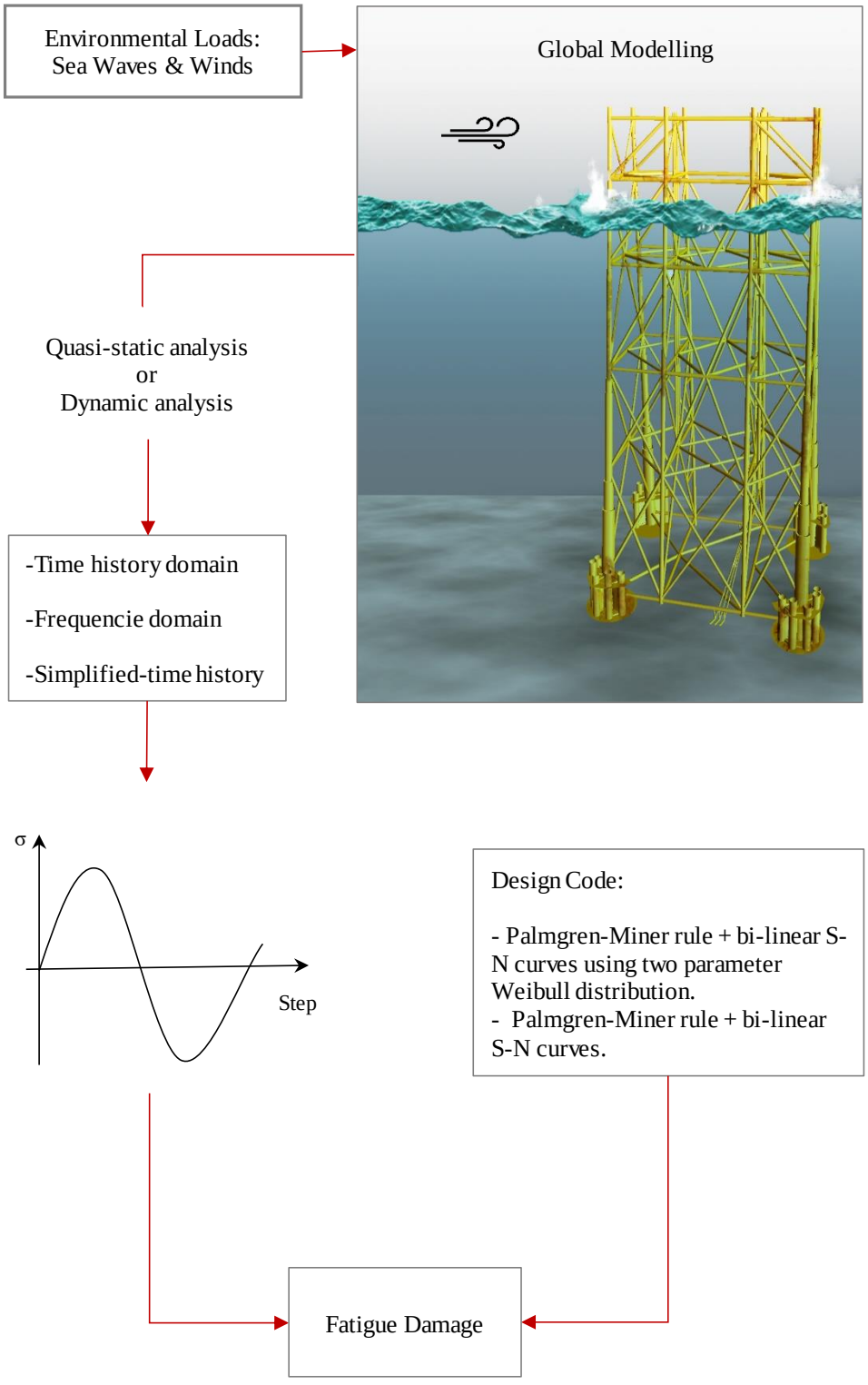

Figure 2.12 –Workflow for the fatigue damage analysis according to DNV-GL.

2.7. FATIGUE EVALUATION BASED ON FRACTURE MECHANICS APPROACHES

A third approach, empiric, is based on fracture mechanics. By integrating the Paris law present in Eq. (2.42), resulting in Eq. (2.43), the fatigue residual life prediction for the propagation phase can be performed, resulting in a number of cycles from initial (a_i) and final crack sizes (a_f).

In the Figure 2.13, a stable crack growth can be found for the majority of the total fatigue life for the propagation phase, however as the crack reaches a certain point in time, crack growth becomes unstable coinciding with the third region of crack propagation leading to collapse.

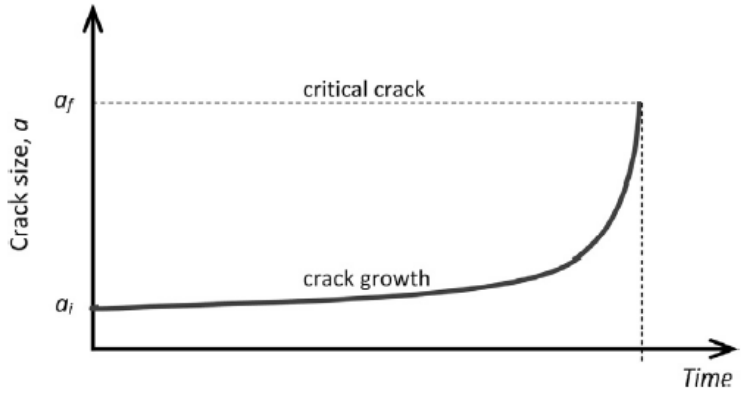

Figure 2.13 – Crack size vs time

The characteristic crack propagation rate curve like the one present in Fig. 2.9 for the material is commonly compared with the design crack propagation curve in BS7910 standard [44], allowing an evaluation of the fatigue residual life.

2.8. FATIGUE ADVANCED APPROACHES IN OFFSHORE STRUCTURES

More advanced approaches can be taken to evaluated fatigue damage and fatigue life, by using for example a local multiaxial approach for instance.

Multiaxial fatigue assessment can be done using several criteria, stress, strain and energy.

A multiaxial fatigue analysis can be done using critical plane orientation using two parameters failure criterion for combined bending and torsion [44]. In this case specifically, both damage criterion are stresses, normal and shear stresses.

$$D_\sigma^i = \frac{1}{N_f} = \frac{1}{N_\sigma} \left(\frac{\sigma_{n,a}}{\sigma_{af}}\right)^{m_\sigma} \tag{2.61}$$

$$D_\tau^i = \frac{1}{N_f} = \frac{1}{N_\tau} \left(\frac{\sigma_{ns,a}}{\sigma_{af}}\right)^{m_\tau} \tag{2.62}$$

In reality, fatigue crack opening and propagation occurs under multiaxial conditions since structures undergo bending both in and out of plane.

S-N curves describe the number of cycles to failure under a single parameter, this way by using the properly selected parameter normal or shear stress on the critical plane, damage is obtained for each of the Eqs. (2.61) and (2.62) and the one that provides the maximum accumulated damage determines the critical plane orientation and fatigue life [44].

2.9. Typical Fatigue Analysis in Offshore Structures Case Studies

Khedmati [45] and his co-authors have performed an assessment of fatigue reliability for a Jacket structure. SACS software was used to simulate the fatigue behaviour as well as stress levels and the platform was evaluated considering wave, sea current, marine growth and soil-structure interaction.

For this analysis, the dynamic behaviour of the offshore structure was considered, and a joint was analysed at 8 different locations of the structure, fatigue damage and so fatigue life was obtained for each of the locations presenting the critical location for the joint with a fatigue life of just over 17 years, the analysis was made using a stress-based approach.

It is also pointed out that several of the parameters used in the analysis like stress concentration factors and interaction with soil play a significant importance, altering the results.

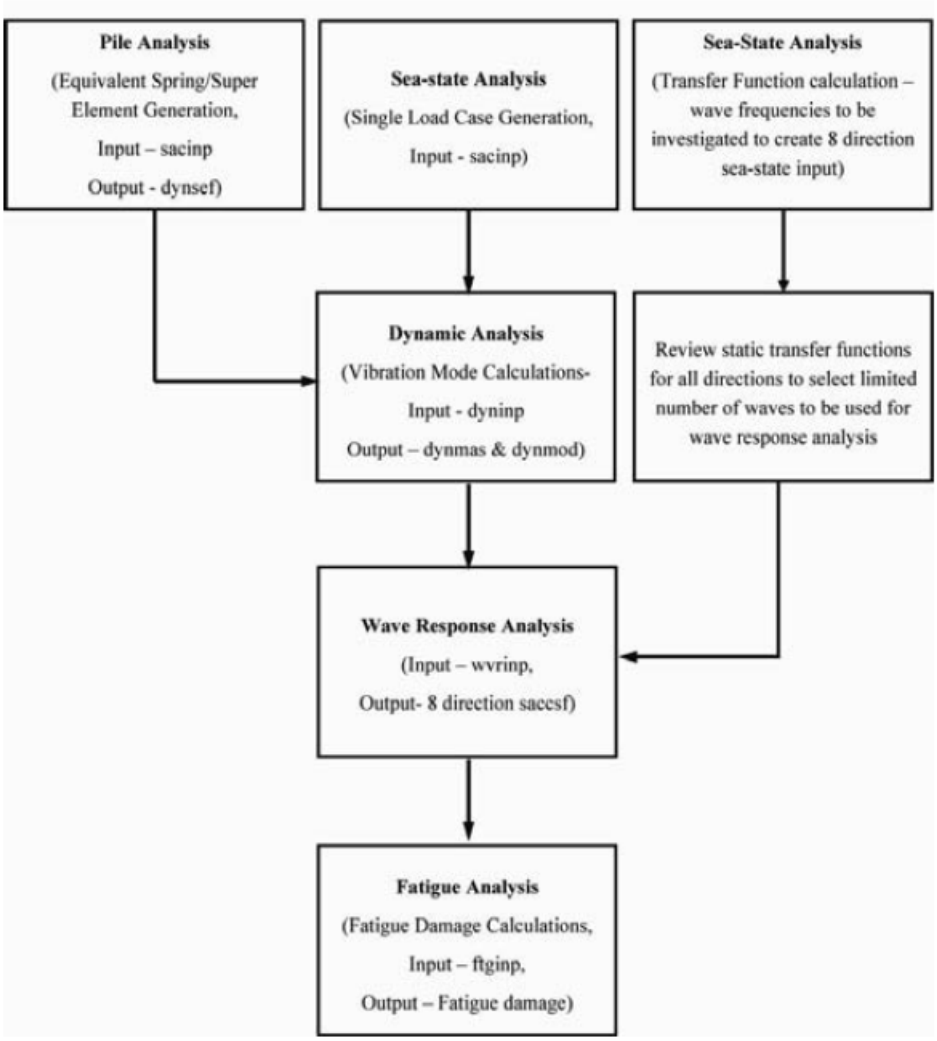

Figure 2.14 – Fluxgram of the steps taken to assess fatigue damage [44].

In another case [46], a fatigue assessment is done to an existing platform in Suez Gulf, Egypt. For this analysis, wave scatter diagrams with increments of 45° are used to characterize the waves resulting in a total of 8 wave directions.

In this paper, a simplified approach based on S-N curve is done.

3
Loads and Structural Response

3.1. REVIEW ON HYDRODYNAMIC ANALYSIS AND SERVICE LOADS

During service life, the offshore structures will undergo a significant number of loads some of which non-linear in nature [47]. These loads can be sorted into one of four categories just like any other structure [48]:

- Permanent Loads
- Live Loads
- Deformation loads
- Environmental loads

The first, related to the weight of the platform itself that remains constant throughout its life, hydrostatic pressure and equipment that like the dead-weight of the structure must persist permanent.

Unlike the previous, live loads result of the direct use of the offshore platform, drilling and pumping operations, cranes, boats, helicopters, and the storage of supplies which are not fixed in time and may be moved.

For deformation loads, these relate to the deformation caused by prestressing and temperature both uniform and differential.

For last, environmental loads, as the name stats, imply all those related to natural causes, such as the wind, waves, ties, ice, earthquakes and others.

Due to the location of the structure, its functionality and the overall aggressiveness of the surrounding environment, the last category will show to be the most unfavourable to the life of the structure. This way, fatigue damage, and therefore, fatigue life, must be obtained with these kind of loading conditions in mind.

For fatigue analysis of the Jacket, wind loads will be ignored since the fatigue damage due to wind is insignificant when compared to the one caused by sea loads. This can be easily understandable since almost the entire structural components are submerged.

3.2. WAVE MEASUREMENT

With aims to simulated and posteriorly achieve the structural response to a certain wave, it is necessary to first determined the waves characteristics, this can be obtained by means of a scatter diagram, which correlates wave periods with wave height, and the number of occurrences for a combination of the two.

Wave measurements can be obtained by using recorders kept either at the surface of below it, from these, the wave rider buoy is the most widely used. For the scatter diagram in Table 3.2 a recording of one year was made in the same circumstances as stated before.

The scatter diagram presented below is valid for the location of the offshore structure presented in chapter 4 and assumes the directions in accordance with the alignment of the structure, being that the same as a small rotation of 5° East to the actual North.

The scatter diagram presented in Table 3.2 corresponds to the sum of the total number of occurrences for a total of 12 directions, from 0° to 360° with increments of 30°.

In the sea-compass presented below in Figure 3.1 it is possible to visualise the probability of the wave in accordance to each direction to the conclusion that the direction 270 and 240 present the highest chances for wave occurrences, in Table 3.1 the accurate percentage is displayed.

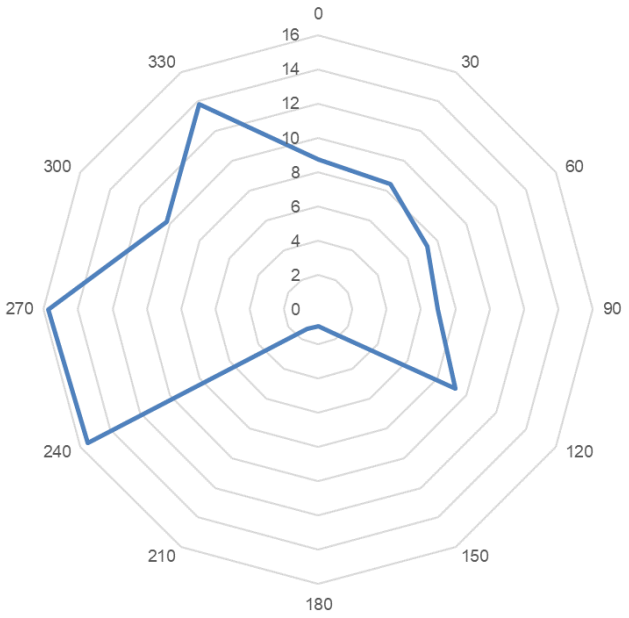

Figure 3.1 – Probability of wave occurrence in a certain direction

Table 3.1 – Probability of wave occurrence in a certain direction

Wave Direction	0	30	60	90	120	150	180	210	240	270	300	330
Probability	8.77	8.44	7.37	7	9.26	1.54	0.96	1.31	15.54	15.76	10.21	13.85

Also, by analysing the scatter diagram below and with the conclusions arrived above regarding the directionality of the wave, it is possible to conclude that most of the waves will be situated in the 0-3 meters height and with a general direction of West.

Since this is the case it is possible to summarize the total of 28 wave heights into only those most relevant to the analysis, this way, mean height and mean period were obtained for the same scatter diagram presented before, where for each interval of wave height the average value was obtained and then multiplied by the number of occurrences for each of the wave period intervals. The same procedure can be extrapolated for the mean period making possible the analysis of 14 waves for every direction instead of 784 waves (28 wave heights for 28 period intervals).

These 14 can be further simplified by pairing waves, resulting in the waves presented in Tables 3.6 to 3.10 instead of the larger number of waves considered in the scatter diagram from Table 3.2. It should also be pointed out that the number of occurrences corresponds to only one year of data.

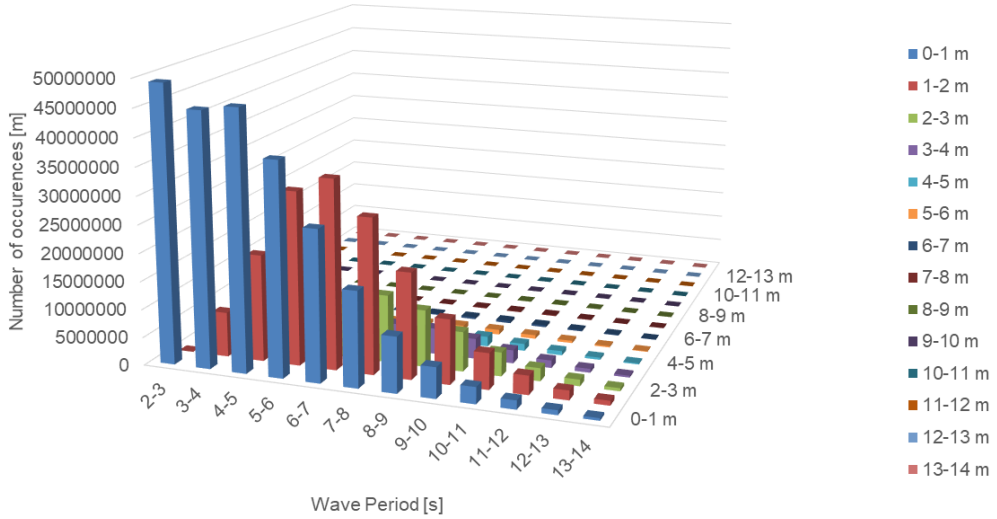

Figure 3.2 – Wave data scatter for the sum of all directions.

	Wave Period (T) - (s)																														
H(m)	2-3	3-4	4-5	5-6	6-7	7-8	8-9	9-10	10-11	11-12	12-13	13-14	14-15	15-16	16-17	17-18	18-19	19-20	20-21	21-22	22-23	23-24	24-25	25-26	26-27	27-28	28-29	29-30	Sum	%	Mean Period
0-1	49231004	45076011	46032294	37804371	26801916	16978883	9916471	5508726	2981834	1592154	842636	443428	232797	122335	64523	34162	18072	9483	4907	2495	1241	601	281	126	54	22	9	4	**243700840**	48.15	4.96
1-2	0	7978447	19033161	30895415	33660781	27625328	18854691	11500942	6456381	3402393	1717259	843972	408379	195946	93698	44751	21276	9974	4562	2024	869	362	146	57	22	8	3	1	**162750848**	32.16	6.95
2-3	0	534297	2625134	6944881	11006331	12048327	10163127	7078418	4269835	2327087	1176703	559347	252713	109832	46440	19258	7832	3101	1191	445	163	58	20	7	2	1	0	0	**59174550**	11.69	7.91
3-4	0	0	404907	1528824	3353192	4650718	4633396	3614650	2359663	1354796	703599	337143	151406	64297	25973	10033	3713	1312	441	142	44	13	4	1	0	0	0	0	**23198267**	4.58	8.55
4-5	0	0	0	363953	941995	1676224	2004043	1776046	1256938	751617	396180	190466	85368	36141	14581	5632	2083	735	248	80	25	7	2	1	0	0	0	0	**9502365**	1.88	9.07
5-6	0	0	0	67437	259010	595074	858742	869289	670298	419476	224396	107067	47046	19520	7785	3014	1137	417	149	51	17	6	2	1	0	0	0	0	**4149934**	0.82	9.49
6-7	0	0	0	12714	69265	205070	359329	418731	355044	235099	128835	61329	26409	10644	4123	1564	588	219	81	30	11	4	1	0	0	0	0	0	**1889090**	0.37	9.86
7-8	0	0	0	0	20212	68553	146587	197858	189872	131386	74495	35762	15231	5989	2247	826	302	111	41	15	6	2	1	0	0	0	0	0	**885496**	0.17	10.19
8-9	0	0	0	0	4931	22301	58252	91486	95849	72891	43148	21099	8976	3475	1271	453	161	57	21	8	3	1	0	0	0	0	0	0	**424383**	0.08	10.49
9-10	0	0	0	0	0	8237	22537	41362	48618	40056	24949	12533	5373	2065	742	258	89	31	11	4	1	1	0	0	0	0	0	0	**206867**	0.04	10.77
10-11	0	0	0	0	0	2451	8503	18298	24252	21779	14369	7468	3251	1250	445	152	51	17	6	2	1	0	0	0	0	0	0	0	**102295**	0.02	11.03
11-12	0	0	0	0	0	718	3134	7929	11899	11708	8230	4454	1981	767	272	91	30	10	3	1	0	0	0	0	0	0	0	0	**51227**	0.01	11.27
12-13	0	0	0	0	0	0	1337	3369	5744	6220	4682	2652	1212	475	169	56	18	6	2	1	0	0	0	0	0	0	0	0	**25943**	0.01	11.52
13-14	0	0	0	0	0	0	458	1405	2730	3265	2643	1575	743	297	106	35	11	4	1	0	0	0	0	0	0	0	0	0	**13273**	0.00	11.74
14-15	0	0	0	0	0	0	155	576	1278	1694	1480	931	456	186	67	22	7	2	1	0	0	0	0	0	0	0	0	0	**6855**	0.00	11.95
15-16	0	0	0	0	0	0	52	233	590	868	822	548	279	117	43	14	5	1	0	0	0	0	0	0	0	0	0	0	**3572**	0.00	12.16
16-17	0	0	0	0	0	0	0	110	269	440	452	321	171	74	27	9	3	1	0	0	0	0	0	0	0	0	0	0	**1877**	0.00	12.37
17-18	0	0	0	0	0	0	0	42	121	220	247	186	104	46	18	6	2	1	0	0	0	0	0	0	0	0	0	0	**993**	0.00	12.57
18-19	0	0	0	0	0	0	0	16	54	109	133	108	63	29	11	4	1	0	0	0	0	0	0	0	0	0	0	0	**528**	0.00	12.74
19-20	0	0	0	0	0	0	0	6	24	54	71	62	38	18	7	3	1	0	0	0	0	0	0	0	0	0	0	0	**284**	0.00	12.93
20-21	0	0	0	0	0	0	0	0	12	26	38	35	23	11	5	2	1	0	0	0	0	0	0	0	0	0	0	0	**153**	0.00	13.15
21-22	0	0	0	0	0	0	0	0	5	13	20	20	14	7	3	1	0	0	0	0	0	0	0	0	0	0	0	0	**83**	0.00	13.26
22-23	0	0	0	0	0	0	0	0	2	6	10	11	8	4	2	1	0	0	0	0	0	0	0	0	0	0	0	0	**44**	0.00	13.45
23-24	0	0	0	0	0	0	0	0	1	3	5	6	5	3	1	0	0	0	0	0	0	0	0	0	0	0	0	0	**24**	0.00	13.50
24-25	0	0	0	0	0	0	0	0	0	2	3	3	3	2	1	0	0	0	0	0	0	0	0	0	0	0	0	0	**14**	0.00	13.71
25-26	0	0	0	0	0	0	0	0	0	1	1	2	2	1	0	0	0	0	0	0	0	0	0	0	0	0	0	0	**7**	0.00	13.64
26-27	0	0	0	0	0	0	0	0	0	0	1	1	1	1	0	0	0	0	0	0	0	0	0	0	0	0	0	0	**4**	0.00	14.00
27-28	0	0	0	0	0	0	0	0	0	0	0	1	1	0	0	0	0	0	0	0	0	0	0	0	0	0	0	0	**2**	0.00	14.00
Sum	**49231004**	**53588755**	**68095496**	**77617595**	**76117633**	**63881884**	**47030814**	**31129492**	**18727313**	**10373363**	**5365407**	**2630530**	**1242053**	**573532**	**262560**	**120347**	**55383**	**25482**	**11665**	**5298**	**2381**	**1055**	**457**	**193**	**78**	**31**	**12**	**5**	**506088818**		
%	9.73	10.59	13.46	15.34	15.04	12.62	9.29	6.15	3.70	2.05	1.06	0.52	0.25	0.11	0.05	0.02	0.01	0.01	0.00	0.00	0.00	0.00	0.00	0.00	0.00	0.00	0.00	0.00			
Mean Height	0.50	0.67	0.87	1.16	1.44	1.71	1.98	2.21	2.40	2.53	2.57	2.55	2.45	2.32	2.15	1.97	1.79	1.62	1.46	1.32	1.20	1.10	1.00	0.93	0.83	0.82	0.75	0.70			

Table 3.2 – Scatter diagram of the total number of occurrences for all directions

Table 3.3 – Simplified wave characteristics in every direction from 1 to 40

Wave number	Wave direction [degrees]	Wave height [m]	Wave period [s]	Number of waves during 1 year
1	0	1	3.58	356458
2	0	3	6.2	72241
3	0	4.5	7.6	8334
4	0	5.5	8.4	3639
5	0	6.5	9.13	1657
6	0	7.5	9.81	776
7	0	9	10.74	554
8	0	14	13.4	181
9	30	1	3.58	343045
10	30	3	6.2	69523
11	30	4.5	7.6	8020
12	30	5.5	8.4	3502
13	30	6.5	9.13	1595
14	30	7.5	9.81	747
15	30	9	10.74	533
16	30	14	13.4	174
17	60	1	3.58	299555
18	60	3	6.2	60709
19	60	4.5	7.6	7003
20	60	5.5	8.4	3058
21	60	6.5	9.13	1393
22	60	7.5	9.81	652
23	60	9	10.74	466
24	60	14	13.4	151
25	90	1	3.58	284516
26	90	3	6.2	57661
27	90	4.5	7.6	6652
28	90	5.5	8.4	2905
29	90	6.5	9.13	1322
30	90	7.5	9.81	620
31	90	9	10.74	442
32	90	14	13.4	144
33	120	1	3.58	376374
34	120	3	6.2	76277
35	120	4.5	7.6	8800
36	120	5.5	8.4	3843
37	120	6.5	9.13	1749
38	120	7.5	9.81	820
39	120	9	10.74	584
40	120	14	13.4	191

Table 3.4 – Simplified characteristics in every direction from 41 to 80.

Wave number	Wave direction [degrees]	Wave height [m]	Wave period [s]	Number of waves during 1 year
41	150	1	3.58	62594
42	150	3	6.2	12685
43	150	4.5	7.6	1463
44	150	5.5	8.4	639
45	150	6.5	9.13	291
46	150	7.5	9.81	137
47	150	9	10.74	97
48	150	13	12.91	31
49	180	1	3.58	39019
50	180	3	6.2	7908
51	180	4.5	7.6	912
52	180	5.5	8.4	399
53	180	6.5	9.13	181
54	180	7.5	9.81	85
55	180	9	10.74	61
56	180	12.5	12.66	19
57	210	1	3.58	53245
58	210	3	6.2	10791
59	210	4.5	7.6	1245
60	210	5.5	8.4	543
61	210	6.5	9.13	248
62	210	7.5	9.81	116
63	210	9	10.74	83
64	210	12.5	12.66	26
65	240	1	3.58	631626
66	240	3	6.2	128007
67	240	4.5	7.6	14767
68	240	5.5	8.4	6449
69	240	6.5	9.13	2936
70	240	7.5	9.81	1376
71	240	9	10.74	981
72	240	14.5	13.63	321
73	270	1	3.58	640568
74	270	3	6.2	129819
75	270	4.5	7.6	14976
76	270	5.5	8.4	6540
77	270	6.5	9.13	2978
78	270	7.5	9.81	1395
79	270	9	10.74	995
80	270	14.5	13.63	326

Table 3.5 – Simplified wave characteristics in every direction from 81 to 96.

Wave number	Wave direction [degrees]	Wave height [m]	Wave period [s]	Number of waves during 1 year
81	300	1	3.58	414987
82	300	3	6.2	84103
83	300	4.5	7.6	9702
84	300	5.5	8.4	4237
85	300	6.5	9.13	1929
86	300	7.5	9.81	904
87	300	9	10.74	644
88	300	14.5	13.63	211
89	330	1	3.58	562936
90	330	3	6.2	114086
91	330	4.5	7.6	13161
92	330	5.5	8.4	5747
93	330	6.5	9.13	2617
94	330	7.5	9.81	1226
95	330	9	10.74	874
96	330	14.5	13.63	287

Table 3.6 –Wave characteristic in every direction from 1 to 16.

Wave number	Wave direction [degrees]	Wave height [m]	Wave period [s]	Number of waves during 1 year
1	0	1	4.96	213726
2	0	2	6.95	142732
3	0	3	7.91	51896
4	0	4	8.55	20345
5	0	5	9.07	8334
6	0	6	9.49	3639
7	0	7	9.86	1657
8	0	8	10.19	777
9	0	9	10.49	372
10	0	10	10.77	181
11	0	11	11.03	90
12	0	12	11.27	45
13	0	13	11.52	23
14	0	14	11.74	12
15	30	1	4.96	205684
16	30	2	6.95	137362

Table 3.7 – Wave characteristics in every direction from 17 to 57.

Wave number	Wave direction [degrees]	Wave height [m]	Wave period [s]	Number of waves during 1 year
17	30	3	7.91	49943
18	30	4	8.55	19579
19	30	5	9.07	8020
20	30	6	9.49	3503
21	30	7	9.86	1594
22	30	8	10.19	747
23	30	9	10.49	358
24	30	10	10.77	175
25	30	11	11.03	86
26	30	12	11.27	43
27	30	13	11.52	22
28	30	14	11.74	11
29	60	1	4.96	179608
30	60	2	6.95	119947
31	60	3	7.91	43612
32	60	4	8.55	17097
33	60	5	9.07	7003
34	60	6	9.49	3059
35	60	7	9.86	1392
36	60	8	10.19	653
37	60	9	10.49	313
38	60	10	10.77	152
39	60	11	11.03	75
40	60	12	11.27	38
41	60	13	11.52	19
42	60	14	11.74	10
43	90	1	4.96	170591
44	90	2	6.95	113926
45	90	3	7.91	41422
46	90	4	8.55	16239
47	90	5	9.07	6652
48	90	6	9.49	2905
49	90	7	9.86	1322
50	90	8	10.19	620
51	90	9	10.49	297
52	90	10	10.77	145
53	90	11	11.03	72
54	90	12	11.27	36
55	90	13	11.52	18
56	90	14	11.74	9
57	120	1	4.96	225667

Table 3.8 – Wave characteristics in every direction from 58 to 98.

Wave number	Wave direction [degrees]	Wave height [m]	Wave period [s]	Number of waves during 1 year
58	120	2	6.95	150707
59	120	3	7.91	54796
60	120	4	8.55	21482
61	120	5	9.07	8799
62	120	6	9.49	3843
63	120	7	9.86	1749
64	120	8	10.19	820
65	120	9	10.49	393
66	120	10	10.77	192
67	120	11	11.03	95
68	120	12	11.27	47
69	120	13	11.52	24
70	120	14	11.74	12
71	150	1	4.96	37530
72	150	2	6.95	25064
73	150	3	7.91	9113
74	150	4	8.55	3573
75	150	5	9.07	1463
76	150	6	9.49	639
77	150	7	9.86	291
78	150	8	10.19	136
79	150	9	10.49	65
80	150	10	10.77	32
81	150	11	11.03	16
82	150	12	11.27	8
83	150	13	11.52	4
84	150	14	11.74	2
85	180	1	4.96	23395
86	180	2	6.95	15624
87	180	3	7.91	5681
88	180	4	8.55	2227
89	180	5	9.07	912
90	180	6	9.49	398
91	180	7	9.86	181
92	180	8	10.19	85
93	180	9	10.49	41
94	180	10	10.77	20
95	180	11	11.03	10
96	180	12	11.27	5
97	180	13	11.52	2
98	180	14	11.74	1

Table 3.9 – Wave characteristics in every direction from 99 to 138.

Wave number	Wave direction [degrees]	Wave height [m]	Wave period [s]	Number of waves during 1 year
99	210	1	4.96	31925
100	210	2	6.95	21320
101	210	3	7.91	7752
102	210	4	8.55	3039
103	210	5	9.07	1245
104	210	6	9.49	544
105	210	7	9.86	247
106	210	8	10.19	116
107	210	9	10.49	56
108	210	10	10.77	27
109	210	11	11.03	13
110	210	12	11.27	7
111	210	13	11.52	3
112	210	14	11.74	2
113	240	1	4.96	378711
114	240	2	6.95	252915
115	240	3	7.91	91957
116	240	4	8.55	36050
117	240	5	9.07	14767
118	240	6	9.49	6449
119	240	7	9.86	2936
120	240	8	10.19	1376
121	240	9	10.49	659
122	240	10	10.77	321
123	240	11	11.03	159
124	240	12	11.27	80
125	240	13	11.52	40
126	240	14	11.74	21
127	270	1	4.96	384073
128	270	2	6.95	256495
129	270	3	7.91	93259
130	270	4	8.55	36560
131	270	5	9.07	14976
132	270	6	9.49	6540
133	270	7	9.86	2977
134	270	8	10.19	1396
135	270	9	10.49	669
136	270	10	10.77	326
137	270	11	11.03	161
138	270	12	11.27	81

Table 3.10 – Wave characteristics in every direction from 139 to 168.

Wave number	Wave direction [degrees]	Wave height [m]	Wave period [s]	Number of waves during 1 year
139	270	13	11.52	41
140	270	14	11.74	21
141	300	1	4.96	248819
142	300	2	6.95	166169
143	300	3	7.91	60417
144	300	4	8.55	23685
145	300	5	9.07	9702
146	300	6	9.49	4237
147	300	7	9.86	1929
148	300	8	10.19	904
149	300	9	10.49	433
150	300	10	10.77	211
151	300	11	11.03	104
152	300	12	11.27	52
153	300	13	11.52	26
154	300	14	11.74	14
155	330	1	4.96	337526
156	330	2	6.95	225410
157	330	3	7.91	81957
158	330	4	8.55	32130
159	330	5	9.07	13161
160	330	6	9.49	5748
161	330	7	9.86	2616
162	330	8	10.19	1226
163	330	9	10.49	588
164	330	10	10.77	287
165	330	11	11.03	142
166	330	12	11.27	71
167	330	13	11.52	36
168	330	14	11.74	18

The reduction from 14, which result in all the waves with a probability of occurrence higher than 0.01% from the scatter diagram in Table 3.2, to 8 waves per direction, result of pairing, may not represent a significant number of wave reduction, however since the wave simulation and structural analysis are made for 24-time steps for each wave, it represents a total reduction of about 43% from 4032 load cases to 2304, reducing significantly the computing time required.

It is relevance to point out that even though Tables 3.6 to 3.10 represents the mean period obtained for each of the corresponding wave heights, in Tables 3.3 to 3.5 the wave periods were obtained using a condition presented in Norsok standard N003 [49] for regular waves:

$$15H_s < \lambda < 25H_s$$

From this interval a middle term (λ=20H) can be used to achieve the wave period that correlates to an exact wave height by using the next formula.

$$\lambda = \frac{g}{2\pi} * T^2 \leftrightarrow T = \sqrt{\frac{\lambda * 2\pi}{g}} \leftrightarrow T = \sqrt{12.8H} \quad (3.1)$$

If the wave heights are fixed as the ones presented in Tables 3.3 to 3.5, then the respective wave periods fall into the limits imposed by the standard.

From this point forward, wave height considered in calculations will be the maximum wave height, $H_{max,}$ which can be taken as 1.86 times the significant wave height H_s, which is presented in Tables 3.3 to 3.5.

3.3. LINEAR WAVE THEORY

When dealing with problems connected with waves, lengthy calculations involving wave characteristics are frequently used [50], so to overcome this problem, mathematical theories were developed to expedite the calculations required.

Even though all wave theories are based on the common assumptions that waves present regular profiles, with a two-dimensional flow, unidirectional propagation involving an impermeable, horizontal sea bed plus an idyllic fluid, inviscid, irrotational and incompressible, same theories are better suited for some conditions than others [51].

One of the theories for example, was developed by Airy, linear in nature and accurate for waves of small heights and infinite water depths [50]. In the light of these limitations, Stokes presented his own theory.

Several theories exist on the subject, and non-linear theories such as Stokes achieve a significant degree of accuracy over the linear theories for cases where the wave amplitude is not small, this way in the figure below it is possible to determine the theory that best suits the case in question, giving several ranges of applicability of various waves correlating the ratio of wave height to the period of the same wave square times the gravitational acceleration and a similar ratio were water depth is used instead.

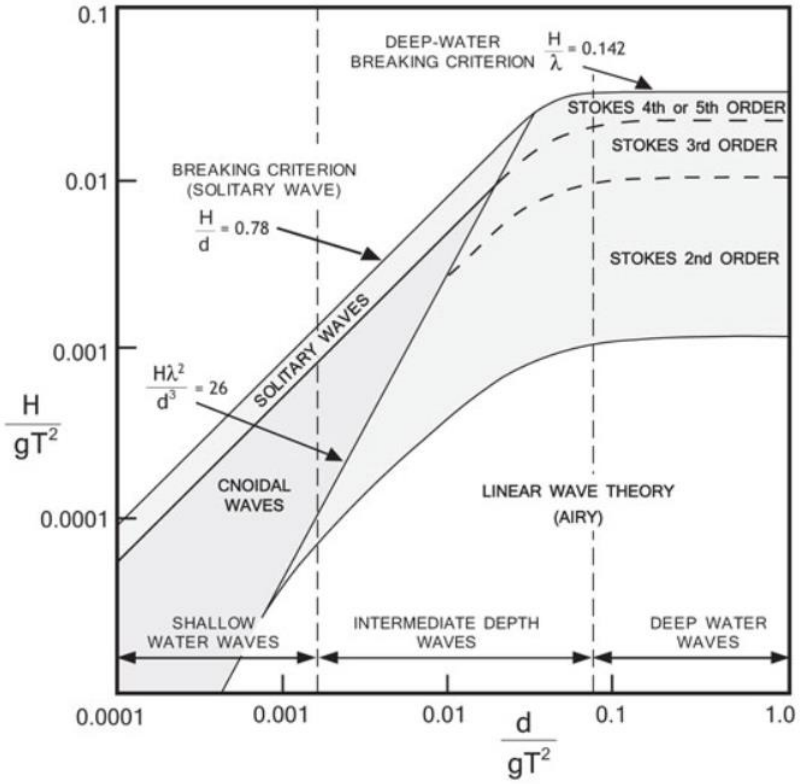

Figure 3.3 – Range of applicability of several wave theories [52].

Table 3.11 – Theory applicability for the waves considered in the case study

Wave number	$\frac{H}{gT^2}$	$\frac{d}{gT^2}$	Theory
1	0.00795362	0.92397225	Stokes 2nd order
2	0.00795553	0.3107163	Stokes 2nd order
3	0.00794175	0.2081092	Stokes 2nd order
4	0.00794575	0.1710793	Stokes 2nd order
5	0.00794882	0.14542676	Stokes 2nd order
6	0.00794427	0.12649403	Stokes 2nd order
7	0.00795362	0.10619853	Stokes 2nd order
8	0.00794785	0.06964016	Stokes 2nd / 3rd order

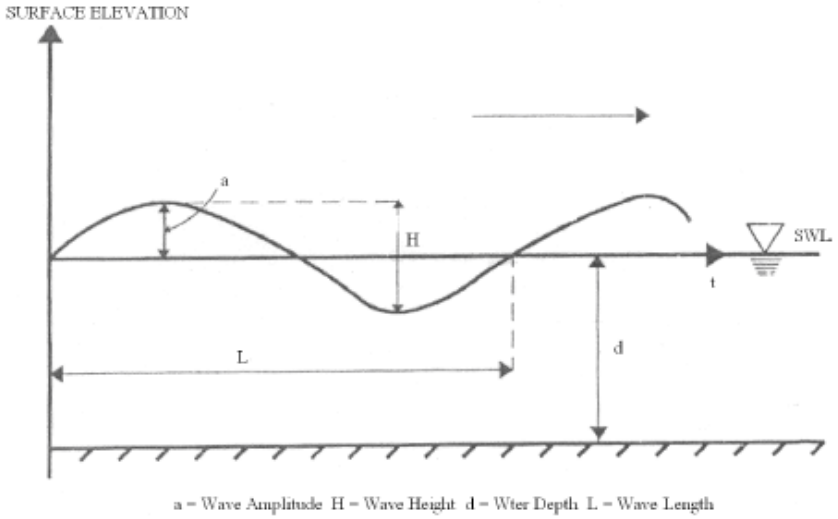

Figure 3.4 – Wave characteristics definition [51].

It is also significant to mention that even though, the wave theories applicability according to the intervals displayed in Table 3.12, as referenced in [53], linear wave theory is possible of being applied, this is because those conditions do not reflect the change in the wave period, which as mentioned before was obtained from Eq. (3.1).

Regardless of any incongruities between which range fits best the waves in question, Airy for both finite and infinite water depth will be studied as well as Stokes 5th Order theory, for it covers all the ranges in figure 3.3 serving as a basis for validating the results.

Table 3.12 - The applicable conditions of wave theory [53]

Condition	Wave theory
$\frac{d}{L} \geq 0.2; \frac{H}{L} \leq 0.2$	Airy wave theory
$0.1 < \frac{d}{L} < 0.2; \frac{H}{L} \geq 0.2$	Stokes wave theory
$0.04 \sim 0.05 < \frac{d}{L} < 0.1$	Conical wave theory; Solitary wave theory

3.3.1. LINEAR WAVE THEORY FOR FINITE WATER DEPTH

Also referred to as small amplitude wave theory, sinusoidal wave theory or just simply Airy theory, this theory assumes the wave height to be significantly inferior to both wave length and water depth.

Since this is a sinusoidal wave, the equation governing the wave can be written as:

$$\xi(x,t) = \xi_a * \sin(\omega t - kx) \tag{3.2}$$

ξ_a - wave amplitude, also referred to in Fig.3.4 as "a";

ω – wave frequency

t – instant in time

k – wave number

x – position of the wave

From this equation the wave profile can be plotted for both time and space [54]. Or a more simplistic equation can be used by fixing x, allowing the representation of a time record of the wave profile, observed at a location along the flume [55].

$$\xi(x,t) = \xi_a * \sin(\omega t) \tag{3.3}$$

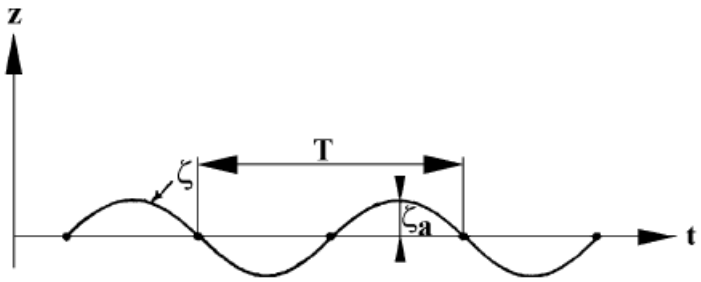

Figure 3.5 – Generic time history wave profile representation

To achieve the waves acceleration and velocity a potential function is required to mathematically express space and time variables, valid for the entire fluid [55]. It has been thought that the derivative of this function in a given direction provides the velocity in that direction, this way the velocity potential (Φ) may be related to the velocity considering the fluid to be irrotational [56].

$$u = \frac{\partial \Phi}{\partial x}\ ; v = \frac{\partial \Phi}{\partial y}\ ; w = \frac{\partial \Phi}{\partial z} \tag{3.4}$$

If the canal is assumed invariable alongside the *y*-axis then the velocity component in that very same direction can be taken as zero [56].

Since the fluid is assumed to be incompressible the following can be said,

$$\frac{\partial u}{\partial x}+\frac{\partial v}{\partial y}+\frac{\partial w}{\partial z}=0 \tag{3.5}$$

This results in Laplace´s equation,

$$\frac{\partial u}{\partial x}+\frac{\partial w}{\partial z}=0 \leftrightarrow \frac{\partial^2 \Phi}{\partial x^2}+\frac{\partial^2 \Phi}{\partial z^2}=0 \tag{3.6}$$

In [57], a method of solving these equations is presented, considering the problems boundary conditions, resulting in the velocity potential presented below, first solved by Airy in 1841.

The velocity potential can be also written as a function of the depth, P(z) [55].

$$\Phi(x,z,t)=P(z)*\cos(wt-kx) \tag{3.7}$$

Which for waves of finite depth, results in the following:

$$\Phi=\frac{g\xi_a}{\omega}\frac{\cosh(k(z+d))}{\cosh(kd)}\cos(wt-kx) \tag{3.8}$$

3.3.2. Linear wave theory for Infinite water depth

Since the velocity potential is directly connected to the water depth, where for a large water depth, $d \rightarrow \infty$, the expression for both velocity potential and dispersion relation given by Eq. (3.9), becomes reduced as presented in Eq. (3.10) and Eq. (3.11) [55].

$$\omega^2=k*g*tanhkd \tag{3.9}$$

$$\omega^2=k*g \tag{3.10}$$

$$\Phi=\frac{g\xi_a}{\omega}*\ e^{kz}*\cos(wt-kx) \tag{3.11}$$

3.3.3. LINEAR WAVE THEORY – SUMMARY

By resorting to differentiation of the velocity potential for both finite and infinite, it can be found in the next table the wave profile, dynamic pressure and the components of both velocity and acceleration for the *x* and *z* directions.

Table 3.13 – Linear wave theory kinematics summary [47].

	Finite water depth	**Infinite water depth**
Velocity potential	$\Phi = \frac{g\xi_a}{\omega}\frac{\cosh(k(z+d))}{\cosh(kd)}\cos(wt-kx)$	$\Phi = \frac{g\xi_a}{\omega}e^{kz}\cos(wt-kx)$
Connection between wave number, k, and wave frequency, w	$\omega^2 = kgtanhkd$	$\omega^2 = kg$
Connection between wave length, λ, abd wave period, T	$\lambda = \frac{g}{2\pi}T^2 tanh\frac{2\pi}{\lambda}d$	$\lambda = \frac{g}{2\pi}T^2$
Wave profile	$\xi = \xi_a * \sin(\omega t - kx)$	$\xi = \xi_a * \sin(\omega t - kx)$
Dynamic pressure	$p_D = \rho g\xi_a\frac{\cosh(k(z+d))}{\cosh(kd)}sin(wt-kx)$	$p_D = \rho g\xi_a e^{kz}\ sin(wt-kx)$
x - component of velocity	$u = \omega\xi_a\frac{\cosh(k(z+d))}{\sinh(kd)}sin(wt-kx)$	$u = \omega\xi_a e^{kz}\ sin(wt-kx)$
z-component of velocity	$w = \omega\xi_a\frac{\sinh(k(z+d))}{\sinh(kd)}cos(wt-kx)$	$w = \omega\xi_a e^{kz}\ cos(wt-kx)$
x-component of acceleration	$\dot{u} = \omega\xi_a\frac{\cosh(k(z+d))}{\sinh(kd)}cos(wt-kx)$	$\dot{u} = \omega\xi_a e^{kz}\ cos(wt-kx)$
z-component of acceleration	$\dot{w} = \omega\xi_a\frac{\sinh(k(z+d))}{\sinh(kd)}sin(wt-kx)$	$\dot{w} = \omega\xi_a e^{kz}\ sin(wt-kx)$

3.4. STOKES WAVE THEORY

Unlike Airy's theory, Stokes is non-linear and assumes that all variations in the *x* direction can be represented with the use of Fourier's series where the coefficients can be written as perturbation parameters (*a*,*b*) which increase with wave height [58].

Since Fourier's series is a trigonometric series used to represent infinite and periodic functions, it is nothing else than the sum of sine or cosines, this way the resulting velocity potential and wave profile are depicted in Eqs (3.12) and (3.13) respectively.

$$\Phi = \sum_{n=1}^{M} b^n \Phi_n(H,T,d)\sin(n\theta) \tag{3.12}$$

$$\xi = \sum_{n=1}^{M} a^n f_n(H,T,d)\cos(n\theta) \tag{3.13}$$

Depending of the order pretend, in this case 5^{th} order, since it is the most complete and accurate when describing water particle kinematics, then there will be five *b* elements and five *a*.

The procedure to obtain wave profile, velocity and acceleration is as follows:

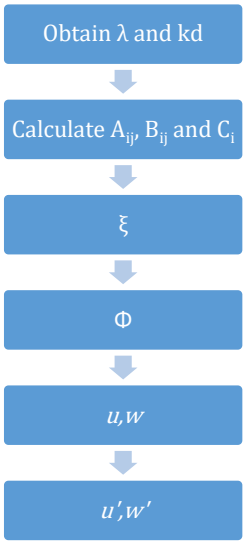

Using the values obtained from the wave scatter and summarized in Tables 3.3 to 3.5, it is possible to obtain λ and *kd* from the two expressions below [51].

$$\frac{1}{kd}[\,\lambda + B_{33}\lambda^2 + (B_{35} + B_{55})\lambda^5] = \frac{H}{2d} \tag{3.14}$$

$$kd \cdot tanh(kd)[1 + C_1\lambda^2 + C_2\lambda^4] = 4\pi^2 \frac{d}{gT^2} \tag{3.15}$$

Since both Eqs. (3.14) and (3.15) are co-dependent of the parameters B_{ij} and C_i, this is an indirect function, requiring iterations until the wanted level of tolerance is reached.

The wave profile formula depicted in Eq. (3.16) as said before, involves the sum of partial velocity profiles Φ_i', which in its turn is dependent of the parameters A_{ij} presented in Annex B.

Step 3 was also calculated using the parameters present in Annex B, alternatively the abacus present in [50], provide the values for all the A_{ij}, B_{ij},C_i parameters in relation to the d/L ratio, where L is the same as λ, wave length.

From here the following steps are a direct use of the formulas, making possible the representation of the wave profile, velocity and acceleration as in the previous cases.

$$\Phi = \frac{\overline{C}}{k}\sum_{n=1}^{5} \Phi_n' \cosh\big(nk(d+z)\big)\sin(n\theta) \tag{3.16}$$

$$\xi = \frac{1}{k}\sum_{n=1}^{5} \xi_n' \sinh\big(nk(d+z)\big)\cos(n\theta) \tag{3.17}$$

All partial parameter for both wave profile and velocity potential are in Annex B.

3.5. MORRISON FORMULA

Once the wave particle kinematics are obtained, it is necessary to transform those into a force capable of applying to the structure in question, for this purpose Morrison's load formula is applicable given that λ>5D [59] and can be calculated by using the equation present in topic 6.2.1, fixed structure in waves and current from the DNV recommended practice, environmental conditions and environmental loads.

$$f_N(t) = \rho(1 + C_A)A\dot{v} + \frac{1}{2}\rho C_D D v|v| \tag{3.19}$$

Where ρ is the mass density of the fluid in [kg/m3] and can be used as 1000. C_A and C_D are the added mass coefficient and drag coefficient respectively, A is the area of the cross section and D the diameter of the same cross section.

To access the added mass coefficient and drag coefficient recommended values were used based on [53], however these can be mathematically achieved as referenced in [59,60].

Both parameters depend on the Reynolds number, a dimensionless parameter dependent of flow velocity, Keulegan-Carpenter number, which depends on wave height and the surface roughness. In [59], tables are presented to facilitate the procurement of the previous.

3.6. APPLICATIONS AND RESULTS

3.6.1. Wave theories

From this point forward, the previous wave theories will be used for different conditions and the results presented.

3.6.1.1. Linear Wave Theory for Finite Water

Figure 3.6 portraits the wave profile using Eq. (3.3) for a fixed instant in time t=0, if *t* where to vary from the initial value zero than the wave profile would simply undergo a translation as seen in Fig. 3.7 where the instant chosen is half the period t=6.815 s. Should be highlighted that this wave profile is correspondent to any multiple wave of 8 (from Table 3.3 to 3.5), the reason for such a choice will be clear in Chapter 4.

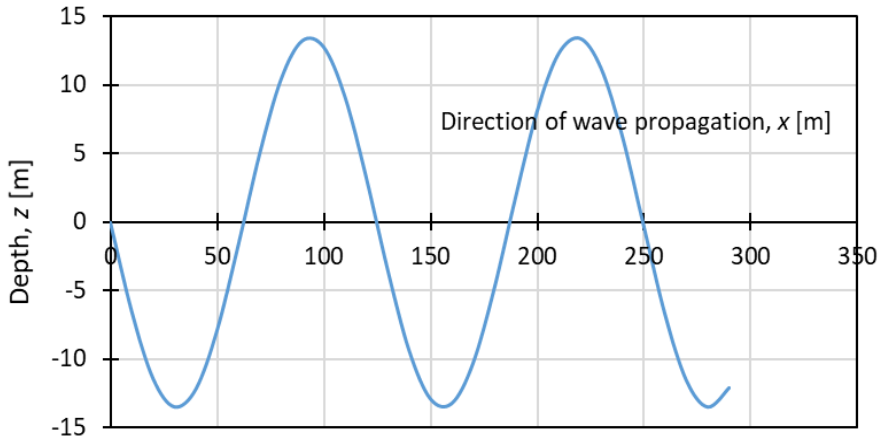

Figure 3.6 – Finite wave profile for instant t=0s.

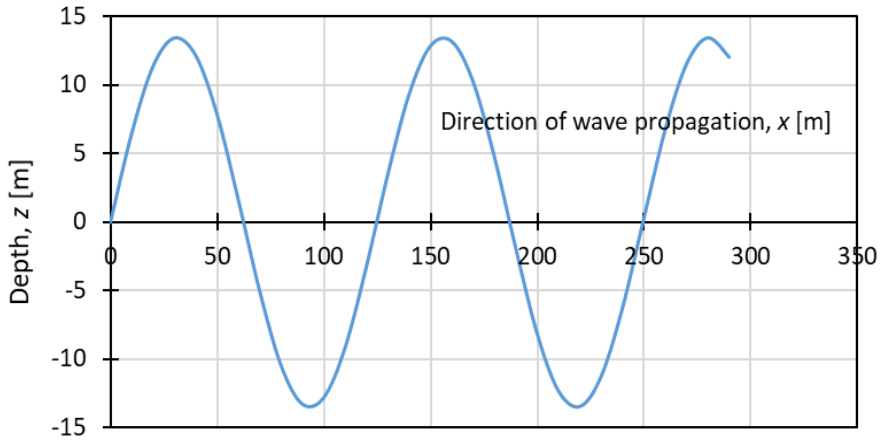

Figure 3.7 – Finite wave profile for instant t=*T*/2

With the velocity potential it is now possible through differentiation to achieve the kinematics characteristics of the wave, velocity, acceleration and pressure, to produce the velocity profile, a value for *x* and an instant *t*, should be fixed because only this way can velocity be charted as a function of *z*, with the same procedure to be extrapolated to the acceleration profile. As such the value of *x* was taken as the correspondent value to the maximum *z* in the wave profile.

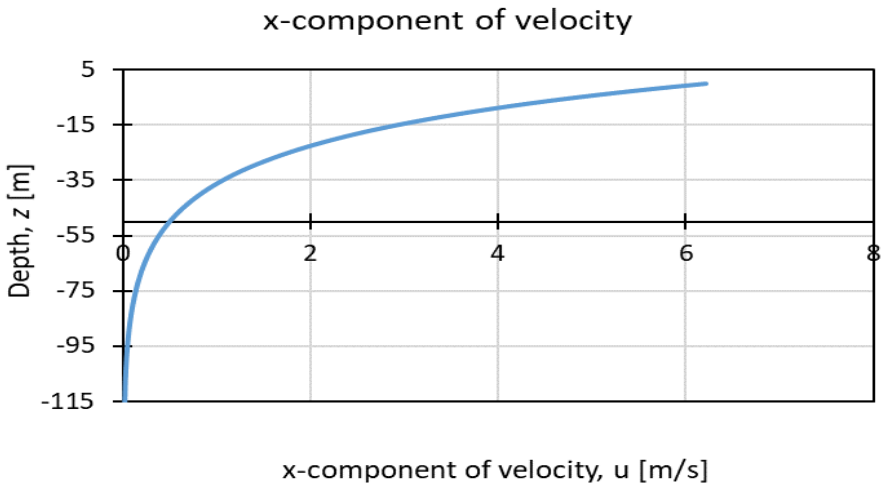

Figure 3.8 – Finite wave velocity profile for t=0s and x=93.6215m.

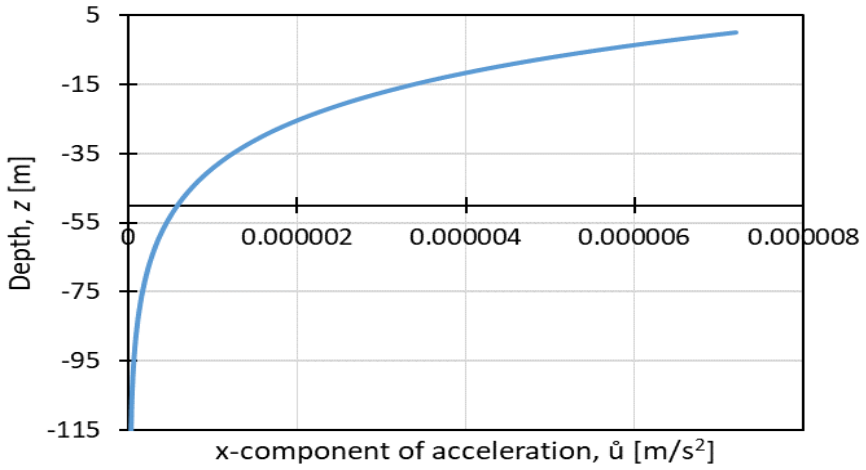

Figure 3.9 – Finite wave acceleration profile for t=0s and x=93.6215m.

As expected the higher the particle the highest the value of both velocity and acceleration.

If the *x*-component of the velocity is plotted for several instants in time instead just for t=0 as presented in Fig. 3.10 then a picture can be formed of the velocity of the wave in time.

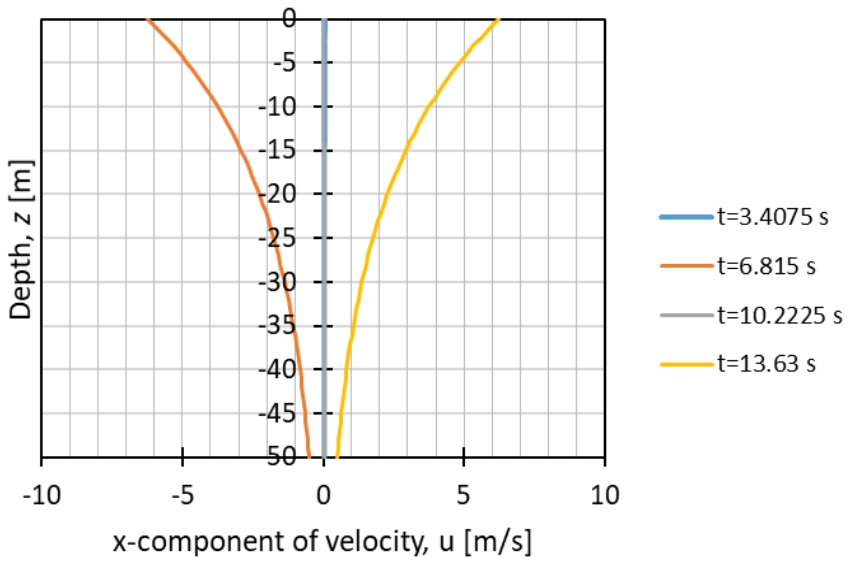

Figure 3.10 – Finite wave velocity profile for quarter intervals of *T*.

3.6.1.2. Linear Wave Theory for Infinite Water

With a coincident wave profile expression as the wave presented in Eq. (3.2) for finite cases, for infinite water depth the wave profile for both t=0 and t=T/2 are presented below in Figs. 3.11 and 3.12 and the velocity and acceleration profiles in Figs. 3.13 and 3.14, respectively.

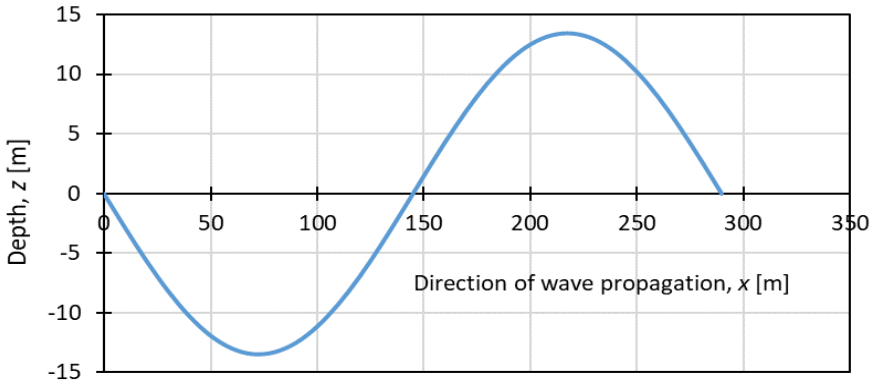

Figure 3.11 – Infinite wave profile for t=0s.

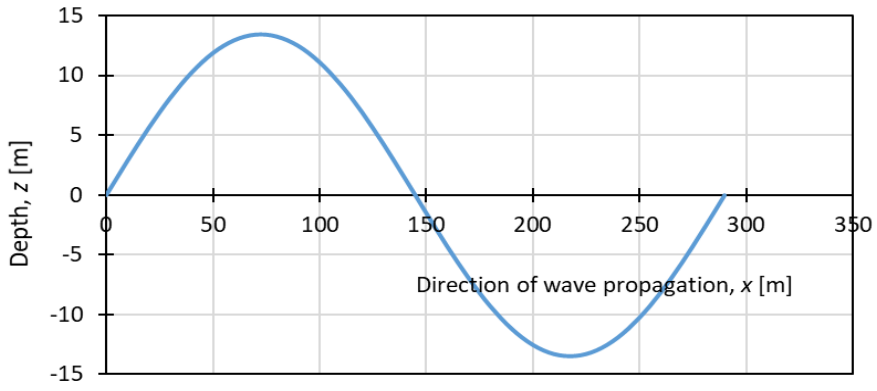

Figure 3.12 – Infinite wave profile for t=*T*/2.

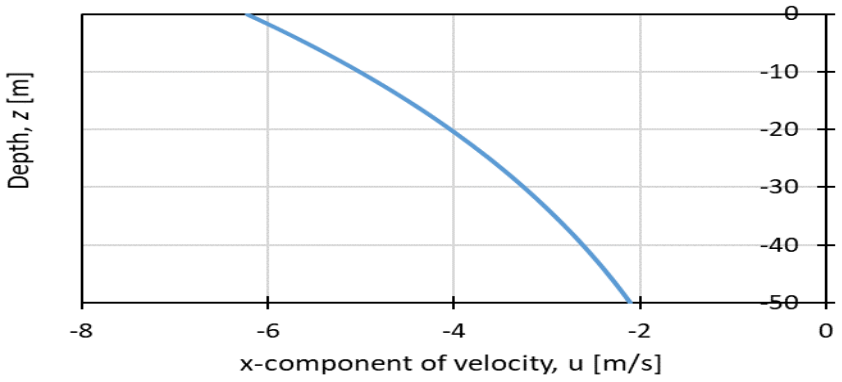

Figure 3.13 – Infinite wave velocity profile for t=0s and x=72.5m.

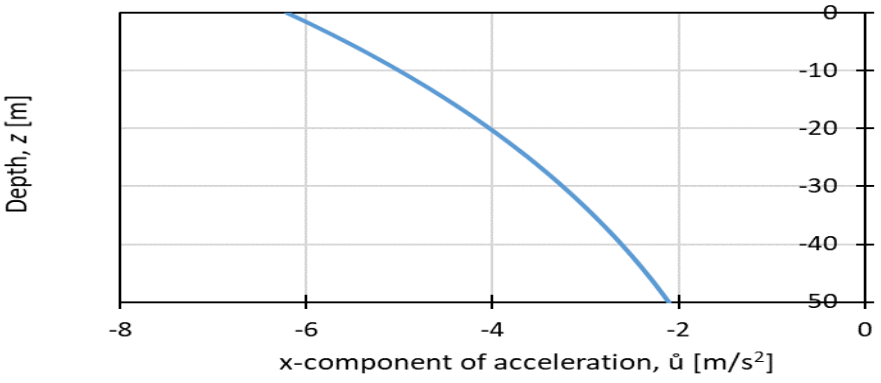

Figure 3.14 – Infinite wave acceleration profile for t=0s and x=72.5m.

If the x-component of the velocity is plotted for quarter intervals of the wave period, the wave velocity profile is as presented in Fig. 3.15 and so a time history representation of the wave velocity profile can be plotted.

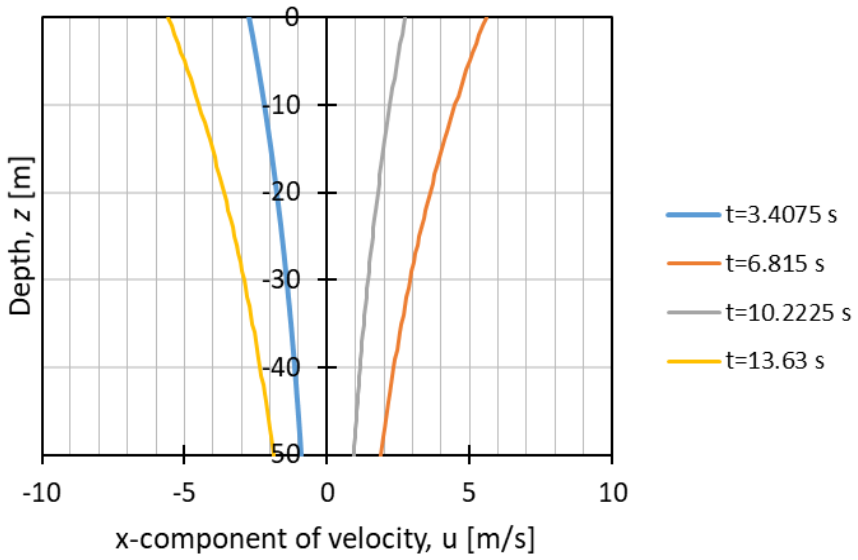

Figure 3.15 – Infinite wave velocity profile for quarter intervals of T

3.6.1.3. Stokes 5th Order Wave Theory

To solve Eqs. (3.14) and (3.15), a VBA routine was put together in excel to accomplish iterations until it reached a tolerance of 1.0E-06, safeguarding an accurate result.

In the previous examples of wave profile, a fixed instant in time was chosen, either zero or half the wave period. Since Stokes wave theory is non-linear, the wave profile can be plotted as both a relation of the direction in which the wave propagates or θ, which depends of both time and location, as presented in Figs. 3.16 to 3.19.

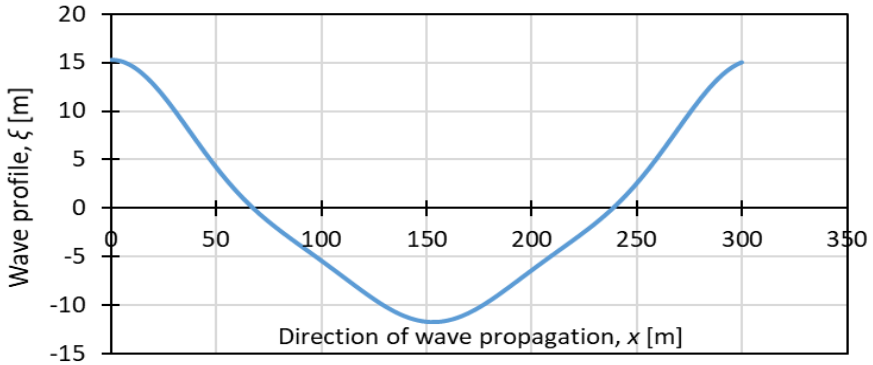

Figure 3.16 – Stokes 5th order wave profile for t=0 and varying *x*.

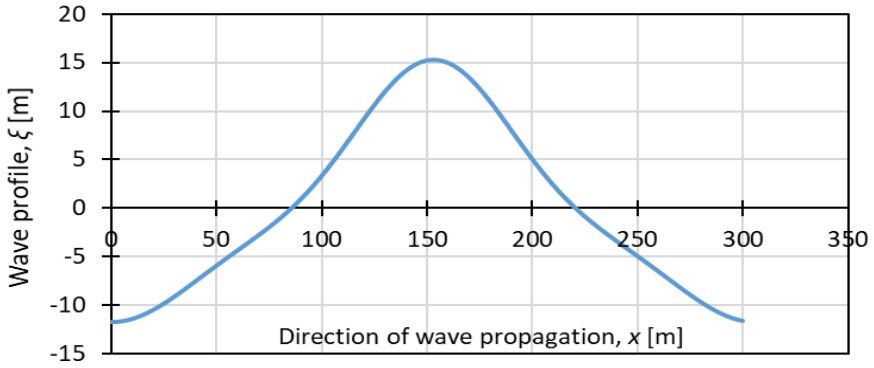

Figure 3.17 – Stokes 5th order wave profile for t=T/2 and varying *x*.

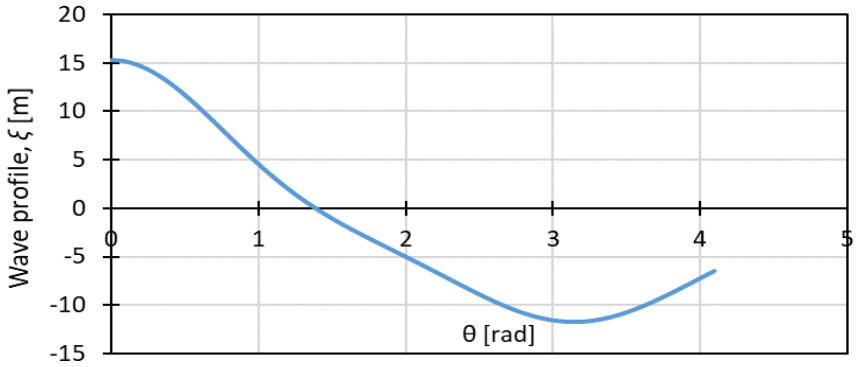

Figure 3.18 – Stokes 5th order wave profile for t=0s and varying *x*, plotted in relation to θ

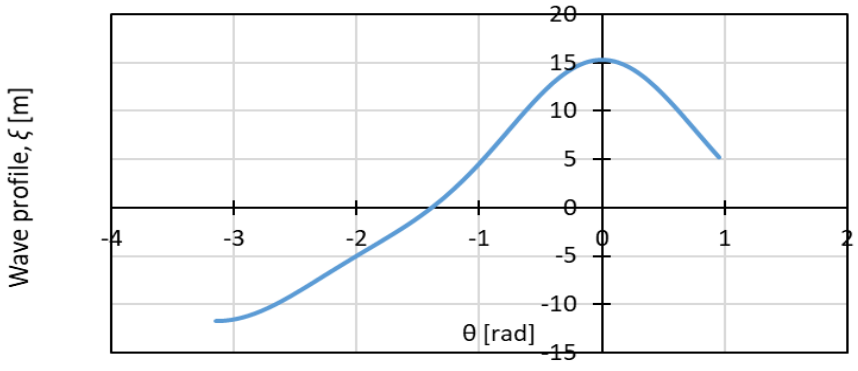

Figure 3.19 – Stokes 5th order wave profile for t=*T*/2s and varying *x*, plotted in relation to θ

If instead of fixing the instant in time, it also varied along with the incremental values of *x*, then the wave profile takes the form presented in Figs. 3.20 and 3.21, plotted in relation to both *x and* θ.

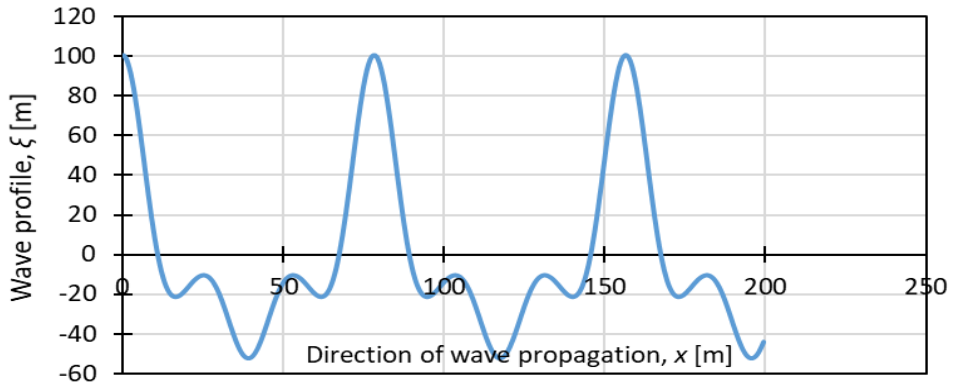

Figure 3.20 – Stokes 5th order wave profile for varying t and x, plotted in relation to the wave propagation direction.

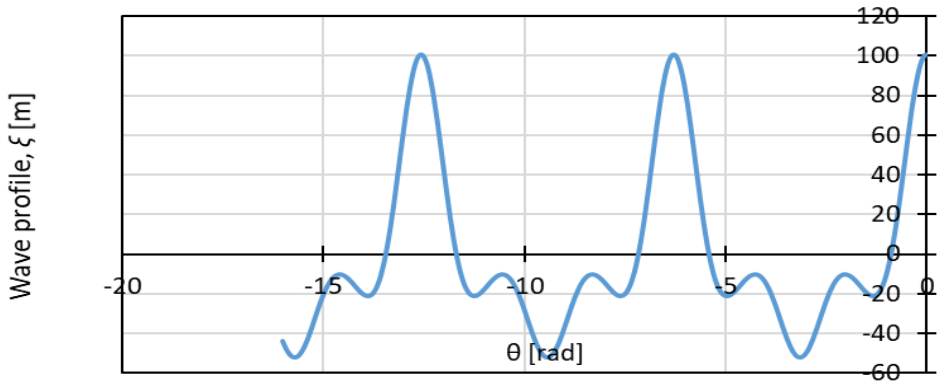

Figure 3.21 – Stokes 5th order wave profile for varying t and x, plotted in relation to θ

Since in Stokes 5th order theory, the velocity depends not only on the position x and time, like the previous theories but θ as well, which depends of both position and time, to plot the velocity profile a fixed value of time was established.

$$\theta = kx - wt \tag{3.18}$$

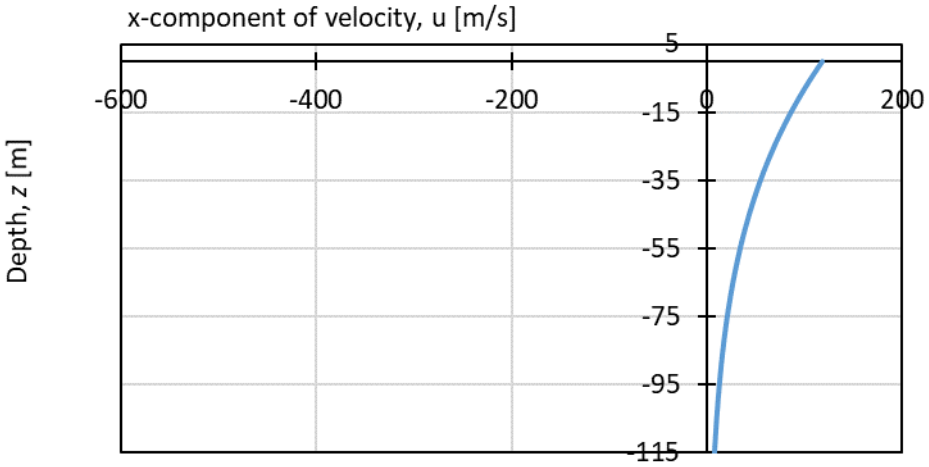

Figure 3.22 – Stokes 5th order velocity profile for t=0 and varying x.

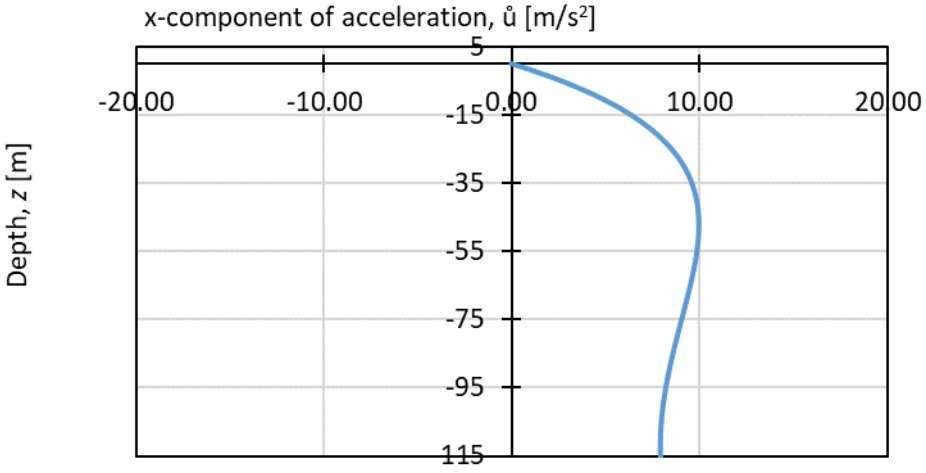

Figure 3.23 – Stokes 5th order acceleration profile for t=0 and varying x.

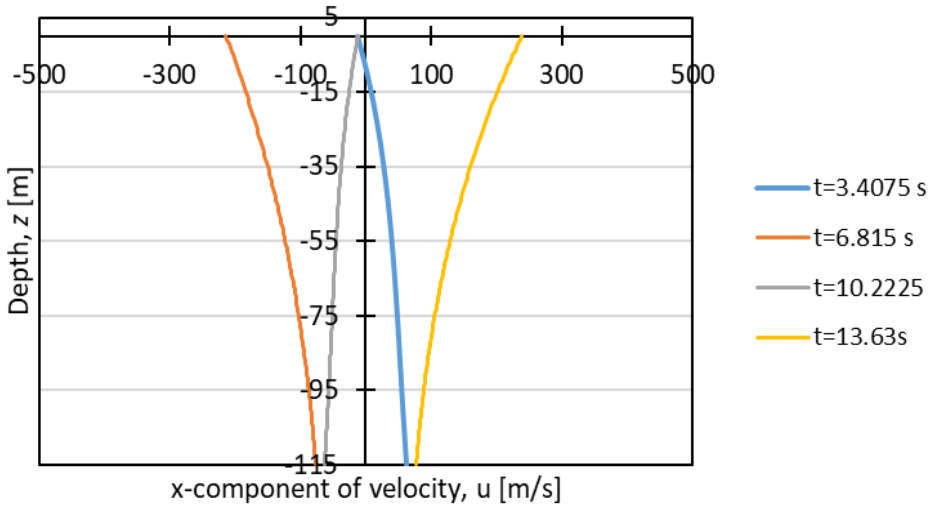

Figure 3.24 – Stokes 5th order velocity profile for quarter intervals of t and varying x.

3.6.2. Morrison Equivalent Forces

The values used for C_A *and* C_D were the following:

- From mudline (z=-115,67 m) to z=-6,3 m: $C_A = 2.2$ *and* $C_D = 0.88$
- From z=-6,3 m to z=0 m: $C_A = 2.0$ *and* $C_D = 0.80$
- Over z=0 m: $C_A = 2.0$ *and* $C_D = 0.65$

The values considered for marine growth were the following:

- From mudline to z=-42 m: 50 mm
- From z=-42 m to z=0 m:100 mm
- Above z=0 m: 0 mm

Since Stokes 5th Order provides a more accurate depiction of the real wave kinematics, the velocity and acceleration used in Morrison formula, v=u and $\dot{v} = \dot{u}$, in the *x*-direction, will result from that theorem.

In the image below, there is a 3D rendering of the critical joint in which this work will be based, more on the structure and its characteristics will be discussed in Chapter 4.

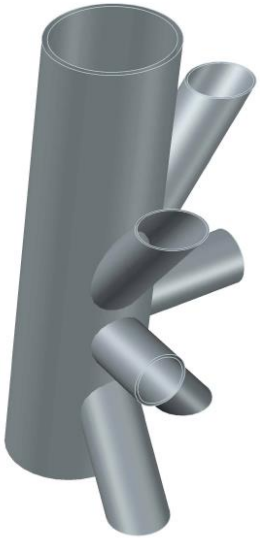

Figure 3.25 – Tubular critical kt-type joint

For simplification, since the Morrison load formula depends on both velocity, acceleration and time, which on its own also depends of the depth considered. The depth considered will be that of every bracing level of the structure to achieve a profile of the force, resulting in a uniform distributed load alongside de vertical element of the structure covering half the length of the main element downward of and another half upward.

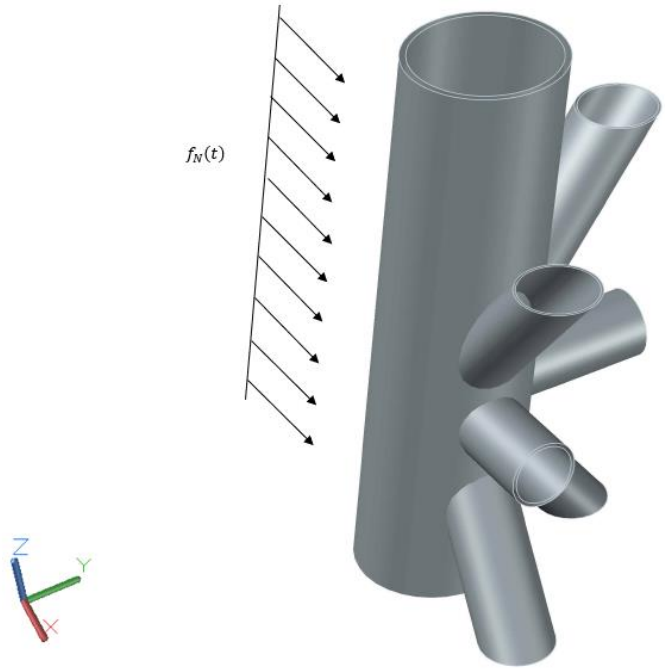

Figure 3.26 – Morrison normal force applied in the jacket-type structure

To achieve this, water depth (*z)* will be fixed but both time and *x* will vary. The time aspect of the mathematical formula will vary from zero to *T* until it reaches 13.63s, the period used will be the one of any multiple wave of 8 and *x* in increments of 0.5m.

Another assumption was made in the calculation of the Morrison normal load force, since the main element is composed of several pilings which vary in diameter with the depth, to arrive at the most accurate value the area and diameter should also change in depth.

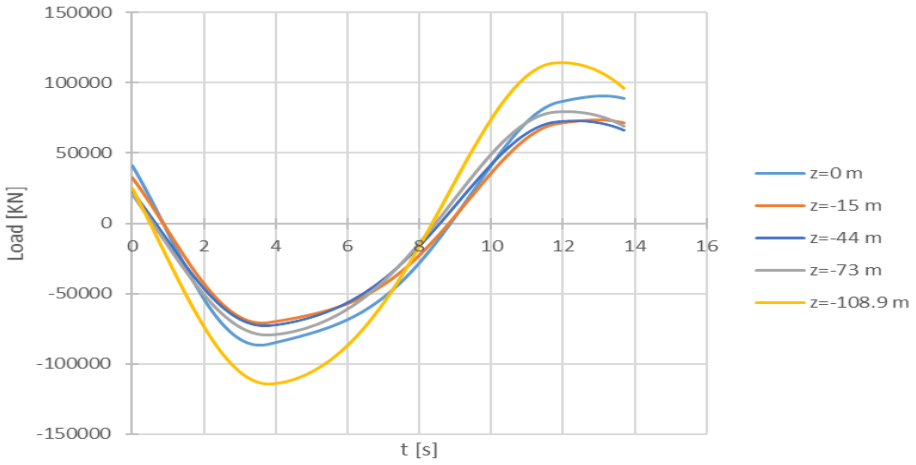

Figure 3.27 – Morrison load force according to Stokes 5th order for several water depths

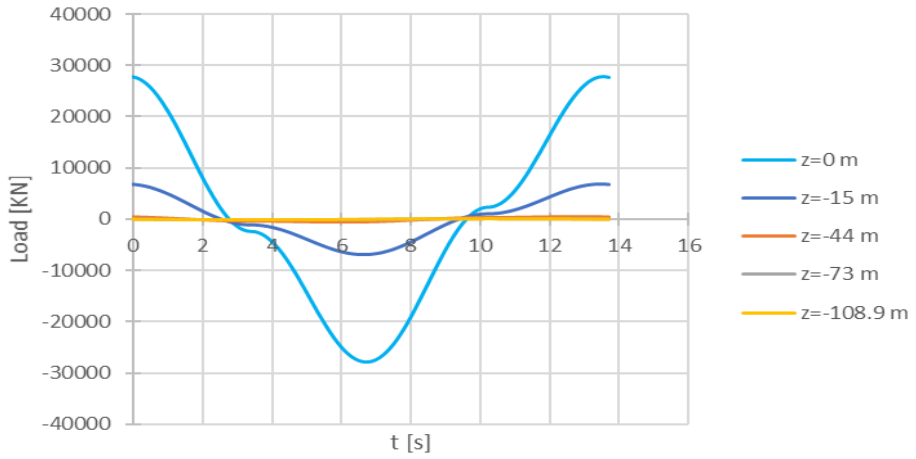

Figure 3.28 – Morrison load force according to Airy Finite water depth theory for several water depths

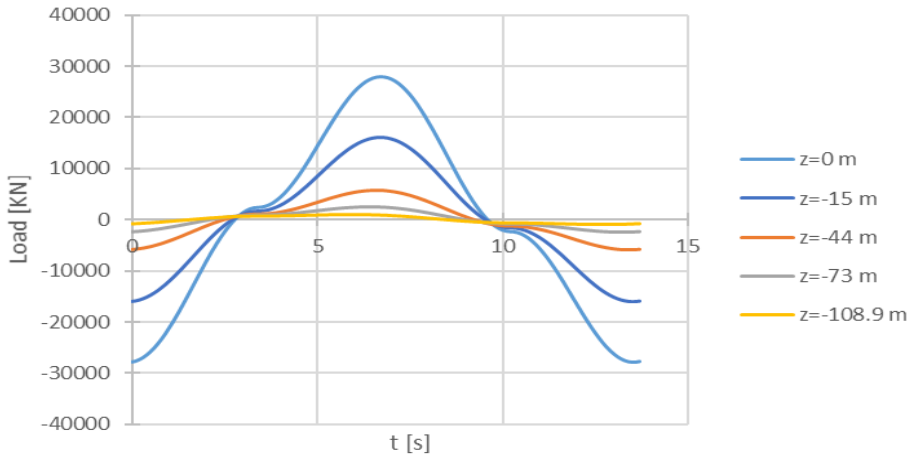

Figure 3.29 – Morrison load force according to Airy Infinite water depth theory for several water depths

Analysing the three charts (Fig. 3.27 to 3.29), a rather significant difference amongst them can be observed, as expected, and for a wave with 14.5 m height, both Airy's finite and infinite water depth theory fail to provide an accurate depiction of the real wave, showing an overwhelming difference of nearly 70 MN for the surface level which cannot be overlooked.

As expected all 3 theories support the idea that as one descends, the force reduces, due to a combination of increased drag and added mass coefficients as well as decreased absolute value of velocity and acceleration.

3.7. Results and Structural Response

Once the normal forces have been obtained it's a matter of applying the load to the structure in a capable structural analysis software. Widely used in the field of offshore structures, SESAM, specially developed by DNV-GL for the specific use in offshore platforms, it allows the design of these kind of constructions providing the structural response of the structure in question when exposed to waves.

Corresponding to the combination of load cases, with all load factor equal to one, the results given by the program are something like the ones below.

Table 3.14 – Sample of SESAM structural response to wave loading for member 4936

Member	Loadcase	Joint/Po D	PX	PY	PZ	MX	MY	MZ
4936.00		5006.00	-0.54	0.00	0.01	-0.02	-0.17	-0.03
	1	0.50	-0.54	0.00	0.01	-0.02	-0.19	-0.03
		JT_RA_6	-0.53	0.00	0.01	-0.02	-0.20	-0.04
4936.00		5006.00	-0.57	0.00	0.01	-0.03	-0.17	-0.03
	2	0.50	-0.57	0.00	0.01	-0.03	-0.19	-0.04
		JT_RA_6	-0.57	0.00	0.01	-0.03	-0.20	-0.04
4936.00		5006.00	-0.60	0.00	0.01	-0.03	-0.17	-0.03
	3	0.50	-0.60	0.00	0.01	-0.03	-0.19	-0.04
		JT_RA_6	-0.60	0.00	0.01	-0.03	-0.21	-0.04

Should be mentioned that the signal of the forces provided by SESAM and so the sample above, follow the following scheme.

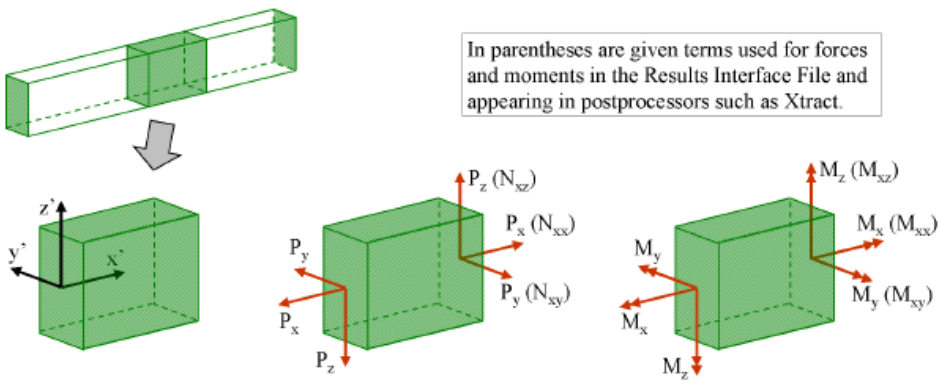

a)

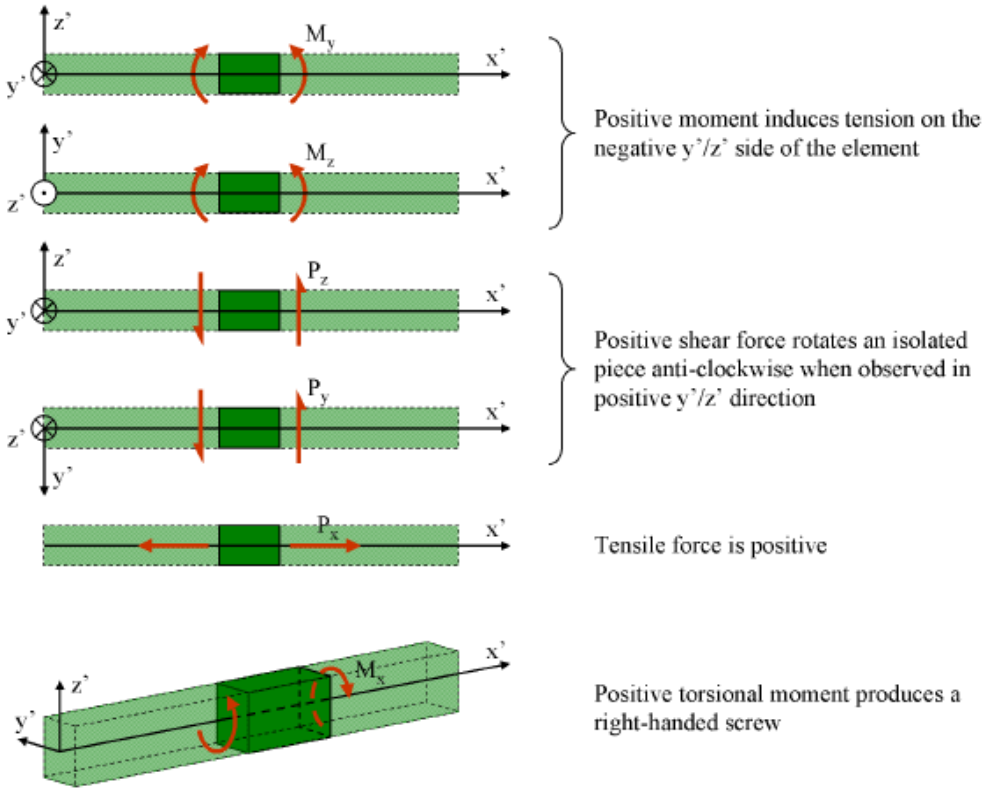

b)

Figure 3.30 – Definition of sign of moments and forces

4

Offshore KT-type Joint Fatigue Analysis

4.1. Outlook into different types of offshore structures

To give answer to an increasing need for raw materials, fuel, ore and energy, frontiers are expanded to the oceans in search of these answers, to the engineers responsible for providing these answers falls the responsibility and the challenges of designing, deploying and guarantying the safe operations of the constructions, situated in environments of adverse and hostile conditions where none have previously existed [60].

Evermore offshore engineers venture in deeper waters, requiring more capable materials and/or new innovative ways to design these structures. An impressive mark was set in 1975 with the first drilling in 2000 ft, however it took 18 years for production to take place revealing the underlying difficulty, yet it has been overcome by employing floating vessels with moorings, this record has been constantly beaten along the years, with sanctioned, installed and operating structures with 2414 m underwater. The word record however from data of March 2017 belongs to RAYA-1, an offshore exploration well off the cost of Uruguay with 3400 meters deep [61].

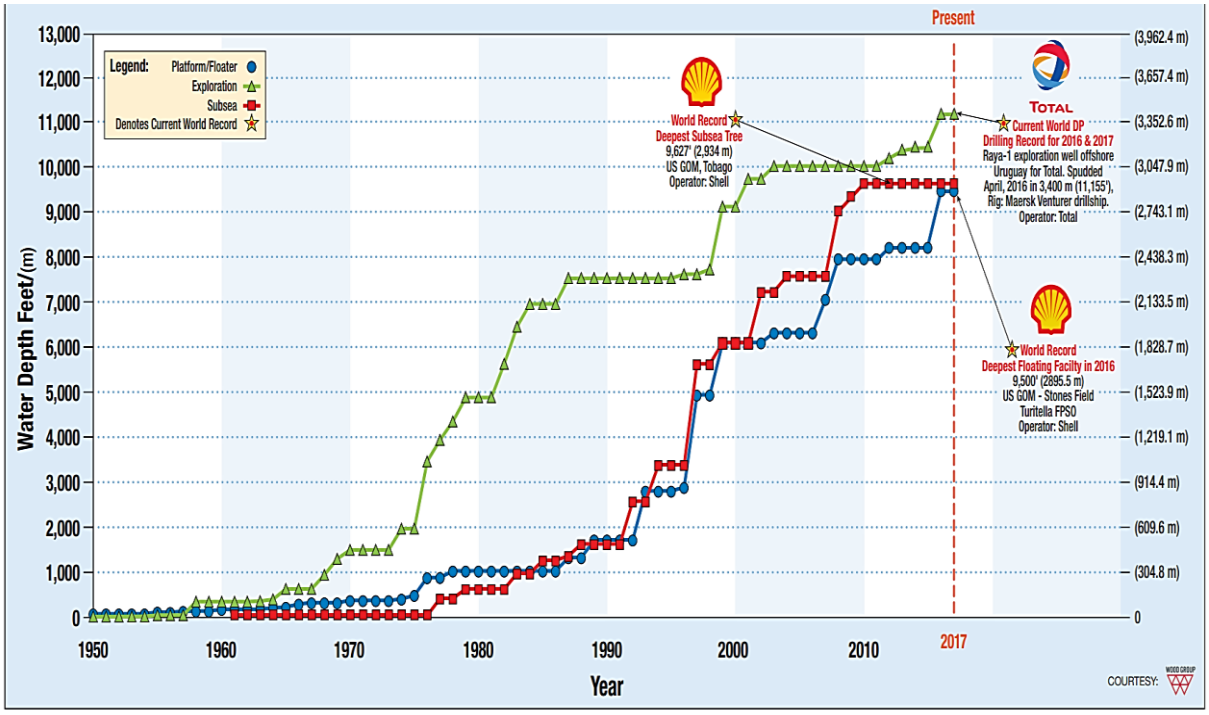

Figure 4.1 – Worldwide progression of water depth capabilities for offshore drilling & production (data as of March 2017) [61].

This serves two show that a lot has changed from the first offshore oil drilling structure build in 1887 of the coast of California [60].

With the recent advancements offshore platforms have experienced a reduce time interval from discovery of the oil field to first production, sitting at 9,9 years from data of March 2017 [61] for semi floating production systems.

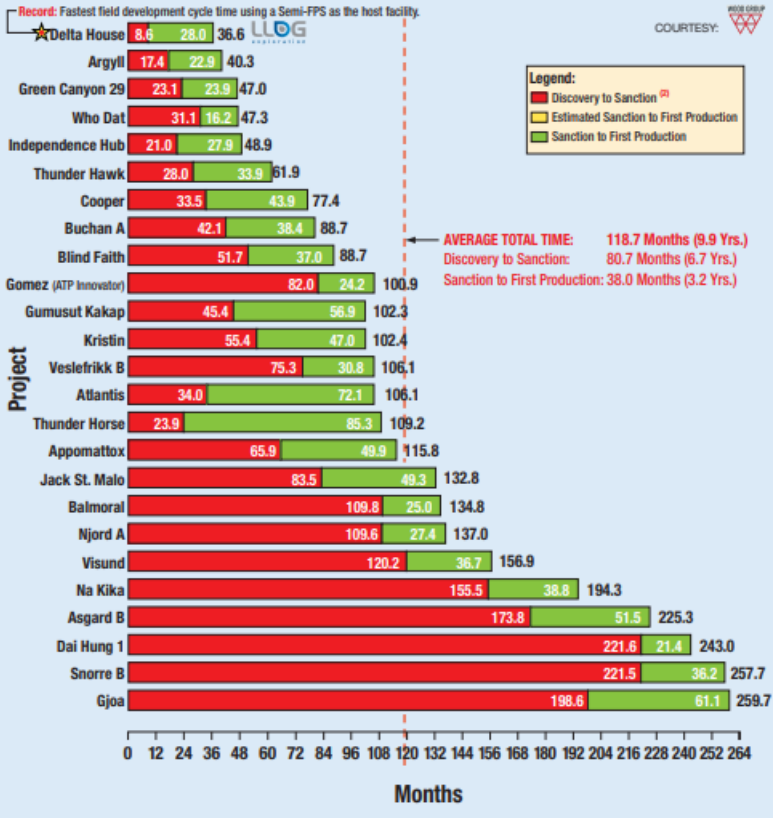

Figure 4.2 – Semi Floating Production Systems time analysis (as of March 2017) [61].

Since environmental loading is persistent and of extreme relevance for life evaluation, site-specific data is of great importance to illustrate, winds, current, waves, temperature… This kind of events take place year-round as they can differ both in short and long periods of time with the most varied ranges and values [60].

To cope with the various challenges presented and pretended use for the structure many options present different advantages and give a solution to a certain specific problem.

First and foremost, offshore structures are divided into two main groups according to the type of support configuration, either bottom supported or floatation offshore structures [61].

Normally constructed of steel tubular elements acting as a truss, fixed or Jacket-type structures are those where the lowest natural frequency is greater than the highest frequency related to wave excitation and behave as a rigid body [62]. Another type is the compliant platform meant for depths from 300 to 800m with close resemblances to the Jacket, although if the loading exceeds the design limit, it makes use of disconnectable pile connections, turning the initial zero degree of freedom to 2 about the seabed [62].

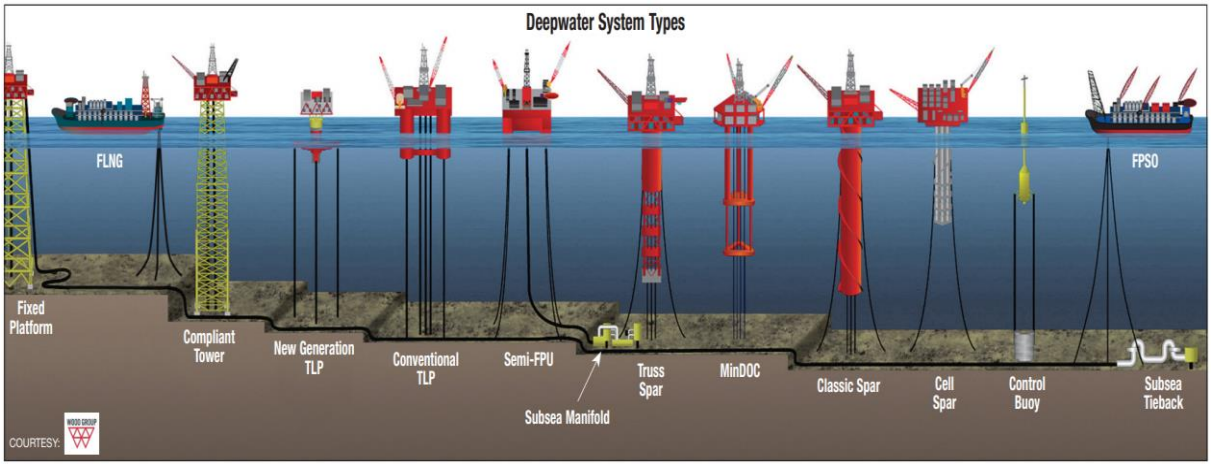

Figure 4.3 – Deepwater System Types [61].

Floating offshore structures such as drill ships, semi-submersibles, spars are unrestrained and so present 6 degrees of freedom.

Positively buoyant structures, designed this way because they present one restrain, heave, guaranteed by cables in tension moored to the sea bed, the case of Tension Leg Platforms. Subsequently weight and weight distribution in the deck is a major concern unlike bottom supported alternative, for each added unit of deck weight for a Tension Leg Platform an additional 1,3 units hull weight are required for buoyancy support and plus 0,65 unit of mooring force [60].

Bottom supported offshore structures:

- Minimal Platforms
- Jacket Structures
- Gravity Base Structures
- Jack-ups

Floating offshore Structures:

Neutrally Buoyant:

- Spars
- Semi-submersible
- FPS – Floating production system
- Ship-Shaped Floating Production, Storage and offloading Vessel
- Drill ships

Positively Buoyant:

- TLP – Tension Leg Platform
- TLWP
- Buoyant tower

The difference between neutrally and positively buoyant is due to the fact that there no restrictions in any of the 6 degrees of freedom, in this case wells are subsea completed, and oil and gas is transported to the platform via risers.

4.2. CASE STUDY – OFFSHORE PLATFORM JACKET-TYPE

4.2.1. STRUCTURE DESCRIPTION

As mentioned throughout this document this work rests on a specific offshore jacket-type structure. Situated in the North Sea, off the west coast of Norway, the platform sets on a sea bed 115,67 m below the sea surface. The structure has 4 frames in the North-South direction and 2 perpendicularly.

A blueprint of the platform is provided in Annex G, where it is possible to observe the dimensions of every element.

Supported by a group of piles on each of the four main vertical elements, the structure is braced at a total of 6 different levels, z = -108,9 m, z = -73 m, z = -44 m, z = -15 m, z = +8m and z = +24m.

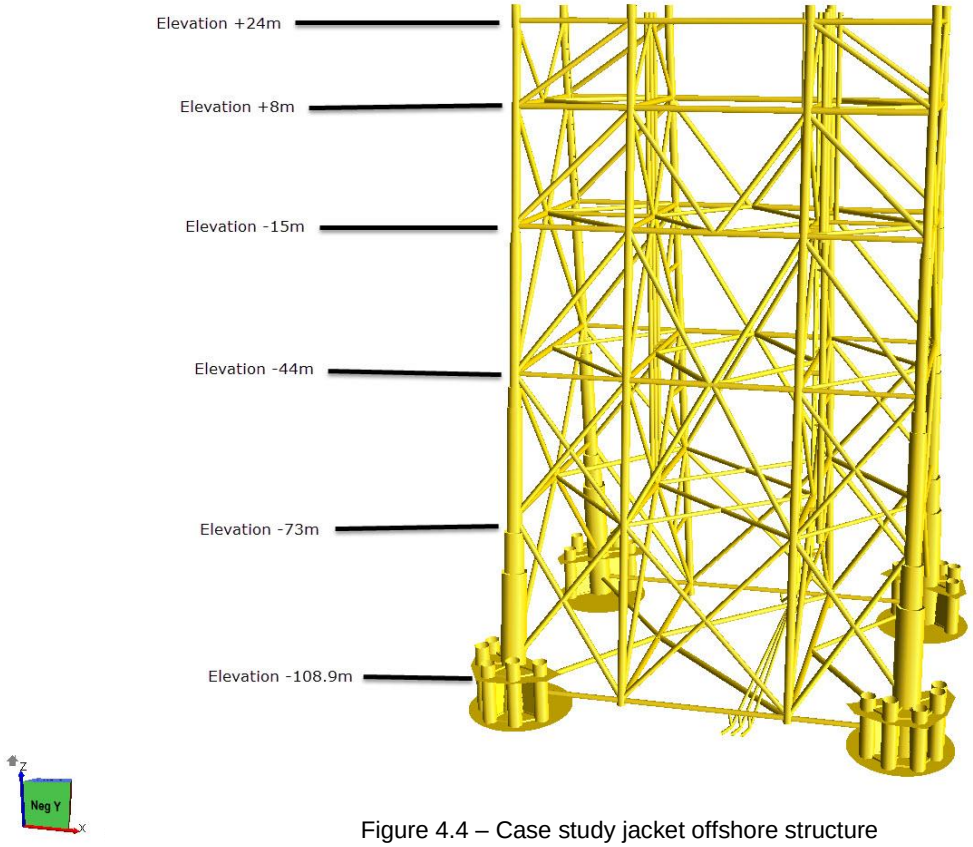

Figure 4.4 – Case study jacket offshore structure

At mudline the structure has 80 x 60 m square meters and 80 x 24 m at topside, reviling the massive size of the metallic structure made from S420 structural steel, with an approximate number of 140 meters of height.

In table 4.1 and 4.2 the chemical composition and mechanical properties of the offshore steel grade used in the structure are comprised.

Table 4.1 – Case study S420 steel chemical composition.

Grade	Standard	Thickness	%C (máx)	%Si	%Mn (máx)	%P	%S
S420G2+M	EN10225-2009	10-100mm	0.14	0.15-0.55	1.65	0.020	0.007

Table 4.2 – Case study S420 steel mechanical properties.

Steel Grade	Tensile Strenght (MPa)		Yield Strenght (MPa)				
	<40mm	40<100mm	<16mm	16 - 25mm	25-40mm	40-63mm	63-100mm
S420G2+M	500 - 660	480 - 640	420	400	390	380	380

Regarding the foundation, the structure was modelled with springs attached underneath each pile at mudline with the following soil stiffness matrix in MN and MN.m (see Table 4.3).

Table 4.3 – Soil Stiffness

K - X	K - Y	K - Z	K – XX	K - YY	K – ZZ
209.5	-16.11	0.00	58.18	1793	0.00
-16.11	208.20	0.00	-1789	-58.18	0.00
0.00	0.00	2471	0.00	0.00	0.00
58.18	-1789	0.00	23860	248.6	0.00
1793	-58.18	0.00	248.6	23880	0.00
0.00	0.00	0.00	0.00	0.00	45l87

4.2.2. Dynamic Analysis

Also provided by SESAM is dynamic response of the structure for mode 1 to 3. Characterized by a modal frequency and shape, dynamic modes are a state wave of excitation, where all the parts of the structure will respond sinusoidally with a specific frequency due to external loads or conditions, such as earthquake or sea waves for example.

Under mode 1, with a frequency of 0.314 Hz the same as saying a period of 3.18s, portraying a global sway in North /South direction.

For mode 2, the structure responds similarly to mode 1, this time with a sway in the East/West direction and a frequency of 0.334 Hz or a period of 2.99 s.

Regarding mode 3, it has a period of 1.90 s which entails a frequency of 0.526 Hz and represents a global twisting about the vertical axis.

A natural frequency was not provided, although not made in this document a comprehensive dynamic analysis of the structure should be conducted since the period related specially to mode 1 and 2 shows some similarity to the smaller waves, that is the waves that occur the most.

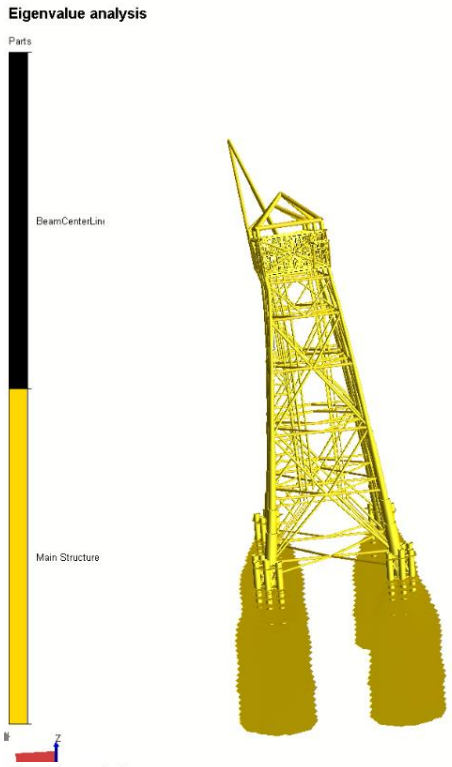

Figure 4.5 – Structure sway in mode 1

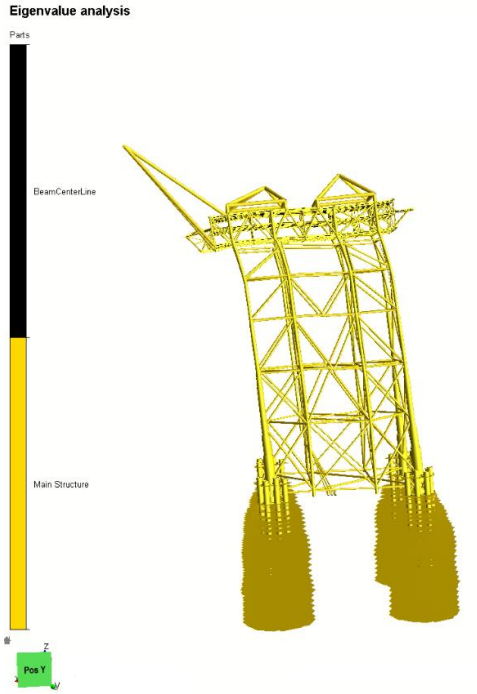

Figure 4.6 – Structure sway in mode 2

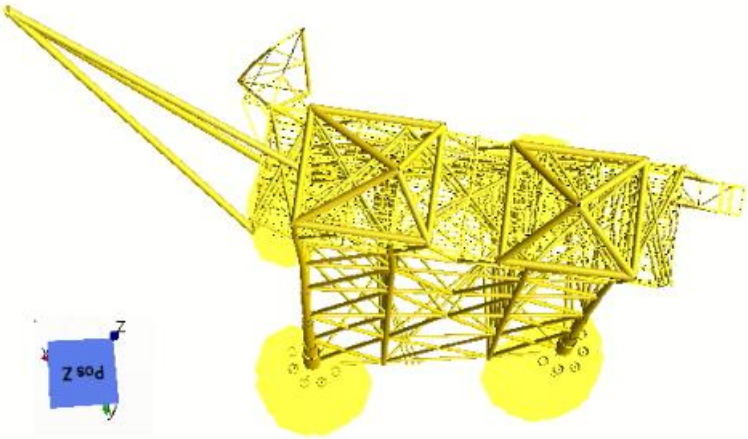

Figure 4.7 – Structural twisting about the vertical axis in mode 3

4.2.3. KT – TYPE OFFSHORE JOINT

In DNVGL recommended practice for fatigue design of offshore steel structures [13], Annex B, several types of joints are exposed.

A KT-type joint is composed by 3 secondary elements in this study case, 6, 3 from the plane XZ and other 3 from YZ. The joint in case in situated ate a depth of 44 meters under water and is denominated JT_RA_6, situated at alignment B4 (see annex F), this joint is deemed critical for this study because in accordance with the results provided by SESAM it shows the biggest range in forces and so becomes relevant for fatigue analysis.

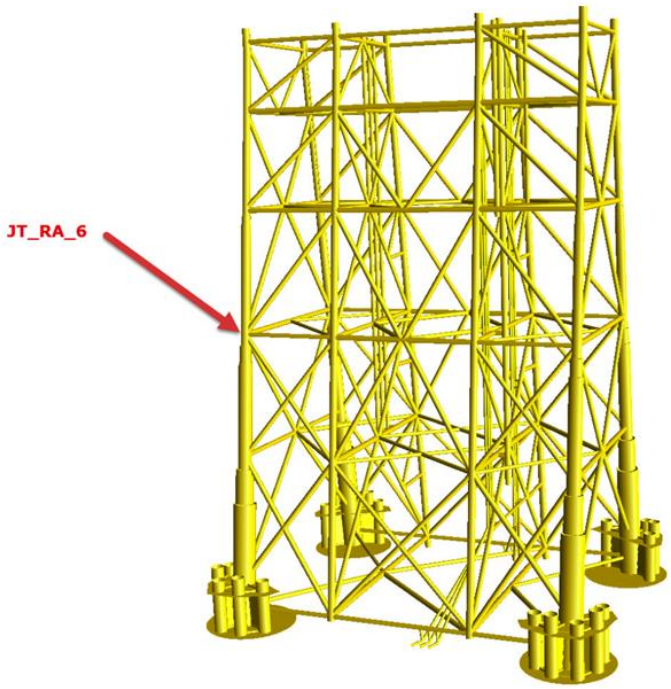

Figure 4.8 – Highlighted KT-type joint

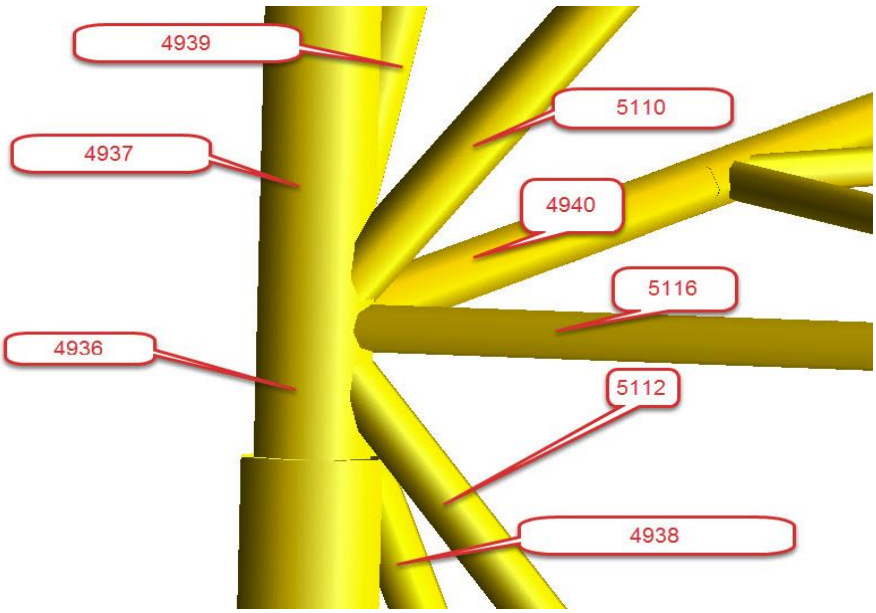

Figure 4.9 – Numbered elements of the critical joint – JT_RA_6

Each element is numbered to facilitate study of each individual member.

In the tables below (Tables 4.4 and 4.5) the geometric dimensions and properties of each primary element (chord) and secondary elements (braces) are given.

Table 4.4 – KT-joint geometrical dimensions

Member #	Diameter [m]	Thickness [m]
4936	2.300	0.095
4937	2.300	0.095
5116	1.000	0.030
4940	1.320	0.055
5110	1.200	0.040
5112	1.100	0.025
4938	1.100	0.025
4939	1.200	0.035

Table 4.5 – KT-joint geometrical properties

Member #	A [m2]	Wel,y	Wel,z
4936	0.3361	0.1854570	0.1854570
4937	0.3361	0.1854570	0.1854570
5116	0.0427	0.0114804	0.0114804
4940	0.065	0.0189428	0.0189428
5110	0.1117	0.0353458	0.0353458
5112	0.0741	0.0215135	0.0215135
4938	0.0427	0.0114804	0.0114804
4939	0.0464	0.0112614	0.0112614

Using the nomenclature present in [13]:

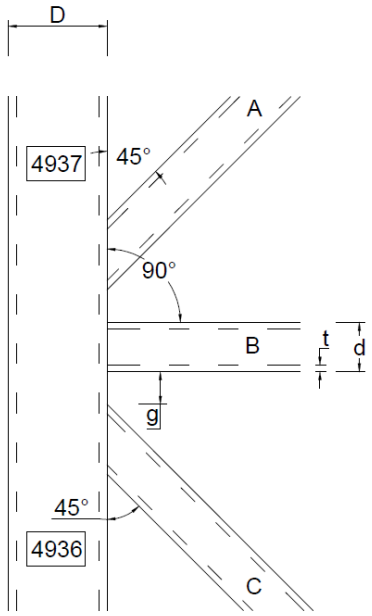

Figure 4.10 – DNV-GL nomenclature for a KT-type joint.

Regarding elements 5110 and 4939 as element A, the other members can be identified as B and C for each of the two planes, with this in mind, θ_A, θ_B and θ_C and the rest of the geometrical parameters take the following values:

Plane XZ:

$\theta_A = 38{,}41849°$

$\theta_B = 90°$

$\theta_C = 38{,}41549°$

g_{AB}=3.52E-01 m

g_{BC}=7.26E-02 m

ξ_{AB}=1.53E-02

ξ_{BC}=3.16E-02

FOR PLANE YZ:

$\theta_A = 30{,}11869°$

$\theta_B = 83{,}23139°$

$\theta_C = 43{,}66527°$

g_{AB}=3.79E-01 m

g_{BC}=7.47E-02 m

ξ_{AB}=1.65E-01

ξ_{BC}=3.25E-02

4.3. CALCULATION OF STRESS CONCENTRATION FACTORS

The geometrical parameters present in Tables 4.6 and 4.8 are within the limits imposed by DNV-GL recommended practice.

Plane XZ:

Table 4.6 – Geometric parameter for plane XZ.

Location	Member	β	τ	γ	α
A	5110	0.521739	0.421053	12.10526	6.835652
B	5116	0.434783	0.315789	12.10526	6.835652
C	5112	0.478261	0.263158	12.10526	6.835652

Table 4.7 – SCF for elements aligned in plane XZ

	Location	SCF_{BAL}	SCF_{IPB}	SCF_{OPB}	SCF_{UOPB}
Chord	A	1.6009775	1.2990365	1.8363963	2.5436804
	B	2.9490646	1.3706252	2.5918459	2.9185857
	C	1.3688033	1	1.0828665	2.1077958
Brace	A	1.8233236	1.6235408	2.6893376	-
	B	3.4089698	2.1717246	3.7857918	-
	C	1.7857226	1.5148	2.9438576	-

Plane YZ:

Table 4.8 – Geometric parameter for plane YZ.

Location	Member	β	τ	γ	α
A	4939	0.521739	0.368421	12.10526	6.835652
B	4940	0.573913	0.578947	12.10526	6.835652
C	4938	0.478261	0.263158	12.10526	6.835652

Table 4.9 –SCF for elements aligned in plane YZ.

	Location	SCF_{BAL}	SCF_{IPB}	SCF_{OPB}	SCF_{UOPB}
Chord	A	1.8318157	1	1.1413502	2.9810327
	B	5.4295072	2.3804706	5.6410504	5.7620280
	C	1.6207604	1	1.2818332	3.2921516
Brace	A	1.7222647	1.4198678	3.3873849	-
	B	4.5199659	2.4921638	4.9807336	-
	C	2.0016058	1.6093898	4.5979906	-

For obtaining the SCF according to the norm a division in two planes must be made, XZ and YZ. Once every geometric parameter present in Tables 4.6 and 4.8 are obtained, the calculation of the SCF according to the parametric formulas in Annex B [13], is made for every A,B,C combination, and so the SCF values can be obtained (see Tables 4.7 and 4.9).

For example, when calculating balanced axial loading condition, in the chord, the $\boldsymbol{\tau_A}, \boldsymbol{\gamma_A}$ and $\boldsymbol{\beta_A}$ are used to achieve SCF_{BAL} for location A, which depending of the plane in question may be element #4939 or #5110.

This process is repeated for every load condition and for every location (secondary element) combination for each of the planes.

Should be mentioned that even though some of the value are present as a 1, this is in reality an assumption because these values in question were lower than 1 which is not physically viable, as such the minimum value was considered, unitary value.

4.4. STRESS LEVELS AND MAXIMUM LOAD CONDITION

Obtained from SESAM, the forces related to each of the 8 elements than compose the joint are given for the total of 96 waves with each wave divided into 24 steps in time, resulting in a simplified time history analysis.

Since DNV-GL considers only the maximum stresses for axial, in-plane-bending and out-of-plane-bending, P_x, M_y and M_z respectively, only these will be considered to obtain the stress levels.

Since each wave load is divided into steps it is necessary to obtain the difference between the maximum and minimum value for each of the 24 step intervals for every loading condition and for each element.

It is now necessary to obtain the load case (wave#) that results in a maximum nominal stress, for it will very likely represent the maximum fatigue damage.

Divided into loading conditions, the maximum force interval is obtained for every element and so doing it is possible to retrieve the correspondent load case.

The next plots provide a view of those maximum values for each of the elements.

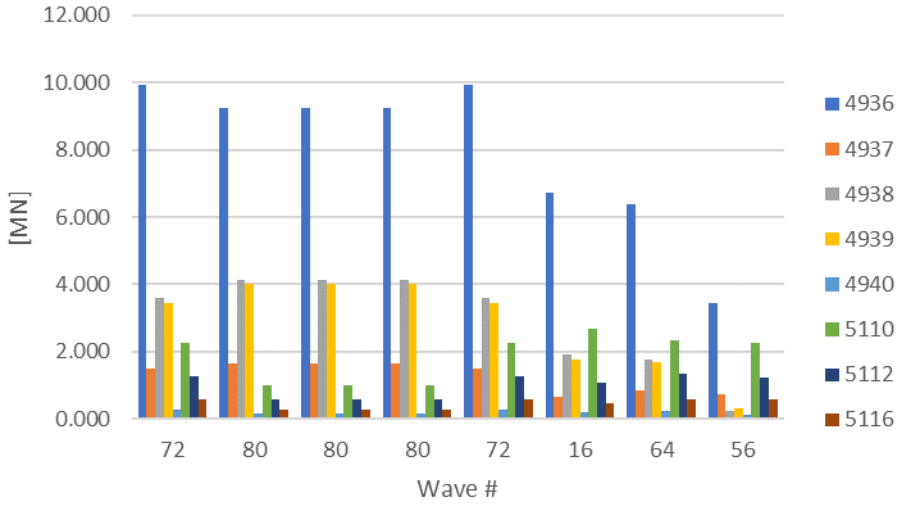

Figure 4.11 – Maximum force intervals for each element and load case for axial loading

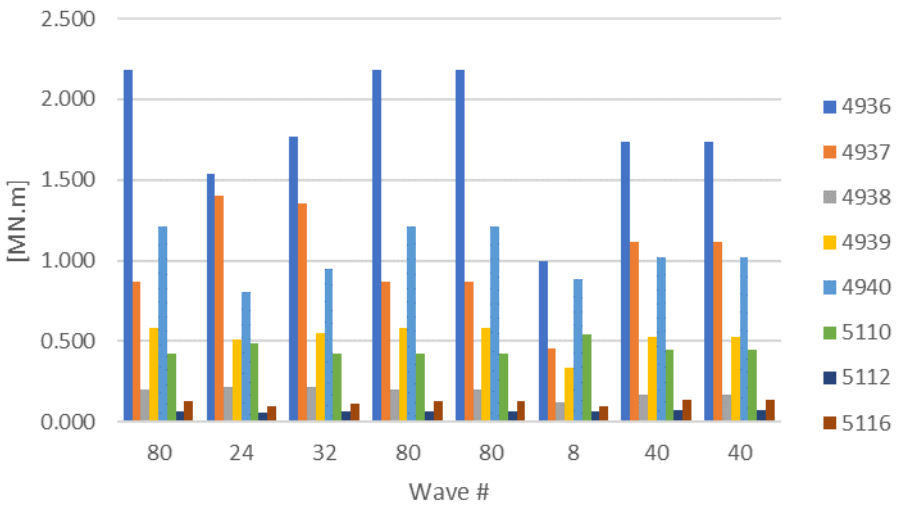

Figure 4.12 – Maximum force intervals for each element and load case for bending moment, MY.

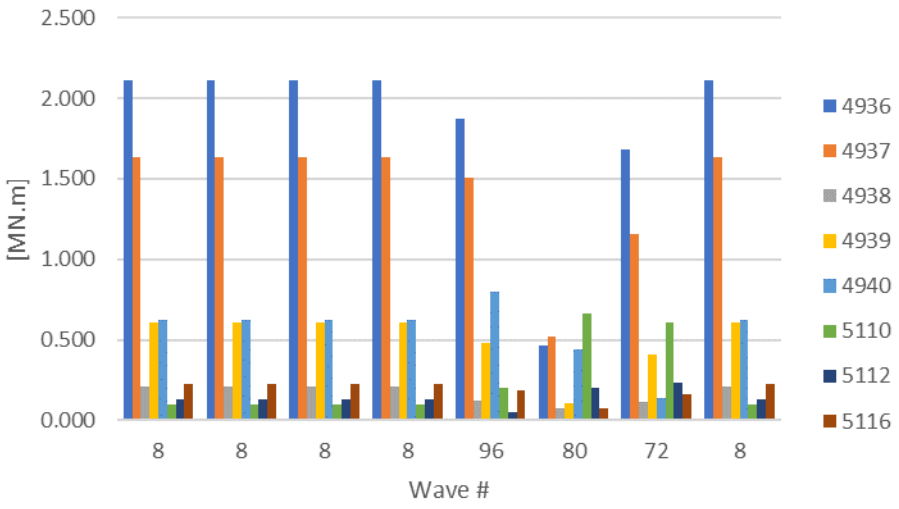

Figure 4.13 – Maximum intervals for each element and load case for bending moment, MZ.

With these summarized load cases, the nominal stresses are obtained resulting in a maximum value for wave number 80. Because wave 80 shows the least number of occurrences and fatigue damage is directly related to both stress and number of occurrences, as an advice from Force Technology, which provided the data related to the case study, waves between 5-7m of height should also be analysed for fatigue damage. This way, all waves from 4.5 to 7.5-meter-high, relating to Tables 3.3 to 3.5, where subjected to analysis. As a comparison wave 73 will be analysed in parallel with wave 80 since it shows the biggest number of occurrences. All other wave analysis and results are presented in Annex D.

4.5. SIMPLIFIED FATIGUE ANALYSIS ACCORDING TO DNV-GL

4.5.1. SIMPLIFIED PROBABILISTIC FATIGUE ANALYSIS USING HOT-SPOT STRESSES

DNV-GL recommended practice for fatigue design in offshore provides several possible ways to deal with the problem, the first, presented in section 5 uses a probabilistic methodology, where a two-parameter Weibull distribution is used to calculate the damage according to a certain level of stress for a year, which needs to be multiplied by the number of years 50 target fatigue life in this case, to retrieve the damage for that same period.

$$D = \left(\frac{n_0}{a}\right) * q^m * \Gamma(1 + \frac{m}{h}) \leq \eta \tag{4.1}$$

Where n_0 is the number of occurrences, q and h are the Weibull distribution parameters and Γ a function of the slope of the S-N curve and h.

Values for the function gamma are listed in table 5.1 of the DNVGL-RP-C203.

The function gamma takes the value 1155.4 for a slope of 5 and a value of 16.6 for a slope of 3.

The norm also contemplates a correction of the hotspot stresses regarding the thickness effect.

$$\sigma_{0,t} = \sigma_{0,tref}\left(\frac{t_{ref}}{t}\right)^k \tag{4.2}$$

Since for this case study, the structure is comprised of tubular elements with a detail category T, and assuming a value of 0.8 for h that correlates to a maximum $\sigma_{0,tref} = 334.2$ MPa for components in seawater with cathodic protection.

For tubular joints Table 2-3 of the same norm provides the characteristics of the S-N curve for several environments, which will be used for every fatigue damage analysis performed in this dissertation apart from the last one, where another curve will be used.

The formula 4.1, provides a simplification of damage calculation, for a more comprehensive analysis the contribution of both slopes can be considered. Regardless of the damage formula chosen for fatigue damage calculation, it should obey the limit imposed by regulation for the usage factor $\eta = {}^1/_{DFF}$ of 1, for a design fatigue factor, DFF of 1. Values for DFF can be 1,2,3,5 and 10, being 10 the most restrictive and the one chosen for this case study.

The design fatigue factors should be chosen according to DNVGL-OS-C101, depending on the accessibility.

In Fig. 4.14 a workflow is presented to provide an overlook into the steeps necessary for the simplified fatigue analysis using hot-spot stresses.

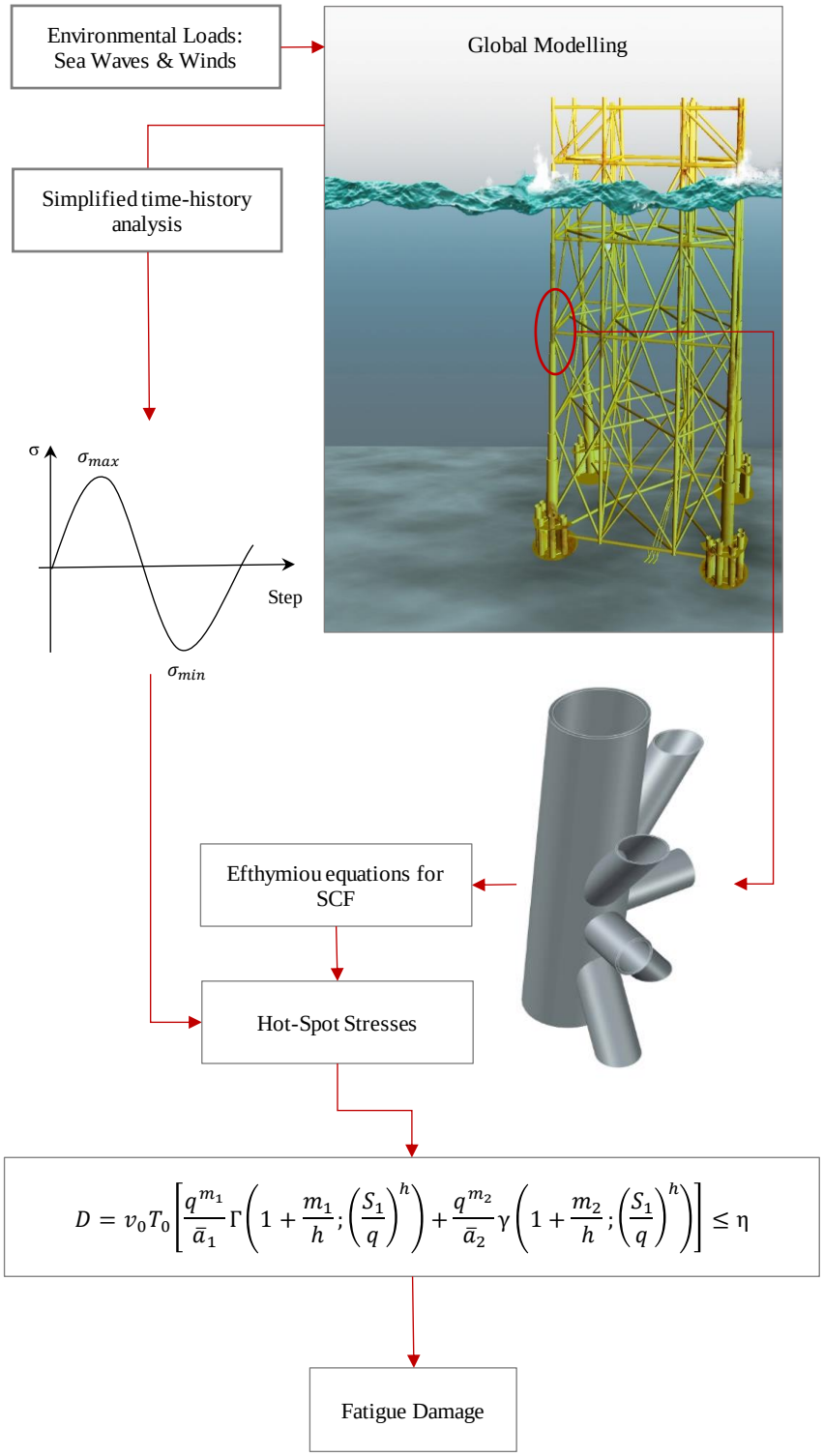

Figure 4.14 – Workflow for a simplified fatigue analysis using hot-spot stresses.

4.5.1.1. HOT-SPOT STRESSES AND SUPERPOSITION OF STRESSES

Once the stress concentration factors are all known, the calculation of the hot-spot stresses is made around the weld in a total of 8 spots using the following expressions specific for tubular joints and members.

In order to acquire the hot-spot stress the norm uses superposition of stresses from the different types of loading to obtain a generalized image of the stress distribution around the welded joint.

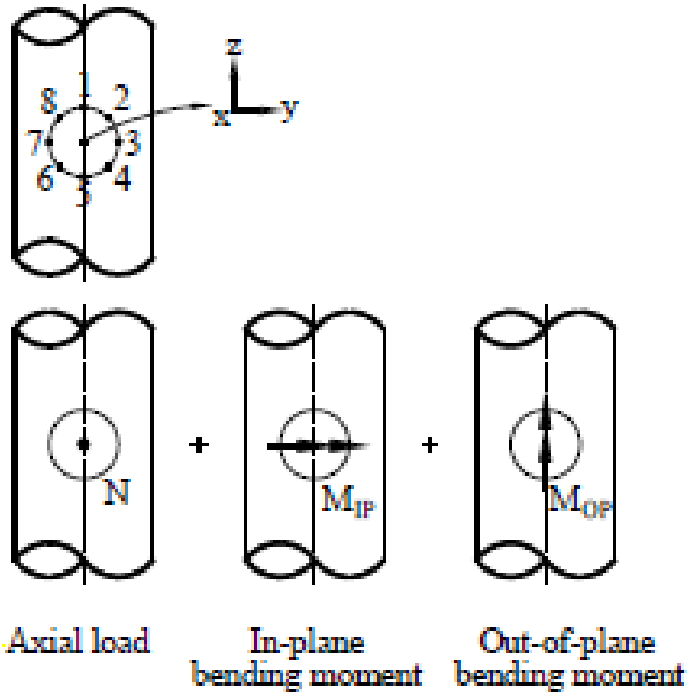

Figure 4.15 – Superposition of stresses [13].

$$\sigma_1 = SCF_{AC} * \sigma_x + SCF_{MIB} * \sigma_{my}$$
$$\sigma_2 = \frac{1}{2}(SCF_{AC} + SCF_{AS})\sigma_x + \frac{1}{2}\sqrt{2}\,SCF_{MIP}\sigma_{my} - \frac{1}{2}\sqrt{2}\,SCF_{MOP}\sigma_{mz}$$
$$\sigma_3 = SCF_{AS} * \sigma_x - SCF_{MOP} * \sigma_{mz}$$
$$\sigma_4 = \tfrac{1}{2}(SCF_{AC} + SCF_{AS})\sigma_x - \tfrac{1}{2}\sqrt{2}\,SCF_{MIP}\sigma_{my} - \tfrac{1}{2}\sqrt{2}\,SCF_{MOP}\sigma_{mz} \qquad (4.3\text{-}4.10)$$
$$\sigma_5 = SCF_{AC} * \sigma_x - SCF_{MIP} * \sigma_{my}$$
$$\sigma_6 = \frac{1}{2}(SCF_{AC} + SCF_{AS})\sigma_x - \frac{1}{2}\sqrt{2}\,SCF_{MIP}\sigma_{my} + \frac{1}{2}\sqrt{2}\,SCF_{MOP}\sigma_{mz}$$
$$\sigma_7 = SCF_{AS} * \sigma_x - SCF_{MOP} * \sigma_{mz}$$
$$\sigma_8 = \frac{1}{2}(SCF_{AC} + SCF_{AS})\sigma_x + \frac{1}{2}\sqrt{2}\,SCF_{MIP}\sigma_{my} + \frac{1}{2}\sqrt{2}\,SCF_{MOP}\sigma_{mz}$$

Since this case only covers KT-type joints and not X-type, SCF_{AC} and SCF_{AS} which are the stress concentration factors for balanced axial loading in the chord and saddle respectively are equal to the SCF for balanced axial loading.

Since wave 80 as stated before is the one that presents the highest nominal stress but the smallest number of occurrences, wave 73 will also be studied because it shows the most number of occurrences.

Table 4.10 – Hot-Spot Stresses for wave #80, MPa.

Plane	Primary Element	Secondary Element	σ1	σ2	σ3	σ4	σ5	σ6	σ7	σ8
		5110	92.32	51.59	39.41	29.94	61.70	36.45	48.62	58.10
	4936	5116	130.23	87.91	74.58	65.06	97.92	74.26	87.58	97.10
		5112	82.42	44.05	34.92	27.38	58.84	31.22	40.35	47.89
		5110	19.90	8.55	2.74	-0.05	7.75	7.26	13.07	15.85
XZ	4937	5116	26.90	13.94	7.27	4.87	14.07	15.18	21.85	24.25
		5112	17.36	7.91	3.71	1.30	8.01	5.61	9.80	12.22
	5110		56.52	-11.41	-58.23	-56.49	-7.24	60.70	107.51	105.78
	5116		44.60	19.96	-4.76	-15.07	-4.93	19.71	44.43	54.74
	5112		32.88	-6.90	-28.56	-19.39	15.23	55.01	76.67	67.50
		4939	95.15	56.68	47.50	40.01	71.57	44.06	53.23	60.72
	4936	4940	210.33	159.12	135.14	119.44	154.22	139.45	163.43	179.13
		4938	89.34	50.62	41.35	33.96	65.77	38.50	47.78	55.17
		4939	19.90	8.55	2.74	-0.05	7.75	7.26	13.07	15.85
YZ	4937	4930	26.90	13.94	7.27	4.87	14.07	15.18	21.85	24.25
		4938	17.36	7.91	3.71	1.30	8.01	5.61	9.80	12.22
	4939		150.15	124.37	88.10	62.59	62.78	88.56	124.83	150.34
	4940		91.65	22.99	-55.54	-97.94	-79.38	-10.72	67.82	110.22
	4938		222.37	192.85	163.79	152.23	164.92	194.44	223.49	235.06

Table 4.11 – Hot-Spot Stresses for wave #73, MPa.

Plane	Primary Element	Secondary Element	σ1	σ2	σ3	σ4	σ5	σ6	σ7	σ8
		5110	1.66	0.85	0.35	0.00	0.46	0.36	0.86	1.21
	4936	5116	2.20	1.31	0.75	0.41	0.93	0.92	1.48	1.82
		5112	1.43	0.74	0.37	0.08	0.51	0.30	0.67	0.95
		5110	0.67	0.06	-0.33	-0.42	-0.01	0.32	0.71	0.79
XZ	4937	5116	0.84	0.08	-0.39	-0.42	0.13	0.62	1.08	1.12
		5112	0.56	0.13	-0.15	-0.24	0.04	0.19	0.47	0.56
	5110		3.75	2.11	-0.45	-2.45	-2.70	-1.06	1.50	3.49
	5116		3.52	1.77	-0.70	-2.43	-2.41	-0.66	1.81	3.54
	5112		1.48	0.73	-0.14	-0.62	-0.43	0.32	1.19	1.68
		4939	1.61	0.91	0.53	0.25	0.68	0.48	0.85	1.13
	4936	4940	3.61	2.28	1.26	0.71	1.40	1.83	2.84	3.39
		4938	1.53	0.81	0.43	0.16	0.60	0.41	0.79	1.07
		4939	0.67	0.06	-0.33	-0.42	-0.01	0.32	0.71	0.79
YZ	4937	4930	0.84	0.08	-0.39	-0.42	0.13	0.62	1.08	1.12
		4938	0.56	0.13	-0.15	-0.24	0.04	0.19	0.47	0.56
	4939		5.44	3.84	0.86	-1.74	-2.46	-0.85	2.12	4.73
	4940		5.12	2.38	-1.44	-4.10	-4.03	-1.28	2.54	5.19
	4938		3.99	2.26	0.11	-1.20	-0.90	0.83	2.98	4.29

The remaining values for Hot Spot Stresses regarding waves in from those wave height intervals are included in Annex E.

4.5.1.2. Fatigue damage results

Described in topic 4.4.1 of this very same document, a fatigue damage assessment is made using parameters from Weibull distribution, the results of that analysis are posted below.

In the case where the absolute value of the hot-spot stresses is below $\Delta\sigma_{nom}$, the stress is below the fatigue limit of the S-N curve and so the damage can be overlooked, and fatigue life considered infinite.

Below, in Fig. 4.16, is a representation of the damage around the same 8 points used to achieve the hot-spot stresses.

As for the wave covering the interval of 4.5 to 7.5 meter in height are not included in this document since they produce an insignificant level of damage in the structure, resulting in the infinite life of the same.

Table 4.12 – Fatigue Damage results from hot-spot probabilistic SFA for wave #80.

Plane	Member	Thickness	Wave	Spot	Δσnom	Δσhot-spot,0	|Δσhot-spot|	n0	q	a	m	Γ , γ	D
-	-	mm	-	-	MPa	MPa	MPa	-	-	-	-	-	-
x-z	5110	40	80	1	63.96	56.5	63.57	326	7.08	1.35E+16	5.00	1155.4	infinite life
				2		-11.4	12.84		1.43	1.35E+16	5.00	1155.4	infinite life
				3		-58.2	65.49		7.30	1.35E+16	5.00	1155.4	infinite life
				4		-56.5	63.54		7.08	1.35E+16	5.00	1155.4	infinite life
				5		-7.2	8.14		0.91	1.35E+16	5.00	1155.4	infinite life
				6		60.7	68.27		7.61	1.35E+16	5.00	1155.4	3.55E-05
				7		107.5	120.91		13.47	1.51E+12	3.00	16.6	4.37E-04
				8		105.8	118.97		13.25	1.51E+12	3.00	16.6	4.16E-04
	5116	30	80	1	23.72	44.6	46.68	326	5.20	1.35E+16	5.00	1155.4	infinite life
				2		20.0	20.89		2.33	1.35E+16	5.00	1155.4	infinite life
				3		-4.8	4.98		0.55	1.35E+16	5.00	1155.4	infinite life
				4		-15.1	15.77		1.76	1.35E+16	5.00	1155.4	infinite life
				5		-4.9	5.16		0.58	1.35E+16	5.00	1155.4	infinite life
				6		19.7	20.63		2.30	1.35E+16	5.00	1155.4	infinite life
				7		44.4	46.50		5.18	1.35E+16	5.00	1155.4	infinite life
				8		54.7	57.29		6.38	1.35E+16	5.00	1155.4	infinite life
	5112	25	80	1	37.17	32.9	32.88	326	3.66	1.35E+16	5.00	1155.4	infinite life
				2		-6.9	6.90		0.77	1.35E+16	5.00	1155.4	infinite life
				3		-28.6	28.56		3.18	1.35E+16	5.00	1155.4	infinite life
				4		-19.4	19.39		2.16	1.35E+16	5.00	1155.4	infinite life
				5		15.2	15.23		1.70	1.35E+16	5.00	1155.4	infinite life
				6		55.0	55.01		6.13	1.35E+16	5.00	1155.4	infinite life
				7		76.7	76.67		8.54	1.35E+16	5.00	1155.4	6.35E-05
				8		67.5	67.50		7.52	1.35E+16	5.00	1155.4	3.36E-05
y-z	4939	35	80	1	98	150.1	163.32	326	18.20	1.51E+12	3.00	16.6	1.08E-03
				2		124.4	135.28		15.07	1.51E+12	3.00	16.6	6.12E-04
				3		88.1	95.83		10.68	1.51E+12	3.00	16.6	2.17E-04
				4		62.6	68.08		7.59	1.35E+16	5.00	1155.4	3.51E-05
				5		62.8	68.29		7.61	1.35E+16	5.00	1155.4	3.56E-05
				6		88.6	96.33		10.73	1.51E+12	3.00	16.6	2.21E-04
				7		124.8	135.78		15.13	1.51E+12	3.00	16.6	6.18E-04
				8		150.3	163.53		18.22	1.51E+12	3.00	16.6	1.08E-03
	4940	55	80	1	48.05	91.6	111.62	326	12.44	1.51E+12	3.00	16.6	3.44E-04
				2		23.0	28.00		3.12	1.35E+16	5.00	1155.4	infinite life
				3		-55.5	67.64		7.54	1.35E+16	5.00	1155.4	3.39E-05
				4		-97.9	119.28		13.29	1.51E+12	3.00	16.6	4.19E-04
				5		-79.4	96.67		10.77	1.51E+12	3.00	16.6	2.23E-04
				6		-10.7	13.05		1.45	1.35E+16	5.00	1155.4	infinite life
				7		67.8	82.59		9.20	1.35E+16	5.00	1155.4	9.21E-05
				8		110.2	134.23		14.96	1.51E+12	3.00	16.6	5.97E-04
	4938	25	80	1	121.08	222.4	222.37	326	24.78	1.51E+12	3.00	16.6	2.72E-03
				2		192.8	192.85		21.49	1.51E+12	3.00	16.6	1.77E-03
				3		163.8	163.79		18.25	1.51E+12	3.00	16.6	1.09E-03
				4		152.2	152.23		16.96	1.51E+12	3.00	16.6	8.71E-04
				5		164.9	164.92		18.37	1.51E+12	3.00	16.6	1.11E-03
				6		194.4	194.44		21.66	1.51E+12	3.00	16.6	1.82E-03
				7		223.5	223.49		24.90	1.51E+12	3.00	16.6	2.76E-03
				8		235.1	235.06		26.19	1.51E+12	3.00	16.6	3.21E-03

Plane	Member	Thickness	Wave	Spot	Δσnom	Δσhot-spot,0	|Δσhot-spot|	n0	q	a	m	Γ , γ	D
-	-	mm	-	-	MPa	MPa	MPa	-	-	-	-	-	-
x-z	5110	40	73	1	2.64	3.75	4.21	640568	0.16	1.35E+16	5.00	1155.4	infinite life
				2		2.11	2.37		0.09	1.35E+16	5.00	1155.4	infinite life
				3		-0.45	0.51		0.02	1.35E+16	5.00	1155.4	infinite life
				4		-2.45	2.75		0.11	1.35E+16	5.00	1155.4	infinite life
				5		-2.70	3.03		0.12	1.35E+16	5.00	1155.4	infinite life
				6		-1.06	1.19		0.05	1.35E+16	5.00	1155.4	infinite life
				7		1.50	1.69		0.07	1.35E+16	5.00	1155.4	infinite life
				8		3.49	3.93		0.15	1.35E+16	5.00	1155.4	infinite life
	5116	30	73	1	1.86	3.52	3.69	640568	0.14	1.35E+16	5.00	1155.4	infinite life
				2		1.77	1.85		0.07	1.35E+16	5.00	1155.4	infinite life
				3		-0.70	0.73		0.03	1.35E+16	5.00	1155.4	infinite life
				4		-2.43	2.54		0.10	1.35E+16	5.00	1155.4	infinite life
				5		-2.41	2.53		0.10	1.35E+16	5.00	1155.4	infinite life
				6		-0.66	0.69		0.03	1.35E+16	5.00	1155.4	infinite life
				7		1.81	1.89		0.07	1.35E+16	5.00	1155.4	infinite life
				8		3.54	3.70		0.14	1.35E+16	5.00	1155.4	infinite life
	5112	25	73	1	1.15	1.48	1.48	640568	0.06	1.35E+16	5.00	1155.4	infinite life
				2		0.73	0.73		0.03	1.35E+16	5.00	1155.4	infinite life
				3		-0.14	0.14		0.01	1.35E+16	5.00	1155.4	infinite life
				4		-0.62	0.62		0.02	1.35E+16	5.00	1155.4	infinite life
				5		-0.43	0.43		0.02	1.35E+16	5.00	1155.4	infinite life
				6		0.32	0.32		0.01	1.35E+16	5.00	1155.4	infinite life
				7		1.19	1.19		0.05	1.35E+16	5.00	1155.4	infinite life
				8		1.68	1.68		0.07	1.35E+16	5.00	1155.4	infinite life
y-z	4939	35	73	1	3.83	5.44	5.92	640568	0.23	1.35E+16	5.00	1155.4	infinite life
				2		3.84	4.17		0.16	1.35E+16	5.00	1155.4	infinite life
				3		0.86	0.94		0.04	1.35E+16	5.00	1155.4	infinite life
				4		-1.74	1.90		0.07	1.35E+16	5.00	1155.4	infinite life
				5		-2.46	2.67		0.10	1.35E+16	5.00	1155.4	infinite life
				6		-0.85	0.93		0.04	1.35E+16	5.00	1155.4	infinite life
				7		2.12	2.31		0.09	1.35E+16	5.00	1155.4	infinite life
				8		4.73	5.14		0.20	1.35E+16	5.00	1155.4	infinite life
	4940	55	73	1	2.36	5.12	6.24	640568	0.24	1.35E+16	5.00	1155.4	infinite life
				2		2.38	2.89		0.11	1.35E+16	5.00	1155.4	infinite life
				3		-1.44	1.76		0.07	1.35E+16	5.00	1155.4	infinite life
				4		-4.10	4.99		0.20	1.35E+16	5.00	1155.4	infinite life
				5		-4.03	4.91		0.19	1.35E+16	5.00	1155.4	infinite life
				6		-1.28	1.56		0.06	1.35E+16	5.00	1155.4	infinite life
				7		2.54	3.09		0.12	1.35E+16	5.00	1155.4	infinite life
				8		5.19	6.32		0.25	1.35E+16	5.00	1155.4	infinite life
	4938	25	73	1	2.6	3.99	3.99	640568	0.16	1.35E+16	5.00	1155.4	infinite life
				2		2.26	2.26		0.09	1.35E+16	5.00	1155.4	infinite life
				3		0.11	0.11		0.00	1.35E+16	5.00	1155.4	infinite life
				4		-1.20	1.20		0.05	1.35E+16	5.00	1155.4	infinite life
				5		-0.90	0.90		0.04	1.35E+16	5.00	1155.4	infinite life
				6		0.83	0.83		0.03	1.35E+16	5.00	1155.4	infinite life
				7		2.98	2.98		0.12	1.35E+16	5.00	1155.4	infinite life
				8		4.29	4.29		0.17	1.35E+16	5.00	1155.4	infinite life

Table 4.13 – Fatigue Damage results from hot-spot probabilistic SFA for wave #73

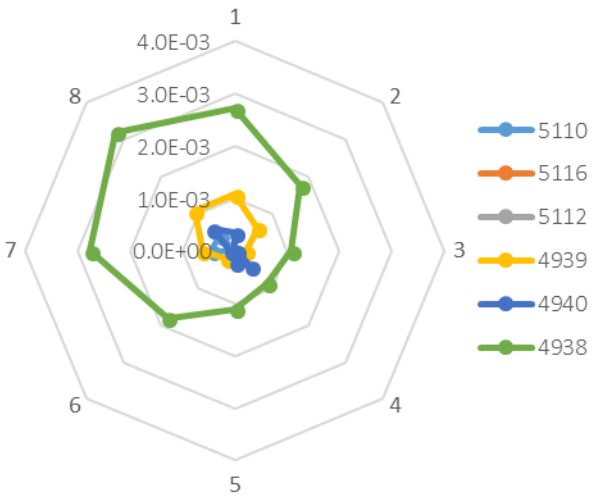

Figure 4.16 – Damage around the 8 spots for different elements for wave 80

4.5.2 Simplified Probabilistic Fatigue analysis using Nominal stresses

Similar to the previous analysis, in this case instead of hot-spot stresses, nominal stresses will be used, even though there is the requirement that for details of this category hot-spot stresses should be used.

In Fig. 4.17 a workflow for this analysis is provided.

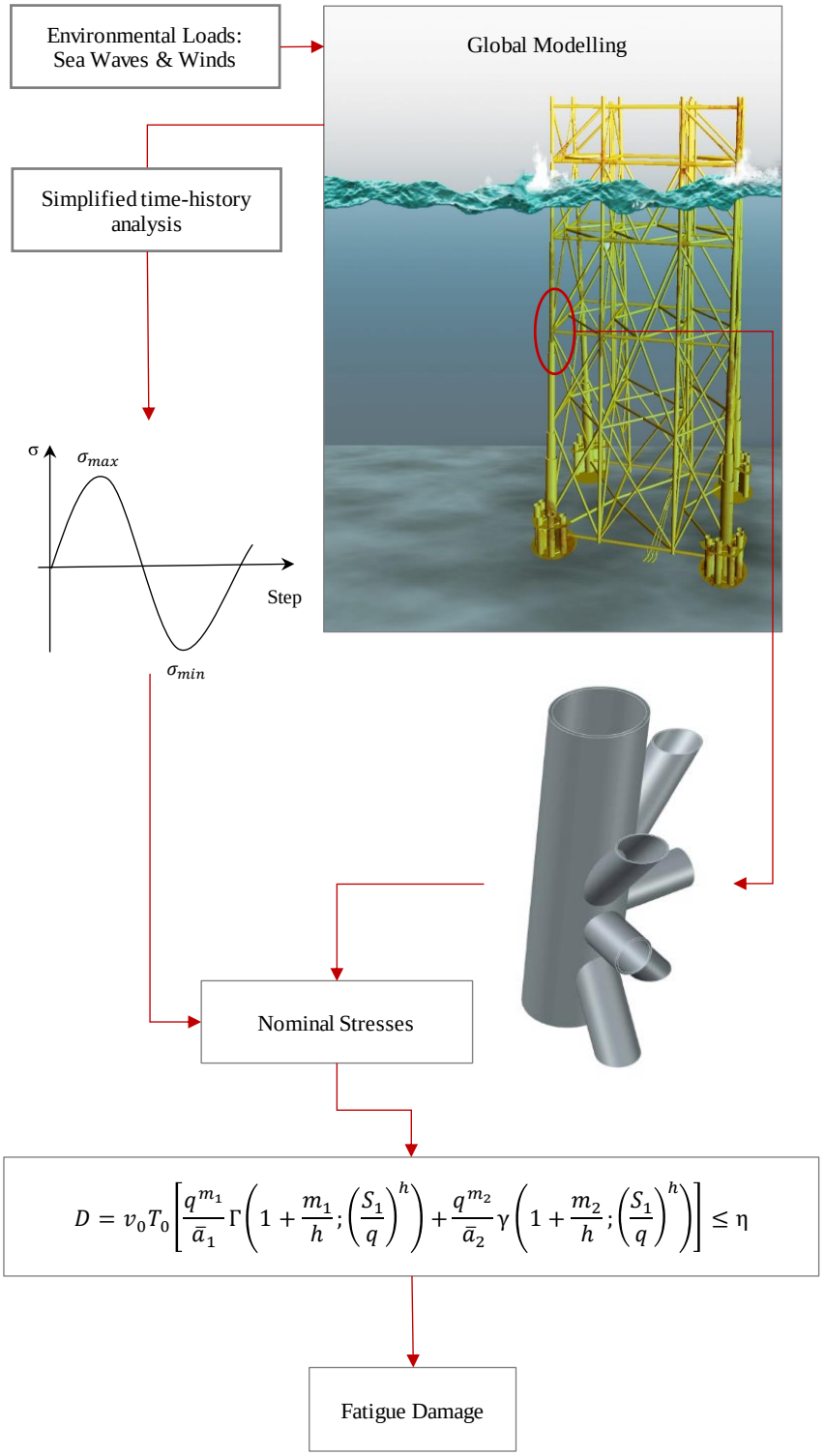

Figure 4.17 – Workflow for a simplified fatigue analysis using nominal stresses.

The fatigue assessment using nominal stress approach for several joints is shown in fatigue classes where a relation between applied stress range, be that normal or shear is compared with fatigue life given by the following equations [27]:

$$N\ \Delta\sigma_{nom}^{m} = C \tag{4.11}$$

$$N\ \Delta\tau_{nom}^{m\tau} = C_{\tau} \tag{4.12}$$

Where, C, C_{τ}, m and m_{τ} are material constants. The material constants m describe the slope of the fatigue strength curves.

The normal and shear stresses effects must be combined in the multiaxial assessment. The EC 3 par 1-9 present three different alternatives to consider their effects [27]:

i) The effects of the shear stress range may be neglected, if the $\Delta\tau_{nom}$<0.15 $\Delta\sigma_{nom}$;
ii) For proportional loading, the maximum principal stress range may be used, in the situation that the plane of the maximum principal stress doesn´t change significantly in the course of a loading event;
iii) For non-proportional loading events, the components of damage for normal and shear stresses should be assessed separately using the interaction equation or the Palmgren-Miner rule:

$$\left(\frac{\Delta\sigma_{eq,nom}}{\Delta\sigma_{c}}\right)^{3} + \left(\frac{\Delta\tau_{eq,nom}}{\Delta\tau_{c}}\right)^{5} \leq 1 \tag{4.13}$$

Where $\Delta\sigma_{c}$ and $\Delta\tau_{c}$ are the reference values of the fatigue strength at 2 million cycles.

$$D_{\sigma} + D_{\tau} \leq 1 \tag{4.14}$$

The computation of the equivalent normal and shear stress ranges are presented, as a function of the normalized stress cycles, N_{ref}:

$$\Delta\tau_{eq,nom} = \sqrt[m\tau]{\sum_{i=1}^{k}(\Delta\tau_{nom,i}^{m\tau}\ n_i)\Big/N_{ref}} \tag{4.15}$$

$$\Delta\sigma_{eq,nom} = \sqrt[m]{\sum_{i=1}^{k}(\Delta\sigma_{nom,i}^{m}\ n_i)\Big/N_{ref}} \tag{4.16}$$

4.5.2.1 Fatigue damage results

In Table 4.14 the results for the simplified fatigue analysis for both waves 80 and 73 are presented.

Table 4.14 – Fatigue damage results from nominal probabilistic SFA for wave 80 and 73.

Plane	Member	Thickness	Wave	Δσnom,0	Δσnom	n0	q	a	m	Γ , γ	D
-	-	mm	-	MPa	MPa	-	-	-	-	-	-
x-z	5110	40	80	63.96	71.93	326	8.01	1.3E+16	5	1155.4	4.62E-05
	5116	30	80	23.72	24.83	326	2.77	1.3E+16	5	1155.4	infinite life
	5112	25	80	37.17	37.17	326	4.14	1.3E+16	5	1155.4	infinite life
y-z	4939	35	80	98.00	106.60	326	11.88	1.5E+12	3	16.6	2.99E-04
	4940	55	80	48.05	58.52	326	6.52	1.3E+16	5	1155.4	infinite life
	4938	25	80	121.08	121.08	326	13.49	1.5E+12	3	16.6	4.39E-04
x-z	5110	40	73	2.64	2.97	640568	0.12	1.3E+16	5	1155.4	infinite life
	5116	30	73	1.86	1.95	640568	0.08	1.3E+16	5	1155.4	infinite life
	5112	25	73	1.15	1.15	640568	0.04	1.3E+16	5	1155.4	infinite life
y-z	4939	35	73	3.83	4.17	640568	0.16	1.3E+16	5	1155.4	infinite life
	4940	55	73	2.36	2.87	640568	0.11	1.3E+16	5	1155.4	infinite life
	4938	25	73	2.60	2.60	640568	0.10	1.3E+16	5	1155.4	infinite life

4.5.3 Miner rule simplified fatigue analysis using nominal stresses

Based on Palmgren-Miner rule of cumulative damage, this approach has been referred to in topic 2.6.

$$D = \sum_{i=1}^{k} \frac{n_i}{N_i} = \frac{1}{\bar{a}} \sum_{i=1}^{k} n_i (\Delta\sigma_i)^m \leq \eta \tag{4.17}$$

Where, $\bar{a}$ is the interception between the design S-N curve with the log N axis.

In this case nominal stresses were used.

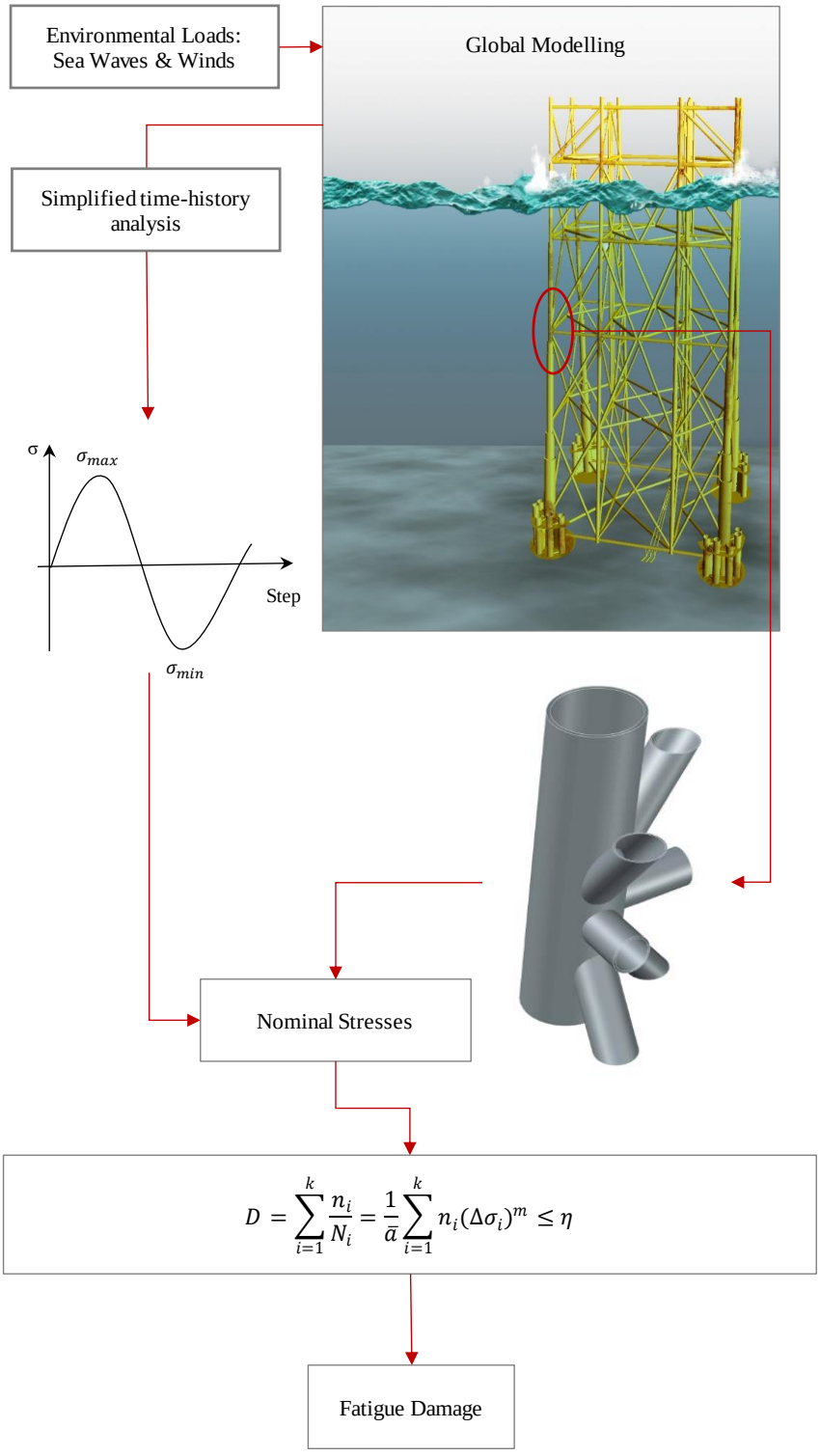

Figure 4.18 – Workflow for the miner rule simplified fatigue analysis using nominal stresses.

4.5.3.1 Fatigue damage results

In Table 4.15 the results for the fatigue damage accumulation analysis using nominal stresses are presented.

Table 4.15 – Fatigue damage results from damage accumulation using nominal stress

Plane	Member	Thickness	Step	$\Delta\sigma_{nom,0}$	$\Delta\sigma_{nom}$	n_0	N_f	D
-	-	mm	-	MPa	MPa	-	-	-
x-z	5110	40	80	63.96	71.93	326	7003381	4.65E-05
	5116	30	80	23.72	24.83	326	10000000	infinite life
	5112	25	80	37.17	37.17	326	10000000	infinite life
y-z	4939	35	80	98.00	106.60	326	1249470	2.61E-04
	4940	55	80	48.05	58.52	326	10000000	infinite life
	4938	25	80	121.08	121.08	326	852673	3.82E-04
x-z	5110	40	73	2.64	2.97	640568	10000000	infinite life
	5116	30	73	1.86	1.95	640568	10000000	infinite life
	5112	25	73	1.15	1.15	640568	10000000	infinite life
y-z	4939	35	73	3.83	4.17	640568	10000000	infinite life
	4940	55	73	2.36	2.87	640568	10000000	infinite life
	4938	25	73	2.60	2.60	640568	10000000	infinite life

Since every other wave load case results in an infinite life of the structure, because the level of stress is below the fatigue limit, those results are of no significance and so will not be included in this document.

4.6 FATIGUE ANALYSIS USING LOCAL APPROACHES

In [17], an estimation of probabilistic fatigue S-N curves for notched structural components is made, resulting in a probabilistic field from a strain-life model. This probabilistic ε-N field for S355 steel is presented in Fig. 4.19. In accordance to the authors findings, the Weibull field should not be used for high- and low-cycle fatigue lives [17].

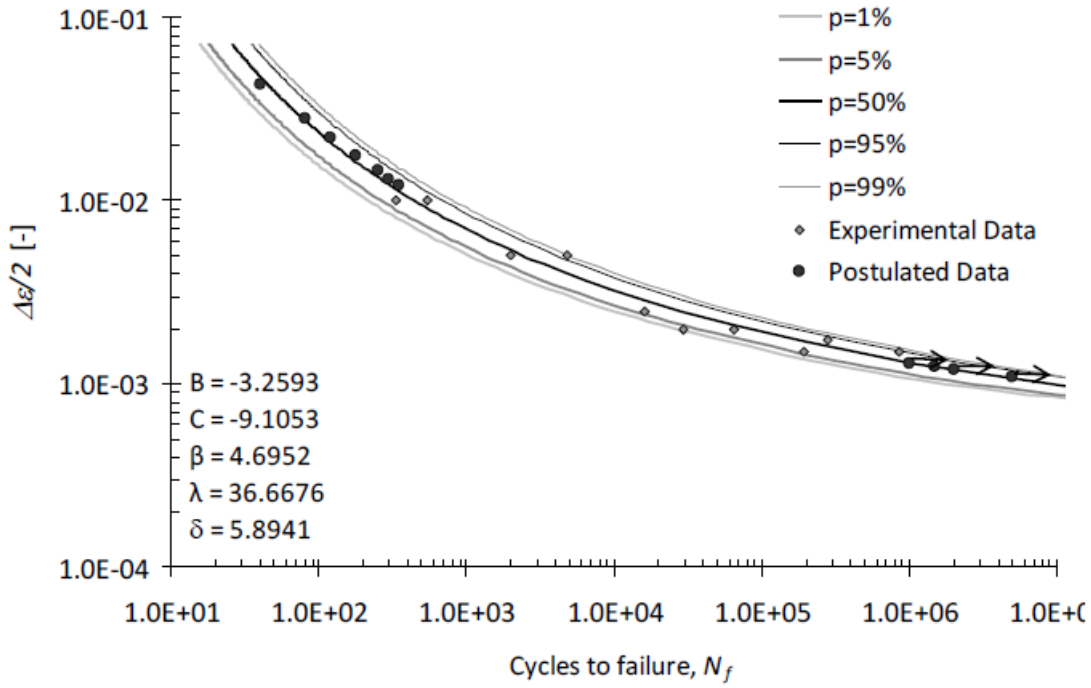

Figure 4.19 – Strain-life data and corresponding probabilistic ε-N field [17].

Neuber and Ramberg-Osgood approach was used alongside Coffin-Manson strain-based approach present in Eq. (4.14).

$$\frac{\Delta\sigma_l^2}{E} + 2\Delta\sigma_l\left(\frac{\Delta\sigma_l}{2K'}\right)^{\frac{1}{n'}} = \frac{k_t^2\Delta\sigma_{nom}^2}{E} \tag{4.12}$$

$$\Delta\varepsilon_l = \frac{\Delta\sigma_l}{E} + 2\left(\frac{\Delta\sigma_l}{2K'}\right)^{\frac{1}{n'}} \tag{4.13}$$

$$\frac{\Delta\varepsilon}{2} = \frac{\left(\sigma_f'\right)(2N_f)^b}{E} + \varepsilon_f' * (2N_f)^c \tag{4.14}$$

Since the curves are so close together this analysis will be made using the mean curve theory, were instead of the characteristic curve, a curve with p=0.50 will be used to calculate damage.

For this analysis the monotonic and cyclic elastoplastic properties of S355 steel were used and are presented in Table 4.16 and in Table 4.17 the Morrow constants for the same material.

Table 4.16 – Monotonic and cyclic elastoplastic properties of the S355 mild steel [27].

E	f_u	f_y	K′	n′
GPa	*MPa*	*MPa*	*MPa*	-
211.60	744.80	422.000	595.85	0.0757

Table 4.17 – Morrow constants of the S355 mild steel [27].

σ'_f	b	ε'_f	c
MPa	-	-	-
952.20	-0.0890	0.7371	-0.6640

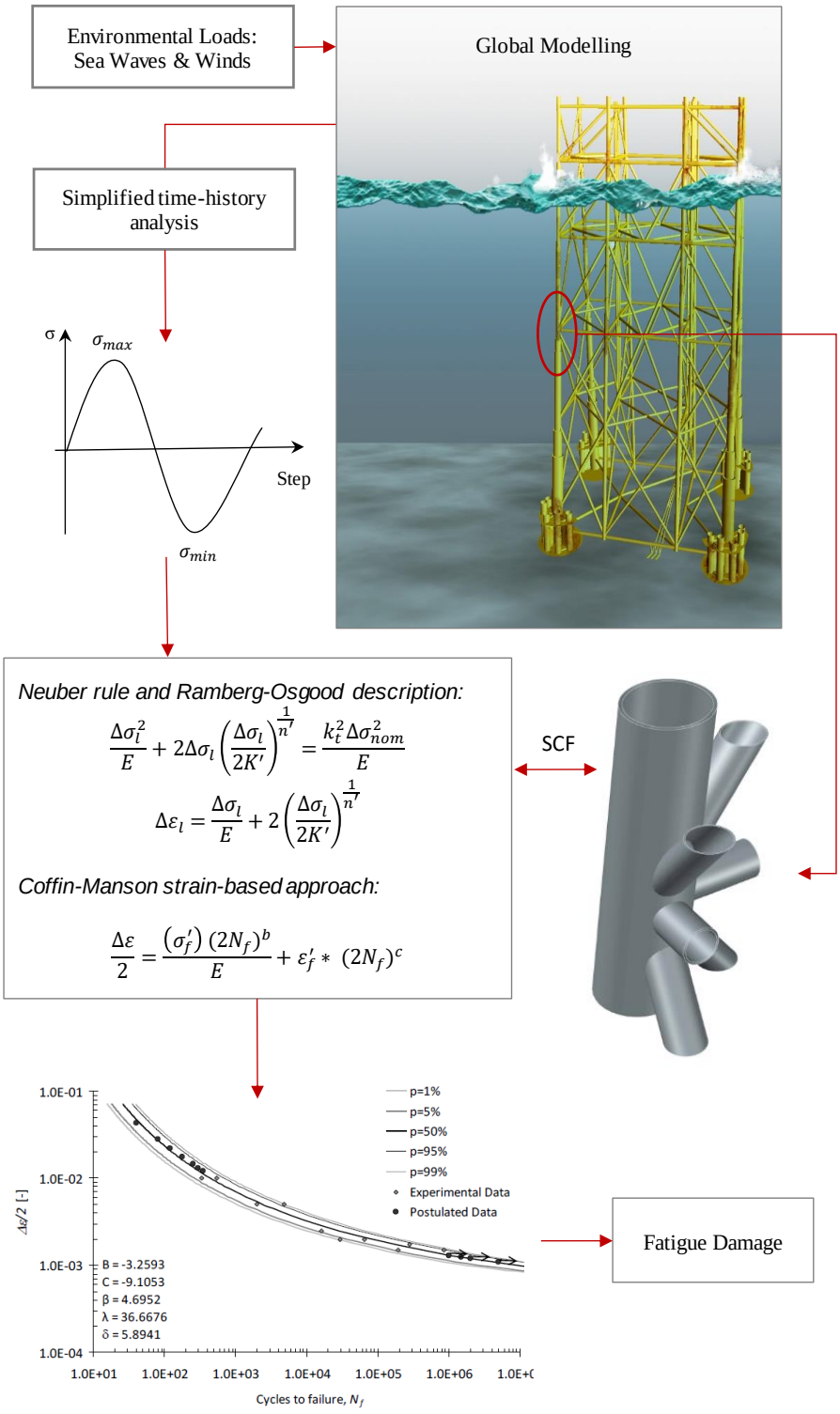

Figure 4.20 – Workflow for the fatigue analysis using local approaches.

4.6.1. Fatigue damage results

In Table 4.18 fatigue damage results using local approach are presented.

Table 4.18 – Fatigue damage results using local approach analysis

Plane	Member	Thickness	Step	SCF	$\Delta\sigma_{nom,0}$	$\Delta\sigma_{nom}$	$\Delta\sigma_{loc,elastoplastic}$	$\Delta\varepsilon_{loc,elastoplastic}$	n_0	$2N_f$	N_f	D
-	-	mm	-	-	MPa	MPa	MPa	-	-	-	-	-
x-z	5110	40	80	2.689338	63.96	71.93	193.46	9.14E-04	326	100000000000	50000000000	3.26E-07
	5116	30	80	3.785792	23.72	24.83	94.01	4.44E-04	326	100000000000	50000000000	3.26E-07
	5112	25	80	2.943858	37.17	37.17	109.44	5.17E-04	326	100000000000	50000000000	3.26E-07
y-z	4939	35	80	3.387385	98.00	106.60	361.08	1.71E-03	326	134949467	67474734	2.42E-04
	4940	55	80	4.980734	48.05	58.52	291.47	1.38E-03	326	1456538183	728269092	2.24E-05
	4938	25	80	4.597991	121.08	121.08	549.21	2.67E-03	326	1441577	720789	2.26E-02
x-z	5110	40	73	2.689338	2.64	2.97	0	0	640568	1E+11	50000000000	0.000641
	5116	30	73	3.785792	1.86	1.95	0	0	640568	1E+11	50000000000	0.000641
	5112	25	73	2.943858	1.15	1.15	0	0	640568	1E+11	50000000000	0.000641
y-z	4939	35	73	3.387385	3.83	4.17	0	0	640568	1E+11	50000000000	0.000641
	4940	55	73	4.980734	2.36	2.87	0	0	640568	1E+11	50000000000	0.000641
	4938	25	73	4.597991	2.60	2.60	0	0	640568	1E+11	50000000000	0.000641

All other results apart from the ones related to wave 80 and wave 73 are presented in the Annex F.

4.7 DISCUSSION AND RESULTS

Once the fatigue damage has been calculated it is possible to draw conclusion as to the remaining life of the structure. Since the damage was calculated for an expected life of 50 years, superior to that of most structures usually endure, it is without a doubt that there is no immediate danger of collapse due to fatigue.

The damage in all occasions except for the local approach, where the maximum damage occurs for element number 4938 with a loading corresponding to wave 80, is far lower than the maximum limit imposed of 0,1 for the usage factor. Regardless of the design fatigue factor chosen, all other fatigue damage values fall within safety limits.

When it comes to the local approach under a condition of loading correspondent to wave number 80, the value is 0.02, which is within the safety margins previously discussed. This value is superior to other analysis, this may be due to the fact that the curve chosen for the local approach is not only the mean curve, where in normal conditions a design curve should be taken, by dimensioning curve is understood one that sits below all values obtained or at least with a percentage of 95%. Furthermore, an argument could be made that the number of specimens used to determine the probabilistic field is not sufficient to account for data scatter and as such underlying error could be present resulting in a fatigue damage superior to what other approaches have demonstrated.

Since fatigue is a phenomenon of the material itself and the local approach is the only one to take that into consideration, then the gap between local approach and reality may in fact be smaller than when using any other type of analysis. Should be referred, that the local approach analysis was made using S355 steel which may result in a superior damage since he actual structure is composed of S420.

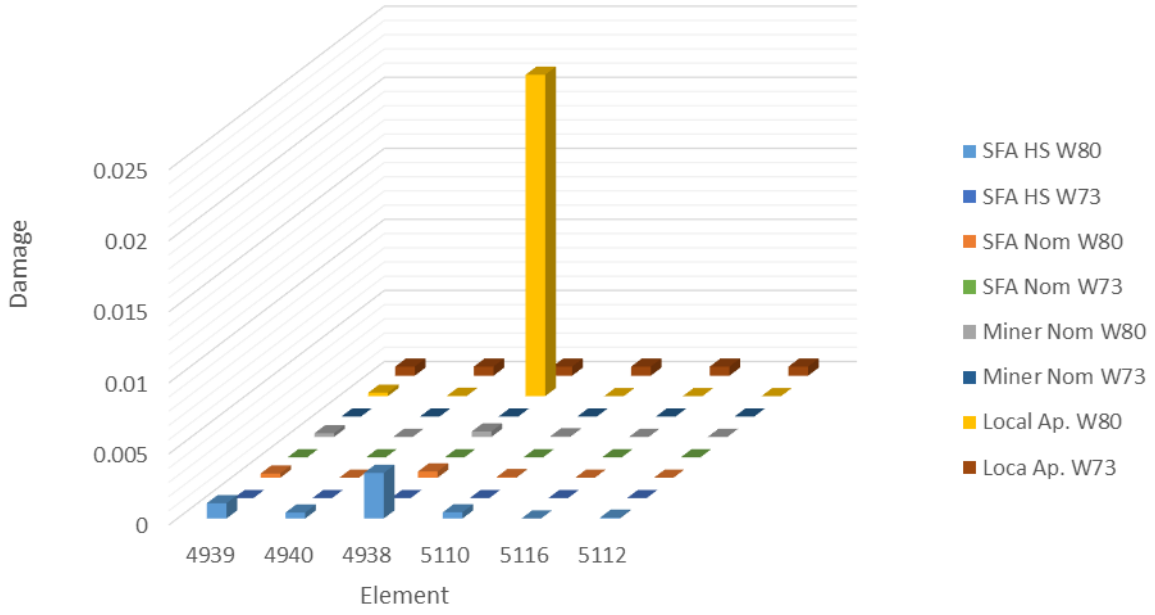

Figure 4.21 – Fatigue damage per element from every approach

5
Conclusions and Future Works

5.1 CONCLUSIONS

Throughout this work it has become clear the influence environmental actions have in an offshore structure and the strict dependency with the wave theory chosen.

Regarding the several wave theories studied, linear wave theory for an infinite water depth even though simple to obtain the wave kinematics, proved inaccurate to predict the proper level of normal force to be applied in the structure. If finite water depth theory were to be applied instead, it would produce a slightly more accurate even though not completely realistic portrait of marine conditions. There is no doubt that Stokes 5^{th} Order, more labour intensive without computerized assistance or abacus, provides the most accurate characterization of the waves.

For the reasons stated in point 4.7, the highest damage is present in element 4938 for wave number 80 under local approach with strain as the damage parameter. The damage obtained in this analysis is in fact lower than the usage factor but higher than other damage analysis which may be explained by the usage of the mean curve to obtain the number of fatigue life cycles for each stress level, which allied with a lower strength steel than the one used in the platform results in higher fatigue damage. These findings are similar to the ones obtained by Force Technology, leading to the conclusion that the degree of damage may be similar to the one experienced by the structure.

5.2 FUTURE WORKS

This work presents a wide analysis both the main contributing factor of fatigue for offshore structures as well as fatigue damage analysis possible of conducing, however, more could be done in both fronts.

A spectral analysis could be done by using Pierson Moskowitz and JONSWAP wave spectrum for the North Sea and a comparison to the wave kinematics and Morrison load force already presented in this work could be done.

It would also be relevant to conduct a local approach fatigue analysis using multiaxial fatigue damage parameters which would represent a more realistic stress state of the structure. For this, an experimental program could be drawn to achieve a S-N and ε-N curves for sea and water environment covering crack initiation in multiaxial loading in light of the works of Adedipe and European project FATHOMS using small scale specimens. For crack propagation CT and CTS specimens could be used and a combination of loading angles and phase/out-of-phase loading could be made for S355 as well as S420 covering mild and high strength steels.

To finalise, it is also recommended a numerical simulation of the critical joint for several load conditions to account for variation between parametric equations proposed for the stress concentration factors and reach an explanation as to why some of the stress concentration factors obtained in this work are below one.

REFERENCES

[1] A. E-10, "Standard Terminology Relating to Fatigue and Fracture Testing," 2010.

[2] W. Schütz, "A history of fatigue," Engineering fracture mechanics, vol. 54, no. 2, pp. 263-300, 1996.

[3] J. Schijve, "Fatigue of structures and materials in the 20th century and the state of the art," International Journal of fatigue, vol. 25, no. 8, pp. 679-702, 2003.

[4] J. Y. Mann, Bibliography on the fatigue of materials, components and structures. Elsevier, 2013.

[5] W. J. M. Rankine, "ON THE CAUSES OF THE UNEXPECTED BREAKAGE OF THE JOURNALS OF RAILWAY AXLES; AND ON THE MEANS OF PREVENTING SUCH ACCIDENTS BY OBSERVING THE LAW OF CONTINUITY IN THEIR CONSTRUCTION," in Minutes of the Proceedings of the Institution of Civil Engineers, 1843, vol. 2, no. 1843, pp. 105-107: Thomas Telford-ICE Virtual Library.

[6] O. Basquin, "The exponential law of endurance tests," in Proc Astm, 1910, vol. 10, pp. 625-630.

[7] R. I. Stephens, A. Fatemi, R. R. Stephens, and H. O. Fuchs, Metal fatigue in engineering. John Wiley & Sons, 2000.

[8] J. Schijve, Fatigue of structures and materials. Springer Science & Business Media, 2001.

[9] J. A. F. de Oliveira Correia, "An integral probabilistic approach for fatigue lifetime prediction of mechanical and structural components," Universidade do Porto (Portugal), 2015.

[10] F. Ellyin, Fatigue damage, crack growth and life prediction. Springer Science & Business Media, 2012.

[11] N. Frost and C. Phillips, "Studies in the formation and propagation of cracks in fatigue specimens," in Proc. Int. Conference on Fatigue of Metals, London, 1956.

[12] European Committee for Standardisation, Eurocode 3: Design of steel structures. EN 2003-1-9: fatigue, Brussels, Belgium, 2003.

[13] D. N. V. DNV, "Recommended practice DNVGL-RP-C203 fatigue design of offshore steel structures," 2016.

[14] A. B. o. S. ABS, "Guide for Fatigue Assessment of Offshore Structures," 2014.

[15] Correia, J.A.F.O., De Jesus, A.M.P., Fernández-Canteli, A. “A procedure to derive probabilistic fatigue crack propagation data”. Int J Struct Integr 3 (2) (2012) 158–183.

[16] Correia, J.A.F.O., De Jesus, A.M.P., Fernández-Canteli, A. “Local unified probabilistic model for fatigue crack initiation and propagation: Application to a notched geometry”. Eng Struct 52 (2013) 394–407.

[17] Correia, J.A.F.O., de Jesus, A.M.P., Fernández-Canteli, A., Calçada, R.A.B. “Modelling probabilistic fatigue crack propagation rates for a mild structural steel”. Frattura ed Integrita Strutturale, Volume 31, 1 January 2015, Pages 80-96.

[18] Sampayo, L.M.C.M.V., Monteiro, P.M.F., Correia, J.A.F.O., Xavier, J.M.C., De Jesus, A.M.P., Fernández-Canteli, A., Calçada, R.A.B. “Probabilistic S-N field assessment for a notched plate

made of puddle iron from the Eiffel bridge with an elliptical hole". Procedia Eng 114 (2015) 691–698.

[19] Huffman, P.J. "A strain energy based damage model for fatigue crack initiation and growth". International Journal of Fatigue 88 (2016) 197–204.

[20] Huffman, P., Correia, J.A.F.O., Mikheevskiy, S., De Jesus, A.M.P., Cicero, S., Fernández-Canteli, A., Berto, F., Glinka, G. "Fatigue evaluation of notched details based on unified local probabilistic approaches". International Symposium on Notch Fracture (ISNF2017), March 29th to 31st, 2017, Santander, Spain.

[21] Noroozi, A.H., Glinka, G., Lambert, S. "A two parameter driving force for fatigue crack growth analysis". International Journal of Fatigue 2005; 27: 1277-1296.

[22] Correia, J.A.F.O., Raposo, P., Muniz-Calvente, M., Blasón, S., Lesiuk, G., De Jesus, A.M.P., Moreira, P.M.G.P, Calçada, R.A.B., Fernández-Canteli, A. "A generalization of the fatigue Kohout-Věchet model for several fatigue damage parameters". Engineering Fracture Mechanics, 2017, in press.

[23] S. S. Manson, "Behavior of materials under conditions of thermal stress," 1954.

[24] L. F. Coffin Jr, "A study of the effects of cyclic thermal stresses on a ductile metal," trans. ASME, vol. 76, pp. 931-950, 1954.

[25] J. Morrow, "Cyclic plastic strain energy and fatigue of metals," in Internal friction, damping, and cyclic plasticity: ASTM International, 1965.

[26] M. Buciumeanu, L. Palaghian, A. Miranda, and F. Silva, "Fatigue life predictions including the Bauschinger effect," International Journal of Fatigue, vol. 33, no. 2, pp. 145-152, 2011.

[27] F. Öztürk, J. Correia, C. Rebelo, A. De Jesus, and L. S. da Silva, "Fatigue assessment of steel half-pipes bolted connections using local approaches," Procedia Structural Integrity, vol. 1, pp. 118-125, 2016.

[28] G. Lesiuk et al., "MULTIAXIAL FATIGUE BEHAVIOUR OF STRUCTURAL STEELS FOR FATIGUE DESIGN OF WIND TOWERS," on Wind Energy Harvesting, 2017.

[29] C. M. Branco and A. A. Fernandes, "Tavares de Castro,"," Fadiga de estruturas soldadas, 1999.

[30] A. Hobbacher, "International Institute of Welding Recommendations for fatigue design of welded joints and components," 2008.

[31] A. Romeijn, "Stress and strain concentration factors of welded multiplanar tubular joints," 1994.

[32] H. Ahmadi and A. Ghaffari, "Probabilistic assessment of degree of bending in tubular X-joints of offshore structures subjected to bending loads," Advances in Civil Engineering, vol. 2015, 2015.

[33] H. Ahmadi and S. Asoodeh, "Parametric study of geometrical effects on the degree of bending (DoB) in offshore tubular K-joints under out-of-plane bending loads," Applied Ocean Research, vol. 58, pp. 1-10, 2016.

[34] H. Ahmadi, M. A. Lotfollahi-Yaghin, and S. Asoodeh, "Degree of bending (DoB) in tubular K-joints of offshore structures subjected to in-plane bending (IPB) loads: study of geometrical effects and parametric formulation," Ocean Engineering, vol. 102, pp. 105-116, 2015.

[35] J. P. M. Ferreira, "Pre-strain effects on fatigue crack propagation behaviour of a pressure vessels steel," 2017.

[36] http://web.mit.edu/3.35/www/Lecture_notes/nlefm.pdf. 21-6-2018

[37] T. R. Gurney, Fatigue of welded structures. CUP Archive, 1979.

[38] P. Paris and F. Erdogan, "A critical analysis of crack propagation laws," Journal of basic engineering, vol. 85, no. 4, pp. 528-533, 1963.

[39] G. Lesiuk, P. Kucharski, J. Correia, A. De Jesus, C. Rebelo, and L. S. da Silva, "Mixed mode (I+ II) fatigue crack growth of long term operating bridge steel," Procedia Engineering, vol. 160, pp. 262-269, 2016.

[40] G. Lesiuk, P. Szata, D.Rozumek, Z. Marciniak, J.A.F.O. Correia and A.M.P. de Jesus, "Energy response of S355 and 41Cr4 steel during fatigue crack growth process", awaiting publication.

[41] O. Adedipe, F. Brennan, and A. Kolios, "Review of corrosion fatigue in offshore structures: Present status and challenges in the offshore wind sector," Renewable and Sustainable Energy Reviews, vol. 61, pp. 141-154, 2016.

[42] O. Adedipe, "Integrity of offshore structures," 2015.

[43] E. Mecozzi et al., "Fatigue behaviour of high-strength steel-welded joints in offshore and marine systems (FATHOMS)," Mecozzi, M. Lecca, S. Sorrentino-Office for Official Publ. of the European Communities, p. 179, 2010.

[44] A. Karolczuk and E. Macha, "Selection of the critical plane orientation in two-parameter multiaxial fatigue failure criterion under combined bending and torsion," Engineering Fracture Mechanics, vol. 75, no. 3-4, pp. 389-403, 2008.

[45] M. R. Khedmati, P. Rigo, A. Amrane, and M. Nazari, "Assessment of fatigue reliability for jacket-type offshore platforms considering dynamic behavior," in ASME 2013 32nd International Conference on Ocean, Offshore and Arctic Engineering, 2013, pp. V02BT02A050-V02BT02A050: American Society of Mechanical Engineers.

[46] A. Khalifa, S. Haggag Aboul, and M. Fayed, "Fatigue Assessment Analysis of Offshore Structures with Application to an Existing Platform in Suez Gulf, Egypt," World Applied Science Journal, vol. 30, pp. 1000-1019, 2014.

[47] O. Faltinsen, Sea loads on ships and offshore structures. Cambridge university press, 1993.

[48] A. Almar-Naess, Fatigue Handbook: Offshore Steel Structures. Tapir, 1985.

[49] N. Standard, "N-003," Actions and Action Effects, Rev, vol. 1, 2007.

[50] L. Skjelbreia and J. Hendrickson, "FIFTH ORDER GRAVITY WAVE THEORY," Coastal Engineering Proceedings, gravity waves; Airy theory; d/L parameter; fifth order gravity theory no. 7, 2011.

[51] http://www.civil.iitb.ac.in/~mcdeo/waves.html. 9-4-2018

[52] https://www.flow3d.com/modeling-capabilities/waves/. 20-6-2018

[53] S.-f. Zhang, C. Chen, Q.-x. Zhang, D.-m. Zhang, and F. Zhang, "Wave Loads Computation for Offshore Floating Hose Based on Partially Immersed Cylinder Model of Improved Morison Formula," The Open Petroleum Engineering Journal, vol. 8, no. 1, 2015.

[54] K. Edvardsen, "Forces on simplified offshore structures according to different wave models," University of Stavanger, Norway, 2015.

[55] J. Journee and J. Pinkster, "Introduction in ship hydromechanics," Delft University of Technology, p. 8, 2002.

[56] Ø. Arntsen and H. Krogstad, "Linear Wave Theory, Part A: Regular Waves," Department of Civil and Transport Engineering, NTNU, Trondheim, 2000.

[57] E. Bækkedal, "Alternative methods of realizing the sea spectrum for time-domain simulations of marine structures in irregular seas," Institutt for marin teknikk, 2014.

[58] J. Fenton, "Nonlinear wave theories," the Sea, vol. 9, no. 1, pp. 3-25, 1990.

[59] G. DNV, "Environmental conditions and environmental loads," Recommend Practice DNV-RP-C205, 2014.

[60] J. F. Wilson, Dynamics of offshore structures. John Wiley & Sons, 2003.

[61] https://www.offshore-mag.com/content/dam/offshore/print-articles/volume-77/05/2017-DeepwaterPoster-D6-Ads.pdf .21-6-2018

[62] S. Chakrabarti, Handbook of Offshore Engineering (2-volume set). Elsevier, 2005.

Annex A: Wave measurements

	Wave Period (T) - (s)																														
H(m)	**2-3**	**3-4**	**4-5**	**5-6**	**6-7**	**7-8**	**8-9**	**9-10**	**10-11**	**11-12**	**12-13**	**13-14**	**14-15**	**15-16**	**16-17**	**17-18**	**18-19**	**19-20**	**20-21**	**21-22**	**22-23**	**23-24**	**24-25**	**25-26**	**26-27**	**27-28**	**28-29**	**29-30**	**Sum**	%	Mean Period
0-1	43176	39532	40370	33154	23505	14890	8697	4831	2615	1396	739	389	204	107	57	30	16	8	4	2	1	1	0	0	0	0	0	0	**213726**	48.15	4.96
1-2	0	6997	16692	27095	29521	24227	16536	10086	5662	2984	1506	740	358	172	82	39	19	9	4	2	1	0	0	0	0	0	0	0	**142732**	32.16	6.95
2-3	0	469	2302	6091	9653	10566	8913	6208	3745	2041	1032	491	222	96	41	17	7	3	1	0	0	0	0	0	0	0	0	0	**51896**	11.69	7.91
3-4	0	0	355	1341	2941	4079	4063	3170	2069	1188	617	296	133	56	23	9	3	1	0	0	0	0	0	0	0	0	0	0	**20345**	4.58	8.55
4-5	0	0	0	319	826	1470	1758	1558	1102	659	347	167	75	32	13	5	2	1	0	0	0	0	0	0	0	0	0	0	**8334**	1.88	9.07
5-6	0	0	0	59	227	522	753	762	588	368	197	94	41	17	7	3	1	0	0	0	0	0	0	0	0	0	0	0	**3639**	0.82	9.49
6-7	0	0	0	11	61	180	315	367	311	206	113	54	23	9	4	1	1	0	0	0	0	0	0	0	0	0	0	0	**1657**	0.37	9.86
7-8	0	0	0	0	18	60	129	174	163	115	65	31	13	5	2	1	0	0	0	0	0	0	0	0	0	0	0	0	**777**	0.17	10.19
8-9	0	0	0	0	4	20	51	80	84	64	38	19	8	3	1	0	0	0	0	0	0	0	0	0	0	0	0	0	**372**	0.08	10.49
9-10	0	0	0	0	0	7	20	36	43	35	22	11	5	2	1	0	0	0	0	0	0	0	0	0	0	0	0	0	**181**	0.04	10.77
10-11	0	0	0	0	0	2	7	16	21	19	13	7	3	1	0	0	0	0	0	0	0	0	0	0	0	0	0	0	**90**	0.02	11.03
11-12	0	0	0	0	0	1	3	7	10	10	7	4	2	1	0	0	0	0	0	0	0	0	0	0	0	0	0	0	**45**	0.01	11.27
12-13	0	0	0	0	0	0	1	3	5	5	4	2	1	0	0	0	0	0	0	0	0	0	0	0	0	0	0	0	**23**	0.01	11.52
13-14	0	0	0	0	0	0	0	1	2	3	2	1	1	0	0	0	0	0	0	0	0	0	0	0	0	0	0	0	**12**	0.00	11.74
14-15	0	0	0	0	0	0	0	1	1	1	1	1	0	0	0	0	0	0	0	0	0	0	0	0	0	0	0	0	**6**	0.00	11.95
15-16	0	0	0	0	0	0	0	0	1	1	1	0	0	0	0	0	0	0	0	0	0	0	0	0	0	0	0	0	**3**	0.00	12.16
16-17	0	0	0	0	0	0	0	0	0	0	0	0	0	0	0	0	0	0	0	0	0	0	0	0	0	0	0	0	**2**	0.00	12.37
17-18	0	0	0	0	0	0	0	0	0	0	0	0	0	0	0	0	0	0	0	0	0	0	0	0	0	0	0	0	**1**	0.00	12.57
18-19	0	0	0	0	0	0	0	0	0	0	0	0	0	0	0	0	0	0	0	0	0	0	0	0	0	0	0	0	**0**	0.00	12.74
19-20	0	0	0	0	0	0	0	0	0	0	0	0	0	0	0	0	0	0	0	0	0	0	0	0	0	0	0	0	**0**	0.00	12.93
20-21	0	0	0	0	0	0	0	0	0	0	0	0	0	0	0	0	0	0	0	0	0	0	0	0	0	0	0	0	**0**	0.00	13.15
21-22	0	0	0	0	0	0	0	0	0	0	0	0	0	0	0	0	0	0	0	0	0	0	0	0	0	0	0	0	**0**	0.00	13.26
22-23	0	0	0	0	0	0	0	0	0	0	0	0	0	0	0	0	0	0	0	0	0	0	0	0	0	0	0	0	**0**	0.00	13.45
23-24	0	0	0	0	0	0	0	0	0	0	0	0	0	0	0	0	0	0	0	0	0	0	0	0	0	0	0	0	**0**	0.00	13.50
24-25	0	0	0	0	0	0	0	0	0	0	0	0	0	0	0	0	0	0	0	0	0	0	0	0	0	0	0	0	**0**	0.00	13.71
25-26	0	0	0	0	0	0	0	0	0	0	0	0	0	0	0	0	0	0	0	0	0	0	0	0	0	0	0	0	**0**	0.00	13.64
26-27	0	0	0	0	0	0	0	0	0	0	0	0	0	0	0	0	0	0	0	0	0	0	0	0	0	0	0	0	**0**	0.00	14.00
27-28	0	0	0	0	0	0	0	0	0	0	0	0	0	0	0	0	0	0	0	0	0	0	0	0	0	0	0	0	**0**	0.00	14.00
Sum	**43176**	**46997**	**59720**	**68071**	**66755**	**56024**	**41246**	**27301**	**16424**	**9097**	**4705**	**2307**	**1089**	**503**	**230**	**106**	**49**	**22**	**10**	**5**	**2**	**1**	**0**	**0**	**0**	**0**	**0**	**0**	**443841**		
%	9.73	10.59	13.46	15.34	15.04	12.62	9.29	6.15	3.70	2.05	1.06	0.52	0.25	0.11	0.05	0.02	0.01	0.01	0.00	0.00	0.00	0.00	0.00	0.00	0.00	0.00	0.00	0.00			
Mean Height	0.50	0.67	0.87	1.16	1.44	1.71	1.98	2.21	2.40	2.53	2.57	2.55	2.45	2.32	2.15	1.97	1.79	1.62	1.46	1.32	1.20	1.10	1.00	0.93	0.83	0.82	0.75	0.70			

Table A.1 – Scatter diagram with mean period and mean wave height for 0°

	Wave Period (T) - (s)																														
H(m)	**2-3**	**3-4**	**4-5**	**5-6**	**6-7**	**7-8**	**8-9**	**9-10**	**10-11**	**11-12**	**12-13**	**13-14**	**14-15**	**15-16**	**16-17**	**17-18**	**18-19**	**19-20**	**20-21**	**21-22**	**22-23**	**23-24**	**24-25**	**25-26**	**26-27**	**27-28**	**28-29**	**29-30**	**Sum**	%	Mean Period
0-1	41551	38044	38851	31907	22621	14330	8370	4649	2517	1344	711	374	196	103	54	29	15	8	4	2	1	1	0	0	0	0	0	0	**205684**	48.15	4.96
1-2	0	6734	16064	26076	28410	23316	15913	9707	5449	2872	1449	712	345	165	79	38	18	8	4	2	1	0	0	0	0	0	0	0	**137362**	32.16	6.95
2-3	0	451	2216	5861	9289	10169	8578	5974	3604	1964	993	472	213	93	39	16	7	3	1	0	0	0	0	0	0	0	0	0	**49943**	11.69	7.91
3-4	0	0	342	1290	2830	3925	3911	3051	1992	1143	594	285	128	54	22	8	3	1	0	0	0	0	0	0	0	0	0	0	**19579**	4.58	8.55
4-5	0	0	0	307	795	1415	1691	1499	1061	634	334	161	72	31	12	5	2	1	0	0	0	0	0	0	0	0	0	0	**8020**	1.88	9.07
5-6	0	0	0	57	219	502	725	734	566	354	189	90	40	16	7	3	1	0	0	0	0	0	0	0	0	0	0	0	**3503**	0.82	9.49
6-7	0	0	0	11	58	173	303	353	300	198	109	52	22	9	3	1	0	0	0	0	0	0	0	0	0	0	0	0	**1594**	0.37	9.86
7-8	0	0	0	0	17	58	124	167	157	111	63	30	13	5	2	1	0	0	0	0	0	0	0	0	0	0	0	0	**747**	0.17	10.19
8-9	0	0	0	0	4	19	49	77	81	62	36	18	8	3	1	0	0	0	0	0	0	0	0	0	0	0	0	0	**358**	0.08	10.49
9-10	0	0	0	0	0	7	19	35	41	34	21	11	5	2	1	0	0	0	0	0	0	0	0	0	0	0	0	0	**175**	0.04	10.77
10-11	0	0	0	0	0	2	7	15	20	18	12	6	3	1	0	0	0	0	0	0	0	0	0	0	0	0	0	0	**86**	0.02	11.03
11-12	0	0	0	0	0	1	3	7	10	10	7	4	2	1	0	0	0	0	0	0	0	0	0	0	0	0	0	0	**43**	0.01	11.27
12-13	0	0	0	0	0	0	1	3	5	5	4	2	1	0	0	0	0	0	0	0	0	0	0	0	0	0	0	0	**22**	0.01	11.52
13-14	0	0	0	0	0	0	0	1	2	3	2	1	1	0	0	0	0	0	0	0	0	0	0	0	0	0	0	0	**11**	0.00	11.74
14-15	0	0	0	0	0	0	0	0	1	1	1	1	0	0	0	0	0	0	0	0	0	0	0	0	0	0	0	0	**6**	0.00	11.95
15-16	0	0	0	0	0	0	0	0	0	1	1	0	0	0	0	0	0	0	0	0	0	0	0	0	0	0	0	0	**3**	0.00	12.16
16-17	0	0	0	0	0	0	0	0	0	0	0	0	0	0	0	0	0	0	0	0	0	0	0	0	0	0	0	0	**2**	0.00	12.37
17-18	0	0	0	0	0	0	0	0	0	0	0	0	0	0	0	0	0	0	0	0	0	0	0	0	0	0	0	0	**1**	0.00	12.57
18-19	0	0	0	0	0	0	0	0	0	0	0	0	0	0	0	0	0	0	0	0	0	0	0	0	0	0	0	0	**0**	0.00	12.74
19-20	0	0	0	0	0	0	0	0	0	0	0	0	0	0	0	0	0	0	0	0	0	0	0	0	0	0	0	0	**0**	0.00	12.93
20-21	0	0	0	0	0	0	0	0	0	0	0	0	0	0	0	0	0	0	0	0	0	0	0	0	0	0	0	0	**0**	0.00	13.15
21-22	0	0	0	0	0	0	0	0	0	0	0	0	0	0	0	0	0	0	0	0	0	0	0	0	0	0	0	0	**0**	0.00	13.26
22-23	0	0	0	0	0	0	0	0	0	0	0	0	0	0	0	0	0	0	0	0	0	0	0	0	0	0	0	0	**0**	0.00	13.45
23-24	0	0	0	0	0	0	0	0	0	0	0	0	0	0	0	0	0	0	0	0	0	0	0	0	0	0	0	0	**0**	0.00	13.50
24-25	0	0	0	0	0	0	0	0	0	0	0	0	0	0	0	0	0	0	0	0	0	0	0	0	0	0	0	0	**0**	0.00	13.71
25-26	0	0	0	0	0	0	0	0	0	0	0	0	0	0	0	0	0	0	0	0	0	0	0	0	0	0	0	0	**0**	0.00	13.64
26-27	0	0	0	0	0	0	0	0	0	0	0	0	0	0	0	0	0	0	0	0	0	0	0	0	0	0	0	0	**0**	0.00	14.00
27-28	0	0	0	0	0	0	0	0	0	0	0	0	0	0	0	0	0	0	0	0	0	0	0	0	0	0	0	0	**0**	0.00	14.00
Sum	**41551**	**45229**	**57473**	**65509**	**64243**	**53916**	**39694**	**26273**	**15806**	**8755**	**4528**	**2220**	**1048**	**484**	**222**	**102**	**47**	**22**	**10**	**4**	**2**	**1**	**0**	**0**	**0**	**0**	**0**	**0**	**427140**		
%	9.73	10.59	13.46	15.34	15.04	12.62	9.29	6.15	3.70	2.05	1.06	0.52	0.25	0.11	0.05	0.02	0.01	0.01	0.00	0.00	0.00	0.00	0.00	0.00	0.00	0.00	0.00	0.00			
Mean Height	0.50	0.67	0.87	1.16	1.44	1.71	1.98	2.21	2.40	2.53	2.57	2.55	2.45	2.32	2.15	1.97	1.79	1.62	1.46	1.32	1.20	1.10	1.00	0.93	0.83	0.82	0.75	0.70			

Table A.2 – Scatter diagram with mean period and mean wave height for 30°

	Wave Period (T) - (s)																														
H(m)	2-3	3-4	4-5	5-6	6-7	7-8	8-9	9-10	10-11	11-12	12-13	13-14	14-15	15-16	16-17	17-18	18-19	19-20	20-21	21-22	22-23	23-24	24-25	25-26	26-27	27-28	28-29	29-30	Sum	%	Mean Period
0-1	36283	33221	33926	27862	19753	12513	7308	4060	2198	1173	621	327	172	90	48	25	13	7	4	2	1	0	0	0	0	0	0	0	**179608**	48.15	4.96
1-2	0	5880	14027	22770	24808	20360	13896	8476	4758	2508	1266	622	301	144	69	33	16	7	3	1	1	0	0	0	0	0	0	0	**119947**	32.16	6.95
2-3	0	394	1935	5118	8112	8880	7490	5217	3147	1715	867	412	186	81	34	14	6	2	1	0	0	0	0	0	0	0	0	0	**43612**	11.69	7.91
3-4	0	0	298	1127	2471	3428	3415	2664	1739	998	519	248	112	47	19	7	3	1	0	0	0	0	0	0	0	0	0	0	**17097**	4.58	8.55
4-5	0	0	0	268	694	1235	1477	1309	926	554	292	140	63	27	11	4	2	1	0	0	0	0	0	0	0	0	0	0	**7003**	1.88	9.07
5-6	0	0	0	50	191	439	633	641	494	309	165	79	35	14	6	2	1	0	0	0	0	0	0	0	0	0	0	0	**3059**	0.82	9.49
6-7	0	0	0	9	51	151	265	309	262	173	95	45	19	8	3	1	0	0	0	0	0	0	0	0	0	0	0	0	**1392**	0.37	9.86
7-8	0	0	0	0	15	51	108	146	137	97	55	26	11	4	2	1	0	0	0	0	0	0	0	0	0	0	0	0	**653**	0.17	10.19
8-9	0	0	0	0	4	16	43	67	71	54	32	16	7	3	1	0	0	0	0	0	0	0	0	0	0	0	0	0	**313**	0.08	10.49
9-10	0	0	0	0	0	6	17	30	36	30	18	9	4	2	1	0	0	0	0	0	0	0	0	0	0	0	0	0	**152**	0.04	10.77
10-11	0	0	0	0	0	2	6	13	18	16	11	6	2	1	0	0	0	0	0	0	0	0	0	0	0	0	0	0	**75**	0.02	11.03
11-12	0	0	0	0	0	1	2	6	9	9	6	3	1	1	0	0	0	0	0	0	0	0	0	0	0	0	0	0	**38**	0.01	11.27
12-13	0	0	0	0	0	0	1	2	4	5	3	2	1	0	0	0	0	0	0	0	0	0	0	0	0	0	0	0	**19**	0.01	11.52
13-14	0	0	0	0	0	0	0	1	2	2	2	1	1	0	0	0	0	0	0	0	0	0	0	0	0	0	0	0	**10**	0.00	11.74
14-15	0	0	0	0	0	0	0	0	1	1	1	1	0	0	0	0	0	0	0	0	0	0	0	0	0	0	0	0	**5**	0.00	11.95
15-16	0	0	0	0	0	0	0	0	0	1	1	0	0	0	0	0	0	0	0	0	0	0	0	0	0	0	0	0	**3**	0.00	12.16
16-17	0	0	0	0	0	0	0	0	0	0	0	0	0	0	0	0	0	0	0	0	0	0	0	0	0	0	0	0	**1**	0.00	12.37
17-18	0	0	0	0	0	0	0	0	0	0	0	0	0	0	0	0	0	0	0	0	0	0	0	0	0	0	0	0	**1**	0.00	12.57
18-19	0	0	0	0	0	0	0	0	0	0	0	0	0	0	0	0	0	0	0	0	0	0	0	0	0	0	0	0	**0**	0.00	12.74
19-20	0	0	0	0	0	0	0	0	0	0	0	0	0	0	0	0	0	0	0	0	0	0	0	0	0	0	0	0	**0**	0.00	12.93
20-21	0	0	0	0	0	0	0	0	0	0	0	0	0	0	0	0	0	0	0	0	0	0	0	0	0	0	0	0	**0**	0.00	13.15
21-22	0	0	0	0	0	0	0	0	0	0	0	0	0	0	0	0	0	0	0	0	0	0	0	0	0	0	0	0	**0**	0.00	13.26
22-23	0	0	0	0	0	0	0	0	0	0	0	0	0	0	0	0	0	0	0	0	0	0	0	0	0	0	0	0	**0**	0.00	13.45
23-24	0	0	0	0	0	0	0	0	0	0	0	0	0	0	0	0	0	0	0	0	0	0	0	0	0	0	0	0	**0**	0.00	13.50
24-25	0	0	0	0	0	0	0	0	0	0	0	0	0	0	0	0	0	0	0	0	0	0	0	0	0	0	0	0	**0**	0.00	13.71
25-26	0	0	0	0	0	0	0	0	0	0	0	0	0	0	0	0	0	0	0	0	0	0	0	0	0	0	0	0	**0**	0.00	13.64
26-27	0	0	0	0	0	0	0	0	0	0	0	0	0	0	0	0	0	0	0	0	0	0	0	0	0	0	0	0	**0**	0.00	14.00
27-28	0	0	0	0	0	0	0	0	0	0	0	0	0	0	0	0	0	0	0	0	0	0	0	0	0	0	0	0	**0**	0.00	14.00
Sum	**36283**	**39495**	**50186**	**57204**	**56099**	**47081**	**34662**	**22942**	**13802**	**7645**	**3954**	**1939**	**915**	**423**	**194**	**89**	**41**	**19**	**9**	**4**	**2**	**1**	**0**	**0**	**0**	**0**	**0**	**0**	**372988**		
%	9.73	10.59	13.46	15.34	15.04	12.62	9.29	6.15	3.70	2.05	1.06	0.52	0.25	0.11	0.05	0.02	0.01	0.01	0.00	0.00	0.00	0.00	0.00	0.00	0.00	0.00	0.00	0.00			
Mean Height	0.50	0.67	0.87	1.16	1.44	1.71	1.98	2.21	2.40	2.53	2.57	2.55	2.45	2.32	2.15	1.97	1.79	1.62	1.46	1.32	1.20	1.10	1.00	0.93	0.83	0.82	0.75	0.70			

Table A.3 – Scatter diagram with mean period and mean wave height for 60°

	Wave Period (T) - (s)																														
H(m)	**2-3**	**3-4**	**4-5**	**5-6**	**6-7**	**7-8**	**8-9**	**9-10**	**10-11**	**11-12**	**12-13**	**13-14**	**14-15**	**15-16**	**16-17**	**17-18**	**18-19**	**19-20**	**20-21**	**21-22**	**22-23**	**23-24**	**24-25**	**25-26**	**26-27**	**27-28**	**28-29**	**29-30**	**Sum**	%	Mean Period
0-1	34462	31553	32223	26463	18761	11885	6942	3856	2087	1115	590	310	163	86	45	24	13	7	3	2	1	0	0	0	0	0	0	0	**170591**	48.15	4.96
1-2	0	5585	13323	21627	23563	19338	13198	8051	4519	2382	1202	591	286	137	66	31	15	7	3	1	1	0	0	0	0	0	0	0	**113926**	32.16	6.95
2-3	0	374	1838	4861	7704	8434	7114	4955	2989	1629	824	392	177	77	33	13	5	2	1	0	0	0	0	0	0	0	0	0	**41422**	11.69	7.91
3-4	0	0	283	1070	2347	3256	3243	2530	1652	948	493	236	106	45	18	7	3	1	0	0	0	0	0	0	0	0	0	0	**16239**	4.58	8.55
4-5	0	0	0	255	659	1173	1403	1243	880	526	277	133	60	25	10	4	1	1	0	0	0	0	0	0	0	0	0	0	**6652**	1.88	9.07
5-6	0	0	0	47	181	417	601	609	469	294	157	75	33	14	5	2	1	0	0	0	0	0	0	0	0	0	0	0	**2905**	0.82	9.49
6-7	0	0	0	9	48	144	252	293	249	165	90	43	18	7	3	1	0	0	0	0	0	0	0	0	0	0	0	0	**1322**	0.37	9.86
7-8	0	0	0	0	14	48	103	139	130	92	52	25	11	4	2	1	0	0	0	0	0	0	0	0	0	0	0	0	**620**	0.17	10.19
8-9	0	0	0	0	3	16	41	64	67	51	30	15	6	2	1	0	0	0	0	0	0	0	0	0	0	0	0	0	**297**	0.08	10.49
9-10	0	0	0	0	0	6	16	29	34	28	17	9	4	1	1	0	0	0	0	0	0	0	0	0	0	0	0	0	**145**	0.04	10.77
10-11	0	0	0	0	0	2	6	13	17	15	10	5	2	1	0	0	0	0	0	0	0	0	0	0	0	0	0	0	**72**	0.02	11.03
11-12	0	0	0	0	0	1	2	6	8	8	6	3	1	1	0	0	0	0	0	0	0	0	0	0	0	0	0	0	**36**	0.01	11.27
12-13	0	0	0	0	0	0	1	2	4	4	3	2	1	0	0	0	0	0	0	0	0	0	0	0	0	0	0	0	**18**	0.01	11.52
13-14	0	0	0	0	0	0	0	1	2	2	2	1	1	0	0	0	0	0	0	0	0	0	0	0	0	0	0	0	**9**	0.00	11.74
14-15	0	0	0	0	0	0	0	0	1	1	1	1	0	0	0	0	0	0	0	0	0	0	0	0	0	0	0	0	**5**	0.00	11.95
15-16	0	0	0	0	0	0	0	0	0	1	1	0	0	0	0	0	0	0	0	0	0	0	0	0	0	0	0	0	**3**	0.00	12.16
16-17	0	0	0	0	0	0	0	0	0	0	0	0	0	0	0	0	0	0	0	0	0	0	0	0	0	0	0	0	**1**	0.00	12.37
17-18	0	0	0	0	0	0	0	0	0	0	0	0	0	0	0	0	0	0	0	0	0	0	0	0	0	0	0	0	**1**	0.00	12.57
18-19	0	0	0	0	0	0	0	0	0	0	0	0	0	0	0	0	0	0	0	0	0	0	0	0	0	0	0	0	**0**	0.00	12.74
19-20	0	0	0	0	0	0	0	0	0	0	0	0	0	0	0	0	0	0	0	0	0	0	0	0	0	0	0	0	**0**	0.00	12.93
20-21	0	0	0	0	0	0	0	0	0	0	0	0	0	0	0	0	0	0	0	0	0	0	0	0	0	0	0	0	**0**	0.00	13.15
21-22	0	0	0	0	0	0	0	0	0	0	0	0	0	0	0	0	0	0	0	0	0	0	0	0	0	0	0	0	**0**	0.00	13.26
22-23	0	0	0	0	0	0	0	0	0	0	0	0	0	0	0	0	0	0	0	0	0	0	0	0	0	0	0	0	**0**	0.00	13.45
23-24	0	0	0	0	0	0	0	0	0	0	0	0	0	0	0	0	0	0	0	0	0	0	0	0	0	0	0	0	**0**	0.00	13.50
24-25	0	0	0	0	0	0	0	0	0	0	0	0	0	0	0	0	0	0	0	0	0	0	0	0	0	0	0	0	**0**	0.00	13.71
25-26	0	0	0	0	0	0	0	0	0	0	0	0	0	0	0	0	0	0	0	0	0	0	0	0	0	0	0	0	**0**	0.00	13.64
26-27	0	0	0	0	0	0	0	0	0	0	0	0	0	0	0	0	0	0	0	0	0	0	0	0	0	0	0	0	**0**	0.00	14.00
27-28	0	0	0	0	0	0	0	0	0	0	0	0	0	0	0	0	0	0	0	0	0	0	0	0	0	0	0	0	**0**	0.00	14.00
Sum	**34462**	**37512**	**47667**	**54332**	**53282**	**44717**	**32922**	**21791**	**13109**	**7261**	**3756**	**1841**	**869**	**401**	**184**	**84**	**39**	**18**	**8**	**4**	**2**	**1**	**0**	**0**	**0**	**0**	**0**	**0**	**354263**		
%	9.73	10.59	13.46	15.34	15.04	12.62	9.29	6.15	3.70	2.05	1.06	0.52	0.25	0.11	0.05	0.02	0.01	0.01	0.00	0.00	0.00	0.00	0.00	0.00	0.00	0.00	0.00	0.00			
Mean Height	0.50	0.67	0.87	1.16	1.44	1.71	1.98	2.21	2.40	2.53	2.57	2.55	2.45	2.32	2.15	1.97	1.79	1.62	1.46	1.32	1.20	1.10	1.00	0.93	0.83	0.82	0.75	0.70			

Table A.4 – Scatter diagram with mean period and mean wave height for 90°

	Wave Period (T) - (s)																														
H(m)	2-3	3-4	4-5	5-6	6-7	7-8	8-9	9-10	10-11	11-12	12-13	13-14	14-15	15-16	16-17	17-18	18-19	19-20	20-21	21-22	22-23	23-24	24-25	25-26	26-27	27-28	28-29	29-30	Sum	%	Mean Period
0-1	45588	41740	42626	35007	24819	15722	9183	5101	2761	1474	780	411	216	113	60	32	17	9	5	2	1	1	0	0	0	0	0	0	**225667**	48.15	4.96
1-2	0	7388	17625	28609	31170	25581	17459	10650	5979	3151	1590	782	378	181	87	41	20	9	4	2	1	0	0	0	0	0	0	0	**150707**	32.16	6.95
2-3	0	495	2431	6431	10192	11157	9411	6555	3954	2155	1090	518	234	102	43	18	7	3	1	0	0	0	0	0	0	0	0	0	**54796**	11.69	7.91
3-4	0	0	375	1416	3105	4307	4291	3347	2185	1255	652	312	140	60	24	9	3	1	0	0	0	0	0	0	0	0	0	0	**21482**	4.58	8.55
4-5	0	0	0	337	872	1552	1856	1645	1164	696	367	176	79	33	14	5	2	1	0	0	0	0	0	0	0	0	0	0	**8799**	1.88	9.07
5-6	0	0	0	62	240	551	795	805	621	388	208	99	44	18	7	3	1	0	0	0	0	0	0	0	0	0	0	0	**3843**	0.82	9.49
6-7	0	0	0	12	64	190	333	388	329	218	119	57	24	10	4	1	1	0	0	0	0	0	0	0	0	0	0	0	**1749**	0.37	9.86
7-8	0	0	0	0	19	63	136	183	172	122	69	33	14	6	2	1	0	0	0	0	0	0	0	0	0	0	0	0	**820**	0.17	10.19
8-9	0	0	0	0	5	21	54	85	89	67	40	20	8	3	1	0	0	0	0	0	0	0	0	0	0	0	0	0	**393**	0.08	10.49
9-10	0	0	0	0	0	8	21	38	45	37	23	12	5	2	1	0	0	0	0	0	0	0	0	0	0	0	0	0	**192**	0.04	10.77
10-11	0	0	0	0	0	2	8	17	22	20	13	7	3	1	0	0	0	0	0	0	0	0	0	0	0	0	0	0	**95**	0.02	11.03
11-12	0	0	0	0	0	1	3	7	11	11	8	4	2	1	0	0	0	0	0	0	0	0	0	0	0	0	0	0	**47**	0.01	11.27
12-13	0	0	0	0	0	0	1	3	5	6	4	2	1	0	0	0	0	0	0	0	0	0	0	0	0	0	0	0	**24**	0.01	11.52
13-14	0	0	0	0	0	0	0	1	3	3	2	1	1	0	0	0	0	0	0	0	0	0	0	0	0	0	0	0	**12**	0.00	11.74
14-15	0	0	0	0	0	0	0	1	1	2	1	1	0	0	0	0	0	0	0	0	0	0	0	0	0	0	0	0	**6**	0.00	11.95
15-16	0	0	0	0	0	0	0	0	1	1	1	1	0	0	0	0	0	0	0	0	0	0	0	0	0	0	0	0	**3**	0.00	12.16
16-17	0	0	0	0	0	0	0	0	0	0	0	0	0	0	0	0	0	0	0	0	0	0	0	0	0	0	0	0	**2**	0.00	12.37
17-18	0	0	0	0	0	0	0	0	0	0	0	0	0	0	0	0	0	0	0	0	0	0	0	0	0	0	0	0	**1**	0.00	12.57
18-19	0	0	0	0	0	0	0	0	0	0	0	0	0	0	0	0	0	0	0	0	0	0	0	0	0	0	0	0	**0**	0.00	12.74
19-20	0	0	0	0	0	0	0	0	0	0	0	0	0	0	0	0	0	0	0	0	0	0	0	0	0	0	0	0	**0**	0.00	12.93
20-21	0	0	0	0	0	0	0	0	0	0	0	0	0	0	0	0	0	0	0	0	0	0	0	0	0	0	0	0	**0**	0.00	13.15
21-22	0	0	0	0	0	0	0	0	0	0	0	0	0	0	0	0	0	0	0	0	0	0	0	0	0	0	0	0	**0**	0.00	13.26
22-23	0	0	0	0	0	0	0	0	0	0	0	0	0	0	0	0	0	0	0	0	0	0	0	0	0	0	0	0	**0**	0.00	13.45
23-24	0	0	0	0	0	0	0	0	0	0	0	0	0	0	0	0	0	0	0	0	0	0	0	0	0	0	0	0	**0**	0.00	13.50
24-25	0	0	0	0	0	0	0	0	0	0	0	0	0	0	0	0	0	0	0	0	0	0	0	0	0	0	0	0	**0**	0.00	13.71
25-26	0	0	0	0	0	0	0	0	0	0	0	0	0	0	0	0	0	0	0	0	0	0	0	0	0	0	0	0	**0**	0.00	13.64
26-27	0	0	0	0	0	0	0	0	0	0	0	0	0	0	0	0	0	0	0	0	0	0	0	0	0	0	0	0	**0**	0.00	14.00
27-28	0	0	0	0	0	0	0	0	0	0	0	0	0	0	0	0	0	0	0	0	0	0	0	0	0	0	0	0	**0**	0.00	14.00
Sum	**45588**	**49623**	**63056**	**71874**	**70485**	**59155**	**43551**	**28826**	**17341**	**9606**	**4968**	**2436**	**1150**	**531**	**243**	**111**	**51**	**24**	**11**	**5**	**2**	**1**	**0**	**0**	**0**	**0**	**0**	**0**	**468639**		
%	9.73	10.59	13.46	15.34	15.04	12.62	9.29	6.15	3.70	2.05	1.06	0.52	0.25	0.11	0.05	0.02	0.01	0.01	0.00	0.00	0.00	0.00	0.00	0.00	0.00	0.00	0.00	0.00			
Mean Height	0.50	0.67	0.87	1.16	1.44	1.71	1.98	2.21	2.40	2.53	2.57	2.55	2.45	2.32	2.15	1.97	1.79	1.62	1.46	1.32	1.20	1.10	1.00	0.93	0.83	0.82	0.75	0.70			

Table A.5 – Scatter diagram with mean period and mean wave height for 120°

	Wave Period (T) - (s)																														
H(m)	**2-3**	**3-4**	**4-5**	**5-6**	**6-7**	**7-8**	**8-9**	**9-10**	**10-11**	**11-12**	**12-13**	**13-14**	**14-15**	**15-16**	**16-17**	**17-18**	**18-19**	**19-20**	**20-21**	**21-22**	**22-23**	**23-24**	**24-25**	**25-26**	**26-27**	**27-28**	**28-29**	**29-30**	**Sum**	%	Mean Period
0-1	7582	6942	7089	5822	4127	2615	1527	848	459	245	130	68	36	19	10	5	3	1	1	0	0	0	0	0	0	0	0	0	**37530**	48.15	4.96
1-2	0	1229	2931	4758	5184	4254	2904	1771	994	524	264	130	63	30	14	7	3	2	1	0	0	0	0	0	0	0	0	0	**25064**	32.16	6.95
2-3	0	82	404	1070	1695	1855	1565	1090	658	358	181	86	39	17	7	3	1	0	0	0	0	0	0	0	0	0	0	0	**9113**	11.69	7.91
3-4	0	0	62	235	516	716	714	557	363	209	108	52	23	10	4	2	1	0	0	0	0	0	0	0	0	0	0	0	**3573**	4.58	8.55
4-5	0	0	0	56	145	258	309	274	194	116	61	29	13	6	2	1	0	0	0	0	0	0	0	0	0	0	0	0	**1463**	1.88	9.07
5-6	0	0	0	10	40	92	132	134	103	65	35	16	7	3	1	0	0	0	0	0	0	0	0	0	0	0	0	0	**639**	0.82	9.49
6-7	0	0	0	2	11	32	55	64	55	36	20	9	4	2	1	0	0	0	0	0	0	0	0	0	0	0	0	0	**291**	0.37	9.86
7-8	0	0	0	0	3	11	23	30	29	20	11	6	2	1	0	0	0	0	0	0	0	0	0	0	0	0	0	0	**136**	0.17	10.19
8-9	0	0	0	0	1	3	9	14	15	11	7	3	1	1	0	0	0	0	0	0	0	0	0	0	0	0	0	0	**65**	0.08	10.49
9-10	0	0	0	0	0	1	3	6	7	6	4	2	1	0	0	0	0	0	0	0	0	0	0	0	0	0	0	0	**32**	0.04	10.77
10-11	0	0	0	0	0	0	1	3	4	3	2	1	1	0	0	0	0	0	0	0	0	0	0	0	0	0	0	0	**16**	0.02	11.03
11-12	0	0	0	0	0	0	0	1	2	2	1	1	0	0	0	0	0	0	0	0	0	0	0	0	0	0	0	0	**8**	0.01	11.27
12-13	0	0	0	0	0	0	0	1	1	1	1	0	0	0	0	0	0	0	0	0	0	0	0	0	0	0	0	0	**4**	0.01	11.52
13-14	0	0	0	0	0	0	0	0	0	1	0	0	0	0	0	0	0	0	0	0	0	0	0	0	0	0	0	0	**2**	0.00	11.74
14-15	0	0	0	0	0	0	0	0	0	0	0	0	0	0	0	0	0	0	0	0	0	0	0	0	0	0	0	0	**1**	0.00	11.95
15-16	0	0	0	0	0	0	0	0	0	0	0	0	0	0	0	0	0	0	0	0	0	0	0	0	0	0	0	0	**1**	0.00	12.16
16-17	0	0	0	0	0	0	0	0	0	0	0	0	0	0	0	0	0	0	0	0	0	0	0	0	0	0	0	0	**0**	0.00	12.37
17-18	0	0	0	0	0	0	0	0	0	0	0	0	0	0	0	0	0	0	0	0	0	0	0	0	0	0	0	0	**0**	0.00	12.57
18-19	0	0	0	0	0	0	0	0	0	0	0	0	0	0	0	0	0	0	0	0	0	0	0	0	0	0	0	0	**0**	0.00	12.74
19-20	0	0	0	0	0	0	0	0	0	0	0	0	0	0	0	0	0	0	0	0	0	0	0	0	0	0	0	0	**0**	0.00	12.93
20-21	0	0	0	0	0	0	0	0	0	0	0	0	0	0	0	0	0	0	0	0	0	0	0	0	0	0	0	0	**0**	0.00	13.15
21-22	0	0	0	0	0	0	0	0	0	0	0	0	0	0	0	0	0	0	0	0	0	0	0	0	0	0	0	0	**0**	0.00	13.26
22-23	0	0	0	0	0	0	0	0	0	0	0	0	0	0	0	0	0	0	0	0	0	0	0	0	0	0	0	0	**0**	0.00	13.45
23-24	0	0	0	0	0	0	0	0	0	0	0	0	0	0	0	0	0	0	0	0	0	0	0	0	0	0	0	0	**0**	0.00	13.50
24-25	0	0	0	0	0	0	0	0	0	0	0	0	0	0	0	0	0	0	0	0	0	0	0	0	0	0	0	0	**0**	0.00	13.71
25-26	0	0	0	0	0	0	0	0	0	0	0	0	0	0	0	0	0	0	0	0	0	0	0	0	0	0	0	0	**0**	0.00	13.64
26-27	0	0	0	0	0	0	0	0	0	0	0	0	0	0	0	0	0	0	0	0	0	0	0	0	0	0	0	0	**0**	0.00	14.00
27-28	0	0	0	0	0	0	0	0	0	0	0	0	0	0	0	0	0	0	0	0	0	0	0	0	0	0	0	0	**0**	0.00	14.00
Sum	**7582**	**8253**	**10487**	**11953**	**11722**	**9838**	**7243**	**4794**	**2884**	**1597**	**826**	**405**	**191**	**88**	**40**	**19**	**9**	**4**	**2**	**1**	**0**	**0**	**0**	**0**	**0**	**0**	**0**	**0**	**77938**		
%	9.73	10.59	13.46	15.34	15.04	12.62	9.29	6.15	3.70	2.05	1.06	0.52	0.25	0.11	0.05	0.02	0.01	0.01	0.00	0.00	0.00	0.00	0.00	0.00	0.00	0.00	0.00	0.00			
Mean Height	0.50	0.67	0.87	1.16	1.44	1.71	1.98	2.21	2.40	2.53	2.57	2.55	2.45	2.32	2.15	1.97	1.79	1.62	1.46	1.32	1.20	1.10	1.00	0.93	0.83	0.82	0.75	0.70			

Table A.6 – Scatter diagram with mean period and mean wave height for 150°

	Wave Period (T) - (s)																														
H(m)	2-3	3-4	4-5	5-6	6-7	7-8	8-9	9-10	10-11	11-12	12-13	13-14	14-15	15-16	16-17	17-18	18-19	19-20	20-21	21-22	22-23	23-24	24-25	25-26	26-27	27-28	28-29	29-30	Sum	%	Mean Period
0-1	4726	4327	4419	3629	2573	1630	952	529	286	153	81	43	22	12	6	3	2	1	0	0	0	0	0	0	0	0	0	0	**23395**	48.15	4.96
1-2	0	766	1827	2966	3231	2652	1810	1104	620	327	165	81	39	19	9	4	2	1	0	0	0	0	0	0	0	0	0	0	**15624**	32.16	6.95
2-3	0	51	252	667	1057	1157	976	680	410	223	113	54	24	11	4	2	1	0	0	0	0	0	0	0	0	0	0	0	**5681**	11.69	7.91
3-4	0	0	39	147	322	446	445	347	227	130	68	32	15	6	2	1	0	0	0	0	0	0	0	0	0	0	0	0	**2227**	4.58	8.55
4-5	0	0	0	35	90	161	192	171	121	72	38	18	8	3	1	1	0	0	0	0	0	0	0	0	0	0	0	0	**912**	1.88	9.07
5-6	0	0	0	6	25	57	82	83	64	40	22	10	5	2	1	0	0	0	0	0	0	0	0	0	0	0	0	0	**398**	0.82	9.49
6-7	0	0	0	1	7	20	34	40	34	23	12	6	3	1	0	0	0	0	0	0	0	0	0	0	0	0	0	0	**181**	0.37	9.86
7-8	0	0	0	0	2	7	14	19	18	13	7	3	1	1	0	0	0	0	0	0	0	0	0	0	0	0	0	0	**85**	0.17	10.19
8-9	0	0	0	0	0	2	6	9	9	7	4	2	1	0	0	0	0	0	0	0	0	0	0	0	0	0	0	0	**41**	0.08	10.49
9-10	0	0	0	0	0	1	2	4	5	4	2	1	1	0	0	0	0	0	0	0	0	0	0	0	0	0	0	0	**20**	0.04	10.77
10-11	0	0	0	0	0	0	1	2	2	2	1	1	0	0	0	0	0	0	0	0	0	0	0	0	0	0	0	0	**10**	0.02	11.03
11-12	0	0	0	0	0	0	0	1	1	1	1	0	0	0	0	0	0	0	0	0	0	0	0	0	0	0	0	0	**5**	0.01	11.27
12-13	0	0	0	0	0	0	0	0	1	1	0	0	0	0	0	0	0	0	0	0	0	0	0	0	0	0	0	0	**2**	0.01	11.52
13-14	0	0	0	0	0	0	0	0	0	0	0	0	0	0	0	0	0	0	0	0	0	0	0	0	0	0	0	0	**1**	0.00	11.74
14-15	0	0	0	0	0	0	0	0	0	0	0	0	0	0	0	0	0	0	0	0	0	0	0	0	0	0	0	0	**1**	0.00	11.95
15-16	0	0	0	0	0	0	0	0	0	0	0	0	0	0	0	0	0	0	0	0	0	0	0	0	0	0	0	0	**0**	0.00	12.16
16-17	0	0	0	0	0	0	0	0	0	0	0	0	0	0	0	0	0	0	0	0	0	0	0	0	0	0	0	0	**0**	0.00	12.37
17-18	0	0	0	0	0	0	0	0	0	0	0	0	0	0	0	0	0	0	0	0	0	0	0	0	0	0	0	0	**0**	0.00	12.57
18-19	0	0	0	0	0	0	0	0	0	0	0	0	0	0	0	0	0	0	0	0	0	0	0	0	0	0	0	0	**0**	0.00	12.74
19-20	0	0	0	0	0	0	0	0	0	0	0	0	0	0	0	0	0	0	0	0	0	0	0	0	0	0	0	0	**0**	0.00	12.93
20-21	0	0	0	0	0	0	0	0	0	0	0	0	0	0	0	0	0	0	0	0	0	0	0	0	0	0	0	0	**0**	0.00	13.15
21-22	0	0	0	0	0	0	0	0	0	0	0	0	0	0	0	0	0	0	0	0	0	0	0	0	0	0	0	0	**0**	0.00	13.26
22-23	0	0	0	0	0	0	0	0	0	0	0	0	0	0	0	0	0	0	0	0	0	0	0	0	0	0	0	0	**0**	0.00	13.45
23-24	0	0	0	0	0	0	0	0	0	0	0	0	0	0	0	0	0	0	0	0	0	0	0	0	0	0	0	0	**0**	0.00	13.50
24-25	0	0	0	0	0	0	0	0	0	0	0	0	0	0	0	0	0	0	0	0	0	0	0	0	0	0	0	0	**0**	0.00	13.71
25-26	0	0	0	0	0	0	0	0	0	0	0	0	0	0	0	0	0	0	0	0	0	0	0	0	0	0	0	0	**0**	0.00	13.64
26-27	0	0	0	0	0	0	0	0	0	0	0	0	0	0	0	0	0	0	0	0	0	0	0	0	0	0	0	0	**0**	0.00	14.00
27-28	0	0	0	0	0	0	0	0	0	0	0	0	0	0	0	0	0	0	0	0	0	0	0	0	0	0	0	0	**0**	0.00	14.00
Sum	**4726**	**5145**	**6537**	**7451**	**7307**	**6133**	**4515**	**2988**	**1798**	**996**	**515**	**253**	**119**	**55**	**25**	**12**	**5**	**2**	**1**	**1**	**0**	**0**	**0**	**0**	**0**	**0**	**0**	**0**	**48585**		
%	9.73	10.59	13.46	15.34	15.04	12.62	9.29	6.15	3.70	2.05	1.06	0.52	0.25	0.11	0.05	0.02	0.01	0.01	0.00	0.00	0.00	0.00	0.00	0.00	0.00	0.00	0.00	0.00			
Mean Height	0.50	0.67	0.87	1.16	1.44	1.71	1.98	2.21	2.40	2.53	2.57	2.55	2.45	2.32	2.15	1.97	1.79	1.62	1.46	1.32	1.20	1.10	1.00	0.93	0.83	0.82	0.75	0.70			

Table A.7 – Scatter diagram with mean period and mean wave height for 180°

	Wave Period (T) - (s)																														
H(m)	**2-3**	**3-4**	**4-5**	**5-6**	**6-7**	**7-8**	**8-9**	**9-10**	**10-11**	**11-12**	**12-13**	**13-14**	**14-15**	**15-16**	**16-17**	**17-18**	**18-19**	**19-20**	**20-21**	**21-22**	**22-23**	**23-24**	**24-25**	**25-26**	**26-27**	**27-28**	**28-29**	**29-30**	**Sum**	%	Mean Period
0-1	6449	5905	6030	4952	3511	2224	1299	722	391	209	110	58	30	16	8	4	2	1	1	0	0	0	0	0	0	0	0	0	**31925**	48.15	4.96
1-2	0	1045	2493	4047	4410	3619	2470	1507	846	446	225	111	53	26	12	6	3	1	1	0	0	0	0	0	0	0	0	0	**21320**	32.16	6.95
2-3	0	70	344	910	1442	1578	1331	927	559	305	154	73	33	14	6	3	1	0	0	0	0	0	0	0	0	0	0	0	**7752**	11.69	7.91
3-4	0	0	53	200	439	609	607	474	309	177	92	44	20	8	3	1	0	0	0	0	0	0	0	0	0	0	0	0	**3039**	4.58	8.55
4-5	0	0	0	48	123	220	263	233	165	98	52	25	11	5	2	1	0	0	0	0	0	0	0	0	0	0	0	0	**1245**	1.88	9.07
5-6	0	0	0	9	34	78	112	114	88	55	29	14	6	3	1	0	0	0	0	0	0	0	0	0	0	0	0	0	**544**	0.82	9.49
6-7	0	0	0	2	9	27	47	55	47	31	17	8	3	1	1	0	0	0	0	0	0	0	0	0	0	0	0	0	**247**	0.37	9.86
7-8	0	0	0	0	3	9	19	26	24	17	10	5	2	1	0	0	0	0	0	0	0	0	0	0	0	0	0	0	**116**	0.17	10.19
8-9	0	0	0	0	1	3	8	12	13	10	6	3	1	0	0	0	0	0	0	0	0	0	0	0	0	0	0	0	**56**	0.08	10.49
9-10	0	0	0	0	0	1	3	5	6	5	3	2	1	0	0	0	0	0	0	0	0	0	0	0	0	0	0	0	**27**	0.04	10.77
10-11	0	0	0	0	0	0	1	2	3	3	2	1	0	0	0	0	0	0	0	0	0	0	0	0	0	0	0	0	**13**	0.02	11.03
11-12	0	0	0	0	0	0	0	1	2	2	1	1	0	0	0	0	0	0	0	0	0	0	0	0	0	0	0	0	**7**	0.01	11.27
12-13	0	0	0	0	0	0	0	0	1	1	1	0	0	0	0	0	0	0	0	0	0	0	0	0	0	0	0	0	**3**	0.01	11.52
13-14	0	0	0	0	0	0	0	0	0	0	0	0	0	0	0	0	0	0	0	0	0	0	0	0	0	0	0	0	**2**	0.00	11.74
14-15	0	0	0	0	0	0	0	0	0	0	0	0	0	0	0	0	0	0	0	0	0	0	0	0	0	0	0	0	**1**	0.00	11.95
15-16	0	0	0	0	0	0	0	0	0	0	0	0	0	0	0	0	0	0	0	0	0	0	0	0	0	0	0	0	**0**	0.00	12.16
16-17	0	0	0	0	0	0	0	0	0	0	0	0	0	0	0	0	0	0	0	0	0	0	0	0	0	0	0	0	**0**	0.00	12.37
17-18	0	0	0	0	0	0	0	0	0	0	0	0	0	0	0	0	0	0	0	0	0	0	0	0	0	0	0	0	**0**	0.00	12.57
18-19	0	0	0	0	0	0	0	0	0	0	0	0	0	0	0	0	0	0	0	0	0	0	0	0	0	0	0	0	**0**	0.00	12.74
19-20	0	0	0	0	0	0	0	0	0	0	0	0	0	0	0	0	0	0	0	0	0	0	0	0	0	0	0	0	**0**	0.00	12.93
20-21	0	0	0	0	0	0	0	0	0	0	0	0	0	0	0	0	0	0	0	0	0	0	0	0	0	0	0	0	**0**	0.00	13.15
21-22	0	0	0	0	0	0	0	0	0	0	0	0	0	0	0	0	0	0	0	0	0	0	0	0	0	0	0	0	**0**	0.00	13.26
22-23	0	0	0	0	0	0	0	0	0	0	0	0	0	0	0	0	0	0	0	0	0	0	0	0	0	0	0	0	**0**	0.00	13.45
23-24	0	0	0	0	0	0	0	0	0	0	0	0	0	0	0	0	0	0	0	0	0	0	0	0	0	0	0	0	**0**	0.00	13.50
24-25	0	0	0	0	0	0	0	0	0	0	0	0	0	0	0	0	0	0	0	0	0	0	0	0	0	0	0	0	**0**	0.00	13.71
25-26	0	0	0	0	0	0	0	0	0	0	0	0	0	0	0	0	0	0	0	0	0	0	0	0	0	0	0	0	**0**	0.00	13.64
26-27	0	0	0	0	0	0	0	0	0	0	0	0	0	0	0	0	0	0	0	0	0	0	0	0	0	0	0	0	**0**	0.00	14.00
27-28	0	0	0	0	0	0	0	0	0	0	0	0	0	0	0	0	0	0	0	0	0	0	0	0	0	0	0	0	**0**	0.00	14.00
Sum	**6449**	**7020**	**8921**	**10168**	**9971**	**8369**	**6161**	**4078**	**2453**	**1359**	**703**	**345**	**163**	**75**	**34**	**16**	**7**	**3**	**2**	**1**	**0**	**0**	**0**	**0**	**0**	**0**	**0**	**0**	**66298**		
%	9.73	10.59	13.46	15.34	15.04	12.62	9.29	6.15	3.70	2.05	1.06	0.52	0.25	0.11	0.05	0.02	0.01	0.01	0.00	0.00	0.00	0.00	0.00	0.00	0.00	0.00	0.00	0.00			
Mean Height	0.50	0.67	0.87	1.16	1.44	1.71	1.98	2.21	2.40	2.53	2.57	2.55	2.45	2.32	2.15	1.97	1.79	1.62	1.46	1.32	1.20	1.10	1.00	0.93	0.83	0.82	0.75	0.70			

Table A.8 – Scatter diagram with mean period and mean wave height for 210°

	Wave Period (T) - (s)																														
H(m)	2-3	3-4	4-5	5-6	6-7	7-8	8-9	9-10	10-11	11-12	12-13	13-14	14-15	15-16	16-17	17-18	18-19	19-20	20-21	21-22	22-23	23-24	24-25	25-26	26-27	27-28	28-29	29-30	Sum	%	Mean Period
0-1	76505	70048	71534	58748	41650	26385	15410	8561	4634	2474	1309	689	362	190	100	53	28	15	8	4	2	1	0	0	0	0	0	0	**378711**	48.15	4.96
1-2	0	12399	29578	48011	52309	42930	29300	17872	10033	5287	2669	1312	635	305	146	70	33	15	7	3	1	1	0	0	0	0	0	0	**252915**	32.16	6.95
2-3	0	830	4079	10792	17104	18723	15793	11000	6635	3616	1829	869	393	171	72	30	12	5	2	1	0	0	0	0	0	0	0	0	**91957**	11.69	7.91
3-4	0	0	629	2376	5211	7227	7200	5617	3667	2105	1093	524	235	100	40	16	6	2	1	0	0	0	0	0	0	0	0	0	**36050**	4.58	8.55
4-5	0	0	0	566	1464	2605	3114	2760	1953	1168	616	296	133	56	23	9	3	1	0	0	0	0	0	0	0	0	0	0	**14767**	1.88	9.07
5-6	0	0	0	105	403	925	1334	1351	1042	652	349	166	73	30	12	5	2	1	0	0	0	0	0	0	0	0	0	0	**6449**	0.82	9.49
6-7	0	0	0	20	108	319	558	651	552	365	200	95	41	17	6	2	1	0	0	0	0	0	0	0	0	0	0	0	**2936**	0.37	9.86
7-8	0	0	0	0	31	107	228	307	289	204	116	56	24	9	3	1	0	0	0	0	0	0	0	0	0	0	0	0	**1376**	0.17	10.19
8-9	0	0	0	0	8	35	91	142	149	113	67	33	14	5	2	1	0	0	0	0	0	0	0	0	0	0	0	0	**659**	0.08	10.49
9-10	0	0	0	0	0	13	35	64	76	62	39	19	8	3	1	0	0	0	0	0	0	0	0	0	0	0	0	0	**321**	0.04	10.77
10-11	0	0	0	0	0	4	13	28	38	34	22	12	5	2	1	0	0	0	0	0	0	0	0	0	0	0	0	0	**159**	0.02	11.03
11-12	0	0	0	0	0	1	5	12	18	18	13	7	3	1	0	0	0	0	0	0	0	0	0	0	0	0	0	0	**80**	0.01	11.27
12-13	0	0	0	0	0	0	2	5	9	10	7	4	2	1	0	0	0	0	0	0	0	0	0	0	0	0	0	0	**40**	0.01	11.52
13-14	0	0	0	0	0	0	1	2	4	5	4	2	1	0	0	0	0	0	0	0	0	0	0	0	0	0	0	0	**21**	0.00	11.74
14-15	0	0	0	0	0	0	0	1	2	3	2	1	1	0	0	0	0	0	0	0	0	0	0	0	0	0	0	0	**11**	0.00	11.95
15-16	0	0	0	0	0	0	0	0	1	1	1	1	0	0	0	0	0	0	0	0	0	0	0	0	0	0	0	0	**6**	0.00	12.16
16-17	0	0	0	0	0	0	0	0	0	1	1	0	0	0	0	0	0	0	0	0	0	0	0	0	0	0	0	0	**3**	0.00	12.37
17-18	0	0	0	0	0	0	0	0	0	0	0	0	0	0	0	0	0	0	0	0	0	0	0	0	0	0	0	0	**2**	0.00	12.57
18-19	0	0	0	0	0	0	0	0	0	0	0	0	0	0	0	0	0	0	0	0	0	0	0	0	0	0	0	0	**1**	0.00	12.74
19-20	0	0	0	0	0	0	0	0	0	0	0	0	0	0	0	0	0	0	0	0	0	0	0	0	0	0	0	0	**0**	0.00	12.93
20-21	0	0	0	0	0	0	0	0	0	0	0	0	0	0	0	0	0	0	0	0	0	0	0	0	0	0	0	0	**0**	0.00	13.15
21-22	0	0	0	0	0	0	0	0	0	0	0	0	0	0	0	0	0	0	0	0	0	0	0	0	0	0	0	0	**0**	0.00	13.26
22-23	0	0	0	0	0	0	0	0	0	0	0	0	0	0	0	0	0	0	0	0	0	0	0	0	0	0	0	0	**0**	0.00	13.45
23-24	0	0	0	0	0	0	0	0	0	0	0	0	0	0	0	0	0	0	0	0	0	0	0	0	0	0	0	0	**0**	0.00	13.50
24-25	0	0	0	0	0	0	0	0	0	0	0	0	0	0	0	0	0	0	0	0	0	0	0	0	0	0	0	0	**0**	0.00	13.71
25-26	0	0	0	0	0	0	0	0	0	0	0	0	0	0	0	0	0	0	0	0	0	0	0	0	0	0	0	0	**0**	0.00	13.64
26-27	0	0	0	0	0	0	0	0	0	0	0	0	0	0	0	0	0	0	0	0	0	0	0	0	0	0	0	0	**0**	0.00	14.00
27-28	0	0	0	0	0	0	0	0	0	0	0	0	0	0	0	0	0	0	0	0	0	0	0	0	0	0	0	0	**0**	0.00	14.00
Sum	**76505**	**83277**	**105820**	**120618**	**118287**	**99272**	**73086**	**48375**	**29102**	**16120**	**8338**	**4088**	**1930**	**891**	**408**	**187**	**86**	**40**	**18**	**8**	**4**	**2**	**1**	**0**	**0**	**0**	**0**	**0**	**786464**		
%	9.73	10.59	13.46	15.34	15.04	12.62	9.29	6.15	3.70	2.05	1.06	0.52	0.25	0.11	0.05	0.02	0.01	0.01	0.00	0.00	0.00	0.00	0.00	0.00	0.00	0.00	0.00	0.00			
Mean Height	0.50	0.67	0.87	1.16	1.44	1.71	1.98	2.21	2.40	2.53	2.57	2.55	2.45	2.32	2.15	1.97	1.79	1.62	1.46	1.32	1.20	1.10	1.00	0.93	0.83	0.82	0.75	0.70			

Table A.9 – Scatter diagram with mean period and mean wave height for 240°

	Wave Period (T) - (s)																														
H(m)	2-3	3-4	4-5	5-6	6-7	7-8	8-9	9-10	10-11	11-12	12-13	13-14	14-15	15-16	16-17	17-18	18-19	19-20	20-21	21-22	22-23	23-24	24-25	25-26	26-27	27-28	28-29	29-30	Sum	%	Mean Period
0-1	77588	71040	72547	59580	42240	26759	15628	8682	4699	2509	1328	699	367	193	102	54	28	15	8	4	2	1	0	0	0	0	0	0	**384073**	48.15	4.96
1-2	0	12574	29996	48691	53049	43538	29715	18125	10175	5362	2706	1330	644	309	148	71	34	16	7	3	1	1	0	0	0	0	0	0	**256495**	32.16	6.95
2-3	0	842	4137	10945	17346	18988	16017	11156	6729	3667	1854	882	398	173	73	30	12	5	2	1	0	0	0	0	0	0	0	0	**93259**	11.69	7.91
3-4	0	0	638	2409	5285	7330	7302	5697	3719	2135	1109	531	239	101	41	16	6	2	1	0	0	0	0	0	0	0	0	0	**36560**	4.58	8.55
4-5	0	0	0	574	1485	2642	3158	2799	1981	1185	624	300	135	57	23	9	3	1	0	0	0	0	0	0	0	0	0	0	**14976**	1.88	9.07
5-6	0	0	0	106	408	938	1353	1370	1056	661	354	169	74	31	12	5	2	1	0	0	0	0	0	0	0	0	0	0	**6540**	0.82	9.49
6-7	0	0	0	20	109	323	566	660	560	371	203	97	42	17	6	2	1	0	0	0	0	0	0	0	0	0	0	0	**2977**	0.37	9.86
7-8	0	0	0	0	32	108	231	312	293	207	117	56	24	9	4	1	0	0	0	0	0	0	0	0	0	0	0	0	**1396**	0.17	10.19
8-9	0	0	0	0	8	35	92	144	151	115	68	33	14	5	2	1	0	0	0	0	0	0	0	0	0	0	0	0	**669**	0.08	10.49
9-10	0	0	0	0	0	13	36	65	77	63	39	20	8	3	1	0	0	0	0	0	0	0	0	0	0	0	0	0	**326**	0.04	10.77
10-11	0	0	0	0	0	4	13	29	38	34	23	12	5	2	1	0	0	0	0	0	0	0	0	0	0	0	0	0	**161**	0.02	11.03
11-12	0	0	0	0	0	1	5	12	19	18	13	7	3	1	0	0	0	0	0	0	0	0	0	0	0	0	0	0	**81**	0.01	11.27
12-13	0	0	0	0	0	0	2	5	9	10	7	4	2	1	0	0	0	0	0	0	0	0	0	0	0	0	0	0	**41**	0.01	11.52
13-14	0	0	0	0	0	0	1	2	4	5	4	2	1	0	0	0	0	0	0	0	0	0	0	0	0	0	0	0	**21**	0.00	11.74
14-15	0	0	0	0	0	0	0	1	2	3	2	1	1	0	0	0	0	0	0	0	0	0	0	0	0	0	0	0	**11**	0.00	11.95
15-16	0	0	0	0	0	0	0	0	1	1	1	1	0	0	0	0	0	0	0	0	0	0	0	0	0	0	0	0	**6**	0.00	12.16
16-17	0	0	0	0	0	0	0	0	0	1	1	1	0	0	0	0	0	0	0	0	0	0	0	0	0	0	0	0	**3**	0.00	12.37
17-18	0	0	0	0	0	0	0	0	0	0	0	0	0	0	0	0	0	0	0	0	0	0	0	0	0	0	0	0	**2**	0.00	12.57
18-19	0	0	0	0	0	0	0	0	0	0	0	0	0	0	0	0	0	0	0	0	0	0	0	0	0	0	0	0	**1**	0.00	12.74
19-20	0	0	0	0	0	0	0	0	0	0	0	0	0	0	0	0	0	0	0	0	0	0	0	0	0	0	0	0	**0**	0.00	12.93
20-21	0	0	0	0	0	0	0	0	0	0	0	0	0	0	0	0	0	0	0	0	0	0	0	0	0	0	0	0	**0**	0.00	13.15
21-22	0	0	0	0	0	0	0	0	0	0	0	0	0	0	0	0	0	0	0	0	0	0	0	0	0	0	0	0	**0**	0.00	13.26
22-23	0	0	0	0	0	0	0	0	0	0	0	0	0	0	0	0	0	0	0	0	0	0	0	0	0	0	0	0	**0**	0.00	13.45
23-24	0	0	0	0	0	0	0	0	0	0	0	0	0	0	0	0	0	0	0	0	0	0	0	0	0	0	0	0	**0**	0.00	13.50
24-25	0	0	0	0	0	0	0	0	0	0	0	0	0	0	0	0	0	0	0	0	0	0	0	0	0	0	0	0	**0**	0.00	13.71
25-26	0	0	0	0	0	0	0	0	0	0	0	0	0	0	0	0	0	0	0	0	0	0	0	0	0	0	0	0	**0**	0.00	13.64
26-27	0	0	0	0	0	0	0	0	0	0	0	0	0	0	0	0	0	0	0	0	0	0	0	0	0	0	0	0	**0**	0.00	14.00
27-28	0	0	0	0	0	0	0	0	0	0	0	0	0	0	0	0	0	0	0	0	0	0	0	0	0	0	0	0	**0**	0.00	14.00
Sum	**77588**	**84456**	**107319**	**122325**	**119961**	**100678**	**74121**	**49060**	**29514**	**16348**	**8456**	**4146**	**1957**	**904**	**414**	**190**	**87**	**40**	**18**	**8**	**4**	**2**	**1**	**0**	**0**	**0**	**0**	**0**	**797598**		
%	9.73	10.59	13.46	15.34	15.04	12.62	9.29	6.15	3.70	2.05	1.06	0.52	0.25	0.11	0.05	0.02	0.01	0.01	0.00	0.00	0.00	0.00	0.00	0.00	0.00	0.00	0.00	0.00			
Mean Height	0.50	0.67	0.87	1.16	1.44	1.71	1.98	2.21	2.40	2.53	2.57	2.55	2.45	2.32	2.15	1.97	1.79	1.62	1.46	1.32	1.20	1.10	1.00	0.93	0.83	0.82	0.75	0.70			

Table A.10 – Scatter diagram with mean period and mean wave height for 270°

	Wave Period (T) - (s)																														
H(m)	2-3	3-4	4-5	5-6	6-7	7-8	8-9	9-10	10-11	11-12	12-13	13-14	14-15	15-16	16-17	17-18	18-19	19-20	20-21	21-22	22-23	23-24	24-25	25-26	26-27	27-28	28-29	29-30	Sum	%	Mean Period
0-1	50265	46023	46999	38598	27365	17335	10125	5624	3044	1626	860	453	238	125	66	35	18	10	5	3	1	1	0	0	0	0	0	0	**248819**	48.15	4.96
1-2	0	8146	19433	31544	34368	28205	19251	11742	6592	3474	1753	862	417	200	96	46	22	10	5	2	1	0	0	0	0	0	0	0	**166169**	32.16	6.95
2-3	0	546	2680	7091	11237	12301	10377	7227	4360	2376	1201	571	258	112	47	20	8	3	1	0	0	0	0	0	0	0	0	0	**60417**	11.69	7.91
3-4	0	0	413	1561	3424	4748	4731	3691	2409	1383	718	344	155	66	27	10	4	1	0	0	0	0	0	0	0	0	0	0	**23685**	4.58	8.55
4-5	0	0	0	372	962	1711	2046	1813	1283	767	404	194	87	37	15	6	2	1	0	0	0	0	0	0	0	0	0	0	**9702**	1.88	9.07
5-6	0	0	0	69	264	608	877	888	684	428	229	109	48	20	8	3	1	0	0	0	0	0	0	0	0	0	0	0	**4237**	0.82	9.49
6-7	0	0	0	13	71	209	367	428	362	240	132	63	27	11	4	2	1	0	0	0	0	0	0	0	0	0	0	0	**1929**	0.37	9.86
7-8	0	0	0	0	21	70	150	202	190	134	76	37	16	6	2	1	0	0	0	0	0	0	0	0	0	0	0	0	**904**	0.17	10.19
8-9	0	0	0	0	5	23	59	93	98	74	44	22	9	4	1	0	0	0	0	0	0	0	0	0	0	0	0	0	**433**	0.08	10.49
9-10	0	0	0	0	0	8	23	42	50	41	25	13	5	2	1	0	0	0	0	0	0	0	0	0	0	0	0	0	**211**	0.04	10.77
10-11	0	0	0	0	0	3	9	19	25	22	15	8	3	1	0	0	0	0	0	0	0	0	0	0	0	0	0	0	**104**	0.02	11.03
11-12	0	0	0	0	0	1	3	8	12	12	8	5	2	1	0	0	0	0	0	0	0	0	0	0	0	0	0	0	**52**	0.01	11.27
12-13	0	0	0	0	0	0	1	3	6	6	5	3	1	0	0	0	0	0	0	0	0	0	0	0	0	0	0	0	**26**	0.01	11.52
13-14	0	0	0	0	0	0	0	1	3	3	3	2	1	0	0	0	0	0	0	0	0	0	0	0	0	0	0	0	**14**	0.00	11.74
14-15	0	0	0	0	0	0	0	1	1	2	2	1	0	0	0	0	0	0	0	0	0	0	0	0	0	0	0	0	**7**	0.00	11.95
15-16	0	0	0	0	0	0	0	0	1	1	1	1	0	0	0	0	0	0	0	0	0	0	0	0	0	0	0	0	**4**	0.00	12.16
16-17	0	0	0	0	0	0	0	0	0	0	0	0	0	0	0	0	0	0	0	0	0	0	0	0	0	0	0	0	**2**	0.00	12.37
17-18	0	0	0	0	0	0	0	0	0	0	0	0	0	0	0	0	0	0	0	0	0	0	0	0	0	0	0	0	**1**	0.00	12.57
18-19	0	0	0	0	0	0	0	0	0	0	0	0	0	0	0	0	0	0	0	0	0	0	0	0	0	0	0	0	**1**	0.00	12.74
19-20	0	0	0	0	0	0	0	0	0	0	0	0	0	0	0	0	0	0	0	0	0	0	0	0	0	0	0	0	**0**	0.00	12.93
20-21	0	0	0	0	0	0	0	0	0	0	0	0	0	0	0	0	0	0	0	0	0	0	0	0	0	0	0	0	**0**	0.00	13.15
21-22	0	0	0	0	0	0	0	0	0	0	0	0	0	0	0	0	0	0	0	0	0	0	0	0	0	0	0	0	**0**	0.00	13.26
22-23	0	0	0	0	0	0	0	0	0	0	0	0	0	0	0	0	0	0	0	0	0	0	0	0	0	0	0	0	**0**	0.00	13.45
23-24	0	0	0	0	0	0	0	0	0	0	0	0	0	0	0	0	0	0	0	0	0	0	0	0	0	0	0	0	**0**	0.00	13.50
24-25	0	0	0	0	0	0	0	0	0	0	0	0	0	0	0	0	0	0	0	0	0	0	0	0	0	0	0	0	**0**	0.00	13.71
25-26	0	0	0	0	0	0	0	0	0	0	0	0	0	0	0	0	0	0	0	0	0	0	0	0	0	0	0	0	**0**	0.00	13.64
26-27	0	0	0	0	0	0	0	0	0	0	0	0	0	0	0	0	0	0	0	0	0	0	0	0	0	0	0	0	**0**	0.00	14.00
27-28	0	0	0	0	0	0	0	0	0	0	0	0	0	0	0	0	0	0	0	0	0	0	0	0	0	0	0	0	**0**	0.00	14.00
Sum	**50265**	**54714**	**69526**	**79248**	**77716**	**65223**	**48018**	**31783**	**19121**	**10591**	**5478**	**2686**	**1268**	**586**	**268**	**123**	**57**	**26**	**12**	**5**	**2**	**1**	**0**	**0**	**0**	**0**	**0**	**0**	**516718**		
%	9.73	10.59	13.46	15.34	15.04	12.62	9.29	6.15	3.70	2.05	1.06	0.52	0.25	0.11	0.05	0.02	0.01	0.01	0.00	0.00	0.00	0.00	0.00	0.00	0.00	0.00	0.00	0.00			
Mean Height	0.50	0.67	0.87	1.16	1.44	1.71	1.98	2.21	2.40	2.53	2.57	2.55	2.45	2.32	2.15	1.97	1.79	1.62	1.46	1.32	1.20	1.10	1.00	0.93	0.83	0.82	0.75	0.70			

Table A.11 – Scatter diagram with mean period and mean wave height for 300°

	Wave Period (T) - (s)																														
H(m)	**2-3**	**3-4**	**4-5**	**5-6**	**6-7**	**7-8**	**8-9**	**9-10**	**10-11**	**11-12**	**12-13**	**13-14**	**14-15**	**15-16**	**16-17**	**17-18**	**18-19**	**19-20**	**20-21**	**21-22**	**22-23**	**23-24**	**24-25**	**25-26**	**26-27**	**27-28**	**28-29**	**29-30**	**Sum**	%	Mean Period
0-1	68185	62430	63755	52359	37121	23516	13734	7630	4130	2205	1167	614	322	169	89	47	25	13	7	3	2	1	0	0	0	0	0	0	**337526**	48.15	4.96
1-2	0	11050	26361	42790	46620	38261	26114	15929	8942	4712	2378	1169	566	271	130	62	29	14	6	3	1	1	0	0	0	0	0	0	**225410**	32.16	6.95
2-3	0	740	3636	9619	15244	16687	14076	9804	5914	3223	1630	775	350	152	64	27	11	4	2	1	0	0	0	0	0	0	0	0	**81957**	11.69	7.91
3-4	0	0	561	2117	4644	6441	6417	5006	3268	1876	974	467	210	89	36	14	5	2	1	0	0	0	0	0	0	0	0	0	**32130**	4.58	8.55
4-5	0	0	0	504	1305	2322	2776	2460	1741	1041	549	264	118	50	20	8	3	1	0	0	0	0	0	0	0	0	0	0	**13161**	1.88	9.07
5-6	0	0	0	93	359	824	1189	1204	928	581	311	148	65	27	11	4	2	1	0	0	0	0	0	0	0	0	0	0	**5748**	0.82	9.49
6-7	0	0	0	18	96	284	498	580	492	326	178	85	37	15	6	2	1	0	0	0	0	0	0	0	0	0	0	0	**2616**	0.37	9.86
7-8	0	0	0	0	28	95	203	274	257	182	103	50	21	8	3	1	0	0	0	0	0	0	0	0	0	0	0	0	**1226**	0.17	10.19
8-9	0	0	0	0	7	31	81	127	133	101	60	29	12	5	2	1	0	0	0	0	0	0	0	0	0	0	0	0	**588**	0.08	10.49
9-10	0	0	0	0	0	11	31	57	67	55	35	17	7	3	1	0	0	0	0	0	0	0	0	0	0	0	0	0	**287**	0.04	10.77
10-11	0	0	0	0	0	3	12	25	34	30	20	10	5	2	1	0	0	0	0	0	0	0	0	0	0	0	0	0	**142**	0.02	11.03
11-12	0	0	0	0	0	1	4	11	16	16	11	6	3	1	0	0	0	0	0	0	0	0	0	0	0	0	0	0	**71**	0.01	11.27
12-13	0	0	0	0	0	0	2	5	8	9	6	4	2	1	0	0	0	0	0	0	0	0	0	0	0	0	0	0	**36**	0.01	11.52
13-14	0	0	0	0	0	0	1	2	4	5	4	2	1	0	0	0	0	0	0	0	0	0	0	0	0	0	0	0	**18**	0.00	11.74
14-15	0	0	0	0	0	0	0	1	2	2	2	1	1	0	0	0	0	0	0	0	0	0	0	0	0	0	0	0	**9**	0.00	11.95
15-16	0	0	0	0	0	0	0	0	1	1	1	1	0	0	0	0	0	0	0	0	0	0	0	0	0	0	0	0	**5**	0.00	12.16
16-17	0	0	0	0	0	0	0	0	0	1	1	0	0	0	0	0	0	0	0	0	0	0	0	0	0	0	0	0	**3**	0.00	12.37
17-18	0	0	0	0	0	0	0	0	0	0	0	0	0	0	0	0	0	0	0	0	0	0	0	0	0	0	0	0	**1**	0.00	12.57
18-19	0	0	0	0	0	0	0	0	0	0	0	0	0	0	0	0	0	0	0	0	0	0	0	0	0	0	0	0	**1**	0.00	12.74
19-20	0	0	0	0	0	0	0	0	0	0	0	0	0	0	0	0	0	0	0	0	0	0	0	0	0	0	0	0	**0**	0.00	12.93
20-21	0	0	0	0	0	0	0	0	0	0	0	0	0	0	0	0	0	0	0	0	0	0	0	0	0	0	0	0	**0**	0.00	13.15
21-22	0	0	0	0	0	0	0	0	0	0	0	0	0	0	0	0	0	0	0	0	0	0	0	0	0	0	0	0	**0**	0.00	13.26
22-23	0	0	0	0	0	0	0	0	0	0	0	0	0	0	0	0	0	0	0	0	0	0	0	0	0	0	0	0	**0**	0.00	13.45
23-24	0	0	0	0	0	0	0	0	0	0	0	0	0	0	0	0	0	0	0	0	0	0	0	0	0	0	0	0	**0**	0.00	13.50
24-25	0	0	0	0	0	0	0	0	0	0	0	0	0	0	0	0	0	0	0	0	0	0	0	0	0	0	0	0	**0**	0.00	13.71
25-26	0	0	0	0	0	0	0	0	0	0	0	0	0	0	0	0	0	0	0	0	0	0	0	0	0	0	0	0	**0**	0.00	13.64
26-27	0	0	0	0	0	0	0	0	0	0	0	0	0	0	0	0	0	0	0	0	0	0	0	0	0	0	0	0	**0**	0.00	14.00
27-28	0	0	0	0	0	0	0	0	0	0	0	0	0	0	0	0	0	0	0	0	0	0	0	0	0	0	0	0	**0**	0.00	14.00
Sum	**68185**	**74220**	**94312**	**107500**	**105423**	**88476**	**65138**	**43114**	**25937**	**14367**	**7431**	**3643**	**1720**	**794**	**364**	**167**	**77**	**35**	**16**	**7**	**3**	**1**	**1**	**0**	**0**	**0**	**0**	**0**	**700934**		
%	9.73	10.59	13.46	15.34	15.04	12.62	9.29	6.15	3.70	2.05	1.06	0.52	0.25	0.11	0.05	0.02	0.01	0.01	0.00	0.00	0.00	0.00	0.00	0.00	0.00	0.00	0.00	0.00			
Mean Height	0.50	0.67	0.87	1.16	1.44	1.71	1.98	2.21	2.40	2.53	2.57	2.55	2.45	2.32	2.15	1.97	1.79	1.62	1.46	1.32	1.20	1.10	1.00	0.93	0.83	0.82	0.75	0.70			

Table A.12 – Scatter diagram with mean period and mean wave height for 330°

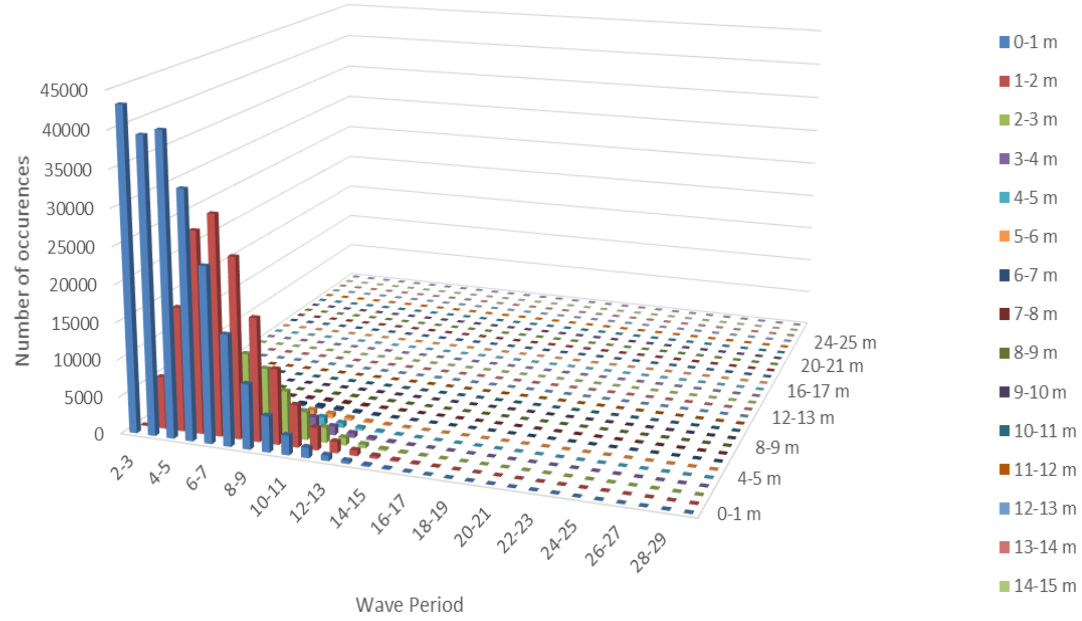

Figure A.13 – Wave data scatter from 0°

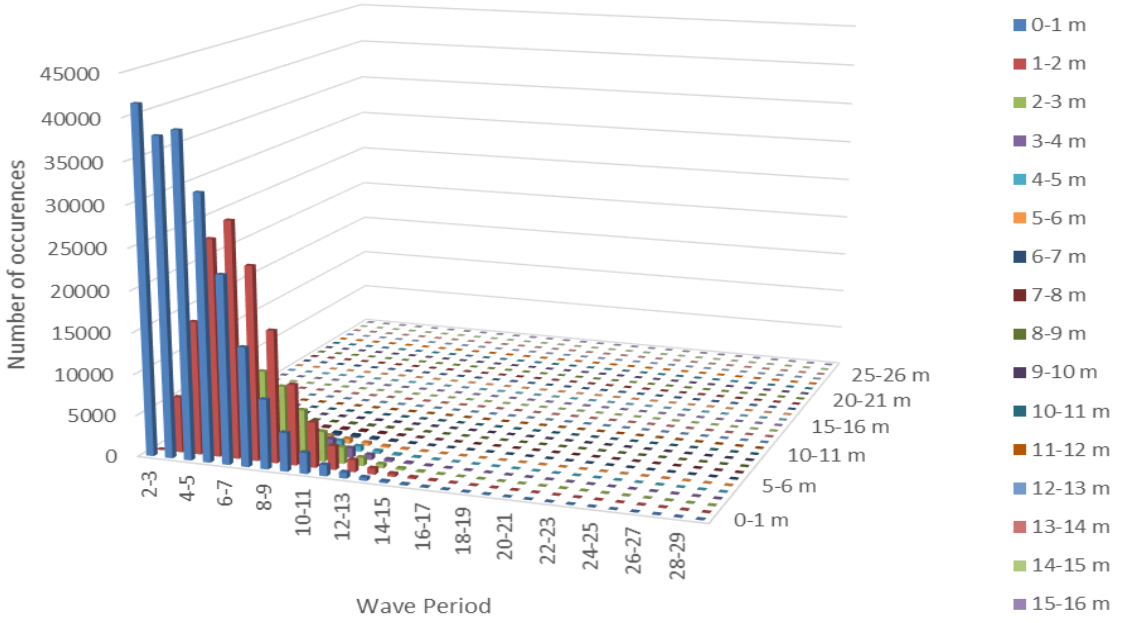

Figure A.14 – Wave data scatter from 30°

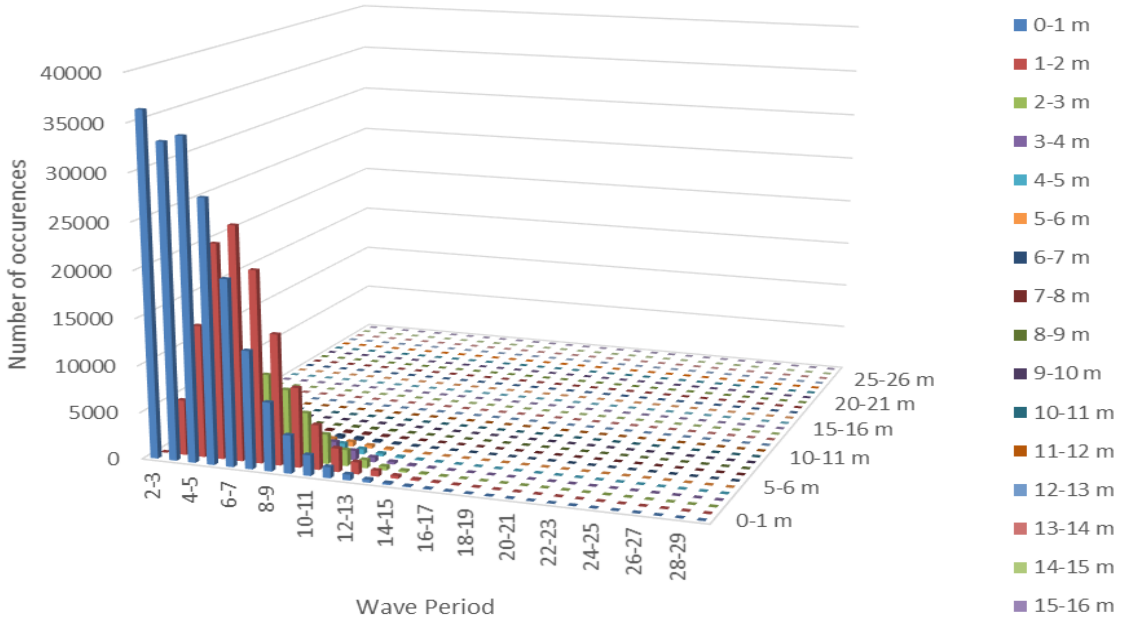

Figure A.15 – Wave data scatter from 60°

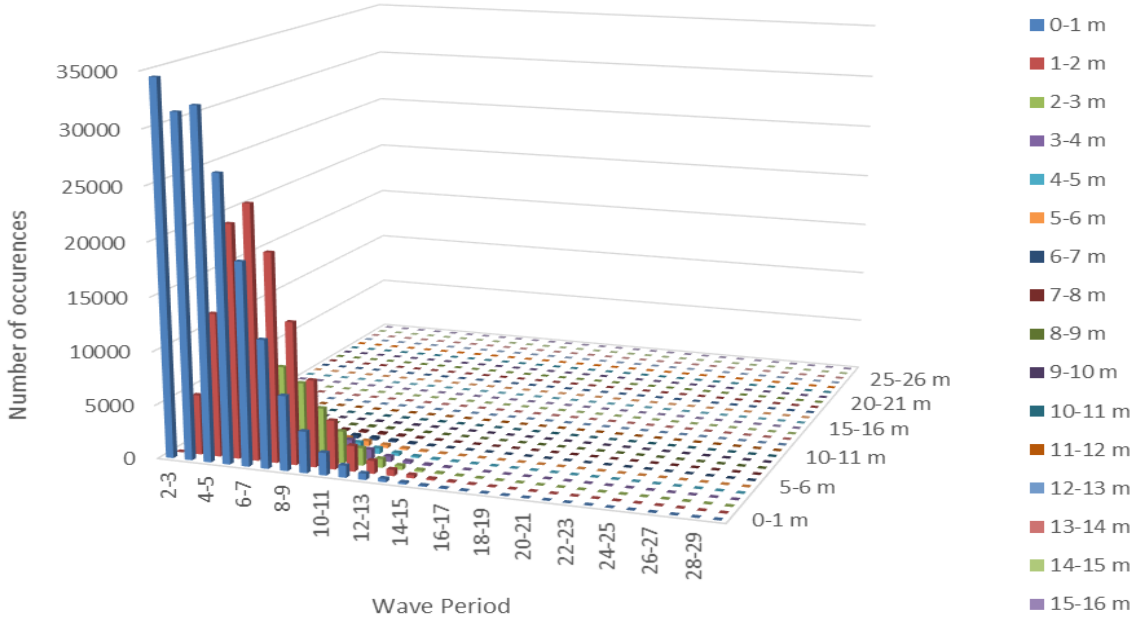

Figure A.16 – Wave data scatter from 90°

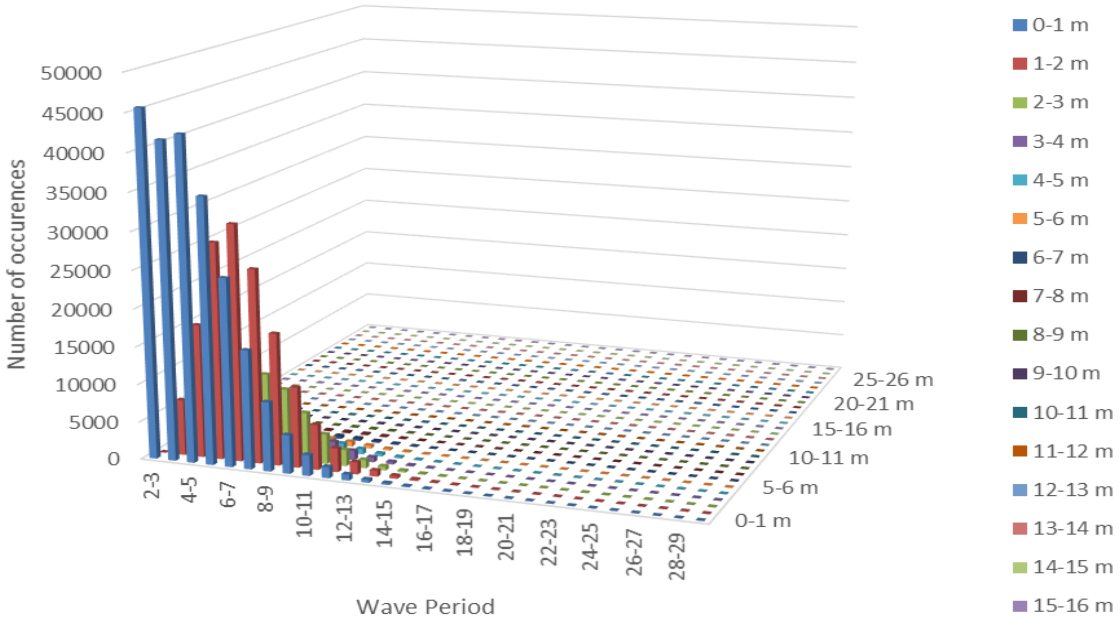

Figure A.17 – Wave data scatter from 120°

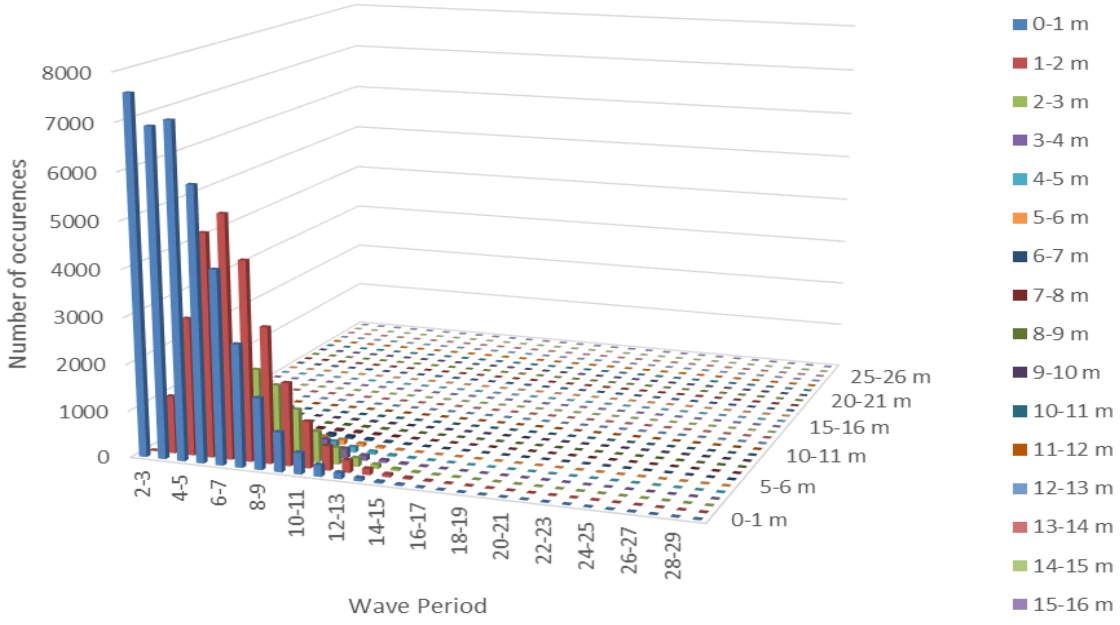

Figure A.18 – Wave data scatter from 150°

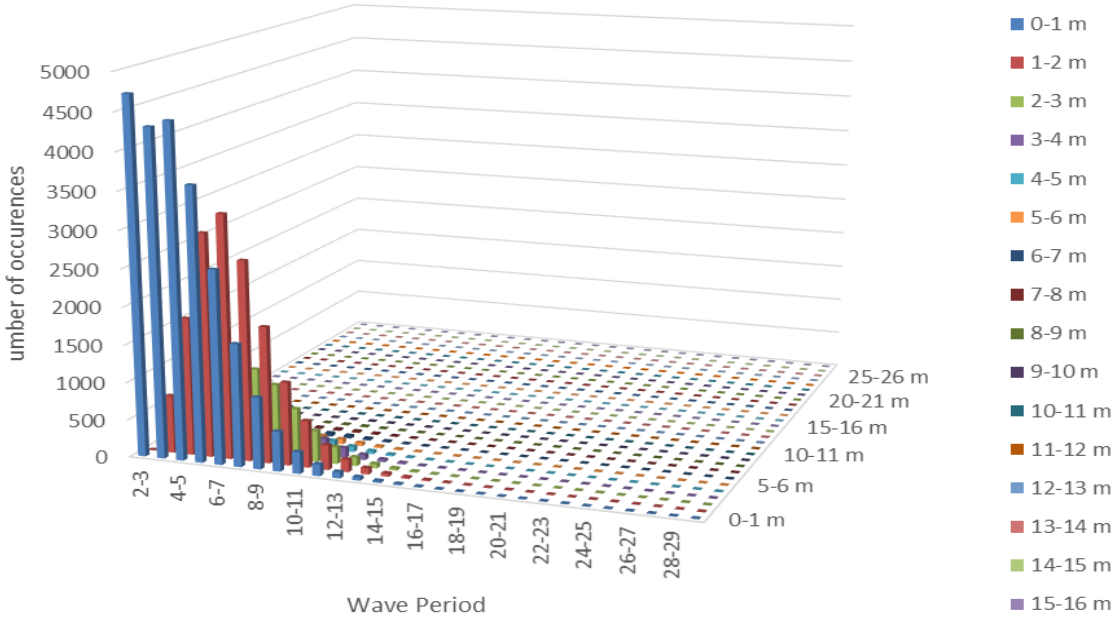

Figure A.19 – Wave data scatter from 180°

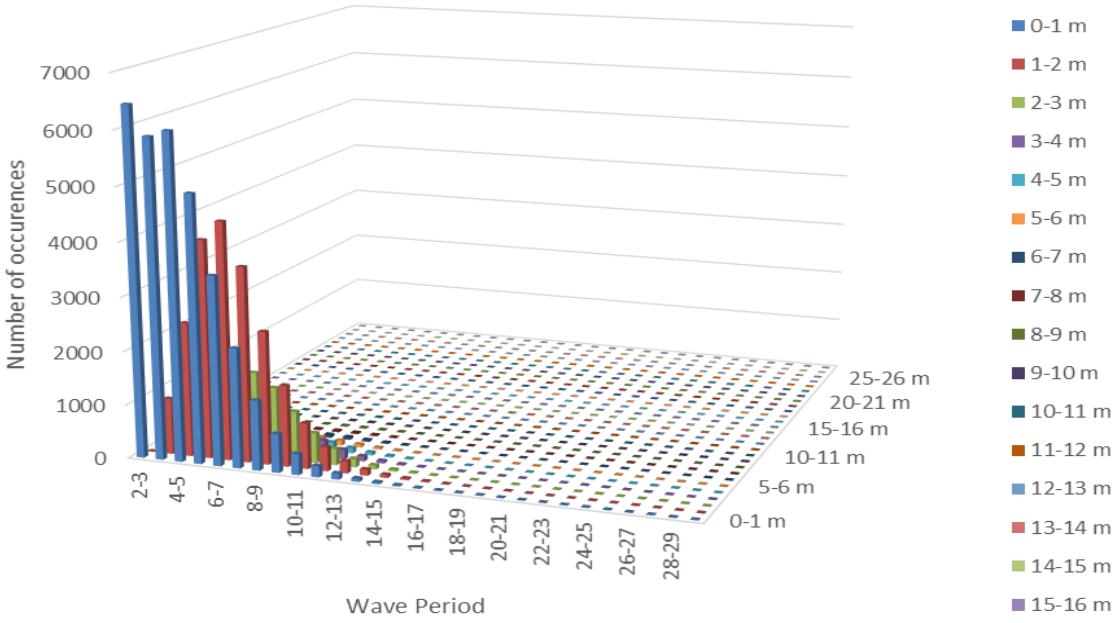

Figure A.20 – Wave data scatter from 210°

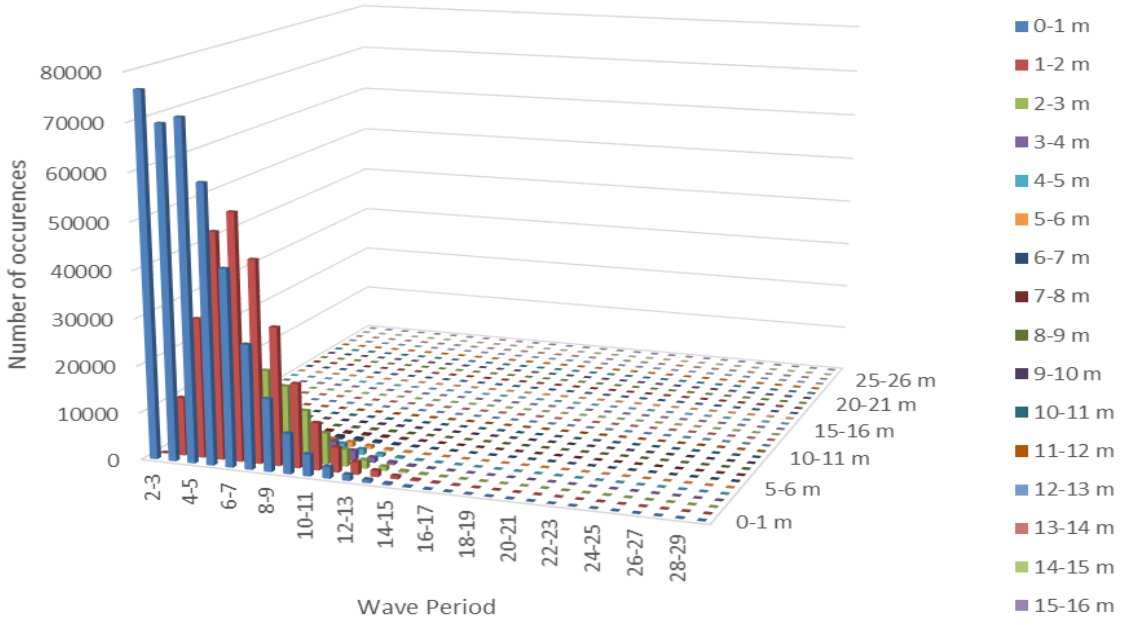

Figure A.21 – Wave data scatter from 240°

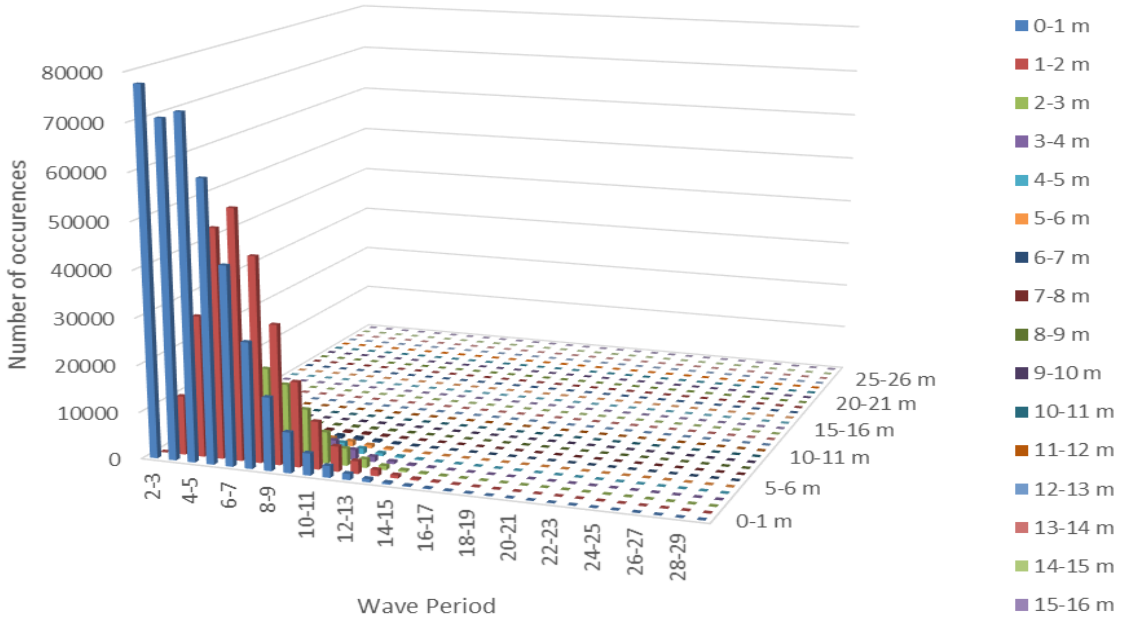

Figure A.22 – Wave data scatter from 270°

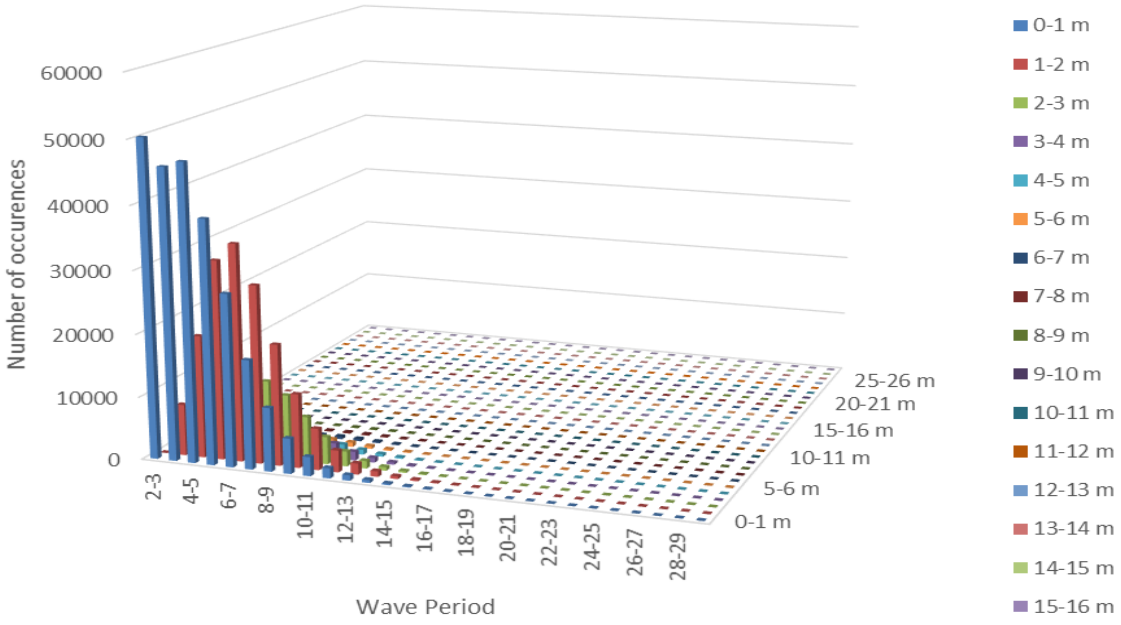

Figure A.23 – Wave data scatter from 300°

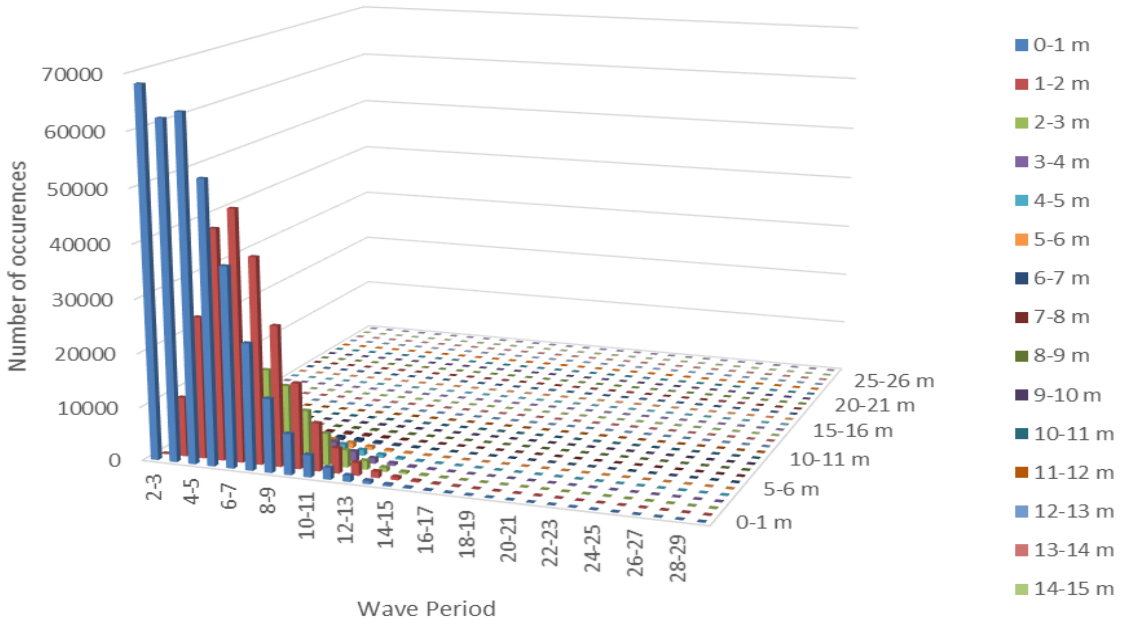

Figure A.24 – Wave data scatter from 330°

Annex B: Stokes 5th Order parameters

$$s = \sinh(kd) \tag{B.1}$$

$$c = \cosh(kd) \tag{B.2}$$

$$A_{11} = \frac{1}{s} \tag{B.3}$$

$$A_{13} = \frac{-c^2(5c^2+1)}{8s^5} \tag{B.4}$$

$$A_{15} = \frac{-(1184c^{10} - 1440c^8 - 1992}{8s^5} \tag{B.5}$$

$$A_{22} = \frac{3}{8s^4} \tag{B.6}$$

$$A_{24} = \frac{(192c^8 - 422c^6 - 312c^4 + 480c^2 - 17)}{748s^{10}} \tag{B.7}$$

$$A_{33} = \frac{(13 - 4c^2)}{64s^7} \tag{B.8}$$

$$A_{35} = \frac{(512c^{12} + 4224c^{10} - 6800c^8 - 12808c^6 + 16704c^4 - 3154c^2 + 107)}{4096s^{13}(6c^2 - 1)} \tag{B.9}$$

$$A_{44} = \frac{(80c^6 - 816c^4 + 1338c^2 - 197)}{1536s^{10}(6c^2 - 1)} \tag{B.10}$$

$$A_{55} = \frac{-(2880c^{10} - 72480c^8 + 324000c^6 - 432000c^4 + 163470c^2 - 16245)}{61440s^{11}(6c^2 - 1)(8c^4 - 11c^2 + 3)} \tag{B.11}$$

$$B_{22} = \frac{(2c^2+1)}{4s^3}c \tag{B.12}$$

$$B_{24} = \frac{c(272c^8 - 504c^6 - 192c^4 + 322c^2 + 21)}{384s^9} \tag{B.13}$$

$$B_{33} = \frac{3(8c^6+1)}{64s^6} \tag{B.14}$$

$$B_{35} = \frac{(88128c^{14} - 208224c^{12} + 70848c^{10} + 54000c^8 - 21816c^6 + 6264c^4 - 52c^2 - 81)}{12288s^{12}(6c^2 - 1)} \tag{B.15}$$

$$B_{44} = \frac{c(768c^{10} - 448c^8 - 48c^6 + 48c^4 + 106c^2 - 21)}{384s^{10}(6c^2 - 1)} \tag{B.16}$$

$$B_{55} = \frac{(192000c^{16} - 262720c^{14} + 83680c^{12} + 20160c^{10} - 7280c^8 + 7160c^6 - 1800c^4}{12288s^{10}(6c^2 - 1)(8c^4 11c^2 + 3)} + \frac{-1050c^2 + 225}{12288s^{10}(6c^2 - 1)(8c^4 11c^2 + 3)} \tag{B.17}$$

$$C_1 = \frac{(8c^4 - 8c^2 + 9)}{8s^4} \tag{B.18}$$

$$C_2 = \frac{(3840c^{12} - 4096c^{10} + 2592c^8 - 1008c^6 + 5944c^4 - 1830c^2 + 147)}{512s^{10}(6c^2 - 1)} \tag{B.19}$$

$$C_3 = -\frac{1}{4sc} \tag{B.20}$$

$$C_4 = \frac{(12c^8 + 36c^6 - 162c^4 + 141c^2 - 27)}{192cs^9} \tag{B.21}$$

$$\Phi_1' = \lambda A_{11} + \lambda^3 A_{13} + \lambda^5 A_{15} \tag{B.22}$$

$$\Phi_2' = \lambda^2 A_{22} + \lambda^4 A_{24} \tag{B.23}$$

$$\Phi_3' = \lambda^3 A_{33} + \lambda^5 A_{35} \tag{B.24}$$

$$\Phi_4' = \lambda^4 A_{44} \tag{B.25}$$

$$\Phi_5' = \lambda^5 A_{55} \tag{B.26}$$

$$\bar{c} = \frac{g}{k}\tanh(kd)\,[1 + C_1\lambda^2 + C_2\lambda^4] \tag{B.27}$$

$$\xi_1' = \lambda \tag{B.28}$$

$$\xi_2' = \lambda^2 B_{22} + \lambda^4 B_{24} \tag{B.29}$$

$$\xi_3' = \lambda^3 B_{33} + \lambda^5 B_{35} \tag{B.30}$$

$$\xi_4' = \lambda^4 B_{44} \tag{B.31}$$

$$\xi_5' = \lambda^5 B_{55} \tag{B.32}$$

$$u = \bar{c}\sum_{n=1}^{5} n\,\Phi_n' \cosh\big(nk(d+z)\big)\cos(n\theta) \tag{B.33}$$

$$\dot{u} = \bar{c}\omega\sum_{n=1}^{5} n^2\,\Phi_n' \cosh\big(nk(d+z)\big)\sin(n\theta) \tag{B.34}$$

$$\dot{w} = \bar{c}\omega \sum_{n=1}^{5} n^2 \, \Phi_n' \sinh\big(nk(d+z)\big) \cos(n\theta) \tag{B.35}$$

Annex C: Efthymiou parametric SCF formula

Balanced axial loading.

CHORD:

$$\tau^{0.9}\gamma^{0.5}\,(0.67-\beta^2+1.16\beta)\sin\theta\,\left(\frac{\sin\theta_{max}}{\sin\theta_{min}}\right)^{0.30}*\left(\frac{\beta_{max}}{\beta_{min}}\right)^{0.30}\,(1.64+0.29\beta^{-0.38}\,\mathrm{ATAN}(8\xi)) \tag{C.1}$$

BRACE:

$$1+(1.97-1.57\beta^{0.25})\tau^{-0.14}(\sin\theta)^{0.7}*\mathrm{SCF}_{BAL,CHORD}+\sin^{1.8}(\theta_{max}+\theta_{min})*\left(0.131-0.084\,\mathrm{ATAN}(14\zeta+4.2\beta)\right)*C\beta^{1.5}\gamma^{0.5}\tau^{-1.22} \tag{C.2}$$

In-plane bending:

CHORD CROWN:

$$1.45\beta\tau^{0.85}\gamma^{(1-0.68\beta)}(\sin\theta)^{0.7} \tag{C.3}$$

BRACE CROWN:

$$1+0.65\beta\tau^{0.4}\gamma^{(1.09-0.77\beta)}(\sin\theta)^{(0.06\gamma-1.16)} \tag{C.4}$$

Unbalanced out-of-plane bending:

$$\gamma\tau\beta(1.7-1.05\beta^3)(\sin\theta)^{1.6} \tag{C.5}$$

Chord saddle SCF adjacent to diagonal brace A:

$$\left(\mathrm{Eq.}\,(C.5)\right)_A*(1-0.08(\beta_B\gamma)^{0.5}\exp(-0.8x_{AB}))(1-0.08(\beta_C\gamma)^{0.5}\exp(-0.8x_{AC}))+\left(\mathrm{Eq.}\,(C.5)\right)_B*(1-0.08(\beta_A\gamma)^{0.5}\exp(-0.8x_{AB}))(2.05\beta_{max}^{0.5}\exp(-1.3x_{AB}))+\left(\mathrm{Eq.}\,(C.5)\right)_B*(1-0.08(\beta_A\gamma)^{0.5}\exp(-0.8x_{AC}))(2.05\beta_{max}^{0.5}\exp(-1.3x_{AC})) \tag{C.6}$$

Where

$$x_{AB}=1+\frac{\xi_{AB}\sin\theta_A}{\beta_A} \tag{C.7}$$

$$x_{AC}=1+\frac{(\xi_{AB}+\xi_{BC}+\beta_B)\sin\theta_A}{\beta_A} \tag{C.8}$$

Chord saddle SCF adjacent to diagonal brace B:

$$\left(\mathrm{Eq.}\,(D.5)\right)_B*(1-0.08(\beta_A\gamma)^{0.5}\exp(-0.8x_{AB}))^{P1}(1-0.08(\beta_C\gamma)^{0.5}\exp(-0.8x_{BC}))^{P2}+\left(\mathrm{Eq.}\,(C.5)\right)_A*(1-0.08(\beta_B\gamma)^{0.5}\exp(-0.8x_{AB}))(2.05\beta_{max}^{0.5}\exp(-1.3x_{AB}))+\left(\mathrm{Eq.}\,(C.5)\right)_C*(1-0.08(\beta_B\gamma)^{0.5}\exp(-0.8x_{BC}))(2.05\beta_{max}^{0.5}\exp(-1.3x_{BC})) \tag{C.9}$$

Where

$$x_{AB}=1+\frac{\xi_{AB}\sin\theta_B}{\beta_B} \tag{C.10}$$

$$x_{BC} = 1 + \frac{\xi_{BC} \sin\theta_B}{\beta_B} \tag{C.11}$$

$$P1 = \left(\frac{\beta_A}{\beta_B}\right)^2 ;\ P2 = \left(\frac{\beta_C}{\beta_B}\right)^2 \tag{C.12}$$

Chord saddle SCF adjacent to diagonal brace C:

$$\begin{aligned}&\left(\text{Eq.}\,(D.5)\right)_C * (1 - 0.08(\beta_B\gamma)^{0.5}\exp(-0.8x_{CB}))(1 - 0.08(\beta_A\gamma)^{0.5}\exp(-0.8x_{CA})) + \\ &\left(\text{Eq.}\,(C.5)\right)_B * (1 - 0.08(\beta_C\gamma)^{0.5}\exp(-0.8x_{CB}))(2.05\beta_{max}^{0.5}\exp(-1.3x_{CB})) + \\ &\left(\text{Eq.}\,(C.5)\right)_B * (1 - 0.08(\beta_C\gamma)^{0.5}\exp(-0.8x_{CA}))(2.05\beta_{max}^{0.5}\exp(-1.3x_{CA}))\end{aligned} \tag{C.13}$$

Where

$$x_{CB} = 1 + \frac{\xi_{CB} \sin\theta_C}{\beta_C} \tag{C.14}$$

$$x_{CA} = 1 + \frac{(\xi_{CB} + \xi_{BA} + \beta_B) \sin\theta_C}{\beta_C} \tag{C.15}$$

Out-of-plane bending brace SCFs:

Out-of-plane bending brace SCFs are obtained directly from the adjacent chord SCFs using:

$$\tau^{-0.54}\gamma^{-0.05}(0.99 - 0.47\beta + 0.08\beta^4) * SCF_{u,OPB} \tag{C.16}$$

Axial load on one brace only:

Chord saddle:

$$\left(\gamma\ \ \tau^{1.1}(1.11 - 3(\beta - 0.52)^2)(sin\ \theta)\ \ \right) * F1 + C_1(0.8\alpha - 6)\tau\beta^2(1 - \beta^2)^{0.5}(\sin 2\theta)^2 * F2 \tag{C.17}$$

Chord Crown:

$$\gamma^{0.2}\tau(2.65 + 5(\beta - 0.65)^2) + \tau\beta(C_2\alpha - 3)\sin\theta \tag{C.18}$$

Brace saddle:

$$1.3 + \gamma\tau^{0.52}\alpha^{0.1}\left(0.187 - 1.25\beta^{1.1}(\beta - 0.96)\right)(\sin\theta)^{(2.7 - 0.01\alpha)} * F1 \tag{C.19}$$

Brace Crown:

$$3 + \gamma^{1.2}(0.12\exp(-4\beta) + 0.011\beta^2 - 0.045) + \beta\tau(C_3\alpha - 1.2) \tag{C.20}$$

Out-of-plane bending on one brace only:

Chord SCF adjacent to diagonal brace A:

$$\left(\text{Eq.}\,(C.5)\right)_A * (1 - 0.08(\beta_B\gamma)^{0.5}\exp(-0.8x_{AB}))(1 - 0.08(\beta_C\gamma)^{0.5}\exp(-0.8x_{AC})) \tag{C.21}$$

Where

$$x_{AB} = 1 + \frac{\xi_{AB} \sin\theta_A}{\beta_A} \tag{C.22}$$

$$x_{AC} = 1 + \frac{(\xi_{AB} + \xi_{BC} + \beta_B)\sin\theta_A}{\beta_A} \quad \text{(C.23)}$$

Chord SCF adjacent to central brace B:

$$\left(\text{Eq.}(C.5)\right)_B * (1 - 0.08(\beta_A\gamma)^{0.5}\exp(-0.8x_{AB}))^{P1} * (1 - 0.08(\beta_C\gamma)^{0.5}\exp(-0.8x_{BC}))^{P2} \quad \text{(C.24)}$$

Where

$$x_{AB} = 1 + \frac{\xi_{AB}\sin\theta_B}{\beta_B} \quad \text{(C.25)}$$

$$x_{BC} = 1 + \frac{\xi_{BC}\sin\theta_B}{\beta_B} \quad \text{(C.26)}$$

$$P1 = \left(\frac{\beta_A}{\beta_B}\right)^2;\ P2 = \left(\frac{\beta_C}{\beta_B}\right)^2 \quad \text{(C.27)}$$

Chord SCF adjacent to diagonal brace C:

$$\left(\text{Eq.}(C.5)\right)_C * (1 - 0.08(\beta_B\gamma)^{0.5}\exp(-0.8x_{CB}))(1 - 0.08(\beta_A\gamma)^{0.5}\exp(-0.8x_{CA})) \quad \text{(C.28)}$$

Where

$$x_{CB} = 1 + \frac{\xi_{CB}\sin\theta_C}{\beta_C} \quad \text{(C.29)}$$

$$x_{CA} = 1 + \frac{(\xi_{CB} + \xi_{BA} + \beta_B)\sin\theta_C}{\beta_C} \quad \text{(C.30)}$$

With short chord correction factors if α<12:

$$F1 = 1 - (0.83\beta - 0.56\beta^2 - 0.02)\gamma^{0.23}\exp(-0.21\,\gamma^{-1.16}\,\alpha^{2.5}) \quad \text{(C.31)}$$

$$F2 = 1 - (1.43\beta - 0.97\beta^2 - 0.03)\gamma^{0.04}\exp(-0.71\,\gamma^{-1.38}\alpha^{2.5}) \quad \text{(C.32)}$$

$$F3 = 1 - 0.55\beta^{1.8}\gamma^{0.16}\exp(-0.49\,\gamma^{-0.89}\,\alpha^{1.8}) \quad \text{(C.33)}$$

$$C1 = 2(C - 0.5) \quad \text{(C.34)}$$

$$C2 = C/2 \quad \text{(C.35)}$$

$$C3 = C/5 \quad \text{(C.36)}$$

$0.5 \le C \le 1.0$, usually 0.7

C is the chord end fixity parameter, 0,7 was used.

Annex D: Axial, In-Plane (My) and Out-of-Plane (Mz) Forces in structural elements

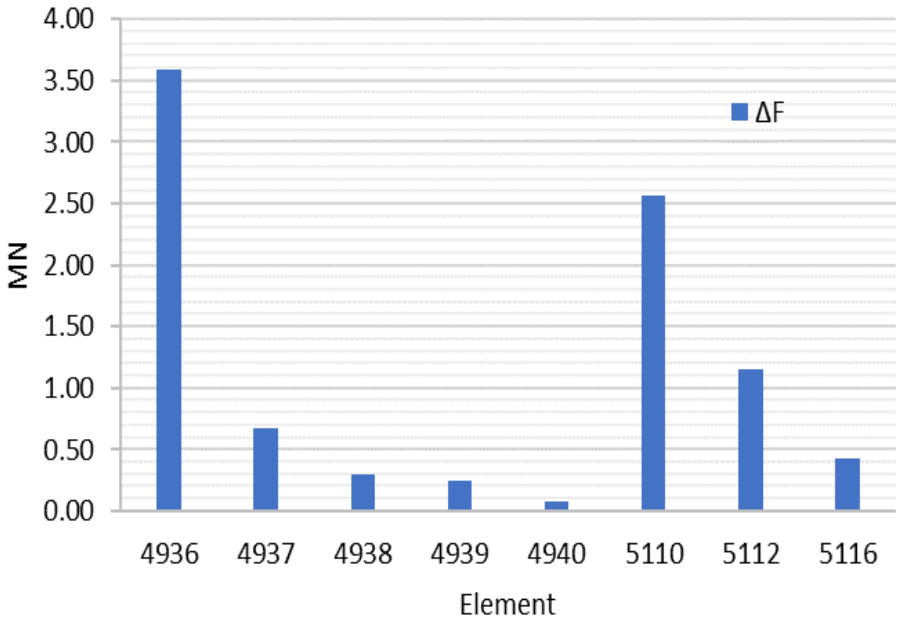

Figure D.1 –Axial forces range for each element – W8

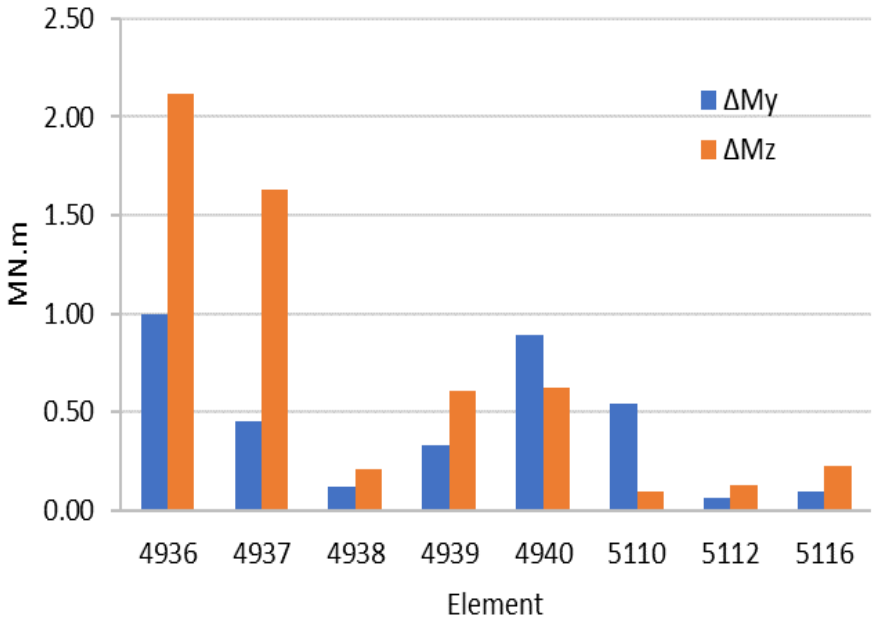

Figure D.2 –Bending forces range for each element – W8

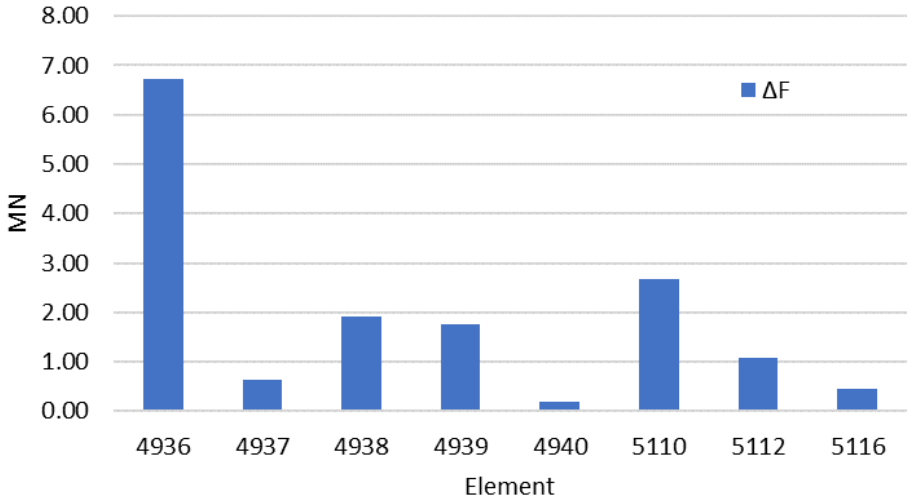

Figure D.3 –Axial forces range for each element – W16

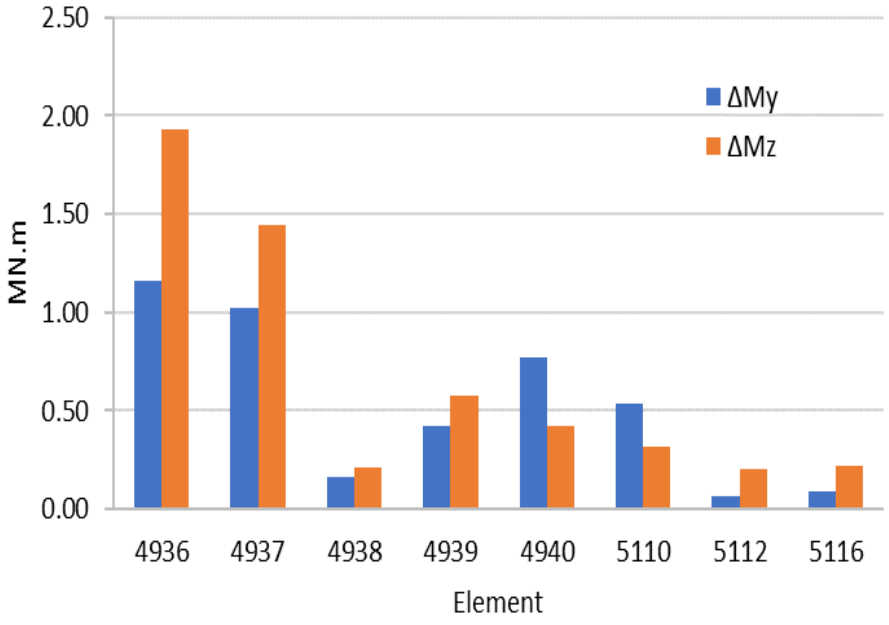

Figure D.4 –Bending forces range for each element – W16

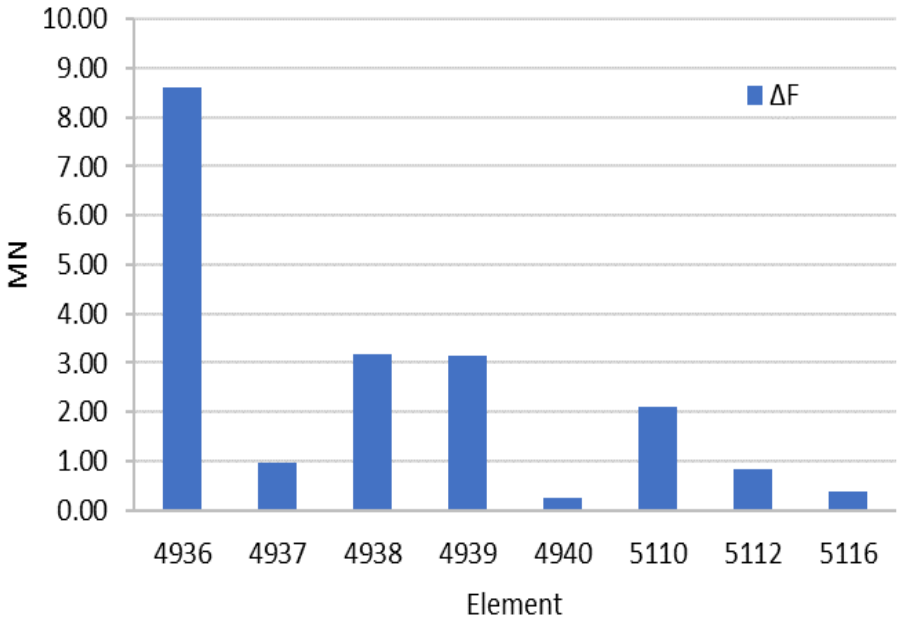

Figure D.5 –Axial forces range for each element – W24

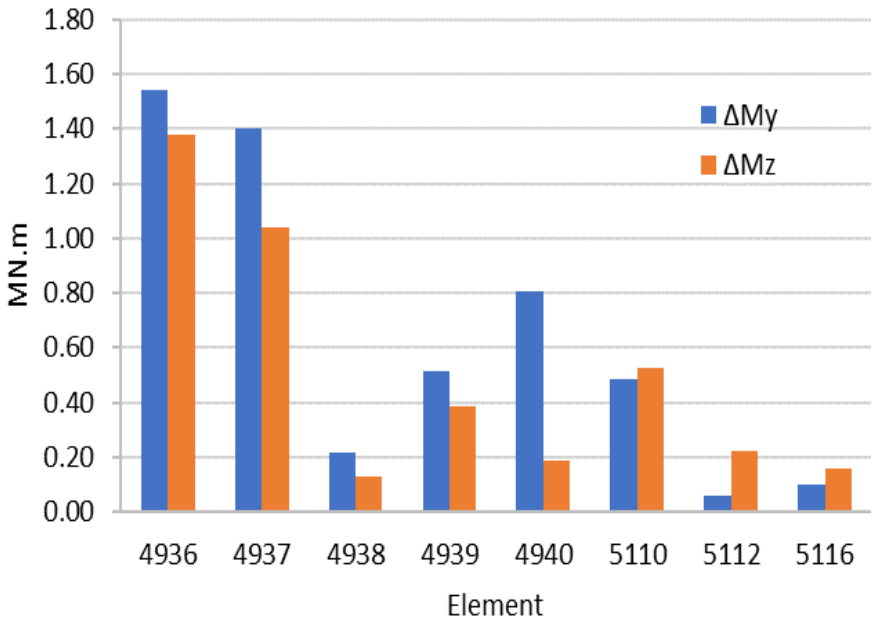

Figure D.6 –Bending forces range for each element – W24

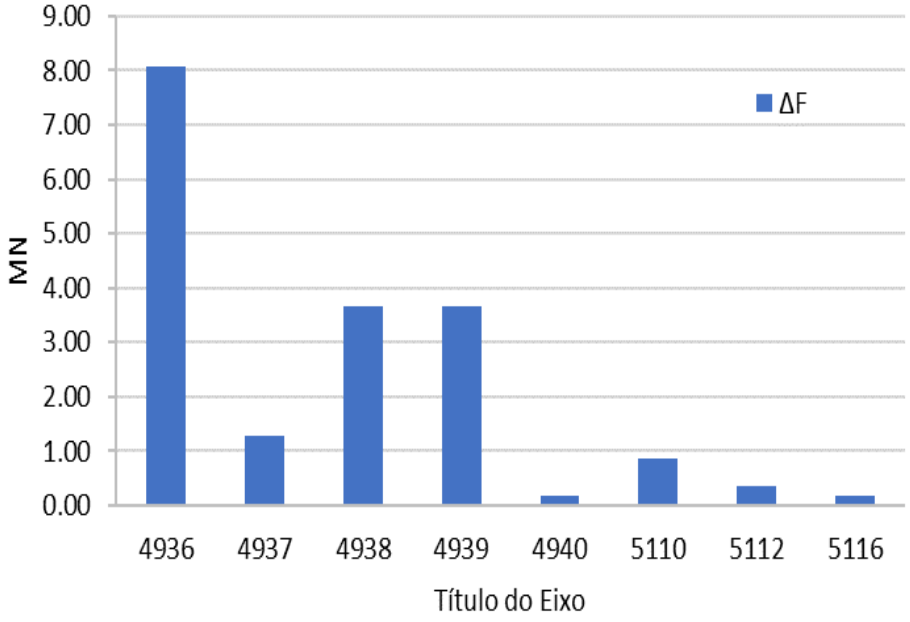

Figure D.7 –Axial forces range for each element – W32

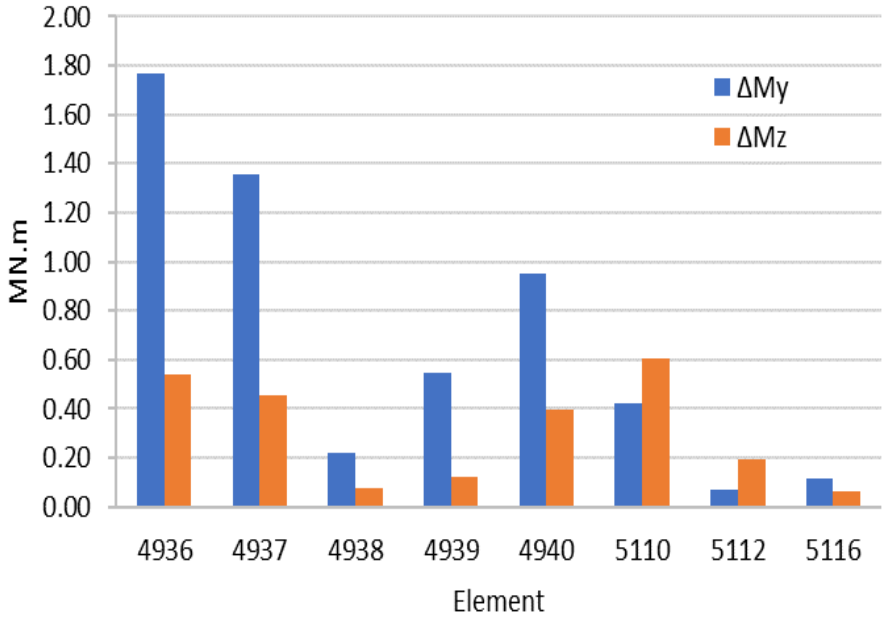

Figure D.8 –Bending forces range for each element – W32

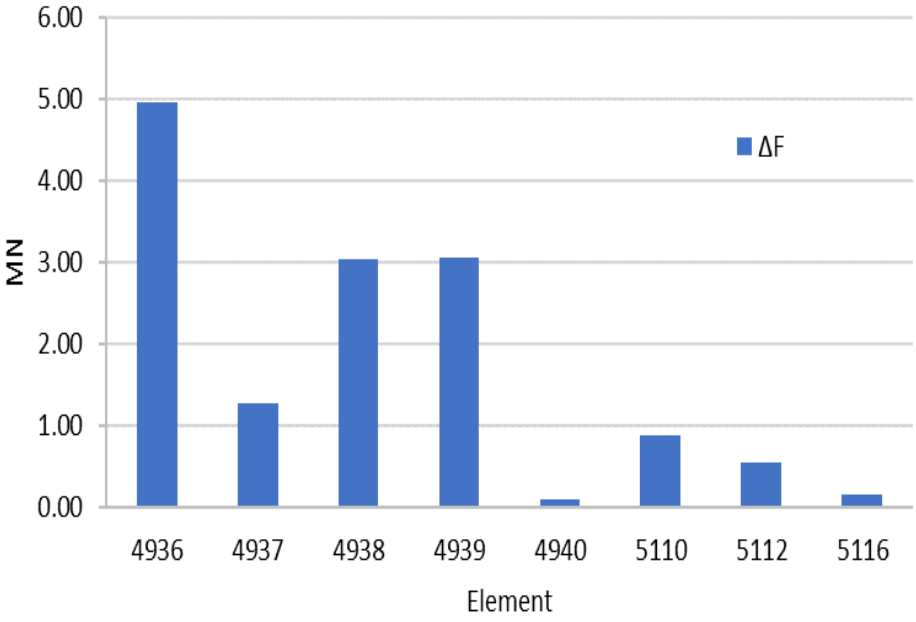

Figure D.9 –Axial forces range for each element – W40

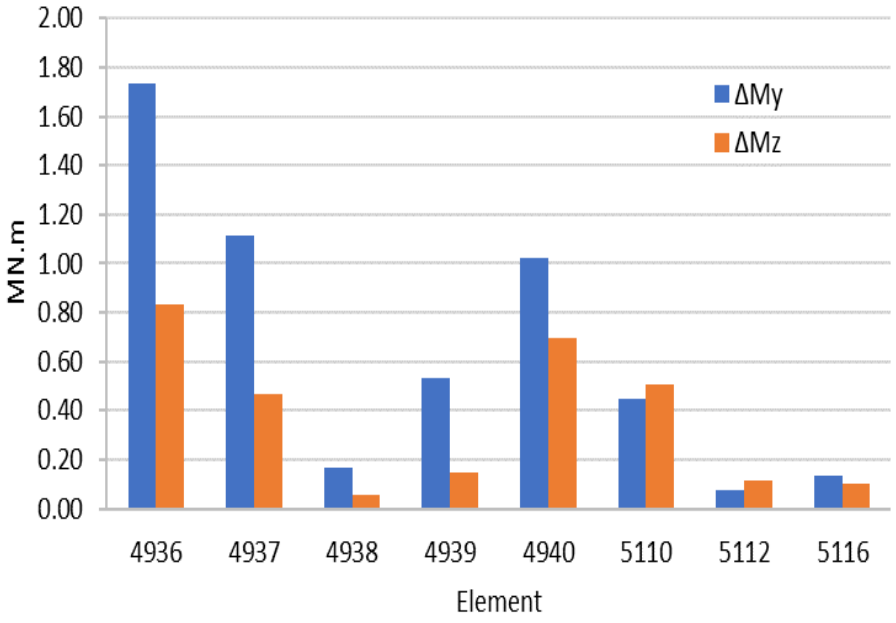

Figure D.10 –Bending forces range for each element – W40

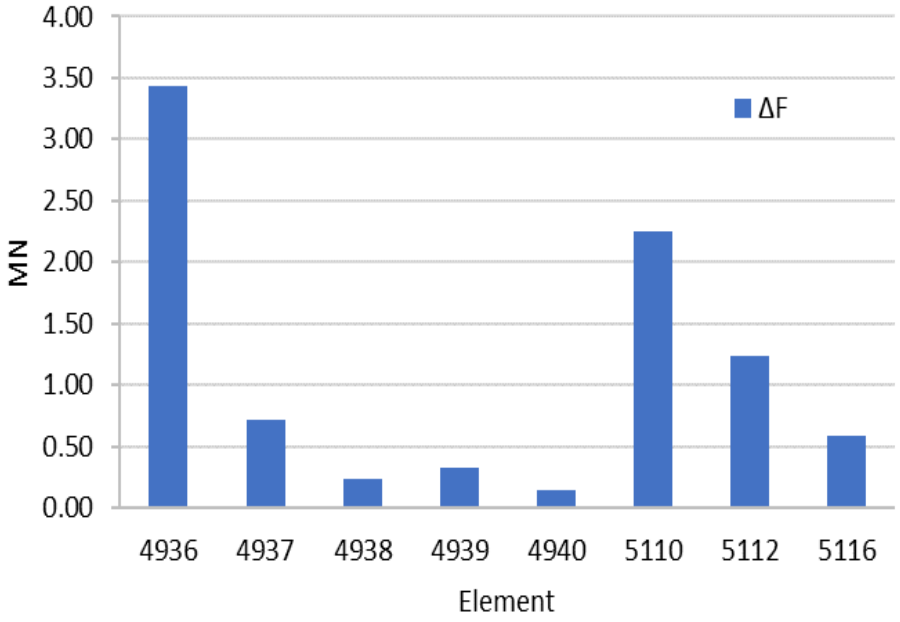

Figure D.11 –Axial forces range for each element – W56

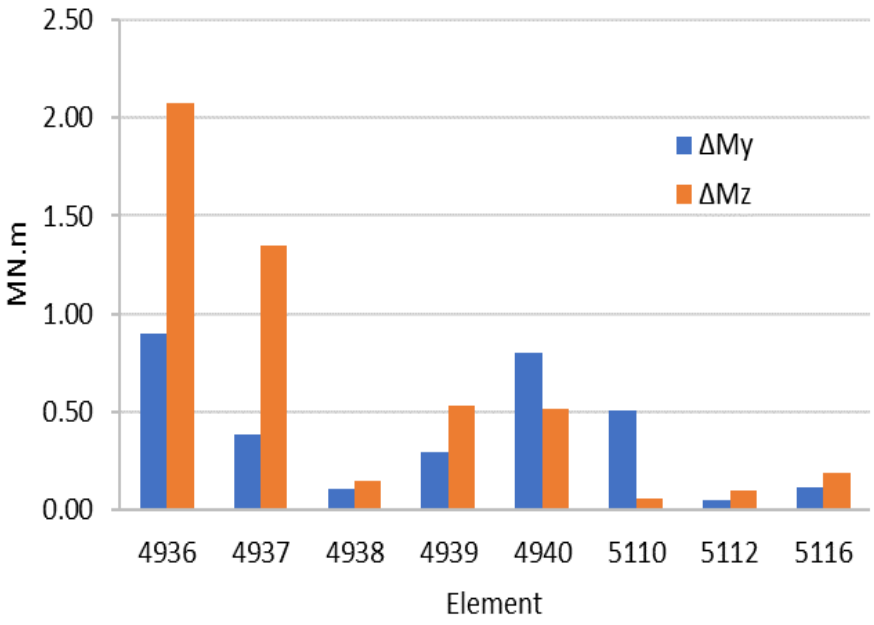

Figure D.12 –Bending forces range for each element – W56

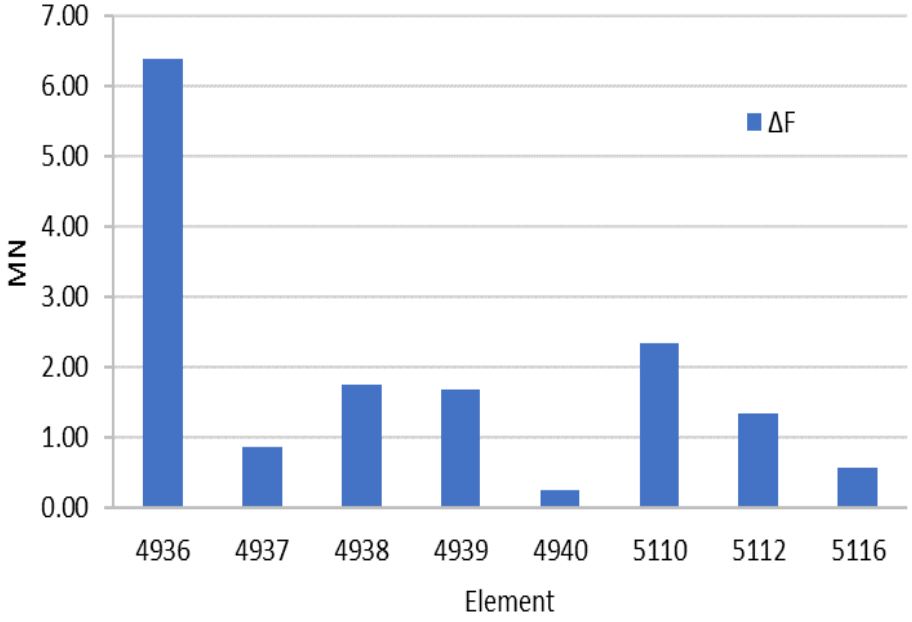

Figure D.13 –Axial forces range for each element – W64

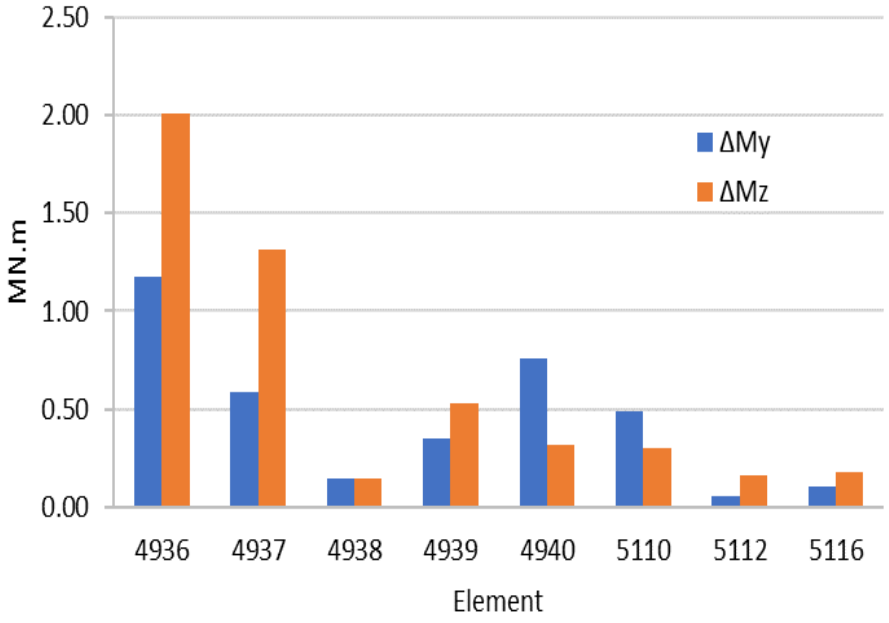

Figure D.14 –Bending forces range for each element – W64

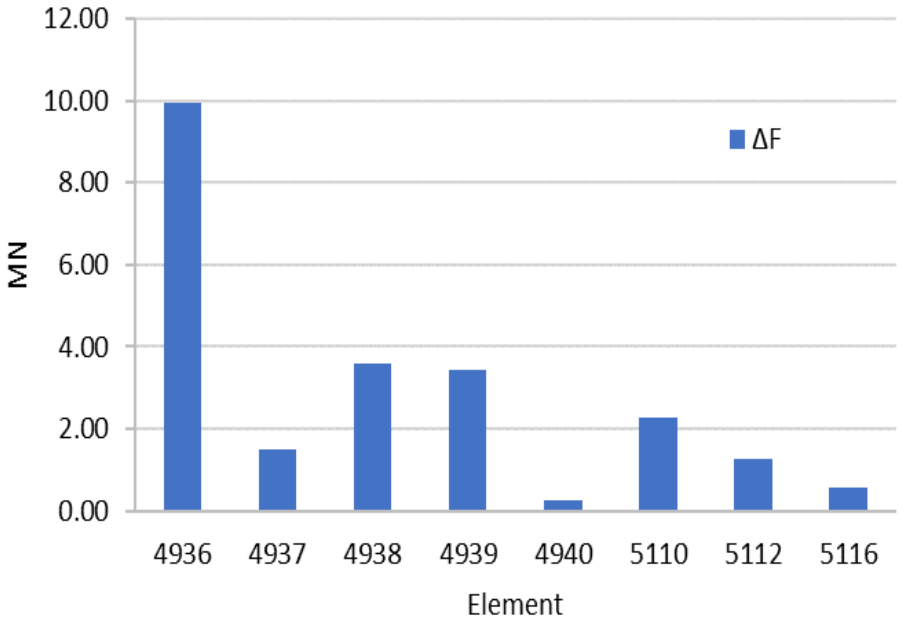

Figure D.15 –Axial forces range for each element – W72

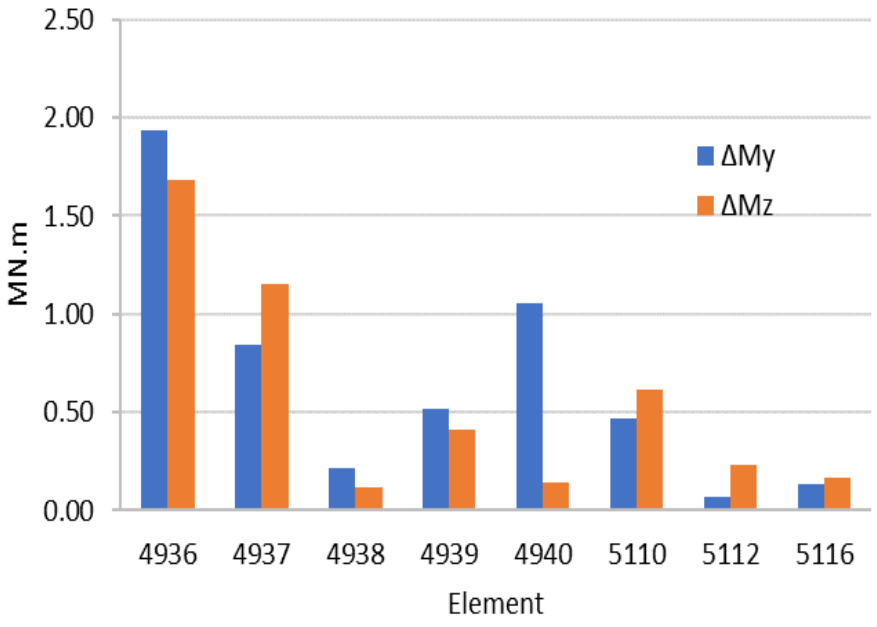

Figure D.16 –Bending forces range for each element – W72

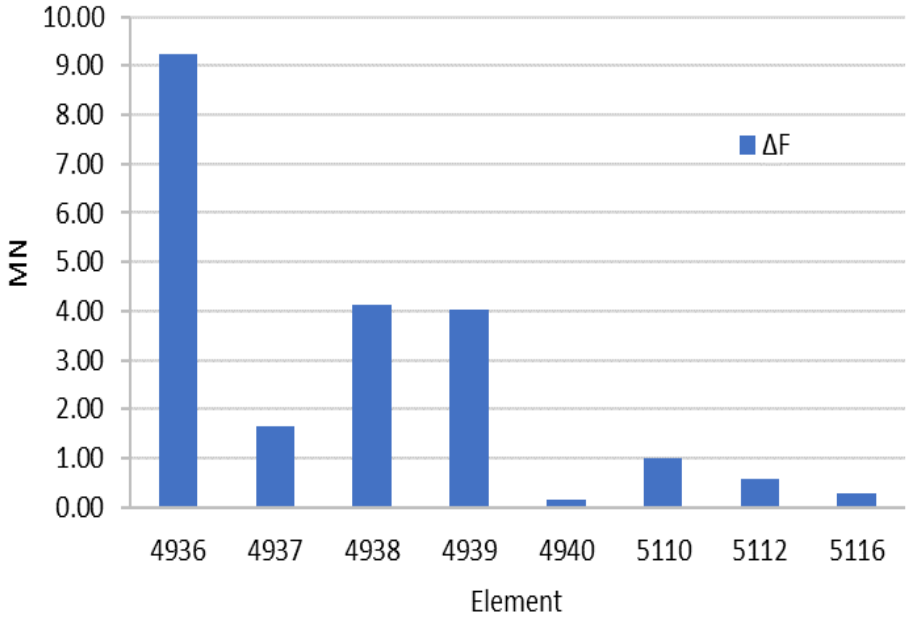

Figure D.17 –Axial forces range for each element – W80

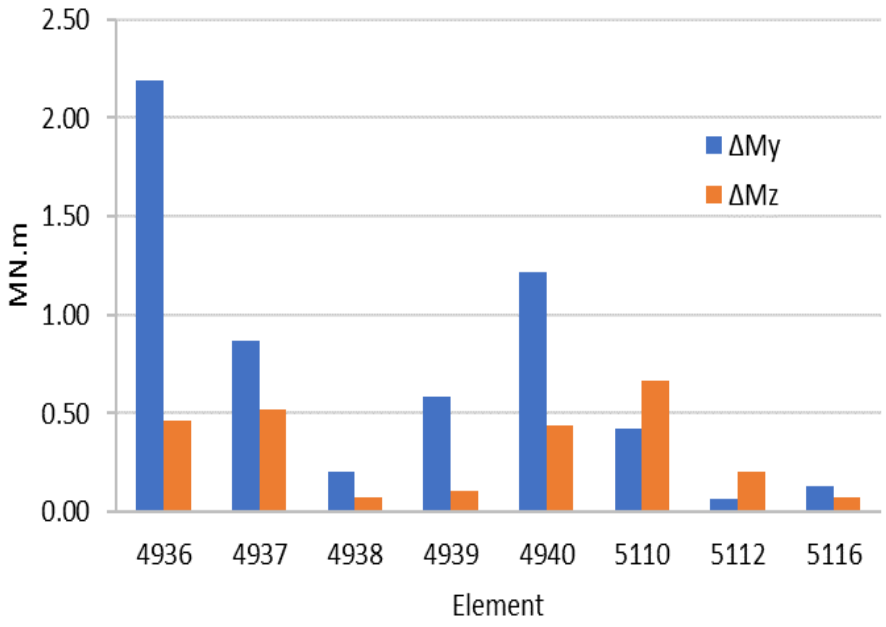

Figure D.18 –Bending forces range for each element – W80

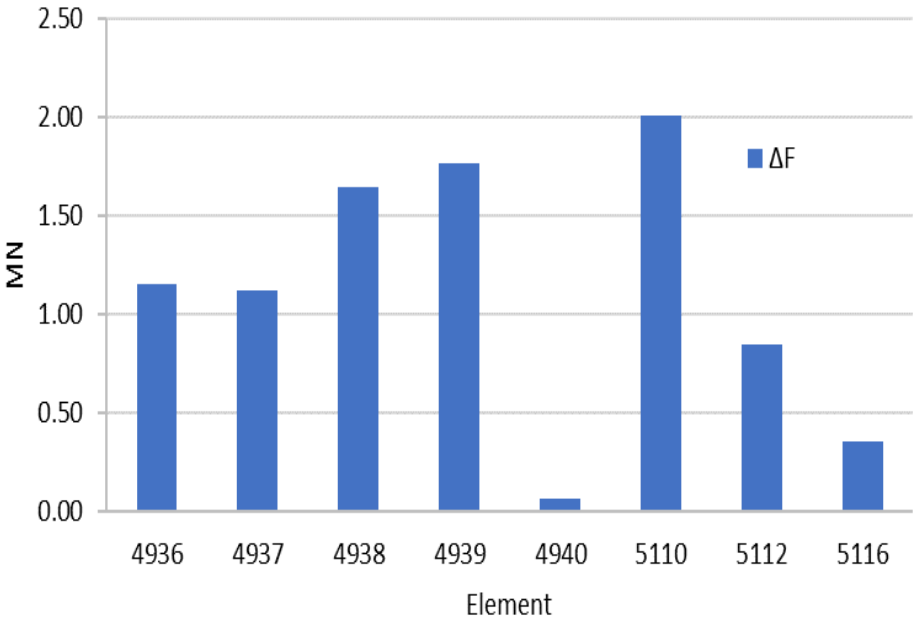

Figure D.19 –Axial forces range for each element – W96

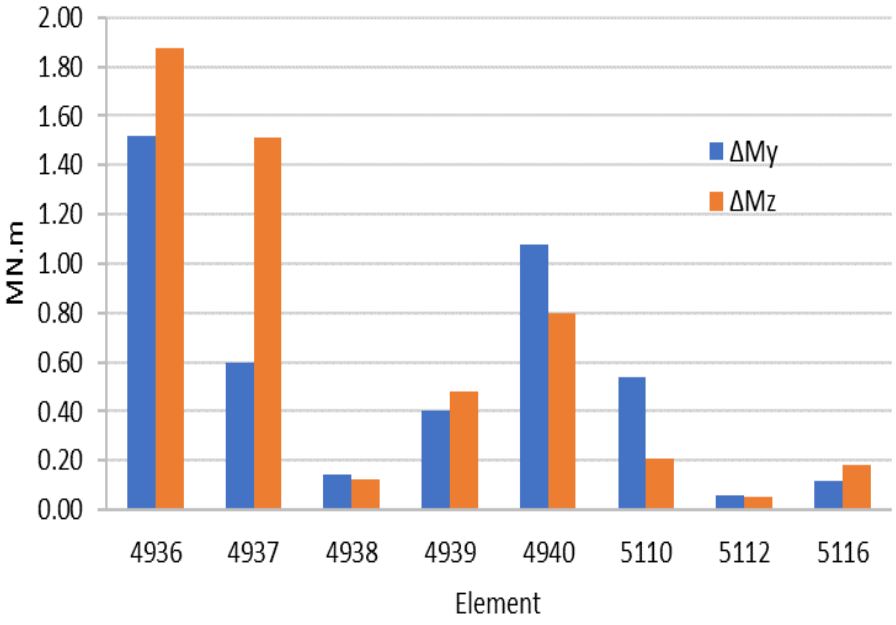

Figure D.20 –Bending forces range for each element – W96

Annex E: Hot-Spot Stresses for each wave load case

Table E.1 – Hot-spot stresses for W3, MPa

Plane	Primary Element	Secondary Element	σ1	σ2	σ3	σ4	σ5	σ6	σ7	σ8
		5110	4.44	0.39	-1.38	-1.24	2.13	3.36	5.13	4.99
	4936	5116	6.08	1.07	-1.14	-0.66	3.64	5.84	8.05	7.57
		5112	3.90	0.87	-0.32	-0.38	2.12	2.33	3.52	3.59
		5110	2.23	-0.93	-2.17	-1.53	1.39	3.00	4.24	3.60
XZ	4937	5116	3.12	-0.98	-2.62	-1.61	2.23	4.79	6.43	5.42
		5112	1.98	-0.22	-1.01	-0.68	1.33	1.99	2.77	2.45
		5110	14.17	9.81	1.61	-5.63	-7.67	-3.31	4.89	12.13
		5116	10.82	3.01	-3.44	-4.73	-0.13	7.69	14.13	15.43
		5112	6.07	2.12	-0.74	-0.83	1.90	5.85	8.71	8.80
		4939	4.44	1.34	0.12	0.09	2.66	2.95	4.17	4.21
	4936	4940	9.88	0.78	-3.64	-2.21	5.65	11.94	16.37	14.93
		4938	4.19	0.92	-0.37	-0.34	2.42	2.88	4.17	4.13
		4939	2.23	-0.93	-2.17	-1.53	1.39	3.00	4.24	3.60
YZ	4937	4930	3.12	-0.98	-2.62	-1.61	2.23	4.79	6.43	5.42
		4938	1.98	-0.22	-1.01	-0.68	1.33	1.99	2.77	2.45
		4939	9.10	-8.63	-20.37	-19.25	-5.92	11.80	23.55	22.43
		4940	11.64	3.60	-5.70	-10.83	-8.78	-0.75	8.56	13.69
		4938	5.24	-0.69	-5.07	-5.34	-1.33	4.60	8.98	9.25

Table E.2 – Hot-spot stresses for W4, MPa

Plane	Primary Element	Secondary Element	σ1	σ2	σ3	σ4	σ5	σ6	σ7	σ8
		5110	3.56	-1.04	-3.65	-3.52	0.05	3.10	5.71	5.58
	4936	5116	4.52	-1.46	-4.71	-4.08	0.82	5.26	8.50	7.88
		5112	3.00	-0.12	-1.88	-2.03	0.30	1.88	3.64	3.79
		5110	2.72	-1.17	-2.83	-2.14	1.35	3.50	5.16	4.47
XZ	4937	5116	3.74	-1.33	-3.49	-2.35	2.30	5.62	7.78	6.64
		5112	2.40	-0.30	-1.36	-1.04	1.34	2.29	3.35	3.03
		5110	21.77	16.53	5.82	-4.10	-7.40	-2.16	8.56	18.47
		5116	10.71	0.04	-7.36	-7.15	0.55	11.22	18.62	18.40
		5112	9.51	3.59	-0.45	-0.25	4.08	10.00	14.04	13.84
		4939	3.30	0.08	-1.73	-1.83	0.60	2.28	4.09	4.19
	4936	4940	7.48	-4.40	-10.88	-8.94	1.05	11.38	17.86	15.93
		4938	3.17	-0.31	-2.22	-2.22	0.46	2.40	4.31	4.31
		4939	2.72	-1.17	-2.83	-2.14	1.35	3.50	5.16	4.47
YZ	4937	4930	3.74	-1.33	-3.49	-2.35	2.30	5.62	7.78	6.64
		4938	2.40	-0.30	-1.36	-1.04	1.34	2.29	3.35	3.03
		4939	10.78	-16.53	-33.20	-29.49	-7.55	19.76	36.44	32.72
		4940	16.51	10.32	-0.89	-10.54	-12.98	-6.78	4.42	14.07
		4938	6.99	-6.63	-14.73	-12.56	-1.40	12.22	20.32	18.16

Table E.3 – Hot-spot stresses for W5, MPa

Plane	Primary Element	Secondary Element	σ1	σ2	σ3	σ4	σ5	σ6	σ7	σ8
		5110	7.05	-0.20	-3.77	-3.58	2.27	5.53	9.10	8.91
	4936	5116	9.43	0.27	-4.18	-3.30	4.39	9.55	14.00	13.12
		5112	6.12	0.90	-1.52	-1.71	2.44	3.66	6.07	6.26
		5110	3.12	-1.72	-3.93	-3.13	1.13	4.15	6.36	5.56
XZ	4937	5116	4.19	-2.16	-5.03	-3.64	2.10	6.63	9.50	8.11
		5112	2.71	-0.57	-2.00	-1.65	1.18	2.64	4.07	3.72
	5110		34.92	28.77	15.29	2.38	-2.39	3.77	17.25	30.15
	5116		15.12	0.44	-9.06	-7.82	3.43	18.10	27.60	26.37
	5112		15.15	7.11	1.67	2.00	7.91	15.95	21.39	21.06
		4939	6.89	1.52	-0.95	-1.08	3.21	4.58	7.05	7.18
	4936	4940	15.42	-1.85	-10.73	-8.04	6.66	19.93	28.81	26.12
		4938	6.54	0.82	-1.79	-1.78	2.86	4.58	7.19	7.18
		4939	3.12	-1.72	-3.93	-3.13	1.13	4.15	6.36	5.56
YZ	4937	4930	4.19	-2.16	-5.03	-3.64	2.10	6.63	9.50	8.11
		4938	2.71	-0.57	-2.00	-1.65	1.18	2.64	4.07	3.72
	4939		12.29	-24.00	-45.30	-39.13	-9.11	27.18	48.48	42.31
	4940		21.46	8.07	-8.92	-19.56	-17.62	-4.24	12.75	23.40
	4938		9.06	-12.30	-24.26	-19.82	-1.57	19.78	31.75	27.31

Table E.4 – Hot-spot stresses for W6, MPa

Plane	Primary Element	Secondary Element	σ1	σ2	σ3	σ4	σ5	σ6	σ7	σ8
		5110	11.31	0.92	-3.70	-3.38	5.23	8.54	13.15	12.84
	4936	5116	15.46	2.56	-3.19	-1.97	9.04	14.85	20.60	19.39
		5112	9.92	2.18	-0.93	-1.13	5.24	5.90	9.01	9.21
		5110	3.66	-2.36	-5.21	-4.22	1.04	5.04	7.89	6.90
XZ	4937	5116	4.87	-3.08	-6.77	-5.04	2.09	8.03	11.72	9.99
		5112	3.17	-0.87	-2.71	-2.30	1.14	3.16	5.01	4.59
	5110		47.19	39.90	23.75	8.18	2.33	9.62	25.77	41.33
	5116		19.98	0.47	-11.75	-9.53	5.84	25.35	37.58	35.35
	5112		21.11	10.83	3.92	4.44	12.08	22.36	29.27	28.75
		4939	11.29	3.36	0.17	0.05	6.61	7.46	10.65	10.77
	4936	4940	25.14	1.66	-9.86	-6.22	14.00	30.39	41.92	38.27
		4938	10.67	2.28	-1.10	-1.03	5.99	7.29	10.67	10.60
		4939	3.66	-2.36	-5.21	-4.22	1.04	5.04	7.89	6.90
YZ	4937	4930	4.87	-3.08	-6.77	-5.04	2.09	8.03	11.72	9.99
		4938	3.17	-0.87	-2.71	-2.30	1.14	3.16	5.01	4.59
	4939		14.97	-29.56	-55.45	-47.55	-10.47	34.06	59.96	52.05
	4940		27.07	4.92	-18.98	-30.63	-23.20	-1.06	22.84	34.49
	4938		11.30	-17.45	-33.20	-26.72	-1.80	26.95	42.70	36.22

Table E.5 – Hot-spot stresses for W11, MPa

Plane	Primary Element	Secondary Element	σ1	σ2	σ3	σ4	σ5	σ6	σ7	σ8
		5110	3.73	0.53	-1.22	-1.47	0.90	2.12	3.86	4.12
	4936	5116	4.92	0.96	-1.15	-1.15	1.94	3.92	6.02	6.03
		5112	3.21	0.84	-0.37	-0.70	1.03	1.42	2.63	2.96
		5110	1.94	-0.61	-2.11	-2.08	-0.14	1.63	3.14	3.11
XZ	4937	5116	2.43	-0.90	-2.76	-2.45	0.23	2.79	4.65	4.34
		5112	1.63	-0.09	-1.11	-1.22	0.02	0.97	1.99	2.10
	5110		14.86	7.33	-2.06	-7.82	-6.56	0.97	10.36	16.12
	5116		6.99	4.05	0.11	-2.51	-2.29	0.65	4.58	7.21
	5112		9.00	5.69	3.05	2.62	4.66	7.97	10.61	11.04
		4939	3.60	1.17	-0.06	-0.37	1.42	1.86	3.09	3.40
	4936	4940	8.07	0.81	-3.31	-2.86	2.88	8.17	12.29	11.84
		4938	3.42	0.86	-0.43	-0.68	1.24	1.82	3.11	3.36
		4939	1.94	-0.61	-2.11	-2.08	-0.14	1.63	3.14	3.11
YZ	4937	4930	2.43	-0.90	-2.76	-2.45	0.23	2.79	4.65	4.34
		4938	1.63	-0.09	-1.11	-1.22	0.02	0.97	1.99	2.10
	4939		17.34	-0.99	-13.61	-13.12	0.18	18.51	31.13	30.64
	4940		11.36	3.02	-5.29	-8.72	-5.25	3.09	11.41	14.83
	4938		17.25	9.34	3.74	3.75	9.34	17.25	22.84	22.84

Table E.6 – Hot-spot stresses for W12, MPa

Plane	Primary Element	Secondary Element	σ1	σ2	σ3	σ4	σ5	σ6	σ7	σ8
		5110	10.48	3.73	1.13	0.65	6.11	5.75	8.35	8.83
	4936	5116	14.59	6.76	3.64	3.50	9.99	10.71	13.83	13.96
		5112	9.29	3.74	1.93	1.36	5.93	4.37	6.18	6.75
		5110	2.67	-0.44	-2.61	-2.95	-0.89	1.46	3.62	3.97
XZ	4937	5116	3.19	-0.85	-3.46	-3.50	-0.56	2.72	5.33	5.37
		5112	2.18	0.10	-1.40	-1.83	-0.55	0.77	2.27	2.70
	5110		26.73	16.60	4.10	-3.44	-1.60	8.53	21.02	28.56
	5116		8.11	4.22	0.55	-0.75	1.08	4.97	8.64	9.94
	5112		13.23	7.62	3.66	3.68	7.65	13.26	17.21	17.20
		4939	10.66	5.03	3.18	2.65	7.30	5.82	7.67	8.20
	4936	4940	23.63	11.07	4.99	5.41	15.63	21.09	27.16	26.74
		4938	10.03	4.21	2.28	1.83	6.67	5.39	7.32	7.77
		4939	2.67	-0.44	-2.61	-2.95	-0.89	1.46	3.62	3.97
YZ	4937	4930	3.19	-0.85	-3.46	-3.50	-0.56	2.72	5.33	5.37
		4938	2.18	0.10	-1.40	-1.83	-0.55	0.77	2.27	2.70
	4939		23.65	-3.64	-21.13	-18.57	2.53	29.81	47.30	44.74
	4940		15.51	3.41	-8.42	-13.04	-7.75	4.36	16.19	20.81
	4938		25.98	10.65	1.14	3.03	15.21	30.54	40.05	38.16

Table E.7 – Hot-spot stresses for W13, MPa

Plane	Primary Element	Secondary Element	σ1	σ2	σ3	σ4	σ5	σ6	σ7	σ8
		5110	17.69	6.77	3.07	2.49	11.64	10.00	13.69	14.27
	4936	5116	24.91	12.40	7.95	7.89	18.54	18.48	22.93	22.99
		5112	15.78	6.60	4.04	3.31	11.12	7.74	10.30	11.03
		5110	3.26	-0.58	-3.53	-4.16	-1.79	1.42	4.37	5.00
XZ	4937	5116	3.76	-1.28	-4.80	-5.05	-1.58	2.83	6.35	6.60
		5112	2.62	0.09	-1.97	-2.66	-1.27	0.63	2.69	3.38
		5110	39.28	25.77	9.50	0.00	2.83	16.34	32.61	42.11
		5116	12.34	3.99	-1.63	-1.22	4.97	13.33	18.95	18.54
		5112	18.07	9.34	3.64	4.32	10.98	19.72	25.41	24.73
		4939	18.20	8.90	6.29	5.61	13.55	10.28	12.89	13.57
	4936	4940	40.25	20.81	12.12	12.98	29.17	36.04	44.74	43.88
		4938	17.10	7.51	4.78	4.22	12.44	9.46	12.19	12.75
		4939	3.26	-0.58	-3.53	-4.16	-1.79	1.42	4.37	5.00
YZ	4937	4930	3.76	-1.28	-4.80	-5.05	-1.58	2.83	6.35	6.60
		4938	2.62	0.09	-1.97	-2.66	-1.27	0.63	2.69	3.38
		4939	30.62	-5.34	-27.95	-23.97	4.28	40.24	62.85	58.86
		4940	20.04	3.36	-12.63	-18.55	-10.94	5.74	21.73	27.65
		4938	35.64	12.90	-0.67	2.88	21.47	44.21	57.79	54.24

Table E.8 – Hot-spot stresses for W14, MPa

Plane	Primary Element	Secondary Element	σ1	σ2	σ3	σ4	σ5	σ6	σ7	σ8
		5110	24.67	9.49	4.66	4.08	17.02	14.34	19.16	19.74
	4936	5116	34.91	17.56	11.71	11.86	26.84	26.33	32.18	32.03
		5112	22.06	9.24	5.91	5.08	16.17	11.13	14.46	15.29
		5110	4.11	-0.76	-4.51	-5.32	-2.33	1.78	5.53	6.33
XZ	4937	5116	4.71	-1.67	-6.15	-6.48	-2.09	3.54	8.02	8.35
		5112	3.29	0.09	-2.53	-3.41	-1.67	0.77	3.39	4.28
		5110	50.74	33.66	13.79	2.76	7.03	24.10	43.98	55.01
		5116	17.40	3.47	-5.16	-3.44	7.63	21.55	30.18	28.46
		5112	22.94	10.64	2.93	4.33	14.02	26.32	34.03	32.63
		4939	25.51	12.53	9.12	8.36	19.62	14.74	18.14	18.90
	4936	4940	56.34	29.61	18.13	19.70	42.32	51.19	62.67	61.11
		4938	23.93	10.56	7.00	6.40	18.05	13.56	17.12	17.72
		4939	4.11	-0.76	-4.51	-5.32	-2.33	1.78	5.53	6.33
YZ	4937	4930	4.71	-1.67	-6.15	-6.48	-2.09	3.54	8.02	8.35
		4938	3.29	0.09	-2.53	-3.41	-1.67	0.77	3.39	4.28
		4939	37.54	-6.26	-33.70	-28.69	5.82	49.63	77.06	72.06
		4940	24.61	2.94	-17.62	-25.02	-14.94	6.73	27.29	34.70
		4938	45.81	16.44	-0.99	3.72	27.82	57.18	74.62	69.90

Table E.9 – Hot-spot stresses for W19, MPa

Plane	Primary Element	Secondary Element	σ1	σ2	σ3	σ4	σ5	σ6	σ7	σ8
		5110	13.24	7.12	5.76	4.96	10.19	6.28	7.63	8.44
	4936	5116	18.97	12.54	11.02	10.27	15.75	12.13	13.66	14.41
		5112	11.92	6.17	5.18	4.51	9.57	5.29	6.28	6.95
		5110	2.57	0.87	-0.60	-1.40	-0.65	0.23	1.70	2.50
XZ	4937	5116	3.12	1.06	-0.61	-1.33	-0.27	0.96	2.63	3.36
		5112	2.12	0.87	-0.21	-0.88	-0.36	0.07	1.15	1.82
		5110	18.80	8.01	-1.83	-4.95	0.47	11.26	21.10	24.22
		5116	7.52	2.78	-1.52	-2.86	-0.45	4.29	8.59	9.93
		5112	10.73	7.90	5.48	4.89	6.48	9.31	11.73	12.32
		4939	13.86	8.08	7.08	6.42	11.51	7.24	8.24	8.90
	4936	4940	30.53	22.66	19.84	18.71	24.94	22.77	25.58	26.72
		4938	12.98	7.15	6.13	5.49	10.63	6.41	7.43	8.07
		4939	2.57	0.87	-0.60	-1.40	-0.65	0.23	1.70	2.50
YZ	4937	4930	3.12	1.06	-0.61	-1.33	-0.27	0.96	2.63	3.36
		4938	2.12	0.87	-0.21	-0.88	-0.36	0.07	1.15	1.82
		4939	27.51	12.96	1.05	-1.23	7.45	22.00	33.90	36.18
		4940	10.36	0.77	-6.90	-8.16	-2.28	7.31	14.99	16.25
		4938	30.37	22.88	16.79	15.67	20.18	27.66	33.75	34.87

Table E.10 – Hot-spot stresses for W20, MPa

Plane	Primary Element	Secondary Element	σ1	σ2	σ3	σ4	σ5	σ6	σ7	σ8
		5110	22.08	11.34	8.80	7.61	16.81	10.89	13.43	14.61
	4936	5116	31.58	20.13	17.20	16.19	26.02	20.81	23.74	24.75
		5112	19.86	9.97	8.14	7.10	15.80	9.03	10.87	11.90
		5110	3.43	1.34	-0.97	-2.47	-1.96	-0.50	1.81	3.31
XZ	4937	5116	3.94	1.40	-1.19	-2.63	-1.75	0.15	2.74	4.18
		5112	2.75	1.25	-0.46	-1.69	-1.40	-0.53	1.18	2.41
		5110	27.56	11.91	-1.50	-4.80	3.94	19.60	33.01	36.31
		5116	10.64	5.21	0.70	-0.26	2.89	8.31	12.82	13.79
		5112	14.42	9.33	5.71	5.68	9.25	14.34	17.96	17.99
		4939	23.07	13.13	11.28	10.26	19.02	12.30	14.15	15.17
	4936	4940	50.85	36.08	30.58	29.24	41.19	39.30	44.80	46.13
		4938	21.61	11.54	9.63	8.67	17.55	10.96	12.87	13.83
		4939	3.43	1.34	-0.97	-2.47	-1.96	-0.50	1.81	3.31
YZ	4937	4930	3.94	1.40	-1.19	-2.63	-1.75	0.15	2.74	4.18
		4938	2.75	1.25	-0.46	-1.69	-1.40	-0.53	1.18	2.41
		4939	40.41	20.13	4.07	1.62	14.23	34.50	50.57	53.02
		4940	15.38	2.31	-8.99	-11.90	-4.71	8.37	19.67	22.58
		4938	48.33	36.83	27.89	26.75	34.08	45.58	54.52	55.66

Table E.11 – Hot-spot stresses for W21, MPa

Plane	Primary Element	Secondary Element	σ1	σ2	σ3	σ4	σ5	σ6	σ7	σ8
		5110	26.75	15.29	15.29	15.29	26.75	15.29	15.29	15.29
	4936	5116	39.63	28.17	28.17	28.17	39.63	28.17	28.17	28.17
		5112	24.53	13.07	13.07	13.07	24.53	13.07	13.07	13.07
		5110	5.00	1.81	-1.44	-3.41	-2.39	-0.31	2.94	4.91
XZ	4937	5116	5.83	1.94	-1.72	-3.57	-1.96	0.81	4.47	6.32
		5112	4.04	1.73	-0.65	-2.29	-1.64	-0.46	1.93	3.56
		5110	36.22	15.13	-2.34	-5.94	6.43	27.52	44.99	48.59
		5116	13.73	7.04	1.67	0.76	4.85	11.54	16.91	17.82
		5112	17.44	9.01	3.76	4.77	11.45	19.88	25.13	24.12
		4939	28.96	17.50	17.50	17.50	28.96	17.50	17.50	17.50
	4936	4940	63.32	51.86	51.86	51.86	63.32	51.86	51.86	51.86
		4938	26.94	15.48	15.48	15.48	26.94	15.48	15.48	15.48
		4939	5.00	1.81	-1.44	-3.41	-2.39	-0.31	2.94	4.91
YZ	4937	4930	5.83	1.94	-1.72	-3.57	-1.96	0.81	4.47	6.32
		4938	4.04	1.73	-0.65	-2.29	-1.64	-0.46	1.93	3.56
		4939	52.96	27.03	6.45	3.28	19.37	45.30	65.88	69.06
		4940	20.86	4.63	-10.61	-15.93	-8.22	8.02	23.26	28.58
		4938	65.92	50.43	38.53	37.19	47.19	62.68	74.58	75.92

Table E.12 – Hot-spot stresses for W22, MPa

Plane	Primary Element	Secondary Element	σ1	σ2	σ3	σ4	σ5	σ6	σ7	σ8
		5110	38.54	18.84	13.79	11.93	28.78	19.64	24.69	26.55
	4936	5116	55.01	33.64	27.74	26.35	44.71	37.24	43.14	44.52
		5112	34.63	16.83	13.23	11.52	27.11	16.07	19.66	21.38
		5110	6.77	2.19	-2.04	-4.35	-2.48	0.26	4.49	6.80
XZ	4937	5116	8.05	2.45	-2.35	-4.45	-1.70	2.06	6.86	8.96
		5112	5.52	2.20	-0.88	-2.83	-1.59	-0.11	2.97	4.92
		5110	44.31	17.86	-3.66	-7.65	8.22	34.67	56.19	60.19
		5116	18.01	7.70	0.12	-0.29	6.70	17.01	24.59	25.00
		5112	21.63	9.19	1.84	3.89	14.14	26.58	33.92	31.87
		4939	40.19	22.27	18.62	16.96	32.68	21.75	25.40	27.07
	4936	4940	88.62	59.73	48.50	47.08	70.72	70.77	82.00	83.42
		4938	37.66	19.44	15.67	14.13	30.14	19.51	23.28	24.83
		4939	6.77	2.19	-2.04	-4.35	-2.48	0.26	4.49	6.80
YZ	4937	4930	8.05	2.45	-2.35	-4.45	-1.70	2.06	6.86	8.96
		4938	5.52	2.20	-0.88	-2.83	-1.59	-0.11	2.97	4.92
		4939	64.31	32.94	8.07	4.27	23.77	55.14	80.01	83.81
		4940	26.93	7.97	-11.21	-19.37	-11.73	7.24	26.42	34.58
		4938	83.14	63.48	48.04	45.85	58.20	77.86	93.30	95.49

Table E.13 – Hot-spot stresses for W27, MPa

Plane	Primary Element	Secondary Element	σ1	σ2	σ3	σ4	σ5	σ6	σ7	σ8
		5110	15.61	8.48	6.99	6.07	12.20	7.41	8.90	9.83
	4936	5116	22.40	14.96	13.29	12.41	18.79	14.32	15.98	16.86
		5112	14.07	7.33	6.23	5.47	11.44	6.26	7.36	8.12
		5110	2.67	1.27	0.00	-0.89	-0.38	0.04	1.31	2.20
XZ	4937	5116	3.31	1.69	0.28	-0.58	0.09	0.73	2.13	3.00
		5112	2.23	1.12	0.17	-0.54	-0.12	0.00	0.95	1.66
		5110	12.31	-1.01	-11.46	-12.90	-4.50	8.83	19.27	20.72
		5116	5.49	1.94	-1.39	-2.56	-0.87	2.68	6.02	7.18
		5112	6.79	4.68	2.71	2.04	3.05	5.17	7.14	7.81
		4939	16.36	9.60	8.50	7.74	13.73	8.58	9.68	10.44
	4936	4940	36.04	27.09	24.02	22.67	29.78	26.81	29.88	31.23
		4938	15.32	8.50	7.38	6.64	12.69	7.59	8.71	9.44
		4939	2.67	1.27	0.00	-0.89	-0.38	0.04	1.31	2.20
YZ	4937	4930	3.31	1.69	0.28	-0.58	0.09	0.73	2.13	3.00
		4938	2.23	1.12	0.17	-0.54	-0.12	0.00	0.95	1.66
		4939	36.04	30.20	21.49	15.02	14.58	20.42	29.13	35.60
		4940	14.42	6.24	-3.22	-8.43	-6.33	1.85	11.31	16.52
		4938	40.87	36.58	31.85	29.44	30.76	35.04	39.78	42.19

Table E.14 – Hot-spot stresses for W28, MPa

Plane	Primary Element	Secondary Element	σ1	σ2	σ3	σ4	σ5	σ6	σ7	σ8
		5110	24.53	13.21	10.61	9.01	18.59	11.44	14.04	15.63
	4936	5116	35.06	23.20	20.28	18.78	28.81	22.20	25.12	26.62
		5112	22.06	11.44	9.52	8.21	17.49	9.64	11.55	12.86
		5110	4.66	2.36	0.35	-1.12	-0.27	0.15	2.16	3.64
XZ	4937	5116	5.86	3.25	1.04	-0.43	0.66	1.38	3.59	5.06
		5112	3.91	2.04	0.54	-0.64	0.12	0.11	1.61	2.79
		5110	16.88	-2.80	-17.27	-18.06	-4.70	14.99	29.46	30.24
		5116	7.93	4.01	-0.03	-1.83	-0.34	3.57	7.62	9.42
		5112	9.88	5.45	2.25	2.16	5.24	9.67	12.87	12.95
		4939	25.62	14.96	13.03	11.73	21.05	13.24	15.17	16.47
	4936	4940	56.46	41.91	36.53	34.22	45.59	41.67	47.06	49.36
		4938	23.99	13.24	11.28	10.01	19.43	11.71	13.67	14.94
		4939	4.66	2.36	0.35	-1.12	-0.27	0.15	2.16	3.64
YZ	4937	4930	5.86	3.25	1.04	-0.43	0.66	1.38	3.59	5.06
		4938	3.91	2.04	0.54	-0.64	0.12	0.11	1.61	2.79
		4939	51.64	43.49	31.62	22.97	22.61	30.75	42.63	51.28
		4940	20.41	8.23	-5.92	-13.74	-10.65	1.54	15.69	23.50
		4938	61.79	55.67	49.13	45.98	48.07	54.18	60.73	63.88

Table E.15 – Hot-spot stresses for W29, MPa

Plane	Primary Element	Secondary Element	σ1	σ2	σ3	σ4	σ5	σ6	σ7	σ8
		5110	32.56	17.50	13.79	11.48	24.04	14.85	18.56	20.87
	4936	5116	46.41	30.59	26.43	24.24	37.43	29.00	33.16	35.35
		5112	29.23	15.15	12.42	10.52	22.68	12.51	15.24	17.14
		5110	6.62	3.36	0.60	-1.43	-0.14	0.35	3.11	5.13
XZ	4937	5116	8.37	4.68	1.64	-0.36	1.24	2.14	5.19	7.19
		5112	5.58	2.90	0.84	-0.78	0.37	0.27	2.32	3.95
		5110	21.06	-4.63	-22.88	-23.00	-4.93	20.75	39.00	39.13
		5116	10.52	6.30	1.35	-1.42	-0.39	3.83	8.78	11.55
		5112	11.94	4.30	-0.56	0.22	6.18	13.82	18.67	17.90
		4939	33.91	19.78	17.03	15.14	27.36	17.24	19.99	21.87
	4936	4940	74.79	55.20	47.54	44.17	59.19	54.52	62.18	65.56
		4938	31.78	17.52	14.71	12.88	25.22	15.24	18.04	19.87
		4939	6.62	3.36	0.60	-1.43	-0.14	0.35	3.11	5.13
YZ	4937	4930	8.37	4.68	1.64	-0.36	1.24	2.14	5.19	7.19
		4938	5.58	2.90	0.84	-0.78	0.37	0.27	2.32	3.95
		4939	65.63	55.11	39.90	28.89	28.54	39.05	54.27	65.28
		4940	26.72	9.92	-9.34	-19.77	-15.26	1.55	20.81	31.23
		4938	81.65	73.39	64.73	60.75	63.78	72.05	80.71	84.68

Table E.16 – Hot-spot stresses for W30, MPa

Plane	Primary Element	Secondary Element	σ1	σ2	σ3	σ4	σ5	σ6	σ7	σ8
		5110	39.85	21.44	16.66	13.61	28.78	17.79	22.57	25.62
	4936	5116	56.68	37.31	31.96	29.06	45.00	34.95	40.30	43.21
		5112	35.73	18.55	15.03	12.53	27.21	14.99	18.51	21.02
		5110	8.58	4.30	0.78	-1.76	0.01	0.61	4.13	6.67
XZ	4937	5116	10.88	6.04	2.15	-0.35	1.84	2.99	6.88	9.39
		5112	7.23	3.73	1.11	-0.93	0.64	0.46	3.08	5.13
		5110	25.89	-5.68	-28.07	-28.15	-5.89	25.68	48.06	48.15
		5116	12.95	7.72	1.48	-2.11	-0.96	4.27	10.51	14.11
		5112	13.69	2.33	-4.55	-2.92	6.27	17.63	24.51	22.87
		4939	41.41	24.16	20.61	18.13	32.89	20.73	24.28	26.75
	4936	4940	91.37	67.28	57.45	52.94	71.08	65.77	75.60	80.11
		4938	38.82	21.41	17.80	15.39	30.30	18.30	21.92	24.33
		4939	8.58	4.30	0.78	-1.76	0.01	0.61	4.13	6.67
YZ	4937	4930	10.88	6.04	2.15	-0.35	1.84	2.99	6.88	9.39
		4938	7.23	3.73	1.11	-0.93	0.64	0.46	3.08	5.13
		4939	78.02	65.15	46.71	33.50	33.27	46.14	64.57	77.78
		4940	33.01	11.27	-13.28	-26.25	-20.05	1.70	26.24	39.21
		4938	100.63	89.81	78.34	72.95	76.79	87.62	99.09	104.48

Table E.17 – Hot-spot stresses for W35, MPa

Plane	Primary Element	Secondary Element	σ1	σ2	σ3	σ4	σ5	σ6	σ7	σ8
		5110	9.18	4.81	3.21	2.18	5.47	3.56	5.16	6.19
	4936	5116	12.81	8.12	6.33	5.35	8.89	7.30	9.09	10.07
		5112	8.15	4.18	3.00	2.16	5.29	2.97	4.15	5.00
		5110	3.30	1.24	0.25	-0.09	1.42	1.46	2.45	2.79
XZ	4937	5116	4.49	2.09	0.94	0.69	2.51	2.88	4.04	4.28
		5112	2.89	1.21	0.51	0.19	1.44	1.10	1.80	2.12
	5110		14.40	1.40	-9.41	-11.70	-4.12	8.88	19.69	21.98
	5116		8.95	2.65	-2.93	-4.52	-1.19	5.10	10.68	12.27
	5112		7.69	5.68	3.80	3.14	4.09	6.10	7.99	8.65
		4939	9.36	5.37	4.18	3.35	6.50	4.21	5.40	6.23
	4936	4940	20.74	14.49	11.20	9.67	13.93	13.91	17.19	18.72
		4938	8.81	4.77	3.56	2.75	5.95	3.71	4.92	5.73
		4939	3.30	1.24	0.25	-0.09	1.42	1.46	2.45	2.79
YZ	4937	4930	4.49	2.09	0.94	0.69	2.51	2.88	4.04	4.28
		4938	2.89	1.21	0.51	0.19	1.44	1.10	1.80	2.12
	4939		29.23	21.69	12.58	7.22	8.76	16.29	25.41	30.76
	4940		15.23	0.74	-12.84	-17.56	-10.66	3.82	17.41	22.13
	4938		29.66	24.91	20.77	19.65	22.21	26.96	31.11	32.22

Table E.18 – Hot-spot stresses for W36, MPa

Plane	Primary Element	Secondary Element	σ1	σ2	σ3	σ4	σ5	σ6	σ7	σ8
		5110	14.73	7.61	4.97	3.34	8.70	5.79	8.43	10.05
	4936	5116	20.54	12.86	9.90	8.36	14.18	11.82	14.78	16.31
		5112	13.07	6.65	4.71	3.37	8.43	4.81	6.75	8.09
		5110	5.05	2.00	0.37	-0.35	1.73	1.87	3.51	4.22
XZ	4937	5116	6.78	3.24	1.35	0.77	3.27	3.90	5.79	6.38
		5112	4.39	1.91	0.73	0.10	1.83	1.41	2.58	3.22
	5110		19.90	1.25	-13.45	-15.57	-3.88	14.77	29.47	31.59
	5116		11.84	3.02	-4.66	-6.69	-1.88	6.95	14.62	16.65
	5112		11.85	8.81	6.17	5.47	7.12	10.16	12.80	13.50
		4939	15.01	8.55	6.59	5.26	10.36	6.78	8.74	10.07
	4936	4940	33.26	22.87	17.41	15.06	22.21	22.57	28.03	30.38
		4938	14.12	7.57	5.57	4.29	9.48	5.99	7.99	9.28
		4939	5.05	2.00	0.37	-0.35	1.73	1.87	3.51	4.22
YZ	4937	4930	6.78	3.24	1.35	0.77	3.27	3.90	5.79	6.38
		4938	4.39	1.91	0.73	0.10	1.83	1.41	2.58	3.22
	4939		42.19	31.26	18.82	12.16	15.18	26.11	38.55	45.21
	4940		21.72	-0.38	-20.62	-27.14	-16.13	5.96	26.20	32.73
	4938		47.18	41.05	35.60	34.03	37.25	43.38	48.83	50.41

Table E.19 – Hot-spot stresses for W37, MPa

Plane	Primary Element	Secondary Element	σ1	σ2	σ3	σ4	σ5	σ6	σ7	σ8
		5110	20.12	10.29	6.55	4.29	11.64	7.87	11.60	13.86
	4936	5116	27.99	17.36	13.15	11.04	19.05	16.08	20.28	22.40
		5112	17.83	9.01	6.27	4.40	11.30	6.51	9.25	11.12
		5110	6.71	2.71	0.42	-0.67	1.93	2.22	4.51	5.60
XZ	4937	5116	8.92	4.29	1.66	0.72	3.87	4.80	7.43	8.37
		5112	5.80	2.56	0.90	-0.04	2.12	1.66	3.31	4.26
		5110	25.01	1.09	-17.38	-19.58	-4.21	19.71	38.17	40.37
		5116	14.81	3.54	-6.22	-8.75	-2.58	8.69	18.45	20.98
		5112	15.43	10.60	6.84	6.37	9.46	14.30	18.05	18.52
		4939	20.45	11.58	8.82	6.97	13.93	9.19	11.95	13.80
	4936	4940	45.35	30.79	23.02	19.80	29.82	30.77	38.54	41.76
		4938	19.25	10.25	7.43	5.64	12.73	8.13	10.95	12.74
		4939	6.71	2.71	0.42	-0.67	1.93	2.22	4.51	5.60
YZ	4937	4930	8.92	4.29	1.66	0.72	3.87	4.80	7.43	8.37
		4938	5.80	2.56	0.90	-0.04	2.12	1.66	3.31	4.26
		4939	54.21	39.98	24.01	15.63	19.77	33.99	49.97	58.34
		4940	27.99	-1.86	-28.86	-37.19	-21.97	7.88	34.88	43.21
		4938	63.87	56.06	49.01	46.84	50.83	58.64	65.70	67.86

Table E.20 – Hot-spot stresses for W38, MPa

Plane	Primary Element	Secondary Element	σ1	σ2	σ3	σ4	σ5	σ6	σ7	σ8
		5110	25.26	12.82	8.01	5.14	14.41	9.85	14.67	17.53
	4936	5116	35.10	21.61	16.18	13.51	23.65	20.16	25.58	28.25
		5112	22.37	11.26	7.73	5.35	14.01	8.13	11.66	14.04
		5110	8.30	3.42	0.48	-1.00	2.06	2.50	5.43	6.92
XZ	4937	5116	10.96	5.31	1.96	0.65	4.38	5.59	8.94	10.25
		5112	7.15	3.20	1.07	-0.20	2.35	1.86	3.99	5.26
		5110	29.99	1.21	-21.02	-23.67	-5.19	23.59	45.81	48.46
		5116	18.12	4.33	-7.54	-10.53	-2.89	10.91	22.78	25.76
		5112	17.71	10.59	5.33	5.00	9.81	16.93	22.19	22.52
		4939	25.65	14.46	10.90	8.55	17.29	11.48	15.04	17.39
	4936	4940	56.89	38.24	28.21	24.18	37.00	38.65	48.68	52.71
		4938	24.15	12.79	9.15	6.88	15.80	10.17	13.80	16.07
		4939	8.30	3.42	0.48	-1.00	2.06	2.50	5.43	6.92
YZ	4937	4930	10.96	5.31	1.96	0.65	4.38	5.59	8.94	10.25
		4938	7.15	3.20	1.07	-0.20	2.35	1.86	3.99	5.26
		4939	65.08	47.87	28.65	18.68	23.80	41.01	60.22	70.19
		4940	34.11	-3.53	-37.35	-47.54	-28.13	9.52	43.34	53.53
		4938	79.91	70.34	61.45	58.45	63.09	72.66	81.55	84.55

Table E.21 – Hot-spot stresses for W43, MPa

Plane	Primary Element	Secondary Element	σ1	σ2	σ3	σ4	σ5	σ6	σ7	σ8
		5110	5.44	1.79	0.13	-0.29	2.50	2.74	4.41	4.82
	4936	5116	7.43	3.14	1.16	0.94	4.33	5.22	7.20	7.41
		5112	4.77	1.85	0.68	0.25	2.51	2.03	3.20	3.63
		5110	2.90	0.31	-0.81	-0.73	1.44	2.17	3.29	3.21
XZ	4937	5116	3.99	0.78	-0.61	-0.31	2.44	3.78	5.18	4.88
		5112	2.55	0.60	-0.15	-0.19	1.43	1.52	2.27	2.31
		5110	14.98	6.19	-3.32	-7.97	-5.05	3.74	13.25	17.91
		5116	11.29	2.11	-4.81	-5.42	0.65	9.83	16.75	17.36
		5112	8.33	5.30	2.91	2.58	4.48	7.52	9.90	10.24
		4939	5.43	2.46	1.26	0.85	3.16	2.74	3.93	4.34
	4936	4940	12.09	4.95	1.11	1.14	6.70	10.44	14.27	14.25
		4938	5.13	2.04	0.80	0.44	2.86	2.55	3.79	4.16
		4939	2.90	0.31	-0.81	-0.73	1.44	2.17	3.29	3.21
YZ	4937	4930	3.99	0.78	-0.61	-0.31	2.44	3.78	5.18	4.88
		4938	2.55	0.60	-0.15	-0.19	1.43	1.52	2.27	2.31
		4939	19.45	4.84	-6.21	-7.23	2.37	16.98	28.04	29.06
		4940	14.02	2.63	-9.05	-14.18	-9.76	1.63	13.31	18.44
		4938	16.75	12.85	9.22	7.99	9.88	13.79	17.41	18.64

Table E.22 – Hot-spot stresses for W44, MPa

Plane	Primary Element	Secondary Element	σ1	σ2	σ3	σ4	σ5	σ6	σ7	σ8
		5110	6.22	1.17	-1.53	-2.00	1.74	3.38	6.08	6.55
	4936	5116	8.26	2.07	-1.18	-1.28	3.53	6.31	9.56	9.66
		5112	5.38	1.58	-0.30	-0.86	1.92	2.31	4.19	4.75
		5110	4.00	0.36	-1.36	-1.34	1.59	2.84	4.55	4.54
XZ	4937	5116	5.41	0.89	-1.23	-0.90	2.87	4.99	7.11	6.79
		5112	3.49	0.79	-0.38	-0.52	1.64	1.94	3.11	3.25
		5110	23.19	10.93	-1.72	-7.35	-2.66	9.61	22.26	27.89
		5116	16.38	3.10	-6.64	-7.13	1.92	15.21	24.95	25.44
		5112	15.42	11.61	8.66	8.28	10.71	14.52	17.48	17.85
		4939	6.03	2.15	0.24	-0.29	2.58	3.05	4.97	5.50
	4936	4940	13.53	2.36	-3.97	-3.45	5.31	13.07	19.40	18.88
		4938	5.73	1.65	-0.35	-0.79	2.28	2.96	4.96	5.40
		4939	4.00	0.36	-1.36	-1.34	1.59	2.84	4.55	4.54
YZ	4937	4930	5.41	0.89	-1.23	-0.90	2.87	4.99	7.11	6.79
		4938	3.49	0.79	-0.38	-0.52	1.64	1.94	3.11	3.25
		4939	25.30	4.12	-10.87	-10.91	4.03	25.20	40.20	40.24
		4940	19.63	1.46	-16.20	-22.99	-14.95	3.22	20.87	27.67
		4938	24.07	16.88	11.35	10.73	15.37	22.57	28.09	28.71

Table E.23 – Hot-spot stresses for W45, MPa

Plane	Primary Element	Secondary Element	σ1	σ2	σ3	σ4	σ5	σ6	σ7	σ8
		5110	7.01	0.41	-3.49	-4.06	0.70	4.00	7.90	8.46
	4936	5116	9.04	0.73	-3.98	-3.98	2.38	7.38	12.09	12.10
		5112	5.96	1.23	-1.47	-2.21	1.10	2.54	5.24	5.98
		5110	5.15	0.30	-2.09	-2.10	1.76	3.65	6.04	6.05
XZ	4937	5116	6.91	0.85	-2.10	-1.68	3.34	6.44	9.38	8.96
		5112	4.48	0.92	-0.71	-0.93	1.87	2.46	4.09	4.31
		5110	32.75	17.07	0.91	-6.27	-0.26	15.41	31.58	38.76
		5116	22.78	5.14	-7.66	-8.12	4.03	21.67	34.47	34.93
		5112	20.36	15.84	12.22	11.61	14.38	18.90	22.53	23.13
		4939	6.60	1.74	-1.02	-1.70	1.74	3.30	6.06	6.74
	4936	4940	14.91	-0.81	-10.02	-8.99	3.33	15.75	24.96	23.93
		4938	6.31	1.14	-1.74	-2.30	1.45	3.32	6.20	6.76
		4939	5.15	0.30	-2.09	-2.10	1.76	3.65	6.04	6.05
YZ	4937	4930	6.91	0.85	-2.10	-1.68	3.34	6.44	9.38	8.96
		4938	4.48	0.92	-0.71	-0.93	1.87	2.46	4.09	4.31
		4939	31.87	4.56	-14.47	-14.06	5.54	32.85	51.88	51.47
		4940	25.51	-1.08	-25.64	-33.80	-20.76	5.82	30.39	38.54
		4938	32.87	22.61	15.17	14.92	22.01	32.28	39.71	39.96

Table E.24 – Hot-spot stresses for W46, MPa

Plane	Primary Element	Secondary Element	σ1	σ2	σ3	σ4	σ5	σ6	σ7	σ8
		5110	8.27	-0.05	-5.17	-5.87	0.05	4.81	9.93	10.63
	4936	5116	10.50	-0.08	-6.27	-6.22	1.82	8.85	15.04	14.98
		5112	6.98	1.12	-2.42	-3.35	0.65	2.94	6.49	7.42
		5110	6.33	0.23	-2.84	-2.87	1.94	4.50	7.57	7.60
XZ	4937	5116	8.45	0.80	-3.00	-2.48	3.81	7.92	11.71	11.19
		5112	5.49	1.05	-1.05	-1.35	2.10	3.00	5.09	5.39
		5110	41.79	23.00	3.38	-5.58	1.37	20.16	39.78	48.74
		5116	28.67	6.88	-8.91	-9.46	5.57	27.37	43.16	43.70
		5112	25.48	20.11	15.67	14.75	17.90	23.27	27.72	28.63
		4939	7.67	1.64	-1.97	-2.84	1.34	3.80	7.41	8.28
	4936	4940	17.39	-3.00	-15.12	-13.66	2.31	19.13	31.26	29.79
		4938	7.36	0.92	-2.86	-3.56	1.02	3.89	7.68	8.37
		4939	6.33	0.23	-2.84	-2.87	1.94	4.50	7.57	7.60
YZ	4937	4930	8.45	0.80	-3.00	-2.48	3.81	7.92	11.71	11.19
		4938	5.49	1.05	-1.05	-1.35	2.10	3.00	5.09	5.39
		4939	38.59	5.86	-17.04	-16.70	6.68	39.41	62.32	61.97
		4940	32.13	-3.75	-35.99	-45.72	-27.24	8.63	40.88	50.61
		4938	41.62	28.57	19.27	19.15	28.29	41.34	50.64	50.76

Table E.25 – Hot-spot stresses for W51, MPa

Plane	Primary Element	Secondary Element	σ1	σ2	σ3	σ4	σ5	σ6	σ7	σ8
		5110	3.62	0.09	-1.62	-1.56	1.29	2.72	4.43	4.37
	4936	5116	4.87	0.43	-1.69	-1.30	2.41	4.74	6.86	6.48
		5112	3.15	0.57	-0.58	-0.70	1.36	1.83	2.99	3.10
		5110	2.06	-0.70	-1.79	-1.28	1.24	2.58	3.67	3.17
XZ	4937	5116	2.88	-0.68	-2.12	-1.30	2.01	4.16	5.59	4.77
		5112	1.83	-0.11	-0.80	-0.56	1.20	1.72	2.42	2.17
		5110	14.56	10.04	1.74	-5.47	-7.37	-2.85	5.45	12.66
		5116	13.07	5.39	-0.88	-2.07	2.53	10.21	16.48	17.67
		5112	5.16	1.28	-1.45	-1.44	1.31	5.18	7.92	7.91
		4939	3.56	0.91	-0.27	-0.36	1.76	2.30	3.49	3.57
	4936	4940	7.95	-0.30	-4.54	-3.32	3.68	9.83	14.06	12.85
		4938	3.37	0.56	-0.69	-0.71	1.58	2.28	3.53	3.55
		4939	2.06	-0.70	-1.79	-1.28	1.24	2.58	3.67	3.17
YZ	4937	4930	2.88	-0.68	-2.12	-1.30	2.01	4.16	5.59	4.77
		4938	1.83	-0.11	-0.80	-0.56	1.20	1.72	2.42	2.17
		4939	8.76	-9.36	-21.27	-19.98	-6.25	11.87	23.78	22.49
		4940	11.37	3.65	-5.49	-10.68	-8.88	-1.16	7.98	13.17
		4938	5.49	-0.10	-4.34	-4.75	-1.09	4.50	8.74	9.15

Table E.26 – Hot-spot stresses for W52, MPa

Plane	Primary Element	Secondary Element	σ1	σ2	σ3	σ4	σ5	σ6	σ7	σ8
		5110	3.38	-1.06	-3.65	-3.56	-0.16	2.90	5.49	5.40
	4936	5116	4.25	-1.55	-4.76	-4.19	0.52	4.94	8.14	7.57
		5112	2.84	-0.16	-1.91	-2.08	0.11	1.73	3.48	3.65
		5110	2.33	-1.09	-2.60	-2.03	0.99	2.99	4.50	3.93
XZ	4937	5116	3.17	-1.30	-3.26	-2.29	1.76	4.80	6.76	5.79
		5112	2.04	-0.30	-1.28	-1.03	1.01	1.93	2.91	2.66
		5110	22.49	17.00	6.30	-3.35	-6.29	-0.80	9.91	19.55
		5116	15.85	4.50	-3.61	-3.74	4.19	15.54	23.66	23.79
		5112	10.91	5.05	1.23	1.70	6.18	12.05	15.86	15.39
		4939	3.10	0.00	-1.79	-1.92	0.38	2.10	3.89	4.02
	4936	4940	7.04	-4.52	-10.92	-9.10	0.57	10.75	17.16	15.34
		4938	2.98	-0.36	-2.26	-2.29	0.26	2.22	4.12	4.15
		4939	2.33	-1.09	-2.60	-2.03	0.99	2.99	4.50	3.93
YZ	4937	4930	3.17	-1.30	-3.26	-2.29	1.76	4.80	6.76	5.79
		4938	2.04	-0.30	-1.28	-1.03	1.01	1.93	2.91	2.66
		4939	10.82	-16.65	-33.41	-29.64	-7.55	19.92	36.68	32.91
		4940	16.03	8.73	-2.83	-11.87	-13.10	-5.81	5.75	14.79
		4938	7.28	-5.11	-12.71	-11.05	-1.12	11.27	18.87	17.22

Table E.27 – Hot-spot stresses for W53, MPa

Plane	Primary Element	Secondary Element	σ1	σ2	σ3	σ4	σ5	σ6	σ7	σ8
		5110	8.01	0.21	-3.46	-3.23	3.15	6.17	9.83	9.61
	4936	5116	10.83	1.06	-3.50	-2.57	5.70	10.69	15.25	14.32
		5112	6.99	1.28	-1.19	-1.37	3.24	4.17	6.64	6.82
		5110	2.88	-1.50	-3.53	-2.84	0.98	3.70	5.73	5.05
XZ	4937	5116	3.86	-1.88	-4.50	-3.30	1.86	5.94	8.56	7.36
		5112	2.50	-0.47	-1.79	-1.50	1.04	2.36	3.67	3.39
		5110	35.31	28.75	15.17	2.54	-1.75	4.82	18.39	31.02
		5116	21.64	4.97	-6.28	-5.53	6.79	23.45	34.71	33.96
		5112	20.69	12.55	7.33	8.08	14.37	22.50	27.73	26.97
		4939	7.91	2.05	-0.48	-0.59	4.17	5.25	7.78	7.89
	4936	4940	17.66	-0.47	-9.59	-6.77	8.75	22.10	31.23	28.40
		4938	7.49	1.27	-1.41	-1.37	3.75	5.18	7.87	7.83
		4939	2.88	-1.50	-3.53	-2.84	0.98	3.70	5.73	5.05
YZ	4937	4930	3.86	-1.88	-4.50	-3.30	1.86	5.94	8.56	7.36
		4938	2.50	-0.47	-1.79	-1.50	1.04	2.36	3.67	3.39
		4939	13.25	-22.59	-43.74	-37.79	-8.24	27.61	48.75	42.81
		4940	21.47	6.64	-11.00	-21.13	-17.80	-2.97	14.67	24.79
		4938	9.21	-9.64	-20.55	-17.12	-1.38	17.47	28.38	24.95

Table E.28 – Hot-spot stresses for W54, MPa

Plane	Primary Element	Secondary Element	σ1	σ2	σ3	σ4	σ5	σ6	σ7	σ8
		5110	12.68	1.24	-3.61	-3.14	6.47	9.70	14.56	14.09
	4936	5116	17.46	3.33	-2.74	-1.30	10.91	16.83	22.90	21.46
		5112	11.17	2.58	-0.68	-0.80	6.39	6.78	10.04	10.16
		5110	3.72	-1.98	-4.63	-3.75	1.22	4.80	7.45	6.57
XZ	4937	5116	4.97	-2.50	-5.93	-4.37	2.34	7.70	11.13	9.56
		5112	3.22	-0.63	-2.36	-1.99	1.30	3.05	4.77	4.41
		5110	47.21	39.46	23.13	7.79	2.43	10.18	26.51	41.85
		5116	28.62	6.28	-8.55	-7.19	9.57	31.91	46.75	45.38
		5112	26.95	16.60	10.01	11.04	19.08	29.43	36.02	35.00
		4939	12.75	3.96	0.62	0.58	7.98	8.57	11.91	11.94
	4936	4940	28.35	2.85	-9.35	-5.19	16.98	34.27	46.47	42.31
		4938	12.03	2.74	-0.80	-0.63	7.25	8.34	11.88	11.71
		4939	3.72	-1.98	-4.63	-3.75	1.22	4.80	7.45	6.57
YZ	4937	4930	4.97	-2.50	-5.93	-4.37	2.34	7.70	11.13	9.56
		4938	3.22	-0.63	-2.36	-1.99	1.30	3.05	4.77	4.41
		4939	16.19	-26.98	-52.38	-45.14	-9.48	33.69	59.09	51.85
		4940	27.86	4.51	-20.15	-31.68	-23.33	0.01	24.68	36.21
		4938	11.31	-13.02	-26.90	-22.20	-1.68	22.64	36.52	31.83

Table E.29 – Hot-spot stresses for W59, MPa

Plane	Primary Element	Secondary Element	σ1	σ2	σ3	σ4	σ5	σ6	σ7	σ8
		5110	4.81	1.37	-0.40	-0.85	1.67	2.34	4.10	4.56
	4936	5116	6.46	2.34	0.24	0.00	3.15	4.49	6.59	6.83
		5112	4.18	1.50	0.26	-0.21	1.77	1.67	2.91	3.38
		5110	1.69	-0.37	-1.65	-1.72	-0.22	1.21	2.49	2.56
XZ	4937	5116	2.09	-0.58	-2.15	-2.01	0.08	2.12	3.69	3.55
		5112	1.41	0.02	-0.86	-1.02	-0.06	0.70	1.58	1.74
		5110	14.65	7.11	-2.29	-8.04	-6.77	0.77	10.17	15.92
		5116	9.68	7.49	4.20	1.74	1.55	3.74	7.03	9.49
		5112	7.74	4.67	2.26	1.91	3.83	6.90	9.31	9.66
		4939	4.72	1.99	0.72	0.28	2.30	2.26	3.52	3.96
	4936	4940	10.55	3.43	-0.63	-0.64	4.80	9.14	13.20	13.21
		4938	4.47	1.62	0.31	-0.09	2.06	2.13	3.45	3.84
		4939	1.69	-0.37	-1.65	-1.72	-0.22	1.21	2.49	2.56
YZ	4937	4930	2.09	-0.58	-2.15	-2.01	0.08	2.12	3.69	3.55
		4938	1.41	0.02	-0.86	-1.02	-0.06	0.70	1.58	1.74
		4939	17.99	-0.39	-13.12	-12.75	0.51	18.89	31.62	31.25
		4940	12.23	4.34	-3.89	-7.62	-4.69	3.20	11.43	15.17
		4938	17.76	9.71	4.08	4.16	9.92	17.98	23.61	23.52

Table E.30 – Hot-spot stresses for W60, MPa

Plane	Primary Element	Secondary Element	σ1	σ2	σ3	σ4	σ5	σ6	σ7	σ8
		5110	12.19	4.56	1.77	1.24	7.50	6.69	9.48	10.01
	4936	5116	17.06	8.27	4.93	4.77	12.11	12.46	15.80	15.96
		5112	10.83	4.48	2.54	1.93	7.22	5.14	7.08	7.69
		5110	2.04	-0.43	-2.32	-2.71	-1.19	0.92	2.81	3.20
XZ	4937	5116	2.33	-0.91	-3.17	-3.31	-1.07	1.81	4.07	4.21
		5112	1.63	0.02	-1.30	-1.74	-0.85	0.40	1.72	2.16
		5110	26.74	16.26	3.66	-3.68	-1.46	9.02	21.62	28.96
		5116	13.70	8.04	3.35	2.36	5.66	11.32	16.01	17.00
		5112	16.55	10.87	7.08	7.39	11.63	17.31	21.10	20.79
		4939	12.46	6.02	4.04	3.47	8.85	6.86	8.83	9.41
	4936	4940	27.60	13.75	7.24	7.67	19.00	24.42	30.92	30.49
		4938	11.72	5.07	3.01	2.52	8.11	6.32	8.39	8.88
		4939	2.04	-0.43	-2.32	-2.71	-1.19	0.92	2.81	3.20
YZ	4937	4930	2.33	-0.91	-3.17	-3.31	-1.07	1.81	4.07	4.21
		4938	1.63	0.02	-1.30	-1.74	-0.85	0.40	1.72	2.16
		4939	24.46	-2.94	-20.59	-18.16	2.93	30.32	47.97	45.54
		4940	17.19	5.91	-5.98	-11.51	-7.44	3.84	15.73	21.26
		4938	27.44	12.79	3.59	5.22	16.74	31.38	40.59	38.95

Table E.31 – Hot-spot stresses for W61, MPa

Plane	Primary Element	Secondary Element	σ1	σ2	σ3	σ4	σ5	σ6	σ7	σ8
		5110	19.79	7.46	3.48	3.04	13.54	11.59	15.57	16.01
	4936	5116	27.99	13.84	9.01	9.18	21.39	21.25	26.08	25.92
		5112	17.69	7.32	4.58	3.92	12.88	8.97	11.71	12.37
		5110	3.13	-0.55	-3.17	-3.62	-1.22	1.63	4.26	4.71
XZ	4937	5116	3.71	-1.08	-4.25	-4.33	-0.89	3.09	6.25	6.34
		5112	2.55	0.10	-1.73	-2.27	-0.80	0.83	2.66	3.20
		5110	39.02	24.80	8.34	-0.73	2.92	17.14	33.60	42.67
		5116	20.56	9.24	1.13	1.00	8.92	20.24	28.35	28.48
		5112	23.78	14.66	8.94	9.97	17.14	26.26	31.98	30.95
		4939	20.45	9.94	7.14	6.54	15.63	11.86	14.66	15.26
	4936	4940	45.17	23.22	13.72	15.12	33.72	41.39	50.89	49.50
		4938	19.19	8.36	5.42	4.96	14.38	10.93	13.87	14.33
		4939	3.13	-0.55	-3.17	-3.62	-1.22	1.63	4.26	4.71
YZ	4937	4930	3.71	-1.08	-4.25	-4.33	-0.89	3.09	6.25	6.34
		4938	2.55	0.10	-1.73	-2.27	-0.80	0.83	2.66	3.20
		4939	32.04	-3.59	-26.20	-22.56	5.21	40.84	63.46	59.81
		4940	23.19	7.41	-9.20	-16.90	-11.19	4.59	21.20	28.90
		4938	38.27	17.64	5.03	7.83	24.39	45.02	57.63	54.83

Table E.32 – Hot-spot stresses for W62, MPa

Plane	Primary Element	Secondary Element	σ1	σ2	σ3	σ4	σ5	σ6	σ7	σ8
		5110	27.12	10.02	4.75	4.45	19.24	16.47	21.75	22.04
	4936	5116	38.49	18.86	12.40	12.98	30.18	29.95	36.40	35.82
		5112	24.29	9.93	6.31	5.64	18.22	12.73	16.34	17.01
		5110	4.45	-0.81	-4.22	-4.56	-0.86	2.86	6.27	6.61
XZ	4937	5116	5.46	-1.37	-5.52	-5.33	-0.14	5.15	9.30	9.11
		5112	3.69	0.13	-2.22	-2.75	-0.40	1.62	3.97	4.51
		5110	50.03	31.84	11.58	1.12	6.59	24.78	45.04	55.50
		5116	27.95	10.39	-1.71	-1.26	11.47	29.03	41.13	40.68
		5112	30.76	17.96	10.28	12.22	22.65	35.46	43.14	41.19
		4939	28.12	13.57	9.87	9.28	22.06	16.75	20.44	21.04
	4936	4940	62.07	31.57	18.81	21.36	47.64	58.29	71.04	68.50
		4938	26.37	11.36	7.48	7.07	20.31	15.46	19.35	19.75
		4939	4.45	-0.81	-4.22	-4.56	-0.86	2.86	6.27	6.61
YZ	4937	4930	5.46	-1.37	-5.52	-5.33	-0.14	5.15	9.30	9.11
		4938	3.69	0.13	-2.22	-2.75	-0.40	1.62	3.97	4.51
		4939	39.46	-3.30	-30.42	-26.03	7.31	50.07	77.19	72.80
		4940	29.31	8.94	-12.72	-22.98	-15.83	4.54	26.21	36.46
		4938	49.21	23.14	7.20	10.73	31.66	57.73	73.67	70.14

Table E.33 – Hot-spot stresses for W67, MPa

Plane	Primary Element	Secondary Element	σ1	σ2	σ3	σ4	σ5	σ6	σ7	σ8
		5110	14.17	7.50	5.82	4.86	10.45	6.58	8.25	9.21
	4936	5116	20.20	13.14	11.25	10.36	16.27	12.78	14.67	15.56
		5112	12.72	6.52	5.30	4.50	9.86	5.51	6.73	7.53
		5110	2.05	0.68	-0.61	-1.34	-0.80	0.03	1.33	2.05
XZ	4937	5116	2.43	0.76	-0.71	-1.37	-0.58	0.56	2.03	2.69
		5112	1.67	0.68	-0.27	-0.88	-0.53	-0.07	0.88	1.49
		5110	19.25	8.46	-1.43	-4.63	0.74	11.53	21.42	24.62
		5116	9.76	4.98	0.67	-0.65	1.80	6.59	10.89	12.21
		5112	13.40	11.06	9.04	8.51	9.80	12.14	14.16	14.69
		4939	14.76	8.53	7.30	6.51	11.89	7.57	8.80	9.60
	4936	4940	32.55	23.64	20.14	18.82	25.73	24.08	27.59	28.91
		4938	13.83	7.54	6.28	5.51	10.97	6.71	7.97	8.73
		4939	2.05	0.68	-0.61	-1.34	-0.80	0.03	1.33	2.05
YZ	4937	4930	2.43	0.76	-0.71	-1.37	-0.58	0.56	2.03	2.69
		4938	1.67	0.68	-0.27	-0.88	-0.53	-0.07	0.88	1.49
		4939	27.92	13.79	2.00	-0.53	7.67	21.80	33.59	36.12
		4940	12.91	2.88	-5.96	-8.45	-3.12	6.91	15.76	18.25
		4938	31.11	23.81	17.90	16.83	21.25	28.55	34.46	35.53

Table E.34 – Hot-spot stresses for W68, MPa

Plane	Primary Element	Secondary Element	σ1	σ2	σ3	σ4	σ5	σ6	σ7	σ8
		5110	23.00	11.48	8.51	7.25	17.01	11.39	14.36	15.63
	4936	5116	32.80	20.38	16.93	15.91	26.47	21.75	25.20	26.22
		5112	20.66	10.19	8.05	6.92	16.04	9.37	11.50	12.63
		5110	3.42	1.36	-0.71	-2.01	-1.34	-0.17	1.90	3.20
XZ	4937	5116	4.05	1.57	-0.74	-1.98	-0.97	0.62	2.93	4.17
		5112	2.78	1.26	-0.26	-1.33	-0.88	-0.24	1.28	2.35
		5110	27.81	11.62	-2.06	-5.22	3.98	20.16	33.85	37.01
		5116	16.41	10.04	4.58	3.24	6.79	13.17	18.63	19.97
		5112	19.48	14.57	11.23	11.43	15.05	19.97	23.30	23.10
		4939	23.96	13.43	11.26	10.17	19.35	12.74	14.90	16.00
	4936	4940	52.85	36.31	29.79	28.54	41.86	41.26	47.78	49.03
		4938	22.46	11.76	9.53	8.50	17.84	11.39	13.62	14.65
		4939	3.42	1.36	-0.71	-2.01	-1.34	-0.17	1.90	3.20
YZ	4937	4930	4.05	1.57	-0.74	-1.98	-0.97	0.62	2.93	4.17
		4938	2.78	1.26	-0.26	-1.33	-0.88	-0.24	1.28	2.35
		4939	41.08	21.28	5.21	2.29	14.23	34.04	50.11	53.03
		4940	19.62	6.04	-7.30	-12.59	-6.72	6.86	20.20	25.49
		4938	49.24	38.64	30.28	29.06	35.69	46.29	54.65	55.87

Table E.35 – Hot-spot stresses for W69, MPa

Plane	Primary Element	Secondary Element	σ1	σ2	σ3	σ4	σ5	σ6	σ7	σ8
		5110	31.88	15.44	11.10	9.54	23.54	16.24	20.58	22.14
	4936	5116	45.45	27.56	22.49	21.34	36.65	30.79	35.86	37.02
		5112	28.63	13.84	10.75	9.30	22.20	13.25	16.34	17.79
		5110	5.32	1.63	-1.38	-2.88	-1.06	0.80	3.82	5.31
XZ	4937	5116	6.52	2.02	-1.43	-2.73	-0.21	2.46	5.91	7.22
		5112	4.41	1.69	-0.49	-1.78	-0.50	0.39	2.57	3.86
		5110	36.07	14.11	-3.69	-6.90	6.35	28.30	46.10	49.32
		5116	21.65	12.50	4.84	3.16	8.44	17.59	25.25	26.93
		5112	24.08	15.49	10.18	11.26	18.09	26.69	32.00	30.92
		4939	33.21	18.31	15.18	13.77	26.78	17.93	21.07	22.48
	4936	4940	73.23	48.83	39.16	38.02	57.94	58.60	68.27	69.41
		4938	31.12	15.97	12.73	11.43	24.70	16.10	19.34	20.64
		4939	5.32	1.63	-1.38	-2.88	-1.06	0.80	3.82	5.31
YZ	4937	4930	6.52	2.02	-1.43	-2.73	-0.21	2.46	5.91	7.22
		4938	4.41	1.69	-0.49	-1.78	-0.50	0.39	2.57	3.86
		4939	53.91	28.62	8.03	4.21	19.39	44.68	65.27	69.09
		4940	26.76	10.22	-7.84	-16.84	-11.51	5.04	23.10	32.10
		4938	67.09	53.38	42.60	41.06	49.66	63.37	74.16	75.70

Table E.36 – Hot-spot stresses for W70, MPa

Plane	Primary Element	Secondary Element	σ1	σ2	σ3	σ4	σ5	σ6	σ7	σ8
		5110	40.16	19.07	13.39	11.52	29.48	20.74	26.42	28.29
	4936	5116	57.22	34.15	27.47	26.18	45.95	39.19	45.86	47.15
		5112	36.05	17.21	13.18	11.39	27.83	16.83	20.86	22.64
		5110	7.10	1.79	-2.09	-3.65	-0.60	1.93	5.81	7.37
XZ	4937	5116	8.87	2.35	-2.15	-3.39	0.76	4.49	8.99	10.23
		5112	5.94	2.04	-0.74	-2.15	0.02	1.14	3.92	5.33
		5110	44.04	16.30	-5.84	-9.43	7.65	35.39	57.54	61.12
		5116	27.85	14.63	4.09	2.41	10.57	23.79	34.33	36.01
		5112	28.78	15.89	8.34	10.55	21.22	34.11	41.67	39.46
		4939	41.81	22.82	18.72	17.00	33.58	22.73	26.83	28.55
	4936	4940	92.21	60.27	47.48	46.43	72.64	74.74	87.53	88.58
		4938	39.18	19.84	15.60	14.03	30.96	20.46	24.70	26.27
		4939	7.10	1.79	-2.09	-3.65	-0.60	1.93	5.81	7.37
YZ	4937	4930	8.87	2.35	-2.15	-3.39	0.76	4.49	8.99	10.23
		4938	5.94	2.04	-0.74	-2.15	0.02	1.14	3.92	5.33
		4939	65.27	34.90	10.21	5.67	23.94	54.31	79.00	83.54
		4940	34.23	15.12	-7.72	-20.91	-16.73	2.38	25.22	38.41
		4938	84.94	67.98	54.20	51.66	61.85	78.80	92.59	95.13

Table E.37 – Hot-spot stresses for W75, MPa

Plane	Primary Element	Secondary Element	σ1	σ2	σ3	σ4	σ5	σ6	σ7	σ8
		5110	16.09	8.84	7.09	5.87	11.88	7.14	8.90	10.12
	4936	5116	22.94	15.39	13.45	12.25	18.50	14.06	16.00	17.20
		5112	14.45	7.60	6.30	5.31	11.21	6.07	7.37	8.36
		5110	2.78	1.20	0.08	-0.57	0.28	0.55	1.67	2.32
XZ	4937	5116	3.58	1.75	0.49	-0.12	0.94	1.47	2.73	3.33
		5112	2.36	1.10	0.28	-0.27	0.44	0.40	1.21	1.76
		5110	12.70	-0.79	-11.44	-13.00	-4.56	8.93	19.57	21.13
		5116	6.75	2.96	-0.85	-2.44	-0.88	2.91	6.71	8.30
		5112	6.65	5.03	3.38	2.67	3.32	4.95	6.59	7.30
		4939	16.76	9.90	8.59	7.60	13.52	8.40	9.71	10.69
	4936	4940	36.96	27.88	24.34	22.42	29.24	26.35	29.89	31.80
		4938	15.70	8.79	7.46	6.50	12.46	7.39	8.72	9.68
		4939	2.78	1.20	0.08	-0.57	0.28	0.55	1.67	2.32
YZ	4937	4930	3.58	1.75	0.49	-0.12	0.94	1.47	2.73	3.33
		4938	2.36	1.10	0.28	-0.27	0.44	0.40	1.21	1.76
		4939	35.79	29.89	21.21	14.83	14.49	20.38	29.06	35.44
		4940	16.20	7.33	-3.72	-10.48	-8.98	-0.11	10.94	17.70
		4938	39.94	35.74	31.29	29.18	30.66	34.85	39.31	41.41

Table E.38 – Hot-spot stresses for W76, MPa

Plane	Primary Element	Secondary Element	σ1	σ2	σ3	σ4	σ5	σ6	σ7	σ8
		5110	25.12	13.73	10.90	8.97	18.38	11.13	13.96	15.89
	4936	5116	35.77	23.89	20.74	18.86	28.66	21.91	25.05	26.94
		5112	22.54	11.83	9.73	8.16	17.35	9.43	11.53	13.10
		5110	4.94	2.34	0.53	-0.64	0.73	0.90	2.71	3.88
XZ	4937	5116	6.42	3.47	1.45	0.33	1.97	2.50	4.52	5.64
		5112	4.22	2.08	0.74	-0.22	0.98	0.69	2.03	2.99
		5110	17.46	-2.54	-17.31	-18.19	-4.68	15.33	30.09	30.97
		5116	10.20	5.86	1.05	-1.40	-0.07	4.26	9.07	11.53
		5112	9.84	5.88	2.97	2.81	5.50	9.47	12.38	12.53
		4939	26.14	15.39	13.27	11.72	20.95	13.06	15.17	16.73
	4936	4940	57.65	43.21	37.47	34.47	45.30	41.11	46.85	49.84
		4938	24.50	13.67	11.52	10.00	19.31	11.50	13.65	15.17
		4939	4.94	2.34	0.53	-0.64	0.73	0.90	2.71	3.88
YZ	4937	4930	6.42	3.47	1.45	0.33	1.97	2.50	4.52	5.64
		4938	4.22	2.08	0.74	-0.22	0.98	0.69	2.03	2.99
		4939	51.52	43.29	31.29	22.54	22.18	30.41	42.41	51.16
		4940	23.99	10.75	-5.95	-16.33	-14.32	-1.08	15.62	26.01
		4938	60.61	54.73	48.68	46.01	48.28	54.16	60.21	62.88

Table E.39 – Hot-spot stresses for W77, MPa

Plane	Primary Element	Secondary Element	σ1	σ2	σ3	σ4	σ5	σ6	σ7	σ8
		5110	33.32	18.25	14.32	11.57	23.88	14.44	18.38	21.12
	4936	5116	47.35	31.61	27.25	24.56	37.38	28.62	32.98	35.66
		5112	29.87	15.70	12.78	10.56	22.59	12.25	15.17	17.39
		5110	6.86	3.25	0.78	-0.81	1.13	1.32	3.79	5.37
XZ	4937	5116	8.94	4.85	2.09	0.57	2.89	3.57	6.33	7.85
		5112	5.87	2.89	1.07	-0.23	1.46	1.02	2.84	4.14
		5110	21.86	-4.47	-23.16	-23.28	-4.75	21.57	40.26	40.38
		5116	13.67	8.77	2.72	-0.93	-0.04	4.86	10.91	14.55
		5112	13.15	5.92	1.16	1.67	7.15	14.38	19.13	18.62
		4939	34.59	20.38	17.44	15.24	27.32	17.03	19.97	22.17
	4936	4940	76.35	57.15	49.20	44.91	59.04	53.73	61.68	65.97
		4938	32.44	18.12	15.13	12.98	25.17	14.98	17.97	20.12
		4939	6.86	3.25	0.78	-0.81	1.13	1.32	3.79	5.37
YZ	4937	4930	8.94	4.85	2.09	0.57	2.89	3.57	6.33	7.85
		4938	5.87	2.89	1.07	-0.23	1.46	1.02	2.84	4.14
		4939	65.57	55.02	39.65	28.45	27.99	38.54	53.92	65.12
		4940	31.54	13.21	-9.59	-23.51	-20.39	-2.06	20.74	34.66
		4938	80.77	73.00	65.17	61.88	65.04	72.82	80.64	83.93

Table E.40 – Hot-spot stresses for W78, MPa

Plane	Primary Element	Secondary Element	σ1	σ2	σ3	σ4	σ5	σ6	σ7	σ8
		5110	40.98	22.53	17.51	13.92	28.80	17.36	22.38	25.97
	4936	5116	58.11	38.85	33.30	29.77	45.26	34.63	40.17	43.71
		5112	36.69	19.35	15.62	12.72	27.31	14.75	18.49	21.38
		5110	8.64	4.03	0.95	-0.98	1.56	1.79	4.87	6.80
XZ	4937	5116	11.28	6.05	2.60	0.77	3.81	4.68	8.13	9.96
		5112	7.40	3.60	1.34	-0.25	1.95	1.38	3.64	5.23
		5110	26.47	-5.76	-28.51	-28.45	-5.62	26.60	49.35	49.29
		5116	17.15	11.11	3.48	-1.27	-0.35	5.70	13.32	18.07
		5112	16.32	5.30	-1.54	-0.20	8.54	19.56	26.40	25.06
		4939	42.45	25.06	21.31	18.44	33.08	20.58	24.33	27.20
	4936	4940	93.74	70.23	60.16	54.46	71.43	65.04	75.11	80.81
		4938	39.82	22.30	18.49	15.67	30.45	18.08	21.89	24.70
		4939	8.64	4.03	0.95	-0.98	1.56	1.79	4.87	6.80
YZ	4937	4930	11.28	6.05	2.60	0.77	3.81	4.68	8.13	9.96
		4938	7.40	3.60	1.34	-0.25	1.95	1.38	3.64	5.23
		4939	77.74	65.03	46.55	33.14	32.64	45.35	63.83	77.24
		4940	38.85	14.91	-14.27	-31.61	-26.93	-2.99	26.19	43.52
		4938	100.37	90.28	80.02	75.59	79.58	89.67	99.93	104.36

Table E.41 – Hot-spot stresses for W83, MPa

Plane	Primary Element	Secondary Element	σ1	σ2	σ3	σ4	σ5	σ6	σ7	σ8
		5110	9.47	4.92	3.15	2.03	5.38	3.56	5.33	6.46
	4936	5116	13.15	8.25	6.28	5.20	8.83	7.37	9.35	10.42
		5112	8.38	4.29	2.99	2.06	5.23	2.97	4.27	5.19
		5110	3.47	1.09	-0.01	-0.27	1.54	1.77	2.88	3.13
XZ	4937	5116	4.73	1.92	0.60	0.48	2.70	3.36	4.68	4.80
		5112	3.04	1.15	0.37	0.10	1.56	1.30	2.08	2.35
		5110	14.11	1.28	-9.37	-11.59	-4.10	8.73	19.38	21.60
		5116	9.96	3.88	-1.73	-3.58	-0.58	5.50	11.11	12.96
		5112	7.89	6.10	4.30	3.54	4.27	6.06	7.87	8.62
		4939	9.61	5.49	4.18	3.26	6.46	4.22	5.53	6.44
	4936	4940	21.31	14.67	11.05	9.37	13.82	14.10	17.73	19.40
		4938	9.05	4.87	3.54	2.64	5.90	3.72	5.05	5.94
		4939	3.47	1.09	-0.01	-0.27	1.54	1.77	2.88	3.13
YZ	4937	4930	4.73	1.92	0.60	0.48	2.70	3.36	4.68	4.80
		4938	3.04	1.15	0.37	0.10	1.56	1.30	2.08	2.35
		4939	29.29	21.88	12.90	7.59	9.08	16.48	25.47	30.77
		4940	15.98	1.20	-12.99	-18.28	-11.56	3.22	17.41	22.69
		4938	29.31	24.62	20.62	19.65	22.29	26.99	30.99	31.95

Table E.42 – Hot-spot stresses for W84, MPa

Plane	Primary Element	Secondary Element	σ1	σ2	σ3	σ4	σ5	σ6	σ7	σ8
		5110	15.01	7.67	4.87	3.18	8.66	5.86	8.66	10.35
	4936	5116	20.88	12.94	9.78	8.20	14.18	11.98	15.13	16.72
		5112	13.30	6.72	4.67	3.26	8.41	4.84	6.90	8.30
		5110	5.32	1.77	-0.03	-0.58	2.00	2.41	4.21	4.76
XZ	4937	5116	7.17	2.98	0.86	0.50	3.66	4.72	6.84	7.20
		5112	4.63	1.81	0.54	0.00	2.08	1.77	3.04	3.57
		5110	19.13	0.92	-13.41	-15.46	-4.02	14.20	28.52	30.57
		5116	13.48	4.91	-2.75	-5.02	-0.55	8.02	15.69	17.95
		5112	11.96	9.72	7.41	6.38	7.24	9.49	11.79	12.82
		4939	15.25	8.63	6.56	5.18	10.36	6.84	8.92	10.30
	4936	4940	33.82	22.93	17.12	14.71	22.19	22.94	28.76	31.17
		4938	14.36	7.64	5.52	4.18	9.47	6.05	8.17	9.51
		4939	5.32	1.77	-0.03	-0.58	2.00	2.41	4.21	4.76
YZ	4937	4930	7.17	2.98	0.86	0.50	3.66	4.72	6.84	7.20
		4938	4.63	1.81	0.54	0.00	2.08	1.77	3.04	3.57
		4939	41.81	30.46	17.95	11.61	15.14	26.49	39.00	45.35
		4940	22.88	0.32	-21.06	-28.74	-18.21	4.35	25.73	33.40
		4938	45.89	39.75	34.51	33.24	36.68	42.82	48.06	49.33

Table E.43 – Hot-spot stresses for W85, MPa

Plane	Primary Element	Secondary Element	σ1	σ2	σ3	σ4	σ5	σ6	σ7	σ8
		5110	20.36	10.26	6.36	4.08	11.61	8.01	11.91	14.19
	4936	5116	28.29	17.32	12.91	10.80	19.07	16.34	20.75	22.86
		5112	18.02	9.03	6.17	4.27	11.30	6.59	9.45	11.35
		5110	6.98	2.27	-0.20	-1.00	2.35	3.05	5.53	6.33
XZ	4937	5116	9.35	3.77	0.86	0.32	4.46	6.04	8.95	9.49
		5112	6.06	2.34	0.59	-0.18	2.49	2.21	3.97	4.73
		5110	23.79	0.53	-17.37	-19.41	-4.41	18.85	36.75	38.79
		5116	16.71	5.55	-4.21	-6.85	-0.81	10.36	20.11	22.75
		5112	14.17	10.54	7.24	6.21	8.04	11.68	14.97	16.01
		4939	20.67	11.61	8.73	6.85	13.94	9.30	12.18	14.05
	4936	4940	45.84	30.62	22.46	19.29	29.82	31.35	39.51	42.68
		4938	19.46	10.26	7.31	5.50	12.73	8.24	11.19	13.00
		4939	6.98	2.27	-0.20	-1.00	2.35	3.05	5.53	6.33
YZ	4937	4930	9.35	3.77	0.86	0.32	4.46	6.04	8.95	9.49
		4938	6.06	2.34	0.59	-0.18	2.49	2.21	3.97	4.73
		4939	53.80	38.30	21.84	14.07	19.54	35.05	51.51	59.28
		4940	29.75	-0.87	-29.73	-39.93	-25.50	5.12	33.98	44.18
		4938	62.67	54.84	48.08	46.33	50.62	58.45	65.21	66.96

Table E.44 – Hot-spot stresses for W86, MPa

Plane	Primary Element	Secondary Element	σ1	σ2	σ3	σ4	σ5	σ6	σ7	σ8
		5110	25.58	12.80	7.76	4.86	14.36	10.03	15.07	17.97
	4936	5116	35.51	21.57	15.87	13.19	23.66	20.49	26.19	28.86
		5112	22.64	11.29	7.60	5.18	14.00	8.23	11.92	14.34
		5110	8.41	2.64	-0.48	-1.48	2.58	3.64	6.76	7.76
XZ	4937	5116	11.22	4.35	0.67	-0.01	5.06	7.22	10.90	11.58
		5112	7.28	2.76	0.55	-0.41	2.79	2.61	4.82	5.78
		5110	28.48	0.48	-21.10	-23.63	-5.63	22.37	43.95	46.48
		5116	19.23	5.46	-6.38	-9.34	-1.69	12.09	23.93	26.88
		5112	16.61	10.77	6.04	5.20	8.73	14.58	19.31	20.15
		4939	25.94	14.51	10.79	8.40	17.30	11.61	15.33	17.72
	4936	4940	57.56	38.04	27.48	23.50	36.99	39.39	49.95	53.93
		4938	24.43	12.81	9.00	6.70	15.79	10.31	14.11	16.42
		4939	8.41	2.64	-0.48	-1.48	2.58	3.64	6.76	7.76
YZ	4937	4930	11.22	4.35	0.67	-0.01	5.06	7.22	10.90	11.58
		4938	7.28	2.76	0.55	-0.41	2.79	2.61	4.82	5.78
		4939	64.84	45.42	25.27	16.18	23.49	42.90	63.05	72.14
		4940	36.99	-2.02	-38.75	-51.69	-33.24	5.77	42.50	55.43
		4938	78.71	69.21	60.76	58.30	63.28	72.78	81.24	83.69

Table E.45 – Hot-spot stresses for W91, MPa

Plane	Primary Element	Secondary Element	σ1	σ2	σ3	σ4	σ5	σ6	σ7	σ8
		5110	5.96	1.91	0.16	-0.18	3.00	3.21	4.96	5.30
	4936	5116	8.19	3.43	1.33	1.22	5.07	6.00	8.10	8.21
		5112	5.25	1.99	0.78	0.38	2.97	2.38	3.60	3.99
		5110	2.99	0.08	-1.16	-0.97	1.50	2.48	3.72	3.53
XZ	4937	5116	4.11	0.48	-1.08	-0.62	2.54	4.25	5.81	5.35
		5112	2.63	0.48	-0.34	-0.32	1.49	1.71	2.54	2.52
		5110	14.03	5.53	-3.76	-8.42	-5.70	2.79	12.09	16.75
		5116	9.75	0.91	-5.84	-6.55	-0.80	8.04	14.79	15.50
		5112	7.67	4.69	2.26	1.79	3.57	6.54	8.98	9.44
		4939	5.99	2.68	1.44	1.07	3.71	3.18	4.42	4.79
	4936	4940	13.31	5.39	1.32	1.56	7.89	11.97	16.04	15.80
		4938	5.65	2.21	0.92	0.60	3.37	2.97	4.26	4.58
		4939	2.99	0.08	-1.16	-0.97	1.50	2.48	3.72	3.53
YZ	4937	4930	4.11	0.48	-1.08	-0.62	2.54	4.25	5.81	5.35
		4938	2.63	0.48	-0.34	-0.32	1.49	1.71	2.54	2.52
		4939	19.74	5.31	-5.65	-6.73	2.72	17.15	28.12	29.19
		4940	14.42	3.79	-7.79	-13.55	-10.10	0.53	12.12	17.87
		4938	16.66	12.11	8.21	7.24	9.78	14.33	18.23	19.20

Table E.46 – Hot-spot stresses for W92, MPa

Plane	Primary Element	Secondary Element	σ1	σ2	σ3	σ4	σ5	σ6	σ7	σ8
		5110	6.89	1.48	-1.22	-1.64	2.47	3.87	6.57	6.99
	4936	5116	9.26	2.69	-0.57	-0.60	4.60	7.17	10.42	10.46
		5112	5.99	1.86	-0.01	-0.54	2.59	2.71	4.58	5.11
		5110	3.98	-0.02	-1.88	-1.70	1.61	3.22	5.07	4.89
XZ	4937	5116	5.38	0.35	-1.96	-1.41	2.89	5.52	7.84	7.29
		5112	3.47	0.56	-0.68	-0.73	1.65	2.17	3.41	3.46
		5110	21.75	10.02	-2.22	-7.81	-3.47	8.26	20.50	26.09
		5116	12.80	0.46	-8.55	-8.95	-0.51	11.83	20.84	21.24
		5112	12.00	8.32	5.29	4.69	6.87	10.55	13.58	14.18
		4939	6.76	2.55	0.64	0.15	3.37	3.57	5.48	5.97
	4936	4940	15.12	3.48	-2.89	-2.24	7.03	14.67	21.03	20.38
		4938	6.41	1.99	-0.01	-0.41	3.01	3.43	5.42	5.83
		4939	3.98	-0.02	-1.88	-1.70	1.61	3.22	5.07	4.89
YZ	4937	4930	5.38	0.35	-1.96	-1.41	2.89	5.52	7.84	7.29
		4938	3.47	0.56	-0.68	-0.73	1.65	2.17	3.41	3.46
		4939	25.38	3.83	-11.26	-11.05	4.33	25.88	40.96	40.76
		4940	19.66	2.97	-14.33	-22.11	-15.80	0.89	18.19	25.97
		4938	23.65	14.30	7.83	8.04	14.80	24.15	30.62	30.41

Table E.47 – Hot-spot stresses for W93, MPa

Plane	Primary Element	Secondary Element	σ1	σ2	σ3	σ4	σ5	σ6	σ7	σ8
		5110	7.58	0.78	-3.04	-3.58	1.40	4.35	8.18	8.72
	4936	5116	9.91	1.43	-3.19	-3.17	3.40	8.03	12.65	12.63
		5112	6.50	1.54	-1.11	-1.82	1.74	2.85	5.50	6.21
		5110	5.06	-0.21	-2.72	-2.48	1.84	4.15	6.66	6.43
XZ	4937	5116	6.81	0.15	-2.99	-2.25	3.41	7.11	10.25	9.51
		5112	4.40	0.61	-1.08	-1.15	1.92	2.77	4.45	4.52
		5110	31.25	16.38	0.79	-6.40	-0.97	13.90	29.50	36.68
		5116	16.81	0.70	-10.80	-10.95	0.33	16.44	27.94	28.09
		5112	15.19	10.82	7.08	6.17	8.61	12.98	16.72	17.63
		4939	7.24	2.15	-0.55	-1.21	2.49	3.72	6.42	7.08
	4936	4940	16.29	0.52	-8.53	-7.48	4.97	16.89	25.94	24.89
		4938	6.90	1.51	-1.32	-1.85	2.15	3.69	6.52	7.05
		4939	5.06	-0.21	-2.72	-2.48	1.84	4.15	6.66	6.43
YZ	4937	4930	6.81	0.15	-2.99	-2.25	3.41	7.11	10.25	9.51
		4938	4.40	0.61	-1.08	-1.15	1.92	2.77	4.45	4.52
		4939	31.57	3.10	-16.31	-15.29	5.56	34.03	53.44	52.42
		4940	25.57	0.71	-23.59	-33.09	-22.23	2.64	26.93	36.43
		4938	31.68	17.69	8.63	9.79	20.51	34.50	43.57	42.40

Table E.48 – Hot-spot stresses for W94, MPa

Plane	Primary Element	Secondary Element	σ1	σ2	σ3	σ4	σ5	σ6	σ7	σ8
		5110	8.22	0.01	-4.99	-5.66	0.21	4.81	9.81	10.47
	4936	5116	10.47	0.04	-6.01	-5.94	2.01	8.84	14.88	14.81
		5112	6.95	1.15	-2.31	-3.21	0.78	2.97	6.42	7.33
		5110	6.11	-0.49	-3.68	-3.33	2.09	5.18	8.36	8.02
XZ	4937	5116	8.19	-0.19	-4.18	-3.19	3.95	8.82	12.81	11.82
		5112	5.30	0.59	-1.55	-1.60	2.21	3.42	5.55	5.61
		5110	39.99	22.29	3.57	-5.21	1.10	18.79	37.51	46.29
		5116	22.06	2.01	-12.06	-11.90	2.40	22.45	36.52	36.36
		5112	19.74	14.52	9.94	8.68	11.48	16.69	21.27	22.53
		4939	7.64	1.68	-1.85	-2.68	1.48	3.83	7.36	8.19
	4936	4940	17.31	-2.72	-14.57	-13.10	2.63	19.06	30.91	29.43
		4938	7.33	0.96	-2.73	-3.40	1.16	3.91	7.60	8.27
		4939	6.11	-0.49	-3.68	-3.33	2.09	5.18	8.36	8.02
YZ	4937	4930	8.19	-0.19	-4.18	-3.19	3.95	8.82	12.81	11.82
		4938	5.30	0.59	-1.55	-1.60	2.21	3.42	5.55	5.61
		4939	38.04	2.99	-20.76	-19.30	6.51	41.57	65.32	63.86
		4940	32.44	-1.68	-34.00	-45.57	-29.62	4.51	36.83	48.40
		4938	40.03	21.72	10.12	12.01	26.29	44.60	56.20	54.31

Annex F: Fatigue Damage for local approach

Table F.1 – Fatigue damage for W3 to W6

Plane	Member	Thickness	Wave	SCF	$\Delta\sigma_{nom,0}$	$\Delta\sigma_{nom}$	$\Delta\sigma_{loc,elastoplas}$	$\Delta\varepsilon_{loc,elastoplas}$	n_0	$2N_f$	N_f	D
-	-	mm	-	-	MPa	MPa	MPa	-	-	-	-	-
	5110	40	3	2.689338	9.12	9.12	28.5129	0.000135	8334	1E+11	5E+10	8.33E-06
x-z	5116	30	3	3.785792	6.41	6.41	25.95491	0.000123	8334	1E+11	5E+10	8.33E-06
	5112	25	3	2.943858	5.21	5.21	18.38277	8.69E-05	8334	1E+11	5E+10	8.33E-06
	4939	35	3	3.387385	12.70	12.70	47.50353	0.000224	8334	1E+11	5E+10	8.33E-06
y-z	4940	55	3	4.980734	5.84	5.84	35.63972	0.000168	8334	1E+11	5E+10	8.33E-06
	4938	25	3	4.597991	4.55	4.55	25.33128	0.00012	8334	1E+11	5E+10	8.33E-06
	5110	40	4	2.689338	13.43	13.43	42.16118	0.000199	3639	1E+11	5E+10	3.64E-06
x-z	5116	30	4	3.785792	7.42	7.42	29.72682	0.00014	3639	1E+11	5E+10	3.64E-06
	5112	25	4	2.943858	8.06	8.06	24.76856	0.000117	3639	1E+11	5E+10	3.64E-06
	4939	35	4	3.387385	17.67	17.67	65.28016	0.000309	3639	1E+11	5E+10	3.64E-06
y-z	4940	55	4	4.980734	6.84	6.84	41.88467	0.000198	3639	1E+11	5E+10	3.64E-06
	4938	25	4	4.597991	7.82	7.82	36.7606	0.000174	3639	1E+11	5E+10	3.64E-06
	5110	40	5	2.689338	20.78	20.78	63.10523	0.000298	1657	1E+11	5E+10	1.66E-06
x-z	5116	30	5	3.785792	10.25	10.25	42.12855	0.000199	1657	1E+11	5E+10	1.66E-06
	5112	25	5	2.943858	12.19	12.19	36.58092	0.000173	1657	1E+11	5E+10	1.66E-06
	4939	35	5	3.387385	22.30	22.30	82.46625	0.00039	1657	1E+11	5E+10	1.66E-06
y-z	4940	55	5	4.980734	10.44	10.44	63.93965	0.000302	1657	1E+11	5E+10	1.66E-06
	4938	25	5	4.597991	11.27	11.27	52.0144	0.000246	1657	1E+11	5E+10	1.66E-06
	5110	40	6	2.689338	27.77	27.77	84.029	0.000397	776	1E+11	5E+10	7.76E-07
x-z	5116	30	6	3.785792	13.56	13.56	53.88122	0.000255	776	1E+11	5E+10	7.76E-07
	5112	25	6	2.943858	16.58	16.58	49.79854	0.000235	776	1E+11	5E+10	7.76E-07
	4939	35	6	3.387385	27.30	27.30	101.5507	0.00048	776	1E+11	5E+10	7.76E-07
y-z	4940	55	6	4.980734	14.71	14.71	89.79685	0.000424	776	1E+11	5E+10	7.76E-07
	4938	25	6	4.597991	14.70	14.70	67.75673	0.00032	776	1E+11	5E+10	7.76E-07

Table F.2 – Fatigue damage for W11 to W14

Plane	Member	Thickness	Wave	SCF	$\Delta\sigma_{nom,0}$	$\Delta\sigma_{nom}$	$\sigma_{loc,elastoplas}$	$\varepsilon_{loc,elastoplas}$	n_0	$2N_f$	N_f	D
-	-	mm	-	-	MPa	MPa	MPa	-	-	-	-	-
	5110	40	11	2.689338	11.18	11.18	36.18382	0.000171	8020	1E+11	5E+10	8.02E-06
x-z	5116	30	11	3.785792	3.42	3.42	0	0	8020	1E+11	5E+10	8.02E-06
	5112	25	11	2.943858	6.54	6.54	22.36407	0.000106	8020	1E+11	5E+10	8.02E-06
	4939	35	11	3.387385	17.73	17.73	65.59763	0.00031	8020	1E+11	5E+10	8.02E-06
y-z	4940	55	11	4.980734	5.69	5.69	35.1677	0.000166	8020	1E+11	5E+10	8.02E-06
	4938	25	11	4.597991	11.17	11.17	51.42747	0.000243	8020	1E+11	5E+10	8.02E-06
	5110	40	12	2.689338	18.76	18.76	57.64188	0.000272	3502	1E+11	5E+10	3.5E-06
x-z	5116	30	12	3.785792	4.03	4.03	19.39491	9.17E-05	3502	1E+11	5E+10	3.5E-06
	5112	25	12	2.943858	9.99	9.99	29.74335	0.000141	3502	1E+11	5E+10	3.5E-06
	4939	35	12	3.387385	25.14	25.14	93.08975	0.00044	3502	1E+11	5E+10	3.5E-06
y-z	4940	55	12	4.980734	8.00	8.00	49.11544	0.000232	3502	1E+11	5E+10	3.5E-06
	4938	25	12	4.597991	17.87	17.87	82.44826	0.00039	3502	1E+11	5E+10	3.5E-06
	5110	40	13	2.689338	27.07	27.07	82.07191	0.000388	1595	1E+11	5E+10	1.6E-06
x-z	5116	30	13	3.785792	6.92	6.92	28.00295	0.000132	1595	1E+11	5E+10	1.6E-06
	5112	25	13	2.943858	14.18	14.18	42.42412	0.0002	1595	1E+11	5E+10	1.6E-06
	4939	35	13	3.387385	32.81	32.81	121.3187	0.000573	1595	1E+11	5E+10	1.6E-06
y-z	4940	55	13	4.980734	10.67	10.67	64.80279	0.000306	1595	1E+11	5E+10	1.6E-06
	4938	25	13	4.597991	25.03	25.03	115.2024	0.000544	1595	1E+11	5E+10	1.6E-06
	5110	40	14	2.689338	34.91	34.91	105.6193	0.000499	747	1E+11	5E+10	7.47E-07
x-z	5116	30	14	3.785792	10.59	10.59	43.01729	0.000203	747	1E+11	5E+10	7.47E-07
	5112	25	14	2.943858	18.58	18.58	55.71937	0.000263	747	1E+11	5E+10	7.47E-07
	4939	35	14	3.387385	40.11	40.11	147.7987	0.000698	747	1E+11	5E+10	7.47E-07
y-z	4940	55	14	4.980734	13.51	13.51	82.16493	0.000388	747	1E+11	5E+10	7.47E-07
	4938	25	14	4.597991	32.20	32.20	148.0652	0.0007	747	1E+11	5E+10	7.47E-07

Table F.3 – Fatigue damage for W19 to W22

Plane	Member	Thickness	Wave	SCF	$\Delta\sigma_{nom,0}$	$\Delta\sigma_{nom}$	$\sigma_{loc,elastoplas}$	$\varepsilon_{loc,elastoplas}$	n_0	$2N_f$	N_f	D
-	-	mm	-	-	MPa	MPa	MPa	-	-	-	-	-
	5110	40	19	2.689338	15.19	15.19	46.04649	0.000218	7003	1E+11	5E+10	7E-06
x-z	5116	30	19	3.785792	4.21	4.21	21.09394	9.97E-05	7003	1E+11	5E+10	7E-06
	5112	25	19	2.943858	7.28	7.28	23.63234	0.000112	7003	1E+11	5E+10	7E-06
	4939	35	19	3.387385	22.06	22.06	81.3532	0.000384	7003	1E+11	5E+10	7E-06
y-z	4940	55	19	4.980734	5.63	5.63	34.40664	0.000163	7003	1E+11	5E+10	7E-06
	4938	25	19	4.597991	17.64	17.64	81.15558	0.000384	7003	1E+11	5E+10	7E-06
	5110	40	20	2.689338	22.33	22.33	67.69519	0.00032	3058	1E+11	5E+10	3.06E-06
x-z	5116	30	20	3.785792	5.37	5.37	22.7203	0.000107	3058	1E+11	5E+10	3.06E-06
	5112	25	20	2.943858	10.41	10.41	31.09724	0.000147	3058	1E+11	5E+10	3.06E-06
	4939	35	20	3.387385	31.95	31.95	117.7339	0.000556	3058	1E+11	5E+10	3.06E-06
y-z	4940	55	20	4.980734	8.09	8.09	50.67366	0.000239	3058	1E+11	5E+10	3.06E-06
	4938	25	20	4.597991	27.91	27.91	128.3875	0.000607	3058	1E+11	5E+10	3.06E-06
	5110	40	21	2.689338	29.67	29.67	90.6364	0.000428	1393	1E+11	5E+10	1.39E-06
x-z	5116	30	21	3.785792	6.78	6.78	28.85229	0.000136	1393	1E+11	5E+10	1.39E-06
	5112	25	21	2.943858	13.70	13.70	41.1917	0.000195	1393	1E+11	5E+10	1.39E-06
	4939	35	21	3.387385	41.60	41.60	153.2865	0.000724	1393	1E+11	5E+10	1.39E-06
y-z	4940	55	21	4.980734	10.63	10.63	64.52799	0.000305	1393	1E+11	5E+10	1.39E-06
	4938	25	21	4.597991	37.99	37.99	174.758	0.000826	1393	1E+11	5E+10	1.39E-06
	5110	40	22	2.689338	36.65	36.65	110.9929	0.000525	652	1E+11	5E+10	6.52E-07
x-z	5116	30	22	3.785792	9.46	9.46	38.55476	0.000182	652	1E+11	5E+10	6.52E-07
	5112	25	22	2.943858	17.94	17.94	54.13128	0.000256	652	1E+11	5E+10	6.52E-07
	4939	35	22	3.387385	50.47	50.47	185.9713	0.000879	652	1E+11	5E+10	6.52E-07
y-z	4940	55	22	4.980734	13.22	13.22	81.34546	0.000384	652	1E+11	5E+10	6.52E-07
	4938	25	22	4.597991	47.97	47.97	220.7044	0.001043	652	3.29E+10	1.64E+10	1.98E-06

Table F.4 – Fatigue damage for W27 to W30

Plane	Member	Thickness	Wave	SCF	$\Delta\sigma_{nom,0}$	$\Delta\sigma_{nom}$	$\Delta\sigma_{loc,elastoplas}$	$\Delta\varepsilon_{loc,elastoplas}$	n_0	$2N_f$	N_f	D
-	-	mm	-	-	MPa	MPa	MPa	-	-	-	-	-
	5110	40	27	2.689338	13.04	13.04	39.53695	0.000187	6652	1E+11	5E+10	6.65E-06
x-z	5116	30	27	3.785792	3.12	3.12	0	0	6652	1E+11	5E+10	6.65E-06
	5112	25	27	2.943858	4.74	4.74	0	0	6652	1E+11	5E+10	6.65E-06
	4939	35	27	3.387385	23.38	23.38	86.88716	0.000411	6652	1E+11	5E+10	6.65E-06
y-z	4940	55	27	4.980734	6.52	6.52	39.68681	0.000188	6652	1E+11	5E+10	6.65E-06
	4938	25	27	4.597991	21.90	21.90	101.7243	0.000481	6652	1E+11	5E+10	6.65E-06
	5110	40	28	2.689338	18.68	18.68	57.08637	0.00027	2905	1E+11	5E+10	2.91E-06
x-z	5116	30	28	3.785792	4.03	4.03	19.39491	9.17E-05	2905	1E+11	5E+10	2.91E-06
	5112	25	28	2.943858	7.57	7.57	24.62923	0.000116	2905	1E+11	5E+10	2.91E-06
	4939	35	28	3.387385	33.40	33.40	123.0951	0.000582	2905	1E+11	5E+10	2.91E-06
y-z	4940	55	28	4.980734	9.48	9.48	57.55603	0.000272	2905	1E+11	5E+10	2.91E-06
	4938	25	28	4.597991	32.97	32.97	151.9897	0.000718	2905	1E+11	5E+10	2.91E-06
	5110	40	29	2.689338	23.93	23.93	72.44078	0.000342	1322	1E+11	5E+10	1.32E-06
x-z	5116	30	29	3.785792	4.98	4.98	21.23668	0.0001	1322	1E+11	5E+10	1.32E-06
	5112	25	29	2.943858	10.24	10.24	32.32254	0.000153	1322	1E+11	5E+10	1.32E-06
	4939	35	29	3.387385	42.52	42.52	156.8276	0.000741	1322	1E+11	5E+10	1.32E-06
y-z	4940	55	29	4.980734	12.72	12.72	78.25816	0.00037	1322	1E+11	5E+10	1.32E-06
	4938	25	29	4.597991	43.62	43.62	200.5694	0.000948	1322	1E+11	5E+10	1.32E-06
	5110	40	30	2.689338	29.42	29.42	89.38979	0.000422	620	1E+11	5E+10	6.2E-07
x-z	5116	30	30	3.785792	6.15	6.15	24.77154	0.000117	620	1E+11	5E+10	6.2E-07
	5112	25	30	2.943858	12.97	12.97	38.36635	0.000181	620	1E+11	5E+10	6.2E-07
	4939	35	30	3.387385	50.70	50.70	186.8275	0.000883	620	1E+11	5E+10	6.2E-07
y-z	4940	55	30	4.980734	16.05	16.05	97.37316	0.00046	620	1E+11	5E+10	6.2E-07
	4938	25	30	4.597991	53.98	53.98	248.2003	0.001173	620	8.81E+09	4.4E+09	7.04E-06

Table F.5 – Fatigue damage for W35 to W38

Plane	Member	Thickness	Wave	SCF	$\Delta\sigma_{nom,0}$	$\Delta\sigma_{nom}$	$\sigma_{loc,elastoplas}$	$\varepsilon_{loc,elastoplas}$	n_0	$2N_f$	N_f	D
-	-	mm	-	-	MPa	MPa	MPa	-	-	-	-	-
	5110	40	35	2.689338	13.93	13.93	43.60505	0.000206	8800	1E+11	5E+10	8.8E-06
x-z	5116	30	35	3.785792	5.27	5.27	24.90571	0.000118	8800	1E+11	5E+10	8.8E-06
	5112	25	35	2.943858	5.20	5.20	18.0793	8.54E-05	8800	1E+11	5E+10	8.8E-06
	4939	35	35	3.387385	20.13	20.13	75.16633	0.000355	8800	1E+11	5E+10	8.8E-06
y-z	4940	55	35	4.980734	8.73	8.73	54.55608	0.000258	8800	1E+11	5E+10	8.8E-06
	4938	25	35	4.597991	16.40	16.40	75.49058	0.000357	8800	1E+11	5E+10	8.8E-06
	5110	40	36	2.689338	19.70	19.70	59.6211	0.000282	3843	1E+11	5E+10	3.84E-06
x-z	5116	30	36	3.785792	7.17	7.17	28.87684	0.000136	3843	1E+11	5E+10	3.84E-06
	5112	25	36	2.943858	8.00	8.00	24.12406	0.000114	3843	1E+11	5E+10	3.84E-06
	4939	35	36	3.387385	29.08	29.08	107.3551	0.000507	3843	1E+11	5E+10	3.84E-06
y-z	4940	55	36	4.980734	12.91	12.91	78.39489	0.00037	3843	1E+11	5E+10	3.84E-06
	4938	25	36	4.597991	25.62	25.62	117.8116	0.000557	3843	1E+11	5E+10	3.84E-06
	5110	40	37	2.689338	25.03	25.03	75.8476	0.000358	1749	1E+11	5E+10	1.75E-06
x-z	5116	30	37	3.785792	9.05	9.05	36.51997	0.000173	1749	1E+11	5E+10	1.75E-06
	5112	25	37	2.943858	10.85	10.85	32.53448	0.000154	1749	1E+11	5E+10	1.75E-06
	4939	35	37	3.387385	37.43	37.43	137.9379	0.000652	1749	1E+11	5E+10	1.75E-06
y-z	4940	55	37	4.980734	17.09	17.09	104.0977	0.000492	1749	1E+11	5E+10	1.75E-06
	4938	25	37	4.597991	34.52	34.52	158.7261	0.00075	1749	1E+11	5E+10	1.75E-06
	5110	40	38	2.689338	30.06	30.06	90.97617	0.00043	820	1E+11	5E+10	8.2E-07
x-z	5116	30	38	3.785792	11.07	11.07	45.6319	0.000216	820	1E+11	5E+10	8.2E-07
	5112	25	38	2.943858	13.18	13.18	39.60994	0.000187	820	1E+11	5E+10	8.2E-07
	4939	35	38	3.387385	45.00	45.00	165.8195	0.000784	820	1E+11	5E+10	8.2E-07
y-z	4940	55	38	4.980734	21.25	21.25	128.9877	0.00061	820	1E+11	5E+10	8.2E-07
	4938	25	38	4.597991	43.13	43.13	198.6981	0.000939	820	1E+11	5E+10	8.2E-07

Table F.6 – Fatigue damage for W43 to W46

Plane	Member	Thickness	Wave	SCF	$\Delta\sigma_{nom,0}$	$\Delta\sigma_{nom}$	$\sigma_{loc,elastoplas}$	$\xi_{loc,elastoplas}$	n_0	$2N_f$	N_f	D
-	-	mm	-	-	MPa	MPa	MPa	-	-	-	-	-
	5110	40	43	2.689338	11.97	11.97	37.5926	0.000178	1463	1E+11	5E+10	1.46E-06
x-z	5116	30	43	3.785792	7.05	7.05	30.05669	0.000142	1463	1E+11	5E+10	1.46E-06
	5112	25	43	2.943858	6.05	6.05	20.60495	9.74E-05	1463	1E+11	5E+10	1.46E-06
	4939	35	43	3.387385	17.40	17.40	64.13601	0.000303	1463	1E+11	5E+10	1.46E-06
y-z	4940	55	43	4.980734	7.49	7.49	46.90689	0.000222	1463	1E+11	5E+10	1.46E-06
	4938	25	43	4.597991	9.68	9.68	44.72533	0.000211	1463	1E+11	5E+10	1.46E-06
	5110	40	44	2.689338	18.05	18.05	55.47211	0.000262	639	1E+11	5E+10	6.39E-07
x-z	5116	30	44	3.785792	10.19	10.19	41.32052	0.000195	639	1E+11	5E+10	6.39E-07
	5112	25	44	2.943858	10.37	10.37	30.8415	0.000146	639	1E+11	5E+10	6.39E-07
	4939	35	44	3.387385	23.55	23.55	86.80019	0.00041	639	1E+11	5E+10	6.39E-07
y-z	4940	55	44	4.980734	11.18	11.18	68.07436	0.000322	639	1E+11	5E+10	6.39E-07
	4938	25	44	4.597991	14.37	14.37	66.97206	0.000317	639	1E+11	5E+10	6.39E-07
	5110	40	45	2.689338	24.78	24.78	74.98847	0.000354	291	1E+11	5E+10	2.91E-07
x-z	5116	30	45	3.785792	13.82	13.82	55.85107	0.000264	291	1E+11	5E+10	2.91E-07
	5112	25	45	2.943858	13.45	13.45	39.74814	0.000188	291	1E+11	5E+10	2.91E-07
	4939	35	45	3.387385	29.93	29.93	110.346	0.000521	291	1E+11	5E+10	2.91E-07
y-z	4940	55	45	4.980734	15.43	15.43	93.60722	0.000442	291	1E+11	5E+10	2.91E-07
	4938	25	45	4.597991	19.75	19.75	90.85483	0.000429	291	1E+11	5E+10	2.91E-07
	5110	40	46	2.689338	31.05	31.05	93.93822	0.000444	137	1E+11	5E+10	1.37E-07
x-z	5116	30	46	3.785792	17.22	17.22	68.73252	0.000325	137	1E+11	5E+10	1.37E-07
	5112	25	46	2.943858	16.70	16.70	50.99683	0.000241	137	1E+11	5E+10	1.37E-07
	4939	35	46	3.387385	36.09	36.09	133.0078	0.000629	137	1E+11	5E+10	1.37E-07
y-z	4940	55	46	4.980734	20.17	20.17	122.3613	0.000578	137	1E+11	5E+10	1.37E-07
	4938	25	46	4.597991	25.02	25.02	115.1433	0.000544	137	1E+11	5E+10	1.37E-07

Table F.7 – Fatigue damage for W51 to W54

Plane	Member	Thickness	Wave	SCF	$\Delta\sigma_{nom,0}$	$\Delta\sigma_{nom}$	$\sigma_{loc,elastoplas}$	$\xi_{loc,elastoplas}$	n_0	$2N_f$	N_f	D
-	-	mm	-	-	MPa	MPa	MPa	-	-	-	-	-
	5110	40	51	2.689338	9.42	9.42	29.09343	0.000137	912	1E+11	5E+10	9.12E-07
x-z	5116	30	51	3.785792	7.01	7.01	29.26012	0.000138	912	1E+11	5E+10	9.12E-07
	5112	25	51	2.943858	4.67	4.67	0	0	912	1E+11	5E+10	9.12E-07
	4939	35	51	3.387385	12.67	12.67	47.21455	0.000223	912	1E+11	5E+10	9.12E-07
y-z	4940	55	51	4.980734	5.69	5.69	35.1677	0.000166	912	1E+11	5E+10	9.12E-07
	4938	25	51	4.597991	4.56	4.56	21.4312	0.000101	912	1E+11	5E+10	9.12E-07
	5110	40	52	2.689338	13.98	13.98	44.23903	0.000209	399	1E+11	5E+10	3.99E-07
x-z	5116	30	52	3.785792	9.23	9.23	36.67765	0.000173	399	1E+11	5E+10	3.99E-07
	5112	25	52	2.943858	8.83	8.83	28.64962	0.000135	399	1E+11	5E+10	3.99E-07
	4939	35	52	3.387385	17.76	17.76	65.77141	0.000311	399	1E+11	5E+10	3.99E-07
y-z	4940	55	52	4.980734	7.03	7.03	42.77055	0.000202	399	1E+11	5E+10	3.99E-07
	4938	25	52	4.597991	7.58	7.58	36.24487	0.000171	399	1E+11	5E+10	3.99E-07
	5110	40	53	2.689338	21.22	21.22	64.20841	0.000303	181	1E+11	5E+10	1.81E-07
x-z	5116	30	53	3.785792	13.00	13.00	51.60857	0.000244	181	1E+11	5E+10	1.81E-07
	5112	25	53	2.943858	15.37	15.37	46.28224	0.000219	181	1E+11	5E+10	1.81E-07
	4939	35	53	3.387385	22.68	22.68	83.58007	0.000395	181	1E+11	5E+10	1.81E-07
y-z	4940	55	53	4.980734	10.86	10.86	66.5494	0.000315	181	1E+11	5E+10	1.81E-07
	4938	25	53	4.597991	10.56	10.56	49.17758	0.000232	181	1E+11	5E+10	1.81E-07
	5110	40	54	2.689338	28.03	28.03	84.91011	0.000401	85	1E+11	5E+10	8.5E-08
x-z	5116	30	54	3.785792	17.29	17.29	69.27012	0.000327	85	1E+11	5E+10	8.5E-08
	5112	25	54	2.943858	19.90	19.90	59.06819	0.000279	85	1E+11	5E+10	8.5E-08
	4939	35	54	3.387385	27.44	27.44	101.1187	0.000478	85	1E+11	5E+10	8.5E-08
y-z	4940	55	54	4.980734	15.27	15.27	93.09804	0.00044	85	1E+11	5E+10	8.5E-08
	4938	25	54	4.597991	13.34	13.34	62.38167	0.000295	85	1E+11	5E+10	8.5E-08

Table F.8 – Fatigue damage for W59 to W62

Plane	Member	Thickness	Wave	SCF	$\Delta\sigma_{nom,0}$	$\Delta\sigma_{nom}$	$\sigma_{loc,elastoplas}$	$\xi_{loc,elastoplas}$	n_0	$2N_f$	N_f	D
-	-	mm	-	-	MPa	MPa	MPa	-	-	-	-	-
	5110	40	59	2.689338	11.08	11.08	34.77926	0.000164	1245	1E+11	5E+10	1.25E-06
x-z	5116	30	59	3.785792	3.89	3.89	19.213	9.08E-05	1245	1E+11	5E+10	1.25E-06
	5112	25	59	2.943858	5.73	5.73	17.90578	8.46E-05	1245	1E+11	5E+10	1.25E-06
	4939	35	59	3.387385	18.13	18.13	66.83602	0.000316	1245	1E+11	5E+10	1.25E-06
y-z	4940	55	59	4.980734	5.77	5.77	36.88027	0.000174	1245	1E+11	5E+10	1.25E-06
	4938	25	59	4.597991	11.48	11.48	54.02428	0.000255	1245	1E+11	5E+10	1.25E-06
	5110	40	60	2.689338	18.96	18.96	57.38431	0.000271	543	1E+11	5E+10	5.43E-07
x-z	5116	30	60	3.785792	6.36	6.36	25.4638	0.00012	543	1E+11	5E+10	5.43E-07
	5112	25	60	2.943858	11.90	11.90	37.03622	0.000175	543	1E+11	5E+10	5.43E-07
	4939	35	60	3.387385	25.65	25.65	94.56815	0.000447	543	1E+11	5E+10	5.43E-07
y-z	4940	55	60	4.980734	8.20	8.20	49.88576	0.000236	543	1E+11	5E+10	5.43E-07
	4938	25	60	4.597991	18.38	18.38	84.58252	0.0004	543	1E+11	5E+10	5.43E-07
	5110	40	61	2.689338	27.32	27.32	83.1514	0.000393	248	1E+11	5E+10	2.48E-07
x-z	5116	30	61	3.785792	10.60	10.60	43.17386	0.000204	248	1E+11	5E+10	2.48E-07
	5112	25	61	2.943858	17.56	17.56	51.83398	0.000245	248	1E+11	5E+10	2.48E-07
	4939	35	61	3.387385	33.50	33.50	123.4826	0.000584	248	1E+11	5E+10	2.48E-07
y-z	4940	55	61	4.980734	11.28	11.28	69.0816	0.000326	248	1E+11	5E+10	2.48E-07
	4938	25	61	4.597991	25.69	25.69	118.1462	0.000558	248	1E+11	5E+10	2.48E-07
	5110	40	62	2.689338	35.12	35.12	106.2996	0.000502	116	1E+11	5E+10	1.16E-07
x-z	5116	30	62	3.785792	15.23	15.23	60.53263	0.000286	116	1E+11	5E+10	1.16E-07
	5112	25	62	2.943858	23.21	23.21	68.90565	0.000326	116	1E+11	5E+10	1.16E-07
	4939	35	62	3.387385	40.78	40.78	150.3567	0.000711	116	1E+11	5E+10	1.16E-07
y-z	4940	55	62	4.980734	14.46	14.46	87.78684	0.000415	116	1E+11	5E+10	1.16E-07
	4938	25	62	4.597991	32.88	32.88	151.4459	0.000716	116	1E+11	5E+10	1.16E-07

Table F.9 – Fatigue damage for W67 to W70

Plane	Member	Thickness	Wave	SCF	$\Delta\sigma_{nom,0}$	$\Delta\sigma_{nom}$	$\sigma_{loc,elastoplas}$	$\xi_{loc,elastoplas}$	n_0	$2N_f$	N_f	D
-	-	mm	-	-	MPa	MPa	MPa	-	-	-	-	-
	5110	40	67	2.689338	15.43	15.43	47.2089	0.000223	14767	1E+11	5E+10	1.48E-05
x-z	5116	30	67	3.785792	4.88	4.88	23.15307	0.000109	14767	1E+11	5E+10	1.48E-05
	5112	25	67	2.943858	8.56	8.56	25.46086	0.00012	14767	1E+11	5E+10	1.48E-05
	4939	35	67	3.387385	22.13	22.13	81.65371	0.000386	14767	1E+11	5E+10	1.48E-05
y-z	4940	55	67	4.980734	6.48	6.48	41.5748	0.000196	14767	1E+11	5E+10	1.48E-05
	4938	25	67	4.597991	17.95	17.95	83.05109	0.000392	14767	1E+11	5E+10	1.48E-05
	5110	40	68	2.689338	22.73	22.73	69.76771	0.00033	6449	1E+11	5E+10	6.45E-06
x-z	5116	30	68	3.785792	7.47	7.47	30.19673	0.000143	6449	1E+11	5E+10	6.45E-06
	5112	25	68	2.943858	13.18	13.18	39.60994	0.000187	6449	1E+11	5E+10	6.45E-06
	4939	35	68	3.387385	32.14	32.14	118.4557	0.00056	6449	1E+11	5E+10	6.45E-06
y-z	4940	55	68	4.980734	9.47	9.47	57.49067	0.000272	6449	1E+11	5E+10	6.45E-06
	4938	25	68	4.597991	28.08	28.08	129.2287	0.000611	6449	1E+11	5E+10	6.45E-06
	5110	40	69	2.689338	30.04	30.04	90.90859	0.00043	2936	1E+11	5E+10	2.94E-06
x-z	5116	30	69	3.785792	10.15	10.15	40.88515	0.000193	2936	1E+11	5E+10	2.94E-06
	5112	25	69	2.943858	17.49	17.49	51.5804	0.000244	2936	1E+11	5E+10	2.94E-06
	4939	35	69	3.387385	41.89	41.89	154.3669	0.00073	2936	1E+11	5E+10	2.94E-06
y-z	4940	55	69	4.980734	12.47	12.47	75.77444	0.000358	2936	1E+11	5E+10	2.94E-06
	4938	25	69	4.597991	38.01	38.01	174.8537	0.000826	2936	1E+11	5E+10	2.94E-06
	5110	40	70	2.689338	37.17	37.17	113.2424	0.000535	1376	1E+11	5E+10	1.38E-06
x-z	5116	30	70	3.785792	13.61	13.61	54.14924	0.000256	1376	1E+11	5E+10	1.38E-06
	5112	25	70	2.943858	22.16	22.16	65.45585	0.000309	1376	1E+11	5E+10	1.38E-06
	4939	35	70	3.387385	50.61	50.61	186.4946	0.000881	1376	1E+11	5E+10	1.38E-06
y-z	4940	55	70	4.980734	15.46	15.46	93.79434	0.000443	1376	1E+11	5E+10	1.38E-06
	4938	25	70	4.597991	48.01	48.01	220.9002	0.001044	1376	3.26E+10	1.63E+10	4.23E-06

Table F.10 – Fatigue damage for W75 to W78

Plane	Member	Thickness	Wave	SCF	$\Delta\sigma_{nom,0}$	$\Delta\sigma_{nom}$	$\sigma_{loc,elastoplas}$	$\xi_{loc,elastoplas}$	n_0	$2N_f$	N_f	D
-	-	mm	-	-	MPa	MPa	MPa	-	-	-	-	-
	5110	40	75	2.689338	13.31	13.31	40.99411	0.000194	14976	1E+11	5E+10	1.5E-05
x-z	5116	30	75	3.785792	3.62	3.62	0	0	14976	1E+11	5E+10	1.5E-05
	5112	25	75	2.943858	4.44	4.44	0	0	14976	1E+11	5E+10	1.5E-05
	4939	35	75	3.387385	23.25	23.25	86.11596	0.000407	14976	1E+11	5E+10	1.5E-05
y-z	4940	55	75	4.980734	7.32	7.32	44.56675	0.000211	14976	1E+11	5E+10	1.5E-05
	4938	25	75	4.597991	21.39	21.39	98.42458	0.000465	14976	1E+11	5E+10	1.5E-05
	5110	40	76	2.689338	19.13	19.13	57.97209	0.000274	6540	1E+11	5E+10	6.54E-06
x-z	5116	30	76	3.785792	4.91	4.91	19.9797	9.44E-05	6540	1E+11	5E+10	6.54E-06
	5112	25	76	2.943858	7.33	7.33	24.72188	0.000117	6540	1E+11	5E+10	6.54E-06
	4939	35	76	3.387385	33.37	33.37	122.9847	0.000581	6540	1E+11	5E+10	6.54E-06
y-z	4940	55	76	4.980734	10.92	10.92	67.30434	0.000318	6540	1E+11	5E+10	6.54E-06
	4938	25	76	4.597991	32.29	32.29	148.4867	0.000702	6540	1E+11	5E+10	6.54E-06
	5110	40	77	2.689338	24.68	24.68	74.66714	0.000353	2978	1E+11	5E+10	2.98E-06
x-z	5116	30	77	3.785792	6.24	6.24	26.01584	0.000123	2978	1E+11	5E+10	2.98E-06
	5112	25	77	2.943858	10.72	10.72	31.74576	0.00015	2978	1E+11	5E+10	2.98E-06
	4939	35	77	3.387385	42.51	42.51	156.7919	0.000741	2978	1E+11	5E+10	2.98E-06
y-z	4940	55	77	4.980734	14.70	14.70	89.68802	0.000424	2978	1E+11	5E+10	2.98E-06
	4938	25	77	4.597991	42.99	42.99	197.9308	0.000935	2978	1E+11	5E+10	2.98E-06
	5110	40	78	2.689338	30.07	30.07	90.99967	0.00043	1395	1E+11	5E+10	1.4E-06
x-z	5116	30	78	3.785792	7.79	7.79	31.67209	0.00015	1395	1E+11	5E+10	1.4E-06
	5112	25	78	2.943858	14.28	14.28	43.28488	0.000205	1395	1E+11	5E+10	1.4E-06
	4939	35	78	3.387385	50.47	50.47	185.9713	0.000879	1395	1E+11	5E+10	1.4E-06
y-z	4940	55	78	4.980734	18.58	18.58	112.7097	0.000533	1395	1E+11	5E+10	1.4E-06
	4938	25	78	4.597991	53.57	53.57	246.6289	0.001166	1395	9.46E+09	4.73E+09	1.48E-05

Table F.11 – Fatigue damage for W83 to W86

Plane	Member	Thickness	Wave	SCF	$\Delta\sigma_{nom,0}$	$\Delta\sigma_{nom}$	$\sigma_{loc,elastoplas}$	$\xi_{loc,elastoplas}$	n_0	$2N_f$	N_f	D
-	-	mm	-	-	MPa	MPa	MPa	-	-	-	-	-
	5110	40	83	2.689338	13.70	13.70	41.77854	0.000197	9702	1E+11	5E+10	9.7E-06
x-z	5116	30	83	3.785792	5.50	5.50	22.28666	0.000105	9702	1E+11	5E+10	9.7E-06
	5112	25	83	2.943858	5.21	5.21	18.38277	8.69E-05	9702	1E+11	5E+10	9.7E-06
	4939	35	83	3.387385	20.11	20.11	74.99528	0.000354	9702	1E+11	5E+10	9.7E-06
y-z	4940	55	83	4.980734	9.07	9.07	56.67936	0.000268	9702	1E+11	5E+10	9.7E-06
	4938	25	83	4.597991	16.20	16.20	75.81011	0.000358	9702	1E+11	5E+10	9.7E-06
	5110	40	84	2.689338	19.07	19.07	57.75645	0.000273	4237	1E+11	5E+10	4.24E-06
x-z	5116	30	84	3.785792	7.56	7.56	31.38769	0.000148	4237	1E+11	5E+10	4.24E-06
	5112	25	84	2.943858	7.68	7.68	23.05298	0.000109	4237	1E+11	5E+10	4.24E-06
	4939	35	84	3.387385	29.03	29.03	107.1395	0.000506	4237	1E+11	5E+10	4.24E-06
y-z	4940	55	84	4.980734	13.46	13.46	81.79007	0.000387	4237	1E+11	5E+10	4.24E-06
	4938	25	84	4.597991	24.96	24.96	114.8383	0.000543	4237	1E+11	5E+10	4.24E-06
	5110	40	85	2.689338	24.06	24.06	72.89133	0.000344	1929	1E+11	5E+10	1.93E-06
x-z	5116	30	85	3.785792	9.58	9.58	38.05247	0.00018	1929	1E+11	5E+10	1.93E-06
	5112	25	85	2.943858	9.56	9.56	31.47818	0.000149	1929	1E+11	5E+10	1.93E-06
	4939	35	85	3.387385	37.74	37.74	139.1426	0.000658	1929	1E+11	5E+10	1.93E-06
y-z	4940	55	85	4.980734	17.95	17.95	108.8911	0.000515	1929	1E+11	5E+10	1.93E-06
	4938	25	85	4.597991	33.91	33.91	156.0084	0.000737	1929	1E+11	5E+10	1.93E-06
	5110	40	86	2.689338	28.86	28.86	87.32111	0.000413	904	1E+11	5E+10	9.04E-07
x-z	5116	30	86	3.785792	11.39	11.39	45.94859	0.000217	904	1E+11	5E+10	9.04E-07
	5112	25	86	2.943858	11.95	11.95	37.8398	0.000179	904	1E+11	5E+10	9.04E-07
	4939	35	86	3.387385	45.78	45.78	168.8511	0.000798	904	1E+11	5E+10	9.04E-07
y-z	4940	55	86	4.980734	22.66	22.66	137.4662	0.00065	904	1E+11	5E+10	9.04E-07
	4938	25	86	4.597991	42.49	42.49	195.4186	0.000924	904	1E+11	5E+10	9.04E-07

Table F.12 – Fatigue damage for W91 to W94

Plane	Member	Thickness	Wave	SCF	$\Delta\sigma_{nom,0}$	$\Delta\sigma_{nom}$	$\sigma_{loc,elastoplas}$	$\xi_{loc,elastoplas}$	n_0	$2N_f$	N_f	D
-	-	mm	-	-	MPa	MPa	MPa	-	-	-	-	-
	5110	40	91	2.689338	11.31	11.31	34.50506	0.000163	13161	1E+11	5E+10	1.32E-05
x-z	5116	30	91	3.785792	6.47	6.47	26.77219	0.000127	13161	1E+11	5E+10	1.32E-05
	5112	25	91	2.943858	5.64	5.64	20.21314	9.55E-05	13161	1E+11	5E+10	1.32E-05
	4939	35	91	3.387385	17.50	17.50	64.52994	0.000305	13161	1E+11	5E+10	1.32E-05
y-z	4940	55	91	4.980734	7.40	7.40	45.38659	0.000214	13161	1E+11	5E+10	1.32E-05
	4938	25	91	4.597991	9.83	9.83	46.11943	0.000218	13161	1E+11	5E+10	1.32E-05
	5110	40	92	2.689338	17.01	17.01	51.53067	0.000244	5747	1E+11	5E+10	5.75E-06
x-z	5116	30	92	3.785792	8.75	8.75	35.60231	0.000168	5747	1E+11	5E+10	5.75E-06
	5112	25	92	2.943858	8.39	8.39	25.90873	0.000122	5747	1E+11	5E+10	5.75E-06
	4939	35	92	3.387385	23.74	23.74	87.51518	0.000414	5747	1E+11	5E+10	5.75E-06
y-z	4940	55	92	4.980734	10.81	10.81	65.98519	0.000312	5747	1E+11	5E+10	5.75E-06
	4938	25	92	4.597991	14.83	14.83	68.65195	0.000324	5747	1E+11	5E+10	5.75E-06
	5110	40	93	2.689338	23.56	23.56	72.11	0.000341	2617	1E+11	5E+10	2.62E-06
x-z	5116	30	93	3.785792	11.42	11.42	46.28819	0.000219	2617	1E+11	5E+10	2.62E-06
	5112	25	93	2.943858	10.47	10.47	31.53583	0.000149	2617	1E+11	5E+10	2.62E-06
	4939	35	93	3.387385	30.23	30.23	111.6372	0.000528	2617	1E+11	5E+10	2.62E-06
y-z	4940	55	93	4.980734	15.03	15.03	91.24734	0.000431	2617	1E+11	5E+10	2.62E-06
	4938	25	93	4.597991	20.31	20.31	93.39228	0.000441	2617	1E+11	5E+10	2.62E-06
	5110	40	94	2.689338	29.55	29.55	90.06222	0.000426	1226	1E+11	5E+10	1.23E-06
x-z	5116	30	94	3.785792	14.53	14.53	57.63292	0.000272	1226	1E+11	5E+10	1.23E-06
	5112	25	94	2.943858	13.39	13.39	39.5083	0.000187	1226	1E+11	5E+10	1.23E-06
	4939	35	94	3.387385	36.74	36.74	135.8024	0.000642	1226	1E+11	5E+10	1.23E-06
y-z	4940	55	94	4.980734	19.87	19.87	120.9051	0.000571	1226	1E+11	5E+10	1.23E-06
	4938	25	94	4.597991	25.84	25.84	118.8666	0.000562	1226	1E+11	5E+10	1.23E-06

Annex G: Offshore platform case study blueprint

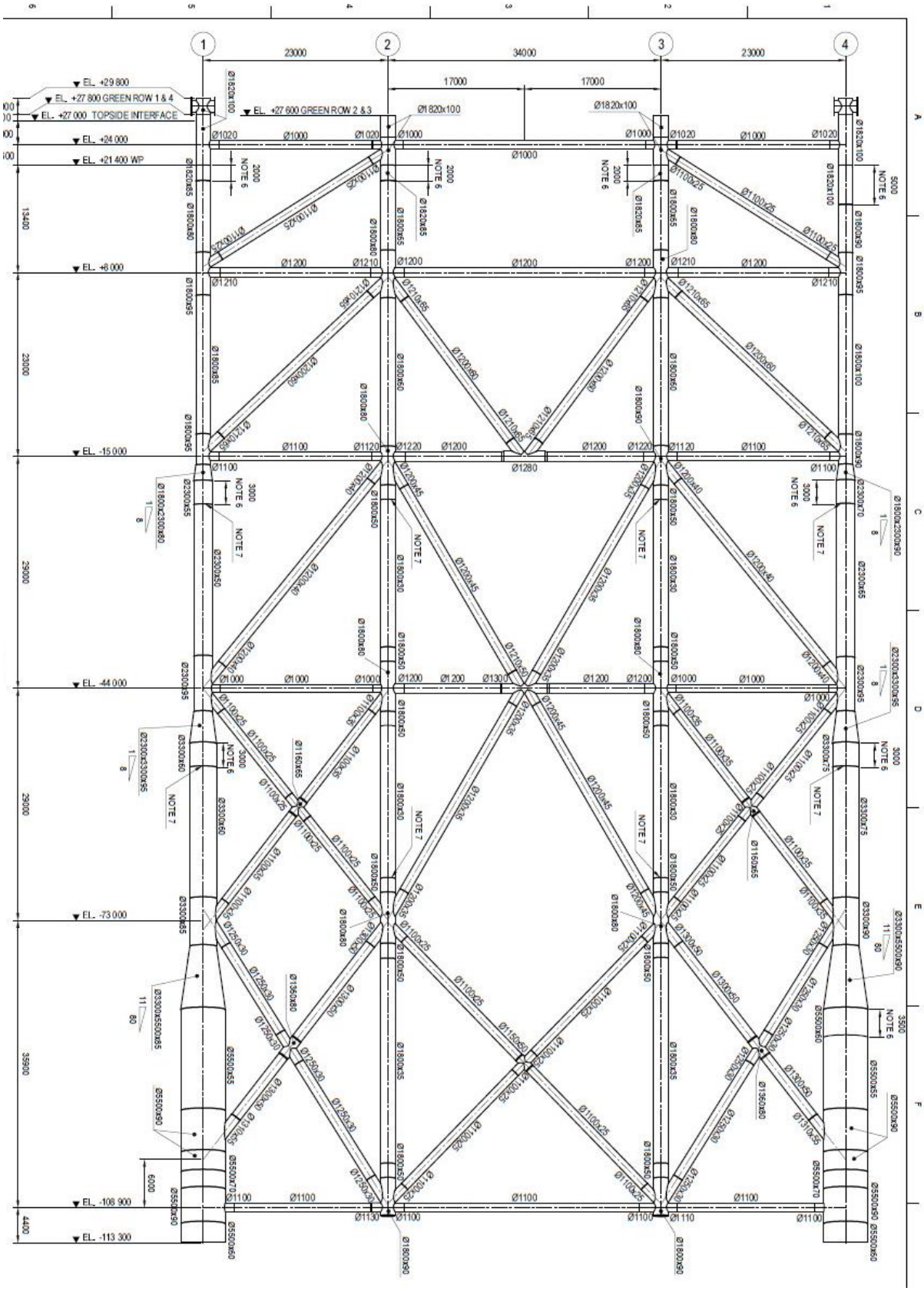

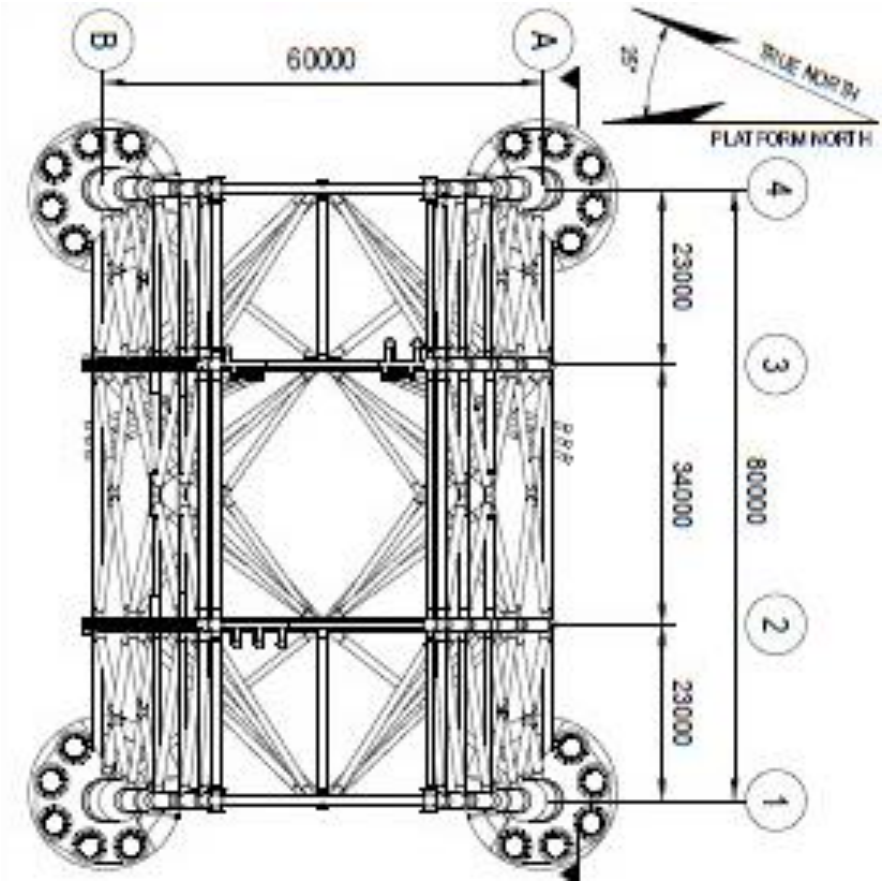
B
A
60000
25°
TRUE NORTH
PLATFORM NORTH
4
3
2
1
23000
34000
23000
80000